1-1-2012

Effect of low endogenous brain-derived neurotrophic factor levels on striatal dopamine dynamics

Francis Kabui Maina
Wayne State University,

EFFECT OF LOW ENDOGENOUS BRAIN-DERIVED NEUROTROPHIC FACTOR LEVELS ON STRIATAL DOPAMINE DYNAMICS

by

FRANCIS KABUI MAINA

DISSERTATION

Submitted to the Graduate School

of Wayne State University,

Detroit, Michigan

in partial fulfillment of the requirements

for the degree of

DOCTOR OF PHILOSOPHY

2011

MAJOR: CHEMISTRY (Analytical)

Approved by:

_____

Advisor Date

_____

_____

_____

DEDICATION

This dissertation is dedicated to my dad (Maina Kabui) and my mom (Eudias Wairimu Maina) for all of the support they have provided.

ACKNOWLEDGMENTS

I would like to start by thanking my mentor, Dr. Tiffany A. Mathews for her support and guidance. She enabled me to learn and be creative on my own in science, but was always available to make sure that everything was done the right way. She went beyond my expectations and really made my life here at Wayne State University successful. Also I would especially like to acknowledge the dissertation committee members: Dr. Mary T. Rodgers, Dr. Christine S. Chow, and Dr. Brandon J. Aragona. Your guidance, comments, suggestions, and availability made quite an impact on my success.

I would like to sincerely thank Kelly Bosse, Ph.D. and Johnna Birbeck, my group members whom we have collaborated with in the BDNF research project. Their results and suggestions helped in solving the BDNF puzzle. Madiha Khalid, her input in making my work a success is highly appreciated. Also I would like to thank the other current group members: Brooke Newman, Aaron Apawu, as well as past members: Jamie Carroll, Ph.D., Rabab Aoun, Ph.D., Stella Wisidamage, Katie Logan, Christopher Rogalla, Marion France, Parvej Khan, Natasha Bohin, and Andrzej Czaja. Thanks for the support, suggestions, comments, potlucks, and laughter. They will always have a special place in my heart because they made graduate school life enjoyable. Also I would like to thank Magdalene Wambua for being a wonderful friend.

Finally, and most important, I would like to sincerely thank my supportive family. Dad, mom, Jeniffer, Anthony, Jane, Harrison, Esther, Loise, Mary, and Nancy; I owe my success to you and your belief in me. Thanks for always being there for me and ensuring that I am able to beat all odds.

TABLE OF CONTENTS

LIST OF TABLES

LIST OF FIGURES

ABBREVIATIONS

3-MT	3-methoxytyramine
7-OH-DPAT	(±)-7-hydroxy-2 dipropylaminotetralin hydrobromide
AADC	L-aromatic amino acid decarboxylase
AC	adenylyl cyclase
aCSF	artificial cerebrospinal fluid
ADC	analog to digital converter
ADHD	attention deficit hyperactivity disorder
Akt	serine/threonine kinase
BAD	BCL2-associated death promoter
BCL2	B-cell lymphoma 2
BDNF	brain-derived neurotrophic factor
cAMP	cyclic adenosine monophosphate
COMT	catechol-O-methyltransferase
CPu	caudate putamen
Cre	site-specific DNA recombinase
CREB	cAMP response element binding protein
DA	dopamine
DAC	digital to analog converter
DAG	diacylglycerol
DAT	dopamine transporter
dATP	2'-deoxyadenosine triphosphate

dCTP	2'-deoxycytidine triphosphate
dGTP	2'-deoxyguanosine triphosphate
DNA	2'-deoxyribonucleic acid
dTTP	deoxythymidine triphosphate
DOPAC	3,4-dihydroxyphenylacetic acid
EC_{50}	half maximal effective concentration
E_d	extraction fraction
EDTA	ethylenediaminetetraacetic acid
ERK	extracellular signal-regulated kinase
EPSP	excitatory post-synaptic potential
f	frequency
FIA	flow injection analysis
Frs-2	fibroblast receptor substrate-2
FSCV	fast scan cyclic voltammetry
GABA	γ-aminobutyric acid
GDNF	glial derived neurotrophic factor
GPCR	G-protein coupled receptor
HPLC	high-performance liquid chromatography
HVA	homovanillic acid
IC_{50}	half maximal inhibitory concentration
i.p.	intraperitoneal
IP3	inositol 1,4,5 triphosphate

IRS	insulin receptor substrate
K252a	tyrosine kinase inhibitor
L-DOPA	L-3,4-dihydroxyphenylalanine
LTP	long-term potentiation
MAO	monoamine oxidase
MAPK	mitogen-activated protein kinase
mIPSC	miniature inhibitory post-synaptic current
MRI	magnetic resonance imaging
mRNA	messenger ribonucleic acid
MS	mass spectrometry
NAc	nucleus accumbens
NGF	nerve growth factor
NT	neurotrophin
p	pulse
PCI	peripheral component interconnections
PCR	polymerase chain reaction
PI3K	phosphatidylinositol-3 kinase
PKC	protein kinase C
PLCγ	phospholipase C, γ
Ras	GTP binding protein
SEM	standard error of the mean
SH2	Src homology domain 2

SHC	adaptor protein containing SH2 domain
SN	substantia nigra
S/N	signal-to-noise ratio
TH	tyrosine hydroxylase
TrkB	tyrosine kinase B
VMAT	vesicular monoamine transporter
V_{max}	maximum velocity
VTA	ventral tegmental area
WT	wildtype

CONTRIBUTIONS

Chapter 2. Materials and Methods

All experiments that used brain-derived neurotrophic factor (BDNF) heterozygote mice as well as their wildtype littermates required in-house breeding and genotyping. Breeding, weaning, and genotypic analysis were performed by Kelly E. Bosse, Ph.D. and Brooke Newman with the assistance from Johnna A. Birbeck, Parvej Khan, Natasha Bohin, Andrzej Czaja, Katie Logan, and Christopher Rogalla. Microdialysis experiments were performed by Kelly E. Bosse, Ph.D. and Johnna A. Birbeck with assistance from Marion France. The experiments encompassed stereotaxic surgery, probe implantation, dialysate collection, HPLC separation with electrochemical detection, chromatographic data analysis, statistical analysis, and graphing. I performed all slice voltammetry experiments, data analysis, statistical analysis, and graphing.

Chapter 3. Functional Fast Scan Cyclic Voltammetry Assay to Characterize Dopamine D2 and D3 Autoreceptors

Wildtype mice were purchased from Jackson Laboratories, thus no genotyping was required. I performed all slice voltammetry experiments, data analysis, statistical analysis, and graphing. Also I performed the literature search and wrote the manuscript which was published in ACS Chemical Neuroscience Journal (Maina and Mathews 2010).

Chapter 4. Aberrant Striatal Dopamine Dynamics in Brain-Derived Neurotrophic Factor-Deficient Mice

Kelly E. Bosse, Ph.D. with assistance from Marion France performed all the microdialysis experiments on young adult mice (3 – 4 months of age). The microdialysis

experiments involved stereotaxic surgery, probe implantation, sample collection, sample analysis that included HPLC separation with electrochemical detection, data and statistical analysis, and graphing. Analyses of L-DOPA content in the tissue were performed by Kelly E. Bosse, Ph.D. with assistance from Joseph Roberts. The experiments involved collection of the tissue samples, sample analysis that included HPLC separation with electrochemical detection, chromatographic and statistical data analysis, and graphing. I performed all slice voltammetry experiments from the caudate putamen and nucleus accumbens, data and statistical analysis, and graphing. Also I performed literature search and wrote the chapter. All the microdialysis results in this chapter and some of the slice voltammetry results from the caudate putamen have been accepted for publication in the Journal of Neurochemistry (Bosse, Maina, *et al,*).

Chapter 5. The Impact of Low Endogenous BDNF Levels and Aging on Striatal Dopamine Dynamics

Johnna A. Birbeck performed all the microdialysis experiments on aged mice (~ 18 months of age). The microdialysis results from the aged mice were compared to those obtained by Kelly E. Bosse, Ph.D. on young adult mice (Chapter 4), with the assistance from Marion France. In all cases, microdialysis experiments conducted by either Kelly E. Bosse, Ph.D. or Johnna A. Birbeck involved stereotaxic surgery, probe implantation, sample collection, HPLC separation with electrochemical detection, chromatographic analysis, statistical data analysis, and graphing. I performed all slice voltammetry experiments from the caudate-putamen and nucleus accumbens, data and statistical analysis, and graphing. Also I performed the literature search and wrote the chapter.

Chapter 6. Effect of Low Endogenous BDNF levels on Dopamine Transporter Function

Kelly E. Bosse, Ph.D. performed all the microdialysis experiments on young adult mice (3 – 4 months of age). Johnna A. Birbeck performed all the microdialysis experiments on aged mice (~ 18 months of age). The experiments involved stereotaxic surgery, probe implantation, sample collection, methamphetamine injection, sample analysis that included HPLC separation with electrochemical detection, chromatographic analysis, statistical data analysis, and graphing. I performed all slice voltammetry experiments, data and statistical analysis, and graphing. I also performed literature search and wrote the chapter.

CHAPTER 1

Introduction and Overview

1.1 Basic neurochemistry

1.1.1 Dopamine neuroanatomy

The brain is a complex structure containing at least 100 billion neurons, with proteins, peptides, and various small molecules working together to execute a variety of functions including movement, emotions, learning, memory, and metabolic functions such as heart rate and breathing (*1, 2*). A disruption in any one of these neurochemical systems can have significant consequences on the organism. One of the most widely investigated chemical messengers within the central nervous system (CNS) is dopamine (DA) due to its involvement in the brain reward pathway, movement, cognition, learning, as well as with several neurological disorders such as schizophrenia, Alzheimer's disease, Huntington's disease, attention deficit hyperactivity disorder (ADHD), and Parkinson's disease (*3, 4*). Under normal physiological conditions, DA regulates locomotor activity. For example, a low dose of a drug of abuse such as cocaine, methamphetamine, or ethanol (also referred to as psychostimulants) increases locomotor activity, which is often attributed to an increase in extracellular DA levels in a specific brain region, the striatum (*5-8*).

Within the brain, DA neurons emanate from two sub-regions located in the midbrain, the substantia nigra (SN) and the ventral tegmental area (VTA; Figure 1.1) (*2*). Cell bodies from the SN project primarily to the dorsal striatum (*from here on in this dissertation the structure will be referred to as the caudate putamen (CPu)),* and constitute the nigrostriatal pathway. This DA projection plays a critical role in initiation

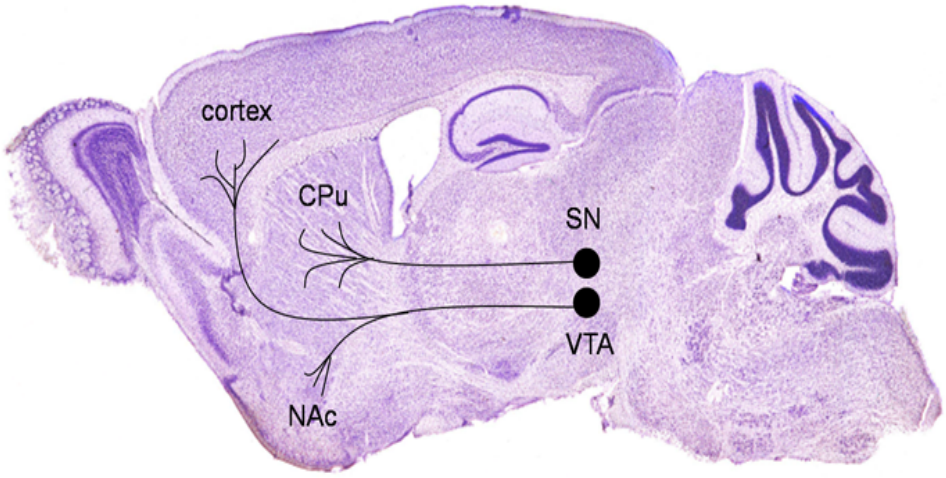

Figure 1.1 Sagittal mouse brain slice (side view) emphasizing major dopamine (DA) projections. DA neurons projecting from the substantia nigra (SN) to the caudate putamen (CPu) make up the nigrostriatal pathway. The mesolimbic pathway is right below the nigrostriatal pathway where DA projections originate from the ventral tegmental area (VTA) and projects to two major targets, the nucleus accumbens (NAc) or the cortex. Figure has been adapted and modified from Mouse Brain Atlas (*9*).

and execution of motor coordination, as well as in learning processes (*10, 11*). The second major source of DA cell bodies are located adjacent to those originating from the SN, in the area referred to as the VTA, and project to numerous brain regions such as the nucleus accumbens (NAc), olfactory bulb, amygdala, hippocampus, and prefrontal cortex. DA neurons that terminate in the NAc from the VTA are often referred to as the mesolimbic pathway, while DA neurons that project to the cortex are typically referred to as the mesocorticolimbic pathway. The mesolimbic pathway is known to be involved in addiction, reward, pleasure, and aggression (*10, 12*). The mesocorticolimbic pathway on the other hand is known to be involved in cognition, motivation, and emotion (*10*).

1.1.2 Dopamine transmission in the brain

Neurons are specialized cells that transmit chemical messengers (neurotransmitters) across a synaptic cleft, a gap between neurons that is a few nanometers wide. Neurotransmitters are released from the sending (presynaptic) to the post-synaptic receiving neuron. Examples of neurotransmitter molecules include: acetylcholine, glutamate, aspartate, glycine, γ-aminobutyric acid (GABA), DA, norepinephrine, and serotonin (*10*). The focus of this section will be on the synthesis and degradation of the neurotransmitter DA.

Cytosolic DA (3,4-dihydroxyphenethylamine) is synthesized in two steps from the amino acid L-tyrosine (Figure 1.2). The rate-limiting first step involves hydroxylation at the third position (C3) of the phenol ring by the tyrosine hydroxylase (TH) enzyme and its co-factors Fe^{2+}, O_2, and tetrahydrobiopterin to generate L-3,4-dihydroxyphenylalanine (L-DOPA). The second step uses L-aromatic amino acid

decarboxylase (AADC) and pyridoxal phosphate, a vitamin B_6 cofactor to convert L-DOPA into DA by removing the carboxyl group. Newly synthesized DA is packaged into synaptic vesicles located in the presynaptic terminal by vesicular monoamine transporter 2 (VMAT2). Vesicular storage protects DA from catabolism by monoamine oxidase (MAO). When recruited by an action potential the vesicles dock and fuse to the plasma membrane, where vesicular DA is rapidly released from the presynaptic neuron to the extracellular environment (Figure 1.3). Once outside the neuron, DA can: (1) bind to post-synaptic receptors to propagate the neurochemical signal, (2) diffuse away from the synapse, (3) be enzymatically degraded into its catabolites, or (4) be taken up by the DA transporter for recycling (reuptake). The DA transporter is a 12 transmembrane protein, whose primary function is to terminate the extracellular DA signaling through rapid reuptake into the presynaptic nerve terminal (*13-15*). This enables DA recycling and limits the duration of receptor activation or signal transmission (*16*). Besides the DA transporter clearing DA from the extraneuronal space, the enzymes MAO and catechol-O-methyltransferase (COMT) enzymatically break down DA into 3,4-dihydroxyphenylacetic acid (DOPAC) and 3-methoxytyramine (3-MT), respectively (*1, 10*). Finally, both DOPAC and 3-MT can be further catabolized to form homovanillic acid (HVA) (*1, 10*).

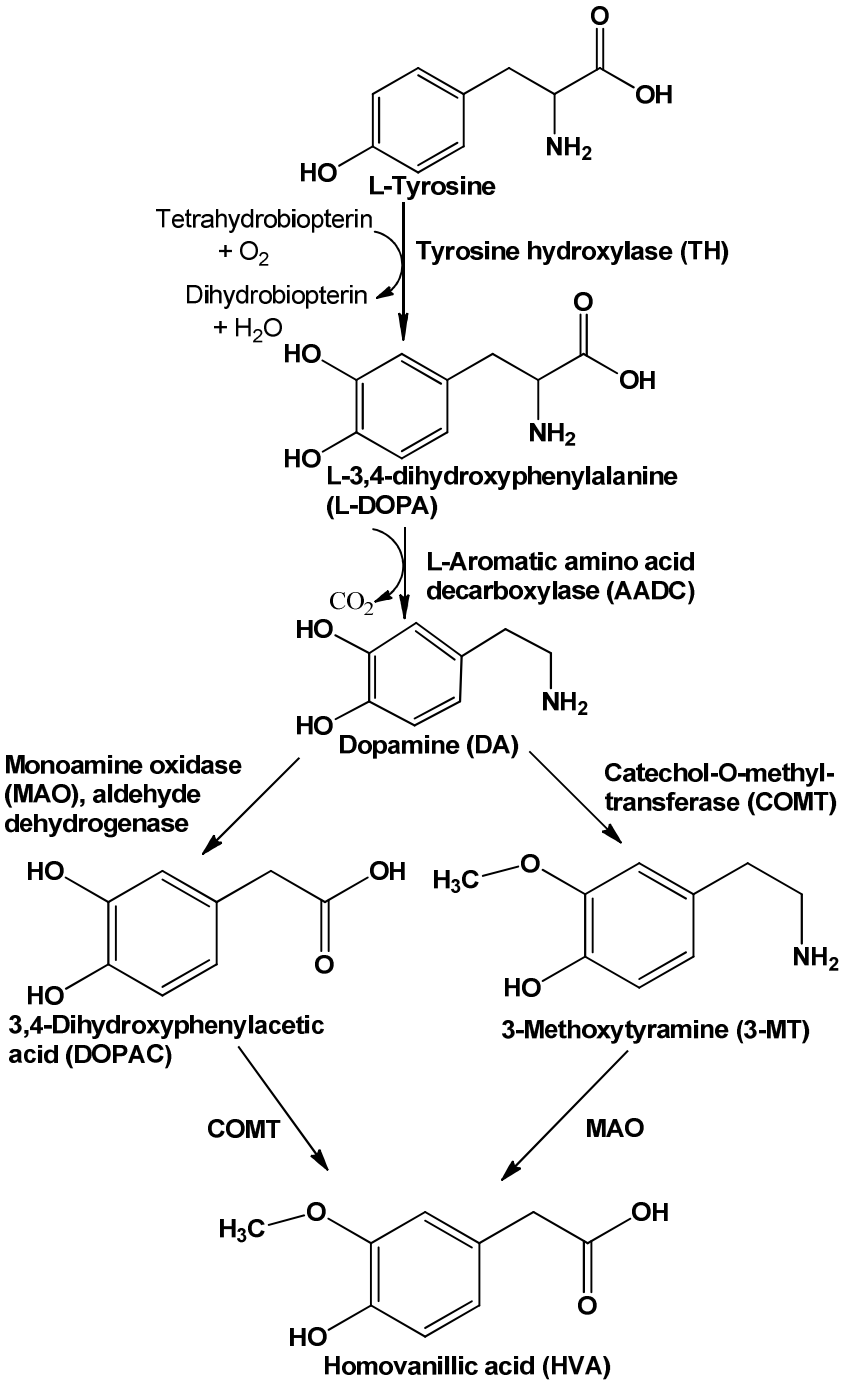

Figure 1.2 Dopamine (DA) synthesis and catabolism.

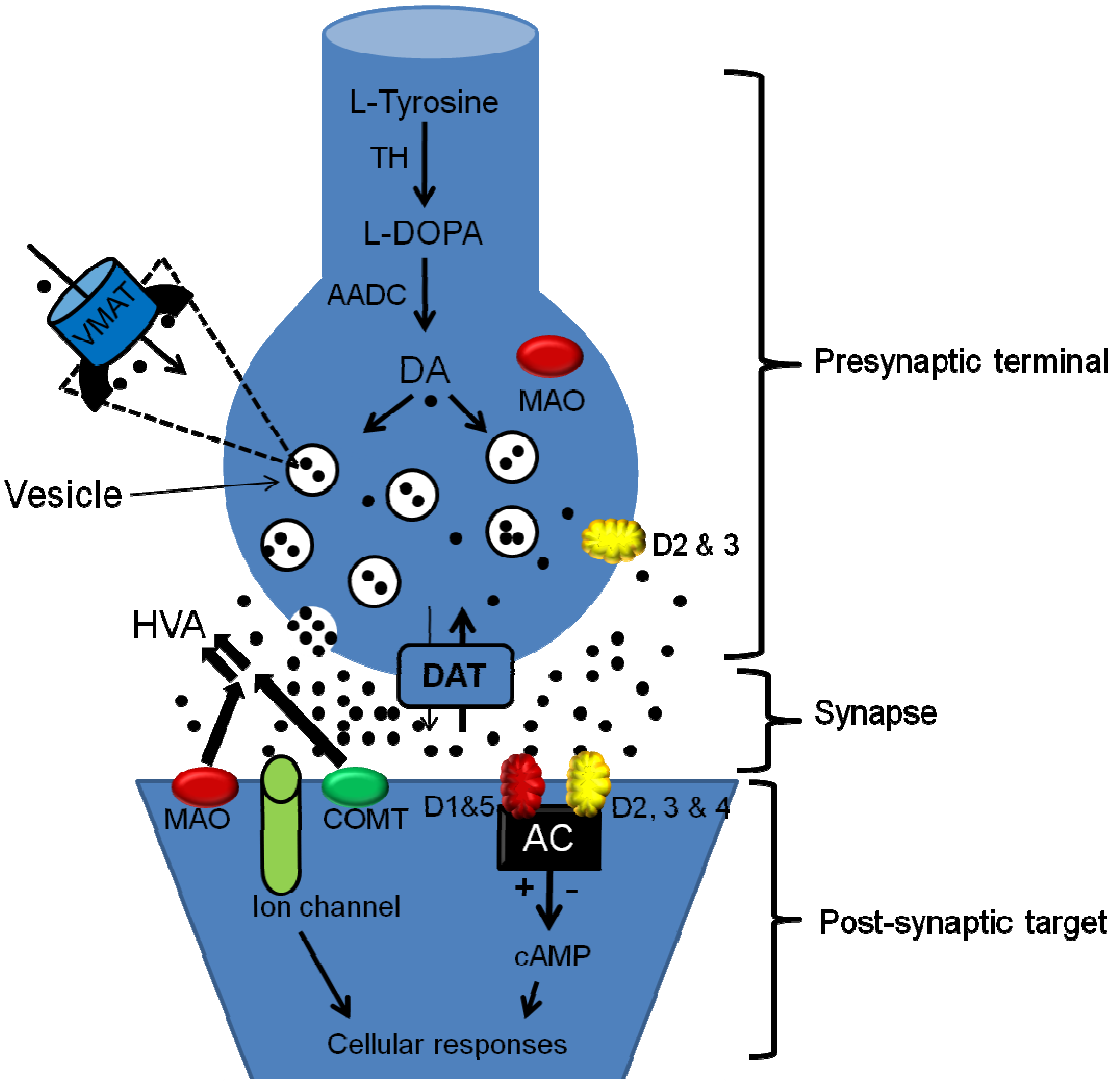

Figure 1.3 A schematic representation of a dopamine (DA) synapse. In the presynaptic neuron, DA is synthesized from L-tyrosine, sequestered in vesicles, and upon an action potential, released into the synapse. The post-synaptic neuron contains the DA receptors, which upon activation by DA, cause signal propagation in the form of secondary messengers to cause cellular responses. Abbreviations: TH, tyrosine hydroxylase; L-DOPA, L-3,4-dihydroxyphenylalanine; AADC, L-aromatic amino acid decarboxylase; VMAT, vesicular monoamine transporter; DAT, DA transporter; HVA, homovanillic acid; MAO, monoamine oxidase; COMT, catechol-O-methyltransferase; AC, adenylyl cyclase; cAMP, cyclic adenosine monophosphate.

Although DA uptake and catabolism are essential to regulate extracellular DA levels, the main purpose of extracellular DA is signaling between neurons. The post-synaptic neuron contains receptors to propagate the DA signal. There are at least five known DA receptor subtypes that belong to the seven-transmembrane G protein-coupled receptor (GPCR) family and are divided into two groups: DA D1-like receptors, which include D1 and D5, and DA D2-like receptors, which include D2, D3, and D4 subtypes (*4, 17, 18*). D1-like receptors stimulate adenylyl cyclase (AC), increasing the levels of secondary messenger cyclic adenosine monophosphate (cAMP) and neuronal activity. However, D2-like receptors inhibit AC, reducing cAMP levels as well neuronal activity. Besides activating post-synaptic receptors, extracellular DA can also stimulate receptors located on the presynaptic terminals, which are referred to as autoreceptors. Depending on whether autoreceptor is D1- or D2-like, activation of these DA autoreceptors can either up- or down-regulate extracellular DA levels, respectively. Specifically, stimulation of DA D2-like receptors reduces extracellular DA levels via a negative feedback mechanism, regulating DA synthesis and/or release (*19, 20*).

1.1.3 Brain-derived neurotrophic factor

Neurotrophic factors are endogenous soluble proteins that regulate the cell cycle, growth, differentiation, and survival of neurons (*21*). Examples of the neurotrophic family are nerve growth factor (NGF), brain-derived neurotrophic factor (BDNF), glial-derived neurotrophic factor (GDNF), neurotrophin-3 (NT-3), and neurotrophin-4 (NT-4) that mediate their functions through protein tyrosine kinase (Trk) receptors. The Trk receptors are glycoproteins that have a molecular weight in the range of 140 – 145 kDa. Each neurotrophin appears to bind to a unique isoform of the Trk receptors. For

example, NGF has greater specificity towards the TrkA receptor, NT-3 interacts with TrkC, while both BDNF and NT-4 bind to TrkB (*10, 22*). BDNF, a 27 kDa homodimeric protein, upon expression is transported to nerve terminals through the axon and undergoes exocytotic release from presynaptic vesicles (*23-25*). Extracellular BDNF binds to TrkB receptors, causing receptor dimerization, which leads to phosphorylation of tyrosine residues within the cytoplasmic domain, activating the kinase (*26*). Phosphorylated tyrosine residues recruit specific proteins, such as GBR2, SHC, and SOS, that activate Raf, a serine/threonine protein kinase (Akt) (*23*). Trk activation induces numerous signaling cascades through three known pathways: the Ras/mitogen activated protein kinase (MAPK), phosphatidylinositol-3-kinase (PI3K), and phospholipase C, γ (PLCγ) (Figure 1.4). Activation of these signaling cascades eventually regulate the transcription factor, cAMP response element binding (CREB), leading to an attenuation or potentiation in gene expression. Continuous activation or inhibition of these signaling events regulate synaptic plasticity, synaptic transmission, neurotransmitter release, neurogenesis, and cell survival (*10, 23, 27-29*).

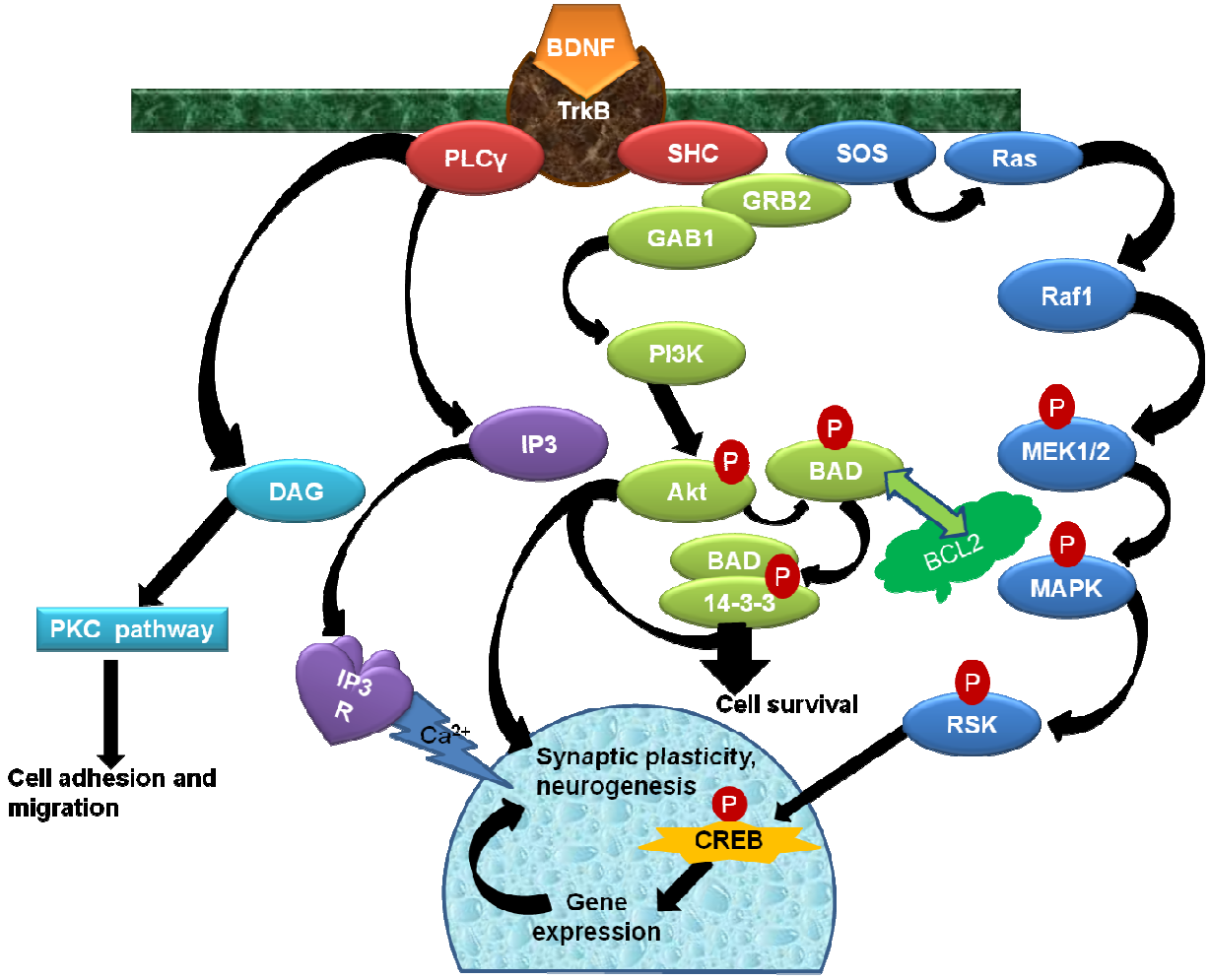

Figure 1.4 Brain-derived neurotrophic factor (BDNF) signaling pathways through the tyrosine kinase (TrkB) receptor. Abbreviations used: PLCγ, phospholipase C, γ; protein kinase C, PKC; Akt, serine/threonine kinase; BCL2, B-cell lymphoma 2; BAD, BCL2-associated death promoter; DAG, diacylglycerol; MAPK, mitogen activated protein kinase; P; phosphorylation; MEK, MAPK kinase; PI3K, phosphatidylinositol-3-kinase; IP3, inositol-1,4,5-triphosphate; IP3 R, IP3 receptor; CREB, cAMP response element binding protein. Modified from Nestler *et al.* (2009), and Kaplan and Miller (2000) (*10, 23*).

1.1.4 Modulation of the dopamine system by BDNF

There is considerable evidence that the interactions between BDNF and the DA system are reciprocal, although the exact mechanism of how BDNF may regulate DA dynamics has remained unknown (*29-31*). BDNF regulates striatal function directly by activating TrkB receptor (Figure 1.4) (*32*). BDNF infused directly into the brain has been shown to influence the survival and function of DA neurons, affect the turnover ratio between DA and its catabolite DOPAC, and potentiate the activity-dependent release of DA (*29-31*). Evidence suggests that BDNF expression can augment DA transmission in the reward pathway of the VTA-NAc circuit (*33*). Mouse models with reduced BDNF expression demonstrate a variety of alterations in the DA system, indicating that BDNF has some influence on this system. Studies have shown that mice lacking one copy of the BDNF gene ($BDNF^{+/-}$) have higher tissue DA concentrations in the striatum, and decreased DA release in superfused striatal tissue fragments (*34, 35*). BDNF knockout ($BDNF^{-/-}$) and $BDNF^{+/-}$ mice have reduced expression and density of DA D3 receptors in the CPu, NAc core and shell, and in the Islands of Calleja (*36-38*). Additionally, BDNF conditional knockout mice show reduced evoked DA release in the CPu and NAc shell but not in the NAc core, and exhibit altered DA D2 receptor expression in the CPu (*39*). Taken together, these studies suggest that BDNF can augment striatal DA functioning in a region-specific manner.

1.1.5 Neurological diseases associated with dysfunction in the dopamine system

It is too simplistic to hypothesize that dysfunction in regulation of one molecule is a direct cause of a neurological disease; rather, it is array of systems and molecules that likely contribute to the progression of a neurological disease. However, at this time

we do not have the scientific tools to evaluate all of these systems simultaneously. Instead, we have taken the novel approach to examine two discrete molecules – BDNF and DA. Interestingly, neurological diseases that primarily involve a dysfunction or dysregulation of the DA system appear to have the BDNF system altered as well. To better understand these systems, we have used a model of reduced BDNF expression to evaluate its impact on the DA system.

Parkinson's disease is characterized by greater than 80% loss of nigrostriatal DA neurons (*10*). The overt symptoms of Parkinson's disease involve the loss of motor function and include a resting tremor, bradykinesia (slowness in movement), and rigidity (*10*). Although a significant loss of DA neurons is observed in Parkinson's disease, the causes of this impairment of the DA system are still unknown. There are several factors that increase one's likelihood of developing Parkinson's disease, such as advanced age (> 65 years old), genetics, and environment (*10, 40*). Besides significant alterations in the DA system, additional studies have shown impairments in BDNF, such as reduced BDNF messenger ribonucleic acid (mRNA) and protein levels in the few surviving DA neurons (*41-43*). These findings suggest that hypofunction of BDNF during one's lifetime may play a role in the neuronal loss. However, it is not understood whether low BDNF levels cause the neuronal degeneration or result from it. Our hypothesis is that low BDNF levels predispose the DA system to neuronal degeneration, because the primary role of BDNF is to ensure survival and maintenance of neurons.

Huntington's disease is a fatal neurodegenerative disorder that is typically inherited (*10, 44*). Huntington's symptoms typically manifest in mid-life, with the mean age of onset being between 35 and 44 years and include the following dysfunctions:

motor, psychiatric, and cognitive (*44*). One of the leading candidates associated with DA neuronal loss is a mutation in the Huntingtin gene, leading to increased expression and accumulation of a mutated Huntingtin protein (*44*). The mutated Huntingtin gene contains excessive CAG trinucleotide repeats, usually greater than 36 (*44, 45*). Interestingly, the Huntingtin gene mutation is hypothesized to decrease the expression of BDNF protein in the cerebral cortex, as well as reduction in BDNF protein transport to the striatum (*46, 47*). However, how the Huntingtin protein regulates BDNF expression and protein levels is unknown.

Finally, a dysregulation in both DA and BDNF has been linked to ADHD, which is characterized by inattention, hyperactivity, and impulsiveness. The cause of the ADHD disorder is not well known, though a dysfunction in the midbrain DA systems is primarily involved (*48, 49*). Additionally, several studies have linked the val66met single nucleotide polymorphism in BDNF to increased susceptibility to ADHD (*50-52*). A decrease in midbrain BDNF activity is thought to be in part involved in the pathogenesis of ADHD as well (*49*).

Besides being involved in several neurological diseases, the DA system is known to play a key role in drug addiction. Drugs of abuse such as cocaine, ethanol, and methamphetamine are known to elevate extracellular DA levels (*5-8*). Recent evidence suggests that underlying genetic susceptibility may contribute to drug addiction; for example, BDNF dysfunction may play a critical role in the addiction process (*53, 54*). Due to the overwhelming studies linking BDNF to DA related neurological diseases and disorders, it is important to study how BDNF levels alone modulate the DA system.

1.2 Neurochemical techniques

Analytical techniques have played a critical role in neurochemical measurements (*55-57*). Most techniques that have been used to monitor extracellular DA dynamics typically focus on electroanalytical methods such as fast scan cyclic voltammetry (FSCV), constant potential amperometry, differential normal pulse voltammetry, high speed chronoamperometry, and *in vivo* microdialysis connected to high performance liquid chromatography (HPLC) with electrochemical detection (*58-62*). An advantage of using *in vivo* microdialysis to sample DA is that it allows for monitoring of multiple analytes (e.g., other monoamines and DA catabolites), because microdialysis samples are coupled to separation techniques (HPLC or capillary electrophoresis, CE) and electrochemical detectors. By sampling at low flow rates, *in vivo* microdialysis measures baseline neurotransmitter levels (without stimulation).

A limitation of microdialysis is that it has poor temporal resolution (i.e., sampling for minutes; typically longer than 5 minutes). On the other hand, using direct electrode approaches such as FSCV, constant potential amperometry, and high-speed chronoamperometry provides sub-second temporal resolution enabling real-time monitoring of the rapid dynamics of DA release and uptake. The analytical advantage of DA is that it is easily oxidized, making it ideally suited for electrochemical monitoring. When FSCV and *in vivo* microdialysis are used together, they complement each other, by measuring different parameters of DA dynamics. FSCV can be used to probe DA sequestration, DA mobilization, DA release, DA uptake and DA autoreceptor functionality (*14, 56, 60, 63-77*). *In vivo* microdialysis on the other hand, enables measurements of baseline levels of extraneuronal DA and DA metabolism (*59, 78-86*).

1.2.1 Fast scan cyclic voltammetry

Voltammetry involves a group of electroanalytical methods in which current is measured as voltage of an electrochemical system is changed. Examples of such techniques are cyclic voltammetry, hydrodynamic voltammetry, square wave voltammetry, and linear sweep voltammetry. What differentiates these techniques from one another is the shape of the applied voltage waveform. For example, cyclic voltammetry uses a triangle waveform versus linear sweep voltammetry, which uses a linear waveform. In either case, the waveform defines how the voltage is applied to the electrode surface. When cyclic voltammetry is used, the potential of the working electrode is made sufficiently positive or negative (depending on the initial and switching potentials that define the triangle waveform) to drive electron transfer. When the working electrode surface becomes sufficiently negative or positive, the analyte of interest either gains electrons from the surface of the electrode or the analyte transfers electrons to the surface, respectively. The electron transfer process generates charge that is measured as current and is proportional to the concentration of the electroactive analyte as defined by Faraday's law (Equation 1).

$$Q = nFN \qquad \textbf{(1)}$$

Where Q (Coulombs) is the total charge, n is the number of moles of electrons transferred per molecule, F is Faraday's constant (9.649×10^4 Coulombs/mole), and N is the number of moles of analyte. At the switching potential (peak of the triangle), the applied voltage is reversed until it reaches its initial potential. If the analyte of interest is chemically reversible, then the corresponding reduction/oxidation peak is observed. The resulting current is recorded and the corresponding current versus voltage plot is

generated. In a reversible system, the voltammetric peak current for forward scan at 25ºC is defined by the Randles-Sevcik equation (Equation 2) (*87, 88*),

$$i_p = (2.69 \times 10^5)\, n^{3/2} A D^{1/2} v^{1/2} C^* \qquad \textbf{(2)}$$

where i_p is the peak current, n is the number of moles of electrons transferred, A is the working electrode surface area, D is the diffusion coefficient of the analyte, v is the scan rate, and C^* is the analyte concentration.

Cyclic voltammetry can be divided into sub-categories depending on the scan rate. FSCV differs from conventional cyclic voltammetry by using scan rates greater than 100 V/s. Advantages of faster scan rates is that they permit enhanced selectivity and lower the limits of detection (Figure 1.5). Because FSCV completes the triangle waveform in less than 10 seconds, real time oxidation/reduction measurements can typically be made every 100 ms. Due to its sub-second time resolution, micrometer-dimension spatial resolution, and the analytical advantage of DA being easily oxidizable has made FSCV an extremely powerful neurochemical technique to measure DA dynamics. The carbon fiber microelectrode used in FSCV is typically less than 10 µm in diameter, making it amenable to placement in anatomically discrete brain regions such as the NAc core versus the shell. *In vivo* FSCV has provided DA measurements from the NAc core and shell of freely moving or anesthetized animals (*66, 89-93*). Similar to *in vivo* FSCV, slice FSCV can be performed in anatomically distinct sub-regions using thin sections of brain tissue (*69, 82, 94-96*).

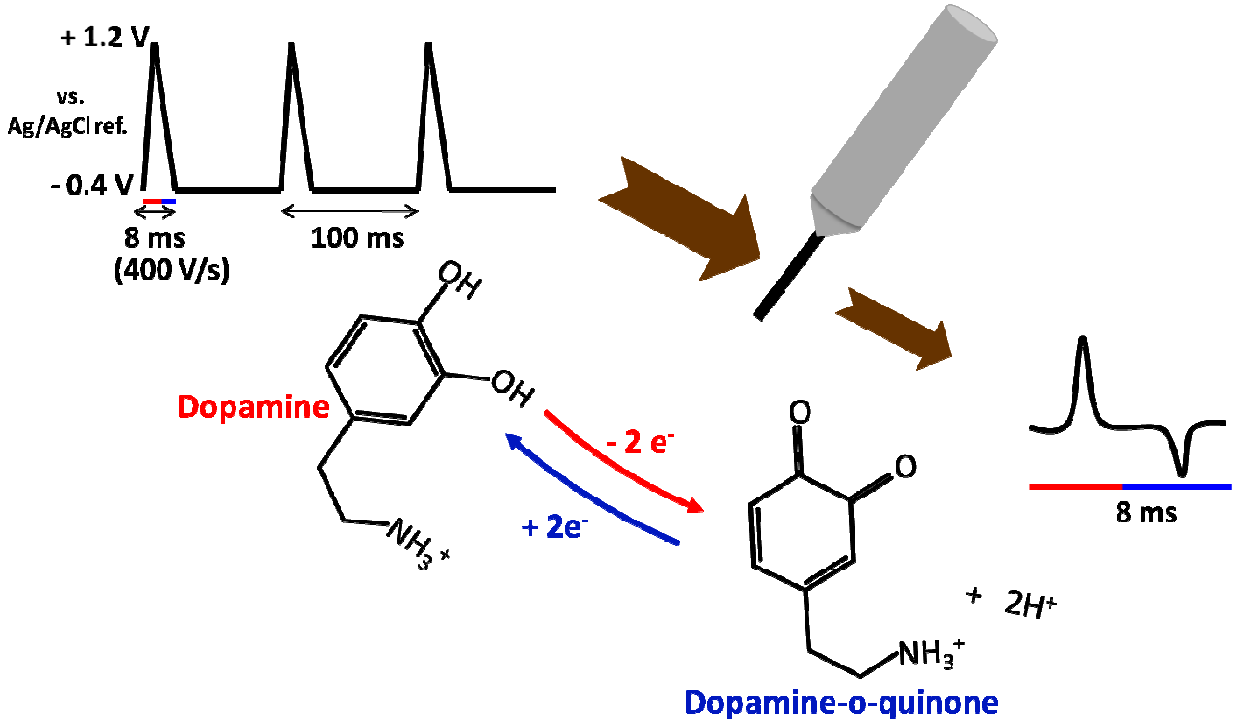

Figure 1.5 Schematic representation of fast scan cyclic voltammetry (FSCV). In the upper left corner: A series of triangle waveforms (each lasting 8 ms) are applied to the microelectrode every 100 ms at a scan rate of 400 V/s. Dopamine (DA) is oxidized to dopamine-o-quinone, which releases 2 moles of electrons and 2 protons during the rise in potential being applied to the carbon fiber (-0.4 to +1.2 V). On the descending phase of the triangle waveform (+1.2 to -0.4 V), any remaining dopamine-o-quinone near the electrode surface is reduced to DA. The carbon fiber microelectrode measures the anodic and cathodic current, respectively (lower right corner).

1.2.2 Slice voltammetry

For more than two decades, brain slices have been used as an important tool for monitoring DA dynamics in guinea pigs, rats, monkeys, and mice (*90, 97-99*). In the 1990's the emergence of genetically modified mice, such as DA D2 receptor knockout mice, DA transporter knockout mice, or transgenic models that mimic certain characteristics of neurological diseases, led to the popularity of fast neurochemical techniques to better understand how the brain adapts to these genetic manipulations. Slice voltammetry allows for the opportunity to probe DA dynamics, such as electrically stimulated DA release, DA uptake, DA autoreceptor function, and heteroreceptor control of presynaptic DA release. All of the above mentioned DA dynamic parameters can be probed with the appropriate pharmacological agents such as DA uptake inhibitors or releasers, DA receptor agonists and antagonists, VMAT inhibitors, and other neurotransmitter systems, such as nicotinic agonists (*70, 96, 100-102*).

Using brain slices to probe DA dynamics allows for control over temperature and stimulation parameters, and reduces interference due to pH changes, which are difficult to control during *in vivo* experiments. Moreover, the use of a slice perfusion chamber allows for easy and reproducible application of pharmacological agents and can be used to probe their effect locally without contributions from connecting brain regions or the periphery. Overall, slice voltammetry (Figure 1.6) allows for an efficient and easy way to assess DA dynamics in the absence or presence of pharmacological agents in various brain regions.

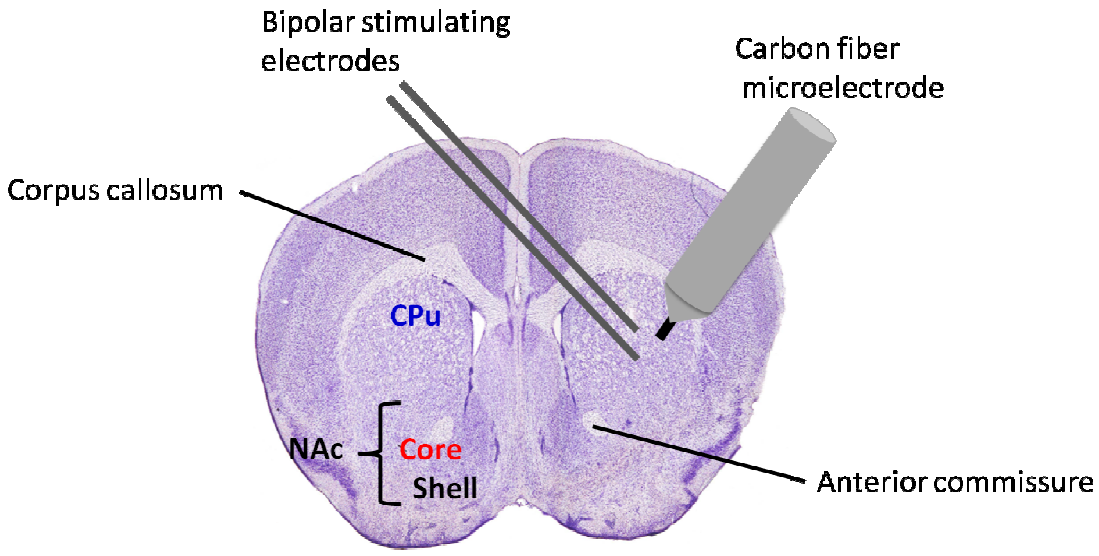

Figure 1.6 Representative image of electrode placement in slice FSCV. In this figure the stimulating and working electrodes are placed on the right side of the caudate putamen (CPu) of a mouse brain slice. The CPu is identified from the anatomical landmarks that are visualized on the slice, such as the corpus callosum and the anterior commissure. The CPu is located between the anterior commissure and the corpus callosum. On the left lower side of the brain slice, approximate locations of the striatal sub-regions of nucleus accumbens (NAc) core and shell are shown. Figure has been adapted and modified from Mouse Brain Atlas (*9*).

Once brain slices are obtained, a carbon fiber working microelectrode is inserted directly into the region of interest. In order to evoke DA release from neurons, a stimulating electrode is placed on top of the brain slice (Figure 1.6). Due to the fast scan rate, a large, but stable background current is generated at the microelectrode. Software is used to subtract the background charging current and therefore generate a meaningful cyclic voltammogram for DA. Using TH-1 software (ESA Inc., Chelmsford, MA), three pieces of data are generated: (1) current versus voltage (CV) plot, (2) current versus time trace, and (3) pseudo-color plot (Figure 1.7). The background subtracted cyclic voltammogram (Figure 1.7A) exhibits a large peak at ~ +0.6 V with respect to a Ag/AgCl reference electrode, which is characteristic of where DA is oxidized, while a second and smaller peak is observed at ~ -0.2 V, representing the reduction of DA-*ortho*-quinone. The locations of the oxidation and reduction peaks in the cyclic voltammogram are used to chemically identify DA. The current versus time plot (Figure 1.7B) indicates current generated at ~ +0.6 V, with electrically evoked DA release (defined as the rising phase in a current), and DA being taken up by the DA transporter (defined as the decay phase in a current). Post-calibration of the electrode with a known concentration of DA is performed at the end of the experiment and the current (nA) is converted into concentration (μM).

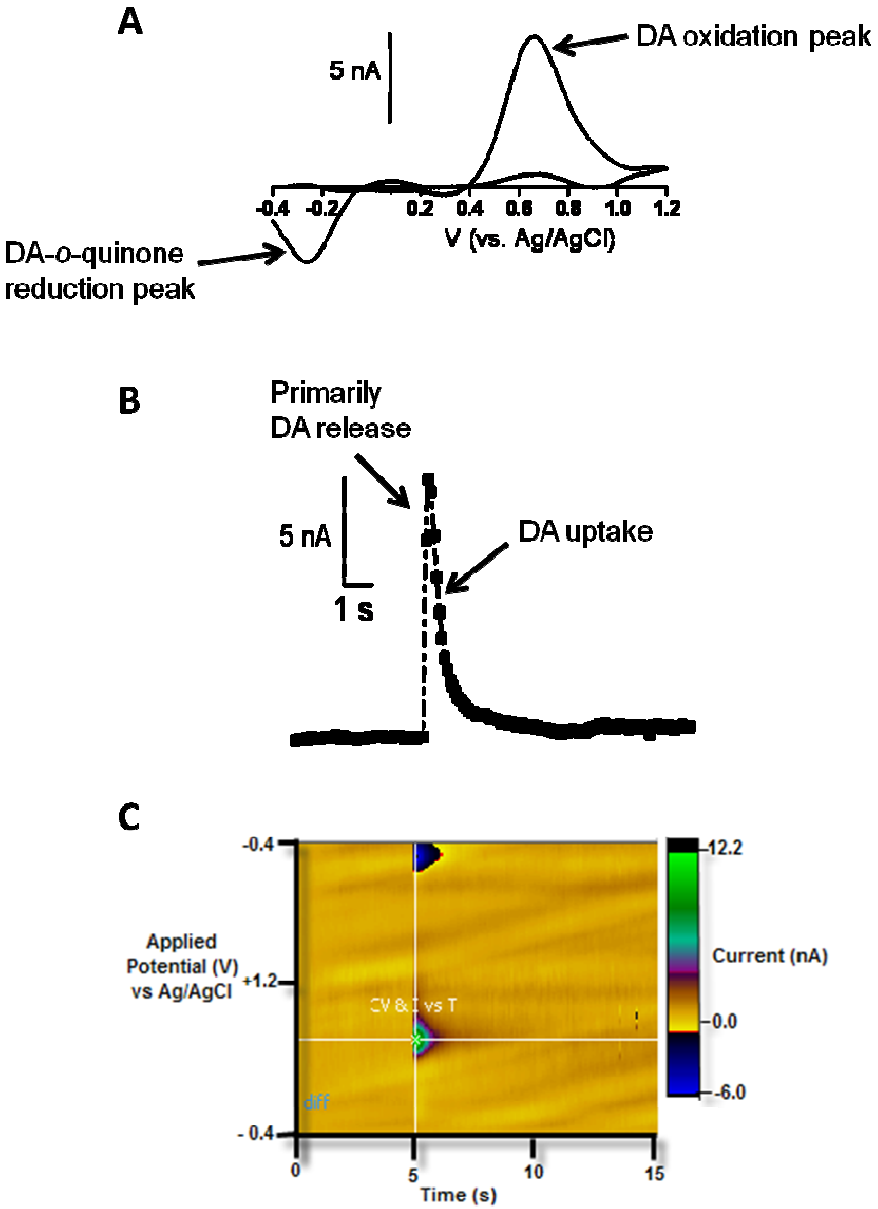

Figure 1.7 Representative FSCV dopamine (DA) measurements from the caudate putamen (CPu) of a mouse brain slice. (A) Corresponding cyclic voltammogram of current (nA) versus voltage (V); (B) Plot of current (nA) versus time (s); (C) Pseudo-color plot. The color plot is a three dimensional plot of the voltammetric current (encoded in color, z-axis) plotted against time (x-axis) and applied potential (y-axis). The color plot is used to visually identify the oxidization of DA and reduction of DA-*ortho*-quinone.

1.2.3 Flow injection analysis

Flow injection analysis (FIA) involves injection of a small but well-defined volume or concentration of an analyte into a continuously flowing carrier stream containing the appropriate buffer, creating a concentration gradient of the sample. In contrast to other conventional continuous flow procedures, FIA does not necessarily require complete mixing of the analyte and reagent(s). With good timing of all events, it is typically not necessary to wait for chemical equilibrium to be attained. Transient signals such as current, voltage, or fluorescence are read out, permitting the measurements to be accomplished within a very short time (usually in less than 30 seconds). FIA is the method by which the carbon fiber microelectrode is calibrated. Using a T-shaped flow cell, the carbon fiber microelectrode is placed in a stream of flowing buffer and a plug of DA is injected manually from a syringe (Figure 1.8). When the sample plug reaches the tip of the carbon fiber microelectrode, the electrode's response is measured (Figure 1.9).

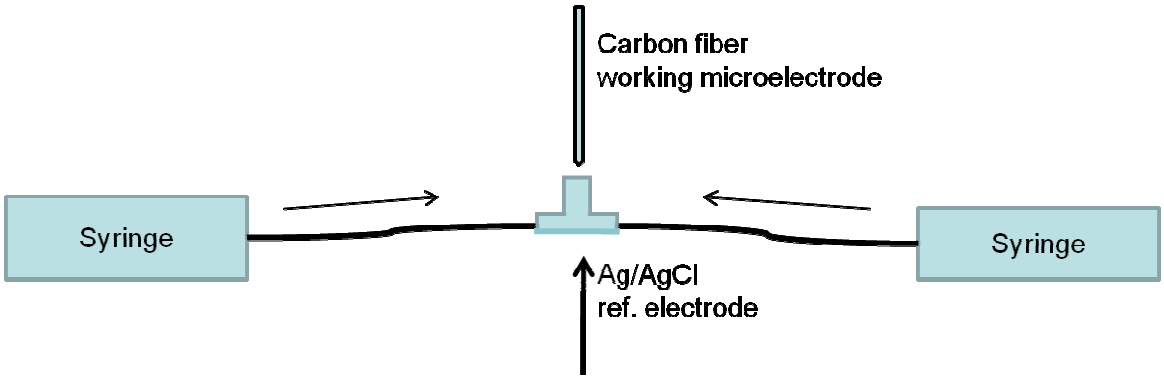

Figure 1.8 Schematic diagram of a flow injection analysis (FIA) set up for microelectrode calibration using a T-shaped flow cell.

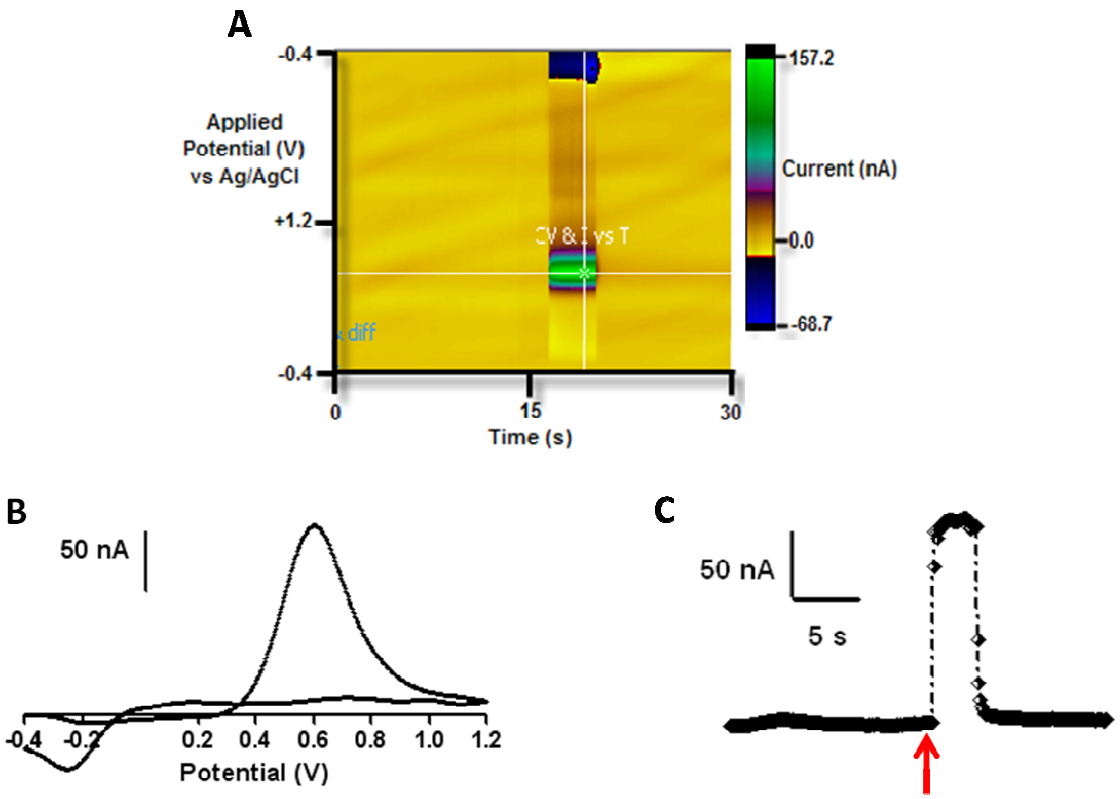

Figure 1.9 Representative data from flow injection analysis used to calibrate the carbon fiber microelectrode. The electrode in this example is calibrated with a 10 µM dopamine (DA) standard. (A) Pseudo-color plot of DA oxidation and reduction, (B) DA cyclic voltammogram, and (C) current versus time plot. The current versus time plot demonstrates the introduction of DA standard solution at ~ 16 s (red arrow) using the flow injection system. The color plot is a visual aide used to identify the oxidization of DA and reduction of DA-*ortho*-quinone.

1.2.4 Chemical selectivity

The main limitation of voltammetry techniques is that oxidation and/or reduction occurs for all electroactive species as long as sufficient voltage is applied to the electrode, making chemical selectivity a primary concern in biological samples. Within the brain, DA is part of the neurotransmitter family known as the monoamines, which is comprised of serotonin and norepinephrine, and all are electroactive (Figure 1.10). Additionally, DOPAC and 5-hydroxyindoleacetic acid, degradation products from DA and serotonin, respectively, are present in 100-fold greater concentrations than their parent molecules and are also electroactive. An advantage of FSCV is that the chemical identity of an electroactive species is defined by both the oxidation and reduction peak potentials. For example, norepinephrine and DA have similar oxidation and reduction potentials at +0.6 V and -0.2 V, respectively. On the other hand, serotonin has oxidation and reduction potentials of +0.7 V and 0.0 V, respectively. Because DA and norepinephrine are structurally similar, it is difficult to distinguish their cyclic voltammograms. However, the carbon fiber microelectrode is more sensitive to DA than norepinephrine, as shown by the larger cathodic current (Figure 1.10).

Chemical species in a cyclic voltammogram can be identified by the ratio of the oxidative and reductive peaks or peak location and shape (*89*). The shape of a cyclic voltammogram is determined by electron transfer kinetics and how strongly the analyte adsorbs on the carbon fiber (*89*). To assist with DA detection in the brain, the electrodes are placed in known dopaminergic-rich regions with little or no norepinephrine or serotonin, like the striatum, which includes the CPu and NAc core and shell.

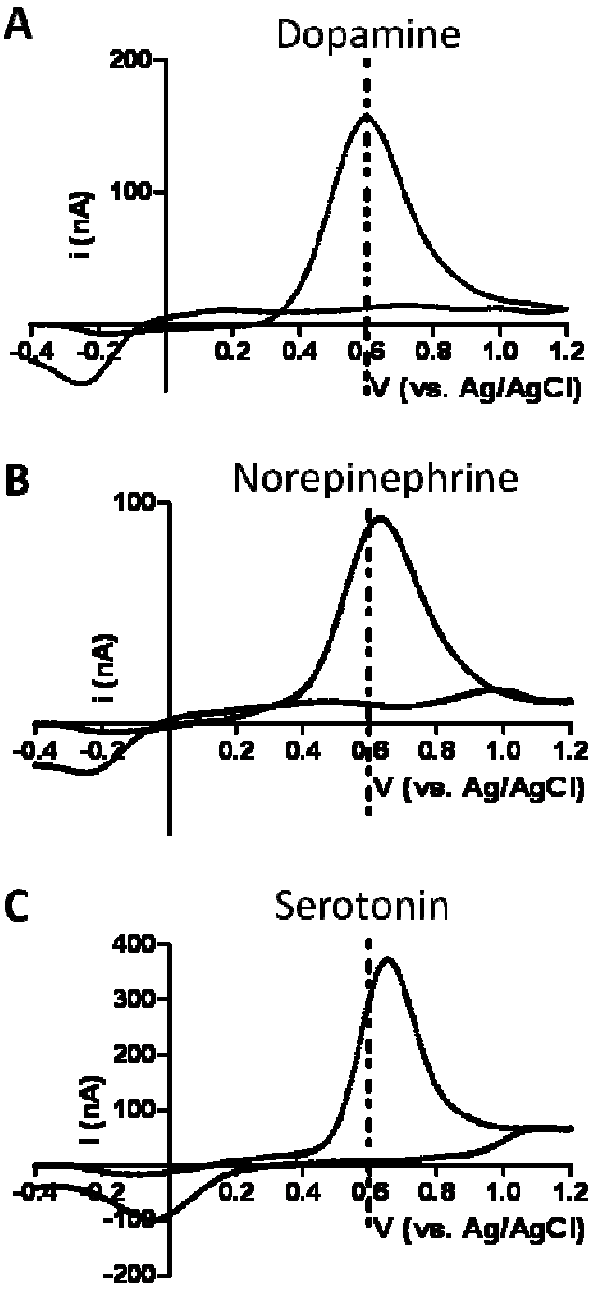

Figure 1.10 Representative cyclic voltammograms for 10 µM: (A) dopamine (DA), (B) norepinephrine, and (C) serotonin. All cyclic voltammograms were obtained using flow injection analysis with a Ag/AgCl reference electrode. A triangle waveform was applied from -0.4 V to +1.2 V and back to -0.4 V at a scan rate of 400 V/s for each neurotransmitter. The dashed line at +0.6 V for all cyclic voltammograms is shown because this represents the voltage where the maximum amount of DA oxidized. Note, for (B) and (C) the peak is slightly shifted from this maximum.

Besides using the characteristic voltammogram to identify DA, pharmacological agents such as DA receptor agonists or antagonists, or DA uptake blockers can be administered to characterize the signal as dopaminergic in nature.

1.2.5 *In vivo* microdialysis

Microdialysis is an *in vivo* neurochemical technique that samples from a freely behaving animal. The microdialysis probe consists of a semi-permeable membrane with a molecular weight cutoff typically in the range of 5 – 30 kDa to allow for exclusion of large molecules, such as proteins, and to provide some selectivity during sampling. The probe is continuously perfused with a buffer like artificial cerebrospinal fluid (aCSF) that mimics the extracellular fluid in the brain. Analytes diffuse from the tissue of interest (high analyte concentration) to the dialysate probe (low analyte concentration) and are collected for analysis (*59, 103*).

Upon stereotaxic surgery, a guide cannula that targets the brain region of interest is implanted and held in place by dental cement and screws. After the animal has recovered (in our lab ~ 4 – 6 hours) the guide cannula is removed and a concentric microdialysis probe is inserted for analyte sampling (Figure 1.11). Concentric probes are commonly used during microdialysis due to their strength and stability (*104*). After an equilibration period (~ 12 – 16 hours) the analytes are sampled in a freely moving and behaving animal (Figure 1.12) (*105*). Syringe pumps are used to infuse the perfusate at very low flow rates of ~ 0.5 – 5.0 µL/min to ensure optimal probe recovery (*106*). The fluid that is collected during microdialysis is referred to as the dialysate and contains the analytes of interest, such as DA and its metabolites. The low volume (5 – 20 µL) dialysate samples are usually free of macromolecules such as proteins.

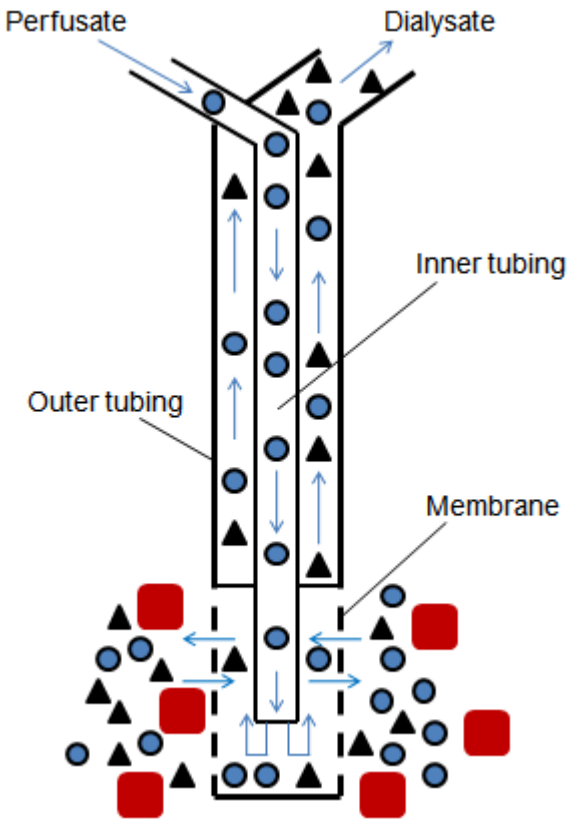

Figure 1.11 A schematic diagram for the semi-permeable membrane of a microdialysis probe. The perfusate buffer (filled circles) is infused through the concentric microdialysis probe. The small molecules such as neurotransmitters (triangles) perfuse down their concentration gradient towards the dialysis probe for collection. Molecules with high molecular weight above the membrane cutoff (e.g., 6 kDa), such as proteins (squares), are excluded.

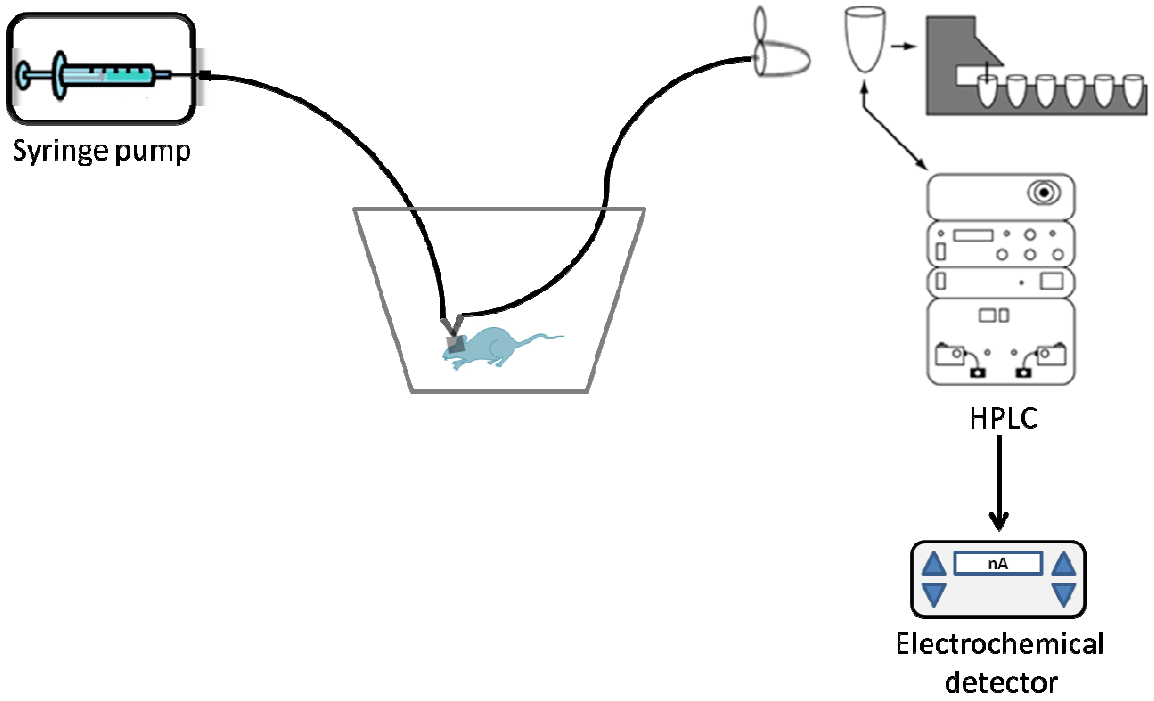

Figure 1.12 Diagram for *in vivo* microdialysis sampling from a freely moving mouse using off-line collection. After off-line dialysate collection is complete, the microdialysis samples are injected, separated using HPLC, and detected with an electrochemical detector.

Analytes in the dialysate must be separated and quantified to determine their *in vivo* concentrations; some of the most common methods of separation include capillary electrophoresis and HPLC (*55*). The separation can be directly connected to the microdialysis set up (on-line) or samples can be collected and analyzed later (off-line). During on-line analysis of dialysate, problems such as sample degradation and handling sub-microliter volumes are reduced (*105*). However, on-line analysis requires complex miniaturization and expensive instrumentation for accurate control of the small volumes. These limitations have made off-line analysis to be the method of choice, where injections are made manually (*8, 59, 83, 84, 107, 108*). In our lab, off-line separation of DA and its metabolites is done using HPLC.

1.2.5.1 Electrochemical detection

An advantage of using microdialysis is that the separation method can easily be coupled to a wide variety of detection techniques such as electrochemical, enzymatic assays, mass spectrometry (MS), or fluorescence (*55, 59, 109, 110*). As stated above, the monoamine neurotransmitter family, which includes DA, DA catabolites (DOPAC and HVA), serotonin, and norepinephrine are electroactive. After separation, detection and quantification of these analytes is typically achieved using electrochemical detection. There are numerous electrochemical detectors commercially available, each with their own inherent advantages and disadvantages. The two most widely used methods to make electrochemical measurements are amperometry and coulometry. These techniques utilize the fact that catecholamines are readily oxidized at potentials that do not oxidize many of the other species in the cerebrospinal fluid. In amperometric cells, a small fraction (< 10%) of the analytes are oxidized (or reduced) at the surface of

the working electrode (*11*). Amperometric cell design requires the HPLC eluent to be perpendicular to the surface of the working electrode, hence approximately only 10% of the analyte reaches the surface and is oxidized. In coulometry, 100% of the analyte is oxidized or reduced by the working electrode surface (*11, 81, 84*). This nearly complete redox of an analyte of interest can be achieved with coulometric detection because the mobile phase is passed directly through the vitreous carbon electrode. Conversion of all of the analyte during coulometric detection does not always imply better detection because the increased background current reduces the signal-to-noise ratio (S/N). In many cases amperometric and coulometric cells provide similar S/N. However, an amperometric electrode is easy to polish and regenerate a 'like new' surface; unlike the flow-through porous carbon electrode (coulometric) where electrode fouling often makes re-using the electrode nearly impossible (*111*). The most desirable figures of merit for these electrochemical detectors are low detection limits, high sensitivity, and selectivity when desired (*11, 81, 111*).

One of the most common methods for detecting analytes from a dialysate sample is using HPLC connected to electrochemical detection as it provides better chemical selectivity compared to electrochemical methods alone (e.g. FSCV). The eluent from HPLC separation is directly monitored for electroactive analytes from the dialysate. Commercially available electrodes typically use a three-electrode system consisting of a working electrode, reference electrode, and auxiliary electrode. A known potential difference is applied to the working electrode relative to the reference electrode and the resulting current is recorded at the working electrode. The electric charge (current) measured is proportional to the analyte concentration (Equation 1).

1.3 Research objectives

The overarching research objective of this thesis is to understand *if and how* BDNF modulates the DA system in the striatum, a brain region that is associated with Parkinson's disease, drug addiction, and ADHD (*46, 54, 112-115*).

1.3.1 Overall Hypothesis: Vulnerability to neurological diseases is a complex interplay between genetics and environment. Recent evidence suggests that alterations in the expression and function of BDNF protein may not only regulate DA dynamics, but also play a critical role in susceptibility to neurological disease (*42, 46, 53, 54, 112, 115-117*). We hypothesize that life-long reduction in BDNF levels may lead to a hyperdopaminergic system, which may increase one's risk factor for developing Parkinson's disease, drug addiction, or ADHD. As a result of a hyperdopaminergic system, we predicted decreases in DA release, DA uptake, and DA D2 and D3 autoreceptor functions in mice lacking one copy of the BDNF gene ($BDNF^{+/-}$) compared to wildtype mice. To understand the long-term consequences of low endogenous BDNF levels on DA dynamics, aged (~ 18 months old) $BDNF^{+/-}$ and wildtype mice were evaluated to determine if the combination of low endogenous BDNF levels and a hyperdopaminergic phenotype lead to an increased susceptibility towards neurodegenerative diseases like Parkinson's disease. We hypothesize that a constitutive reduction in BDNF levels would lead to more severe impairments in the DA system of $BDNF^{+/-}$ mice as compared to their control wildtype littermates. We tested our overall hypothesis through four research objectives as outlined below.

1.3.2 Research objective 1: *Develop a voltammetric assay to characterize the functionality of DA D2 and D3 autoreceptors in the mouse striatum. Parts have been previously published in the manuscript by Francis K. Maina and Tiffany A. Mathews in ACS Chemical Neuroscience, 2010 (94).*

DA D2 and D3 autoreceptors are located on presynaptic terminals and are known to control the release and synthesis of DA. DA D3 receptors have a fairly restricted pattern of expression in the mammalian brain. Their localization in the NAc core and shell is of particular interest because of their association with the rewarding properties of drugs of abuse. Current tools to evaluate DA D2 and D3 receptor function include microdialysis, autoradiography, voltammetry, and magnetic resonance imaging (MRI) (*118-123*). FSCV has been used extensively to characterize the DA D2 receptor functionality throughout the striatum. However, its use to characterize the DA D3 receptor has been limited (*14, 70, 71, 76, 124-126*). Using background subtracted FSCV, our goal was to investigate the effects of DA D2 and D3 agonists on electrically stimulated DA release and uptake rates in the mouse CPu and NAc core and shell. We hypothesized that, due to the differential expression of DA D2-like receptors in the striatum, FSCV will be able to distinguish the functionality between DA D2- and D3-receptors agonists. To our knowledge, this was the first time that the functionality of DA D2 and D3 autoreceptors was compared across the different regions of interest; CPu, NAc core, and NAc shell in the striatum using FSCV.

1.3.3 Research objective 2: *To determine if low endogenous neuronal BDNF levels influence the dopaminergic system using wildtype and BDNF $^{+/-}$ mutant mice*

The long-term objective of the Mathews' laboratory[1] is to use BDNF$^{+/-}$ mice as an animal model in two discrete disease models: alcoholism and aging. However, before using the BDNF$^{+/-}$ mice in behavioral protocols, it is necessary to understand if BDNF has the ability to influence DA dynamics in these mice. For example, with respect to the serotonin system, *in vivo* microdialysis studies have revealed that in the hippocampus, BDNF$^{+/-}$ mice have increased basal extracellular serotonin levels and decreased serotonin uptake compared to their wildtype littermate controls (*127*). There has been considerable interest in the serotonin-BDNF relationship due to the hypothesized dual role in the effectiveness of anti-depressants (*29, 128*). Despite the fact that BDNF levels regulate the expression of the DA D3 receptor, few studies have investigated whether BDNF levels influence other facets of DA dynamics (*36*). To understand the role of endogenous BDNF on the dopaminergic system *in vivo*, BDNF$^{+/-}$ mice were evaluated using a variety of neurochemical techniques including *in vivo* microdialysis and slice FSCV. Low BDNF levels in BDNF$^{+/-}$ mice are hypothesized to lead to a poorly developed dopaminergic system (*35*). *In vivo* microdialysis was used to determine extracellular levels of DA and its catabolites. This was to provide information on the overall tone of the DA system. FSCV was used to measure DA release and uptake dynamics more discretely. An advantage of using FSCV to evaluate the dopaminergic system is that it provides an opportunity to probe DA release, DA uptake, DA

[1] Since the goal of the Mathews' laboratory is to understand the biological role of BDNF *in vivo*, to strengthen and support our hypothesis from my voltammetric results on the *in vivo* role of BDNF some of the results in the following chapters show collaborative work from other Mathews' laboratory group members. The roles of each can be found in the contribution section of this dissertation as well as in the individual chapters.

autoreceptor functionality, and the ability of exogenous BDNF to influence DA release and uptake. We hypothesized that an impaired DA system due to low BDNF levels would lead to attenuated presynaptic DA dynamics of release and uptake.

1.3.4 Research objective 3*: Do lifelong BDNF reductions negatively influence striatal dopamine dynamics?*[2]

Results from research objective 2 indicated that $BDNF^{+/-}$ mice have a 2.5-fold increase in basal extracellular DA levels as compared to their wildtype littermates at 3 months of age. A leading hypothesis in neurodegenerative diseases is that too much DA could be neurotoxic because is easily oxidized by reactive oxygen species (*129-131*). Aged $BDNF^{+/-}$ mice (9 to 21 months) exhibit reduced locomotor activity as compared to their wildtype littermates (*34, 132*). Often locomotor activity measurements are an indirect way to assess the function of the DA system. Furthermore, the Dluzen laboratory has suggested that low BDNF levels are associated with an attenuation in nigrostriatal DA system function, which would agree with locomotor activity results in aged $BDNF^{+/-}$ mice (*35*). To understand if lifelong decrements in BDNF levels negatively influence the nigrostriatal pathway, mice deficient in BDNF were evaluated at 3 (see above *research objective #2)* and ~ 18 months of age and compared to their littermate controls. Because young $BDNF^{+/-}$ mice have reduced BDNF levels and elevated DA levels, our working hypothesis was that these mice are more susceptible to age-related changes in the striatum versus wildtype mice. Similar to research objective #2,

[2] The objective consists of collaborative work from Kelly Bosse Ph.D. and Johnna A. Birbeck who performed *in vivo* microdialysis experiments to complement the slice voltammetry experiments. For the specific and detailed roles of each please see the contribution section of this dissertation as well as chapter 5.

neurochemical techniques including slice FSCV and *in vivo* microdialysis were used to evaluate striatal DA dynamics.

1.3.5 Research objective 4: *How do low endogenous BDNF levels influence the function of the dopamine transporter?*[3]

One commonality between all drugs of abuse such as methamphetamine, cocaine, and alcohol is their ability to elevate terminal extracellular DA levels, although through different mechanisms. Specifically, methamphetamine increases extracellular concentrations of DA mainly by competitively inhibiting DA uptake at the DA transporter. Our studies from *Research Objective #2* suggest that DA uptake is reduced in $BDNF^{+/-}$ mice. Additionally, autoradiographic studies have shown that DA transporter density in $BDNF^{+/-}$ does not differ from that of wildtype mice (*37, 133*). Furthermore, when BDNF-deficient mice were exposed to a neurotoxic dose of methamphetamine, they were found to be less susceptible to methamphetamine-induced neurotoxicity in the nigrostriatal dopaminergic system as compared to wildtype mice (*35, 134*). Taken together, these results suggest that DA transporter function is impaired or reduced in the CPu of $BDNF^{+/-}$ mice.

To understand how low endogenous neuronal BDNF levels influence DA transporter function, the effect of methamphetamine on the DA transporter was evaluated in both wildtype and $BDNF^{+/-}$ mice at two discrete time points using slice FSCV and *in vivo* microdialysis. We hypothesized that the reduced DA clearance

[3] The objective includes collaborative work from Kelly E. Bosse Ph.D. and Johnna A. Birbeck who performed *in vivo* microdialysis experiments to determine the role of BDNF deficiency on DA transporter function *in vivo*. The microdialysis results complement the slice (*in vitro*) voltammetry results, overall providing a better understanding on the role of BDNF. For the detailed roles of each please see the contribution section of this dissertation as well as chapter 6.

observed in the CPu of young BDNF-deficient mice is a result of reduced DA transporter function and aging would further impair it.

CHAPTER 2

Materials and Methods

The objective of this chapter is to describe experimental protocols that are common to all chapters in this dissertation. Any variations or changes in these protocols are directly addressed in the relevant chapter.

2.1 Animals

Mice having only one active brain-derived neurotrophic factor (BDNF) gene ($BDNF^{+/-}$) on a C57Bl/6 genetic background and wildtype C57Bl/6 mice were obtained from Jackson Laboratory (Bar Harbor, ME) at 3 – 5 weeks old. Male and female breeders were then paired and housed in the animal care facilities at Wayne State University. BDNF wildtype (will be referred to as wildtype) and $BDNF^{+/-}$ mice offspring were bred and raised in house. Genotype identification was performed using polymerase chain reaction (PCR) analysis of tail DNA (Section 2.2). The mice were kept in groups of 3 – 5 animals per cage with food and water *ad libitum* on a 12 hr light-dark cycle. All procedures were designed to minimize discomfort to the animals. Experiments were conducted during the light cycle (0600 – 1800 h) with young adult mice aged 3 – 4 months or at least 18 months for studies in aged mice. Experimental protocols adhered to the National Institutes of Health Animal Care Guidelines and were approved by the Wayne State University Institutional Animal Care and Use Committee.

2.2 Genotyping

Breeding, weaning, and genotypic analysis were performed and overseen by Kelly E. Bosse, Ph.D. and Brooke Newman with the assistance from Johnna Birbeck, Parvejz Khan, Natasha Bohin, Andrezj Czaja, Katie Logan, and Christopher Rogalla.

Immediately after mice were weaned, genomic DNA was obtained from tail tissue (~ 0.3 – 0.5 cm) and frozen (-80℃) until needed. T ails were lysed in 500 µL of lysis buffer (100 mM Tris-base, 1.5 mM NaCl, 5 mM EDTA, 0.2% sodium dodecyl sulfate; pH 8.5) containing 0.1 mg/mL proteinase K (New England BioLabs, Ipswich, MA). Tail lysis was completed within 15 hours at 55℃, with agitation. Tail lysis samples were centrifuged (Eppendorf, Hauppauge, NY) for 32 minutes at high speed (20,000 x g) to remove tissue and cellular debris. Isopropyl alcohol (500 µL) was added to the supernatant to extract genomic DNA followed by centrifugation at 20,000 x g for 16 minutes. A DNA pellet at the bottom of the vial was retained and washed by adding 500 µL of 75% ethanol (v/v) followed by centrifugation for 5 minutes at 20,000 x g. The supernatant was carefully removed and discarded, leaving the DNA pellet. Nanopure water (6 µL) was added to the DNA pellet and placed in a desiccator with the cap open. The genomic DNA was re-suspended in 85 µL TE buffer (10 mM Tris-base and 1 mM EDTA at pH 8.5) followed by centrifugation for 30 seconds at 20,000 x g. Samples were then stored at 4℃ for at least 24 hours before use.

An approximation of how much DNA present was determined by measuring ultraviolet (UV) light absorbance at 260 nm (UV-1800 Shimadzu (Shimadzu, Columbia, MD)). DNA was diluted to a final concentration of 350 ng/mL, from which 2 µL was added to PCR reagents. Wildtype and BDNF mutant targeted alleles were separately amplified using the following primers: wildtype: 5’-CCAGCAGAAAGAGTAGAGGAG-3’; BDNF mutant: 5’-GGGAACTTCCTGACTAGGGG-3’; and common: 5’-ATGAAAGAAGTAAACGTCCAC-3’ as specified by Jackson Laboratories. The PCR reagent (22.8 µL) contained 0.096 mM of each deoxyribonucleotide triphosphate

(dNTP's: dATP, dCTP, dGTP, dTTP), 1.28 mM $MgCl_2$, 1 µM of one of the primers, and 1.2 µL PCR buffer A (10 mM Tris–HCl, 1.5 mM $MgCl_2$, 50 mM KCl; pH 9.0) in 15.9 µL nanopure water. Then, 0.2 µL *Taq* DNA polymerase (1 unit) was added to each sample. PCR was performed using a thermocycler (Robocycler® gradient 96, Stratagene (Agilent), Santa Clara, CA). The cycling conditions were: 94℃ (melting) for 5 minutes, 58℃ (annealing) for 1 minute, 72℃ (extension) for 2 minutes, followed by 35 cycles at 95℃ for 1 minute, 58℃ for 1 minute, and 72℃ for 2 minutes. PCR reaction products were then separated on 2% agarose gels (6 µL:lane) in TBE buffer (89 mM Tris–base; 89 mM boric acid; 1 mM EDTA; 1 mM NaOH, pH 8.0) at 125 – 135 V and visualized using ethidium bromide. Wildtype mice were identified from genomic DNA that yields only one band for the active BDNF gene in the first column. The $BDNF^{+/-}$ mice were identified from two separate bands; the first band identifies genomic DNA for the active BDNF gene, while the second band identifies the inactive BDNF gene (Figure 2.1). The BDNF gene is inactivated by insertion of a neomycin (NEO) resistant cassette, and has a higher molecular weight compared to the active BDNF gene and travels less during gel electrophoresis (Figure 2.1).

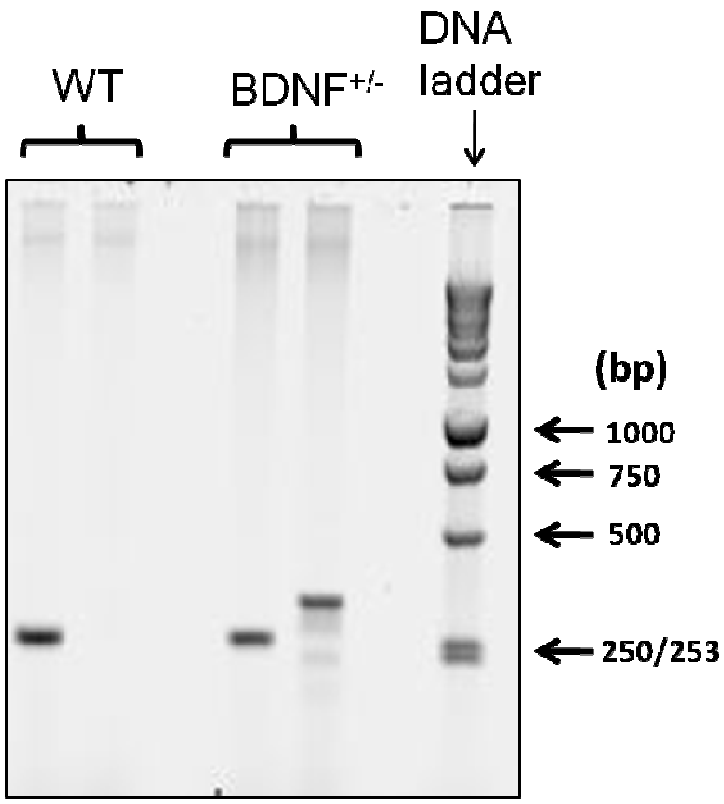

Figure 2.1 Representative gel electrophoresis image of wildtype (WT) and BDNF$^{+/-}$ mice. Five lanes are shown; the first 2 lanes illustrate genotype identification of a WT mouse, while the second 2 lanes highlight genotype identification of a BDNF$^{+/-}$ mouse, with the final lane showing the base pair (bp) ladder. A mouse is identified as a wildtype mouse when only the first lane exhibits one band (275 bp) and there is no band present in the second lane. A mouse is identified as a BDNF$^{+/-}$ mouse when both lanes exhibit a band. Similar to the wildtype mice the band for the WT BDNF gene is present in the first column, and the second lane determines the presence of mutant BDNF (340 bp), which is only present in BDNF$^{+/-}$ mice. *Image courtesy of Brooke Newman.*

2.3 Brain slices

Mice were anesthetized with CO_2 and the brain was rapidly removed and cooled in a pre-oxygenated (95% O_2 / 5% CO_2) high sucrose-artificial cerebrospinal fluid (aCSF) buffer for 10 minutes. The sucrose-aCSF buffer consisted of: 180 mM sucrose, 30 mM NaCl, 4.5 mM KCl, 1 mM $MgCl_2$, 26 mM $NaHCO_3$, 1.2 mM NaH_2PO_4, and 10 mM D-glucose (*135*). The brain was sectioned with a vibrating tissue slicer (Vibratome, St. Louis, MO) into 400-µm-thick coronal slices. Brain slices containing dopamine (DA) rich regions of interest such as the caudate putamen (CPu) and nucleus accumbens (NAc) were obtained. Slices were maintained in oxygenated aCSF at room temperature for 1 hour before use. A slice was transferred to a custom made submersion recording chamber (Custom Scientific, Denver, CO) and allowed to equilibrate in oxygenated aCSF at 32℃ for 30 minutes before DA measurements we re performed.

2.4 Fast scan cyclic voltammetry

2.4.1 Microelectrode fabrication

Carbon fiber microelectrodes were fabricated in house using a previously described method with minor modifications (*58*). First, a 7 µm diameter carbon fiber (Goodfellow, Oakdale, PA) was aspirated through a borosilicate glass capillary (A-M Systems, Carlsborg, WA) using vacuum suction. The capillary containing the carbon fiber was heated and pulled using a micropipette puller (Narishige, Tokyo, Japan) to generate two microelectrodes with a tight glass seal around the carbon fiber. The exposed carbon fiber was trimmed to a length of 50 – 200 µm beyond the glass carbon fiber seal (Figure 2.2).

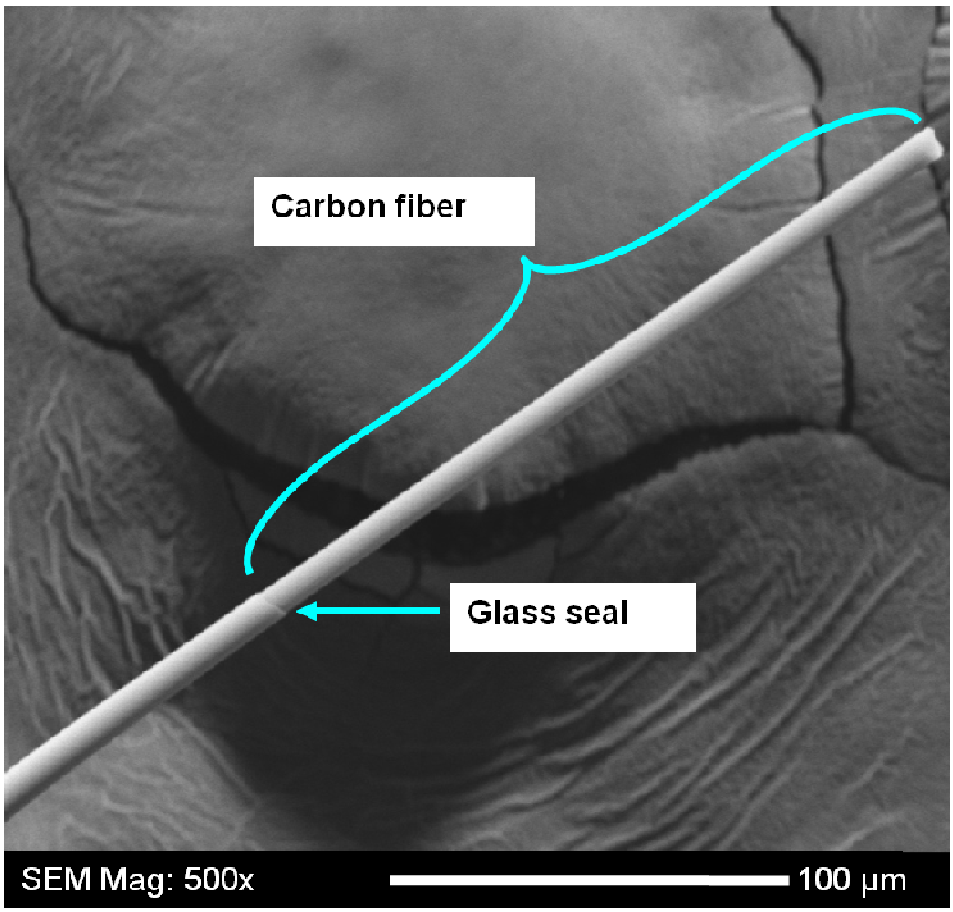

Figure 2.2 Representative scanning electron microscope image showing a microelectrode at 500x magnification (acceleration voltage, 25 kV). The length of the carbon fiber that extends beyond the glass seal is ~ 190 µm.

The microelectrode was then backfilled with 150 mM KCl and a lead wire (Squires Electronics, Cornelius, OR) was inserted to make an electrical connection with the carbon fiber. The silver/silver chloride (Ag/AgCl) reference electrode was made from a 250 µm diameter silver wire (A-M Systems, Carlsborg, WA). The silver wire was coated with a thin layer of silver chloride by anodizing at (+1 V) in a solution of 1 M HCl for 5 – 10 minutes. A two electrode configuration with a working carbon fiber microelectrode and Ag/AgCl reference electrode was used to determine DA release and uptake rates in the CPu and NAc.

2.4.2 Stimulator calibration

To detect DA from a brain slice, an additional electrode known as the stimulating electrode was placed on top of the brain slice to apply an electrical current, inducing DA release from surrounding neurons. To ensure consistent stimulating current output, the stimulator was calibrated. Previously, John *et al.* described the stimulation parameters to evoke DA release from the mouse striatum (includes CPu and NAc). The optimal current to be supplied to the stimulating electrode was determined to be 350 µA (*62, 136*). In order to determine the voltage that would provide a 350 µA current, a Neurolog® stimulator (Digitmeter, Hertfordshire, England) was calibrated. Using National Instruments Labview™ software (Austin, TX), the voltage output to the stimulator was varied from 2.5 – 5.75 V and the resulting current measured using a digital multimeter MTI-058 (Megatone Electronics, Taipei, Taiwan). Interpolation of a linear plot of current versus voltage was used determine that the voltage needed to generate a current of 350 µA was 4.5 V (Figure 2.3).

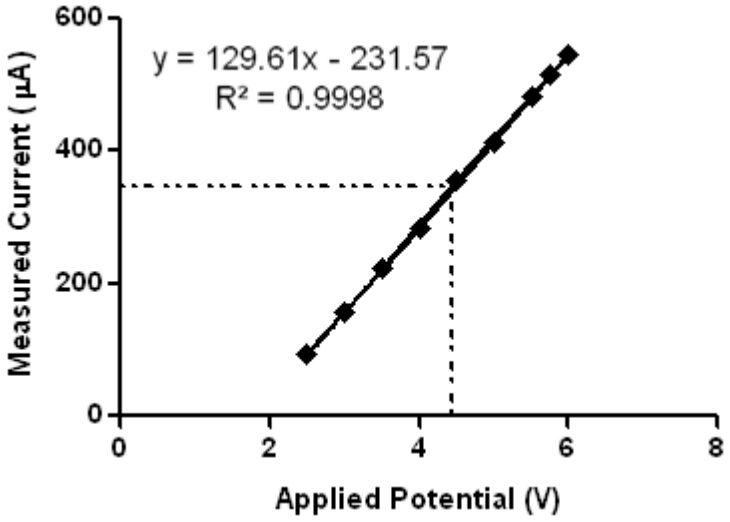

Figure 2.3 Calibration plot for the Neurolog® stimulator. The dashed line indicates the optimal applied potential voltage of 4.5 V to obtain the desired current of 350 µA.

2.4.3 Data acquisition

The potential at a carbon fiber microelectrode was held at -0.4 V versus the reference electrode, ramped to +1.2 V and back to -0.4 V (400 V/s) every 100 ms (10 Hz) (*62, 71, 73, 74, 92, 137*). All electrode and stimulation parameters were controlled by TH software (ESA Inc., Chelmsford, MA). The data collection system uses two peripheral component interconnections (PCI) 6221 boards manufactured by National Instruments (Austin, TX). The main board has an analog to digital converter (ADC) and a digital to analog converter (DAC) (Figure 2.4). This main board is responsible for generating the waveform input, as well as recording the current difference at the microelectrode. The second board contains a DAC output that stimulates when triggered. When the triangle waveform is applied, a stable background current is produced before DA is released. This background is digitally subtracted from the voltammograms following DA stimulation (*89*). Characteristic background subtracted voltammograms for DA demonstrate peak oxidation currents for DA at approximately +0.6 V and the peak reduction currents for DA-ortho-quinone at approximately -0.2 V. A low-noise ChemClamp potentiostat (Dagan Corporations, Minneapolis, MN) was used for FSCV measurements. The slice chamber was perfused at 1 mL/min with 32°C oxygenated aCSF. DA was evoked every 5 minutes by either one (monophasic, 350 µA, and 4 ms pulse width) or multiple pulse stimulation from the adjacent stimulating tungsten electrodes (Plastics One, Roande, VA) generated from the Neurolog® stimulator. The stimulating electrode was placed directly on the slice, approximately 100 – 200 µm away from the carbon fiber electrode (*62, 74*). The microelectrode was placed approximately 75 µm below the surface of the slice.

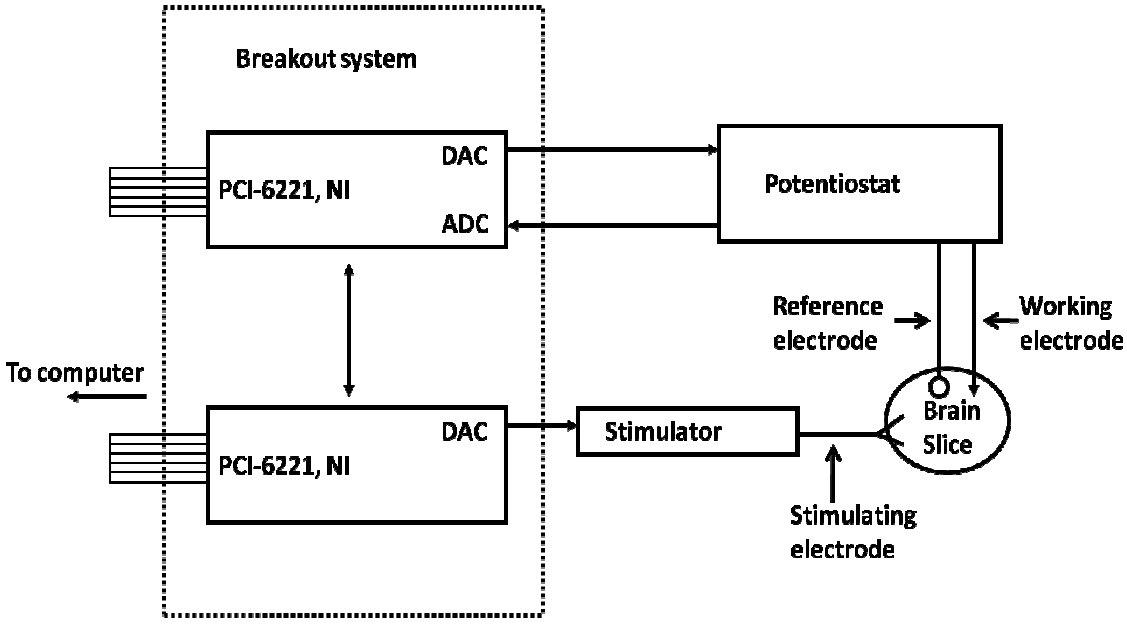

Figure 2.4 Schematic diagram showing the experimental set up for fast scan cyclic voltammetry measurements. National Instruments (NI) peripheral component interconnections (PCI) 6221 boards link the computer to the potentiostat, and convert signal from analog to digital converter (ADC) or digital to analog converter (DAC) during the measurements.

2.4.4 Microelectrode post-calibration

Flow injection analysis (FIA) was used to determine the electrode response to the 3 µM concentration of DA at the end of the experiment. The microelectrode was placed in a stream of calibration buffer (Figure 1.8), which was a modified artificial cerebrospinal fluid (aCSF) solution consisting of (in mM): NaCl (126), KCl (2.5), NaH_2PO_4 (1.2), $CaCl_2$ (2.4), $MgCl_2$ (1.2), and $NaHCO_3$ (25); pH 7.4. The modified aCSF was pumped continuously at a flow rate 2 mL/min using a syringe pump through a T-shaped flow cell. The second syringe contained a known concentration of DA (3 µM), which was manually injected. The electrode measures the amount of current generated from the oxidation of the known concentration of DA. The calibration factor for the electrode was defined as the amount of current per micromolar concentration (nA/µM). Implanting electrodes in brain tissue decreases the sensitivity of the electrode, resulting in a decreased response time. Every effort was made to obtain a post-calibration factor for each electrode to determine the sensitivity.

2.4.5 Data analysis

The resulting current versus time plots obtained were fitted by nonlinear regression as described by Jones *et al.* in software written in Labview™ (National Instruments, Austin, TX) (*62, 68, 138*). The electrically stimulated DA release and uptake rates were determined using a set of Michaelis-Menten based equations (Equation 3) (*62, 68, 90, 138*).

$$\frac{d[\mathrm{DA}]}{dt} = f[\mathrm{DA}]_p \quad \frac{V_{max}}{(K_m/[\mathrm{DA}]+1)} \qquad \textbf{(3)}$$

The apparent K_m is a constant, which correlates the affinity of DA to DA transporter and was set during the analysis of stimulated [DA] and maximal uptake rates as maximum velocity (V_{max}). The K_m value (0.16 µM) used in all data analysis was obtained from the literature (*62, 68, 139, 140*). Stimulated DA release per pulse ($[DA]_p$) at a given stimulation frequency *f* and maximal uptake rates (V_{max}) were then evaluated. It is assumed that each stimulation pulse evokes a constant amount of DA and uptake of DA by DA transporter is a saturable process (*62, 68, 71*). The rise in electrically stimulated DA signal after electrical stimulation is a competition between release and uptake, where release mechanisms dominate. On the other hand, the decay phase of the electrically stimulated DA is attributed to diffusion, enzymatic breakdown of DA, and DA uptake (*77, 141*). However, diffusion and enzymatic breakdown of DA are considered 'slow' events when using FSCV, and therefore the decay phase is primarily attributed to uptake (*77, 141*).

2.5 *In vivo* microdialysis

Stereotaxic surgery and all *in vivo* microdialysis experiments were performed by *Kelly Bosse, Ph.D.* or *Johnna Birbeck* as previously described (*142*). Briefly, young adult mice aged 8 – 16 weeks were anesthetized with an intraperitoneal (i.p.) injection of Avertin (20 mL/kg). Shaving and sterilization of the skin covering the skull was done with two applications of Betadine and alcohol. To limit discomfort, mice were placed on a heating pad (~ 37℃) and lidocaine (0.5 mg/kg) was su bcutaneously injected near the surgical site. After ensuring surgical plane anesthesia, a small incision was made to expose the skull and the area was cleaned and dehydrated using 10% hydrogen peroxide. The head was secured on a Kopf® stereotaxic frame (David Kopf Instruments,

Tujunga, CA) using two ear bars that do not puncture the tympanic membrane. Two small holes were drilled into the skull for the probe placement and a support screw. The CPu coordinates (in mm: Anterior (A), +0.80; Lateral (L), -1.3; Ventral (V) -2.5 from Bregma) were determined from Paxinos and Franklin mouse atlas (*9*). A CMA/7 guide cannula (CMA Microdialysis, Chelmsford, MA) was implanted in the CPu and anchored to the skull with dental cement and a screw (BAS, Lafayette, IN). The microdialysis probe (CMA/7, 2 mm length, 240 µm diameter, Cuprophane, 6 kDa cut-off; CMA Microdialysis, Chelmsford, MA) was inserted into the guide cannula upon mouse recovery. Artificial CSF (composition in mM: 147 NaCl, 3.5 KCl, 2 Na_2HPO_4, 1.0 $CaCl_2$, 1.2 $MgCl_2$; pH 7.4) was perfused through the probe overnight at a flow rate of 0.4 µL/min. After approximately 12 hours, the flow rate was increased to 1.1 µL/min for an hour of equilibration. Afterwards, dialysate samples containing DA and other small molecules were collected offline from freely moving mice at 20 minutes intervals.

Zero net flux is a quantitative microdialysis technique that allows for estimation of basal extracellular concentration of analyte in a tissue. The x-intercept of the zero net flux regression line gives an estimate of the “true” extracellular concentration of the analyte that is corrected for the probe recovery (*103, 143*). The technique also approximates relative “*in vivo*” probe recovery using extraction fraction (E_d) values, determined from the slopes of the zero net flux regression lines (*143*). The E_d, also referred to as extraction efficiency, is a measure of diffusion between the effluent dialysate and the analyte concentration in the extracellular space of the tissue surrounding the probe (*79*). To determine the “true” basal extracellular DA concentration in freely behaving mice, an infusion pump (CMA/402) was used to perfuse a known

amount of DA (0, 5, 10, or 20 nM in aCSF) through the microdialysis probe, where each concentration was delivered to the CPu for 90 minutes (*83, 103, 144*). The dialysate was analyzed using HPLC coupled to an electrochemical detector as described in Section 2.6.

A high K^+ concentration in aCSF depolarizes neurons, inducing exocytotic release of neurotransmitters like DA and subsequently elevating extracellular levels. First three stable baseline samples were collected, then the aCSF was switched to a solution containing high K^+ (composition in mM: 120 KCl, 30.5 NaCl, 2.0 Na_2HPO_4, 1.2 $MgCl_2$, 1.0 mM $CaCl_2$; pH 7.4), which was infused through the microdialysis probe for 20 minutes (*83*). After the 20 minute perfusion with high K^+ aCSF, the perfusate was switched back to standard aCSF solution.

2.6 High performance liquid chromatography (HPLC) and electrochemical detection

Kelly E. Bosse, Ph.D. and Johnna A. Birbeck performed all HPLC analysis, which included HPLC separation with electrochemical detection and data analysis.

DA and its catabolites, 3,4-dihydroxyphenylacetic acid (DOPAC) and homovanillic acid (HVA) levels from dialysate samples were separated and quantified using HPLC coupled to an electrochemical detector. Dialysis samples (20 µL) were manually injected onto a C_{18} (2)-HST HPLC column (100 mm x 3 mm, 2.5 µm particle size) (Phenomenex, Torrance, CA) for separation followed by detection using an ESA 5014B microdialysis cell (E_1 = -150 mV; E_2 = +220 mV; ESA Coulochem III (ESA Inc., Chelmsford, MA). An ESA 5020 guard cell (ESA Inc., Chelmsford, MA) was placed in-line before the injection loop and set at +350 mV potential. The mobile phase

composition was: 75 mM NaH_2PO_4, 1.4 – 1.8 mM 1-octanesulfonic acid, 0.025 mM EDTA, 10% acetonitrile, and 0.002% triethylamine; pH = 3.0, adjusted with 85% phosphoric acid, delivered at a flow rate of 0.4 mL/min by an isocratic LC-20AD pump (Shimadzu, Columbia, MD). DOPAC, DA, and HVA retention times were ~ 5, 6, and 12.5 minutes, respectively. Analyte peak area was integrated and quantified against known standards using LC Solutions Software (Shimadzu, Columbia, MD). After microdialysis experiments, mice were euthanized by CO_2 inhalation and their brains were rapidly removed for histological verification of probe placement in the CPu.

2.7 L-DOPA tissue content

Tissue content studies for the analysis of L-DOPA content were performed by Kelly E. Bosse, Ph.D. assisted by Joseph Roberts. The tissue content studies involved collection of the tissue samples, analysis that included HPLC separation with electrochemical detection, and data analysis.

The activity of tyrosine hydroxylase (TH), the rate-limiting enzyme in DA biosynthesis, was evaluated by measuring L-3,4-dihydroxyphenylalanine (L-DOPA) accumulation in brain tissue samples. Briefly, the L-aromatic amino acid decarboxylase (AADC) enzyme was inhibited with 3-hydrazineomethyl phenol dihydrochloride (NSD-1015) and γ-butyrolactone (GBL) was used to minimize autoreceptor feedback effects during the regulation of DA biosynthesis (*145*). Mice were injected with GBL (750 mg/kg, i.p.) and 5 minutes later with NSD-1015 (100 mg/kg, i.p.). Mice were first sacrificed 40 minutes after NSD-1015 injection and the brain was rapidly removed. The CPu was then rapidly dissected and frozen in liquid nitrogen. Brain tissue samples were stored at -80℃ until time of analysis. To measure L-DO PA tissue accumulation,

samples were weighed and homogenized in 0.1 M $HClO_4$ using an Microson™ ultrasonic cell disruptor (Qsonica, Newtown, CT) and centrifuged for 10 minutes at 9000 x g. L-DOPA was quantified from the resulting supernatant using HPLC separation with a Luna C_{18} reverse phase column (50 x 2 mm, 3 µm particle size) (Phenomenex) and electrochemical detection was achieved with an ESA 5011A analytical cell (E_1 = -150 mV, E_2 = +200 mV) and Coulochem III detector (ESA Inc.). The mobile phase was composed of 1 mM EDTA, 2.4 mM sodium octanesulfonate, 7.8 mM chloroacetic acid, 10 mM NaH_2PO_4, 80 mM citric acid, and 3% acetonitrile; pH 3 and delivered by LC-20 AD isocratic pump at a flow rate of 0.4 mL/min. L-DOPA peak area was integrated and quantified against known standards using LC Solutions Software.

2.8 Chemicals

Components of the mobile phase, buffers, genotyping reagents, NSD-1015, GBL, Avertin, standards (DA, DOPAC, L-DOPA, and HVA) were either of HPLC grade or the highest purity available and purchased from Sigma-Aldrich (St. Louis, MO) and Fisher Scientific (Pittsburgh, PA). Concentrated HNO_3, $HClO_4$, boric acid, triethylamine, agarose PCR plus, and citric acid were obtained from EMD (Gibbstown, NJ). Primers, $MgCl_2$, and dNTP's were obtained from Invitrogen (Carlsbad, California).

2.9 Statistical data analysis

Statistical analysis and graphing of the microdialysis results was performed by Kelly E. Bosse, Ph.D. or Johnna A. Birbeck.

Briefly, all statistical analyses were carried out using GraphPad Prism (GraphPad Software Inc., San Diego, CA). Data are shown as means ± standard errors of the means (SEMs). When a comparison between two means was required, these data were

analyzed by Student's t-tests. When three or more means needed to be compared, these results were analyzed by a one-way analysis of variance (ANOVA) with the appropriate post-hoc tests. When the mean's interaction needed to be assessed between two independent variables like genotype and treatment, a two-way ANOVA was performed. In all cases, statistical significance was defined as $P < 0.05$.

CHAPTER 3

Functional Fast Scan Cyclic Voltammetry Assay to Characterize Dopamine D2 and D3 Autoreceptors

(Adapted from Maina and Mathews (2010) *ACS Chemical Neuroscience* 1, 450-462)

(Copyright License Number: 2633741370556)

3.1 Introduction

Dopaminergic histological and neurochemical studies demonstrate regional differences within the striatum, which can be further subdivided into three distinct anatomical regions (the caudate-putamen (CPu), the nucleus accumbens (NAc) core, and the NAc shell) (*93, 146, 147*). Dopamine (DA) cell bodies, which innervate the NAc and the CPu, arise from two distinct areas in the midbrain, the ventral tegmental area (VTA) and the substantia nigra (SN), respectively (*2*). A variety of neurochemical studies have demonstrated differences in DA levels between these regions. For example, the CPu is known to have higher extracellular DA levels and greater DA uptake as compared to the NAc (*90, 96, 148, 149*). Within the NAc, the core is known to exhibit greater electrically evoked DA release and uptake than the shell (*150*). *In vivo* microdialysis data also confirm that extracellular DA levels are greater in the core than the shell (*78, 151*). However, it is not clear whether these observations are solely due to the reduced expression of the DA transporter from the dorsal to ventral striatum, or if they are impacted by varied expression levels of DA autoreceptors.

Stimulation of D2 receptors on presynaptic terminals results in feedback inhibition, reducing extracellular levels of DA via regulation of DA synthesis and release (*19, 20*). Additionally, there is evidence that implies the DA D3 receptor also regulates

DA release in terminal regions such as the NAc (*108, 152, 153*). Importantly, the anatomical distribution of the D2 and D3 receptors is very distinct. Specifically, the D3 receptor shows localization in the mesolimbic pathway, including the NAc, Islands of Calleja, and olfactory tubercles (*20, 154, 155*). The highest levels of this receptor in the striatum appear to occur in the NAc shell, not the core (*36, 156*). In contrast, evidence suggests that the DA D2 receptors are more homogeneously distributed throughout the striatum (*157, 158*).

There is intense interest in characterizing the functional effects of DA D2 and D3 agonists because of their potential therapeutic involvement in diseases such as schizophrenia and Parkinson's. However, a major problem with characterizing these agonists is their lack of selectivity for a given receptor. The development of D2 and D3 receptor knockout animals has facilitated the characterization and classification of D2 and D3 receptor agonists. Both microdialysis and voltammetric techniques have been used to examine D2-like agonists in D2 and D3-receptor knockout mice (*70, 80, 123, 125, 159*). However, conflicting neurochemical results obtained in these experiments, which used D2 or D3 knockout mice, highlight a concern with respect to using knockout mice: lifelong constitutive reduction could easily alter other facets of the DA system, which may make it more difficult to characterize selective D2-like agonist as either D2 or D3 specific (*123, 159*). Therefore, it is critical to develop new strategies to better identify the functional properties of potential D2 and D3 agonists.

Current tools to evaluate DA D2 and D3 presynaptic receptor function include microdialysis, voltammetry, and magnetic resonance imaging (MRI) (*67, 71, 80, 118*). Typically, microdialysis is used in neurochemical studies because of its ability to sample

numerous neurotransmitters and provides greater sensitivity of these baseline levels. However, the limitation with using microdialysis to characterize DA autoreceptor function is its poor temporal resolution and inability to discriminate sub-anatomical brain regions such as the NAc core from shell, especially in mice. Recently, Chen *et al.* demonstrated that pharmacological MRI is a valuable tool for characterizing DA receptor function, because it is a non-invasive technique that allows for multiple, simultaneous measurements in a variety of brain regions and provides the ability to perform longitudinal studies (*118*). However, few labs have the expertise or MRI equipment to perform these studies. On the other hand, voltammetry has been used routinely *in vitro* and *in vivo* to characterize the functionality of DA receptors (*70, 71, 76, 82, 124-126, 160*). The advantages of using voltammetry are its' fast temporal resolution (100 ms), which allows for the measurements of both release and uptake in the presence of D2-like agonists, and the small size of the carbon fiber microelectrodes, which allows for sampling from discrete sub-anatomical regions such as the NAc core versus shell. Additionally, it is well established that D2-like agonists mediate DA release, and there is increasing evidence that D2 like autoreceptors may mediate DA uptake (*152, 161-166*). Thus, voltammetry is particularly useful to characterize both of these parameters that are influenced by DA agonists.

This study characterized the functional effects of DA D2 and D3 receptor agonists in the CPu, NAc core, and shell. Fast scan cyclic voltammetry (FSCV) with a carbon fiber microelectrode (~ 7 µm in diameter) was used, allowing for discrete anatomical detection of electrically stimulated DA. We have decided to use *in vitro* FSCV (slice FSCV) experiments to eliminate contributions from the DA cell bodies.

Commercially available D2, D3, or mixed D2/D3 agonists (e.g. quinpirole, 7-OH-DPAT, and (+)-PD 128907) were used to evaluate autoreceptor function (*70, 76, 124, 159, 160, 167*). The effect of B-HT 920 was also examined, because it is a reported DA D2 agonist, but with very limited use in voltammetry and microdialysis studies (*85*). Although there are many voltammetric studies that have examined autoreceptor functionality, to our knowledge this is the first reported study that examines anatomically distinct brain regions to characterize D2-like agonists as either selective D2 or D3 agonists, or mixed D2/D3 agonists (*70, 71, 76, 124-126, 160*). The results here suggest that the mode of action for DA agonists' functionality can be specifically assigned based upon their potency and efficacy within the discrete anatomical sub-regions. The utility of this functional voltammetric assay will assist future characterization of selective agonists that could be used as potential therapeutic agents.

3.2 Materials and methods

Male C57Bl/6 mice aged 8 – 16 weeks purchased from Jackson Laboratory were used. Coronal brain slices containing DA rich regions of interest such as CPu and NAc were prepared as described in Section 2.3. FSCV experiments to measure electrically-evoked DA release and uptake rates were performed as described in Section 2.4. Briefly, after at least 3 stable DA baseline recordings (≥ 30 minutes), 0.001 – 10 µM DA agonist solutions of (−)-quinpirole hydrochloride, (4aR,10bR)-3,4a,4,10b-tetrahydro-4-propyl-2H,5H-[1]benzopyrano-[4,3-b]-1,4-oxazin-9-ol hydrochloride ((+)-PD 128907), 5,6,7,8-Tetrahydro-6-(2-propen-1-yl)-4H-thiazolo[4,5-d]azepin-2-amine dihydrochloride (B-HT 920) or (±)-7-hydroxy-2-dipropylaminotetralin hydrobromide (7-OH-DPAT) were perfused over the slice for 30 minutes at a flow rate of 1 mL/min. The chemical

structures of the DA D2 and D3 agonists are shown in Figure 3.1. A cumulative dose response curve was chosen because John and Jones previously demonstrated that cumulative concentrations of drugs do not affect release or uptake as compared to applying only a single concentration of the drug (*62*). The effect of each drug concentration was recorded for 30 minutes. In the reversing experiments both agonists and antagonists were used. A single dose of the D2 or D3 agonist (300 nM) was perfused over the slice for 30 minutes. Then to determine if the antagonist could reverse the effects of the agonist, 10 μM of (S)-(-)-sulpiride or nafadotride (Figure 3.1) was perfused over the slice immediately after the agonist for 30 minutes. The peak oxidation current for DA was converted into concentration from a post electrode calibration with 3 μM DA as described in Section 2.4.4. Current versus time plots were analyzed as described in Section 2.4.5 to determine electrically stimulated DA release and uptake rates.

3.2.1 Chemicals

All of the DA agonists and antagonists were purchased from Tocris Bioscience (Ellisville, MO) except quinpirole, which was purchased from Sigma-Aldrich (St. Louis, MO). All solutions of the drugs and DA were diluted in the aCSF from stock solutions.

3.2.2 Statistical data analysis

All statistical analyses were carried out using GraphPad Prism. Data are shown as means ± standard errors of the means (SEMs) of at least five brain slices, derived from different animals. When DA agonists were used the change in the current versus time profile was evaluated as a change in $[DA]_p$, which represents the inhibition of DA release via the D2-like autoreceptors. This change in electrically stimulated DA release

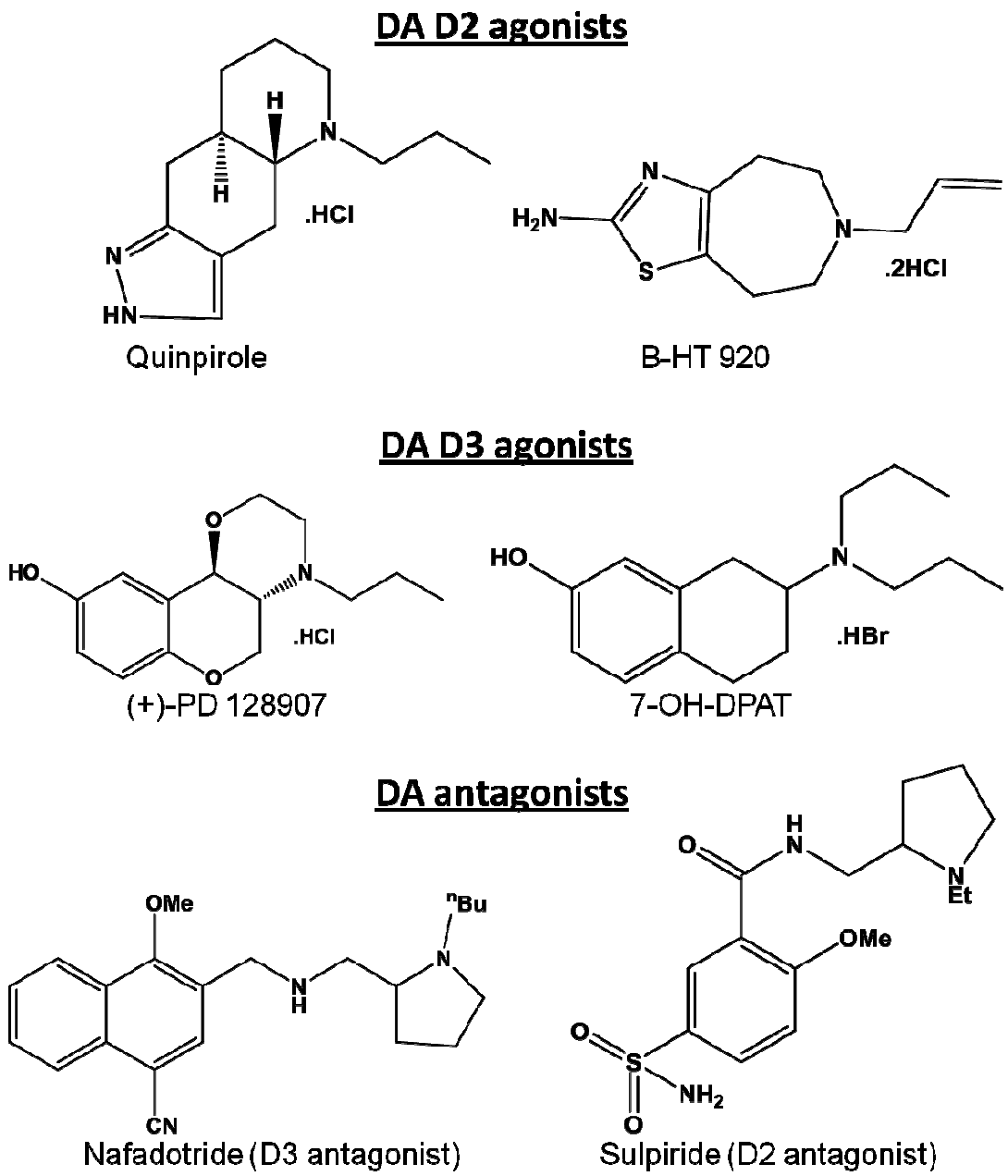

Figure 3.1 Chemical structures of the dopamine D2 and D3 receptor agonists and antagonists.

was compared to pre-drug values (each animal served as their own control), leading to a percent change in stimulated DA efflux. Using GraphPad Prism, the dose response curve was plotted as a log concentration (M) of agonist versus percent of baseline (maximal stimulated DA release); the data was fitted using a non-linear regression curve fit to determine half maximal effective concentration (EC_{50}). The log EC_{50} obtained after administration of DA D2 or D3 agonists were subjected to a one-way ANOVA with Tukey post-test by comparing CPu, NAc core, and shell. Effect of DA D2 or D3-like agonists on DA uptake was analyzed using a one-way ANOVA with Dunnett's post-test by comparing pre-drug V_{max} values to DA agonist treatment. In all cases, statistical significance was defined as $P < 0.05$.

3.3 Results and Discussion

3.3.1 Effect of dopamine D2 agonists on electrically stimulated dopamine

DA autoreceptors regulate the extracellular levels of DA through a negative feedback mechanism in which increasing agonist concentration results in a reduction in extracellular DA. The most common method for evaluation of DA receptor density is autoradiography, which employs the use of radioactive ligands to quantify receptor levels (*119-122, 158*). Within the striatum (including the CPu and NAc), it is well known that the D2 density is fairly homogeneous, while the D3 receptor density is greatest in the NAc shell region (*17, 155, 158, 168, 169*). The striatum was chosen as the region of interest to take advantage of this divergent D2 and D3 receptor distribution in order to better differentiate D2 and D3 receptor agonists and antagonists. Using FSCV, the activity of DA release-regulating autoreceptors was evaluated in the dorsal CPu, and separately in the core and the shell of the NAc. In all brain regions evaluated, increasing

concentrations of the D2 or D3 receptor agonists (0.001 – 10 µM) were added to slices at 30-minute intervals. Upon addition of each agonist, a plateau in DA release was reached within 15 – 25 minutes. The peak DA release was determined during this plateau and expressed as a percent of the pre-drug (control) concentration.

The two D2 agonists, quinpirole and B-HT 920, were evaluated by first examining their effects on DA release stimulated by a single electrical pulse in the CPu, NAc core, and NAc shell. Representative voltammetric traces of electrically evoked DA in the CPu in the absence or presence of quinpirole (0.03, 0.1, and 1 µM) are shown in Figure 3.2A. The observed responses for these two agonists were nearly indistinguishable (Figure 3.3). The amount of DA evoked before drug application was approximately 2 µM (n = 10), 1 µM (n = 10), and 0.6 µM (n = 10) for CPu, NAc core, and NAc shell, respectively. Similarly, the log EC_{50} values and corresponding EC_{50}'s for B-HT 920 were – 7.0 ± 0.2 (102 ± 32 nM, n = 5), – 7.1 ± 0.2 (82 ± 29 nM, n = 5), and – 7.2 ± 0.1 (70 ± 18 nM, n = 5) for CPu, NAc core, and shell, respectively. The EC_{50} values for quinpirole and B-HT 920 are summarized in Table 3.1. No difference was observed for quinpirole (one-way ANOVA (Tukey post-test); $F_{2,19} = 0.60$; $P = 0.56$) or B-HT 920 ($F_{2,14} = 0.52$; $P = 0.61$) between their EC_{50} values in the CPu, NAc core, or NAc shell. The results with both D2 agonists show that DA D2 receptors have a fairly homogeneous expression throughout the striatum (from the CPu to the NAc) as evidenced by similar functional effects of D2 agonists on DA release across the striatum. Our results correlate with autoradiography studies that have shown that DA D2 receptor density is fairly homogeneous throughout the striatum (*17, 155, 158, 168, 169*).

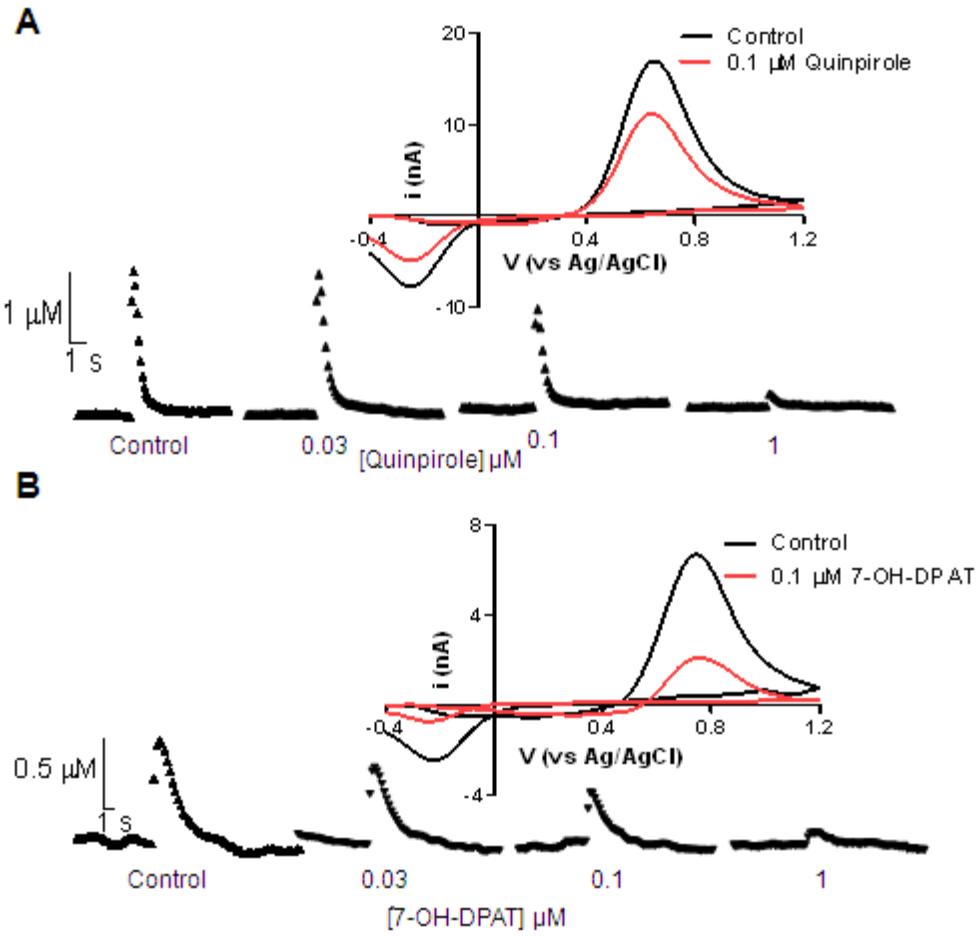

Figure 3.2 Representative concentration versus time plots showing the concentration dependent effects of agonist on stimulated DA efflux and uptake. (A) D2 agonist quinpirole in the CPu and (B) D3 agonist 7-OH-DPAT in the NAc shell. Insets are representative cyclic voltammograms.

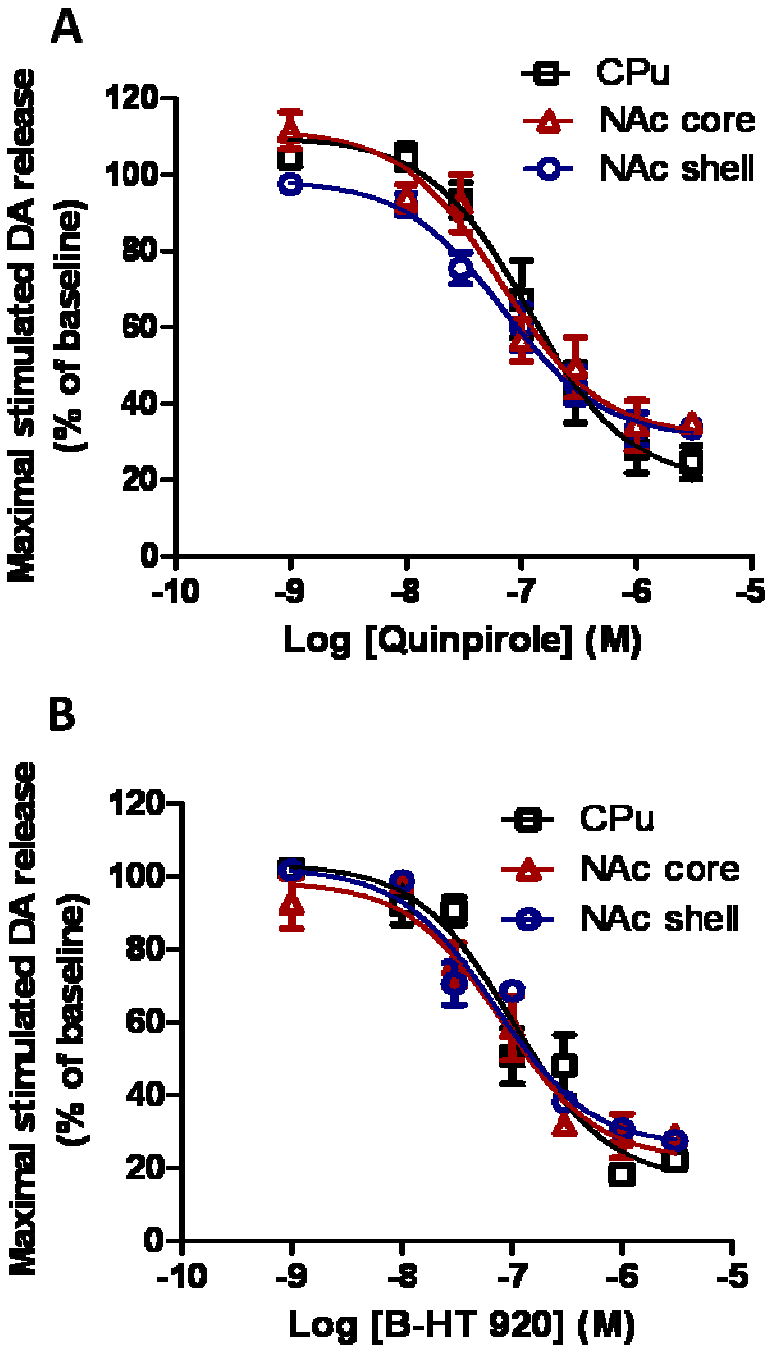

Figure 3.3 Concentration-response relationship of D2 agonist, quinpirole (A) and B-HT 920 (B) on inhibiting electrically stimulated DA efflux in the CPu (■), NAc core (Δ) and shell (●). No difference was observed for quinpirole (one-way ANOVA (Tukey post-test); $F_{2,19}$ = 0.60; *P* = 0.56) or B-HT 920 ($F_{2,14}$ = 0.52; *P* = 0.61) between their half maximal effective concentrations (EC_{50}) in the CPu, NAc core, or NAc shell.

Table 3.1 Potency (EC_{50}, nM) and efficacy (%) values for dopamine D2 and D3 agonists in the striatum, determined using voltammetry.

	Caudate putamen		**Nucleus accumbens core**		**Nucleus accumbens shell**	
Drug	EC_{50} ± SEM (nM)	Mean ± SEM Efficacy (%)	EC_{50} ± SEM (nM)	Mean ± SEM Efficacy (%)	EC_{50} ± SEM (nM)	Mean ± SEM Efficacy (%)
7-OH-DPAT	325 ± 119	48 ± 9	59 ± 9	23 ± 1	44 ± 8	19 ± 2
(+)-PD 128907	250 ± 77	43 ± 5	163 ± 47	36 ± 6	65 ± 12	29 ± 3
Quinpirole	114 ± 35	28 ± 6	66 ± 33	34 ± 6	69 ± 16	33 ± 4
B-HT 920	102 ± 32	18 ± 3	82 ± 29	28 ± 6	70 ± 18	30 ± 2

The reported efficacy values are at a dose of 1 µM for all agonists.

3.3.2 Effect of dopamine D3 agonists on electrically stimulated dopamine release

The effect of the D3 agonists 7-OH-DPAT and (+)-PD 128907 on a single pulse stimulated DA release was evaluated as described above for D2 agonists. Concentrations of 7-OH-DPAT greater than 30 nM significantly reduced electrically-stimulated DA release in all striatal regions ($P < 0.0001$). Representative voltammetric plots of DA concentration versus time in the NAc shell in the absence and presence of 7-OH-DPAT (0.03, 0.1, and 1 µM) are shown in Figure 3.2B. Similar to the DA D2 agonists, dose response curves were analyzed by curve fitting analysis, which revealed the potency (EC_{50}) and efficacy of the DA D3 agonist to decrease electrically stimulated DA release in the striatum. The log EC_{50} values and corresponding EC_{50}s for 7-OH-DPAT were – 6.5 ± 0.2 (325 ± 119 nM, n = 5) for CPu, – 7.2 ± 0.07 (59 ± 9 nM, n = 5) for NAc core, and – 7.4 ± 0.09 (44 ± 8 nM, n = 5) for NAc shell. The log EC_{50} values and corresponding EC_{50}'s for (+)-PD 128907 were – 6.6 ± 0.2 (250 ± 77 nM, n = 5), – 6.8 ± 0.1 (163 ± 47 nM, n = 5), and – 7.2 ± 0.08 (65 ± 12 nM, n = 5) for CPu, NAc core, and NAc shell, respectively. The EC_{50} values for 7-OH-DPAT are presented in Table 3.1.

Unlike the DA D2 agonists, the EC_{50} values for the D3 agonist 7-OH-DPAT were significantly different across the brain regions in the striatum as analyzed with one-way ANOVA ($F_{2,14} = 7.0$; $P < 0.01$; Figure 3.4A). A Tukey post-test revealed a significant leftward shift toward lower values in the EC_{50} between the dorsal CPu and the NAc core ($P < 0.05$) and the dorsal CPu to the NAc shell ($P < 0.05$). However, the Tukey post-test revealed no difference between the 7-OH-DPAT EC_{50} values in the core versus the shell. This shift in EC_{50} values indicates that the DA D3 receptors function is higher in

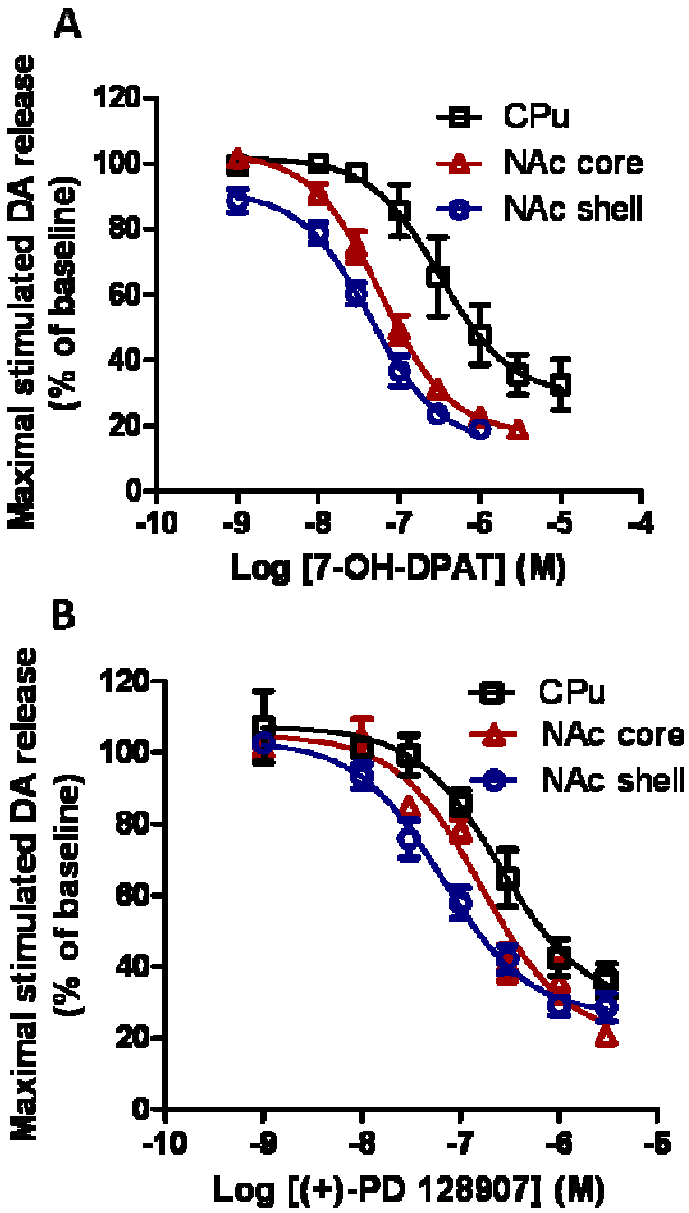

Figure 3.4 Concentration-response relationship of D3 agonists 7-OH-DPAT (A) and (+)-PD 128907 (B) on inhibiting electrically stimulated DA efflux in the CPu (■), NAc core (Δ) and shell (●). The dose response curves across these striatal brain regions were significantly different for the D3 agonists, 7-OH-DPAT ($F_{2,14}$ = 7.0; P < 0.01) and (+)-PD 128907 ($F_{2,14}$ = 11.24; P < 0.01) as analyzed by a one-way ANOVA (Tukey post-test).

the NAc (includes both the core and shell), suggesting higher DA D3 receptor density in the NAc versus the CPu. These results are also consistent with autoradiography experiments, which showed that the DA D3 density is greater in the NAc as compared to the CPu (*20*).

The effect of the DA D3-preferring agonist (+)-PD 128907 on electrically stimulated DA release was similar to that of 7-OH-DPAT. Increasing concentrations of (+)-PD 128907 decreased electrically stimulated DA in a dose-dependent manner (Figure 3.4B). The EC_{50} values for (+)-PD 128907 are summarized in Table 3.1. The (+)-PD 128907 EC_{50} values across these striatal brain regions were significantly different as analyzed by a one-way ANOVA ($F_{2,14} = 11.24$; $P < 0.01$). A Tukey post-test revealed the EC_{50} values in the NAc shell exhibited the greatest shift to lower values as compared to the CPu ($P < 0.01$) and NAc core ($P < 0.05$). However, the Tukey post-test showed no difference between the EC_{50} values for (+)-PD 128907 in the CPu and NAc core. Based on the EC_{50} values, 7-OH-DPAT and (+)-PD 128907 had significant but different effects on the brain regions studied. The ability of these DA D3 agonists to lower the concentration of stimulated DA was greatest in the NAc shell and least effective in the CPu. This suggests regional difference in potency of these agonists to inhibit electrically stimulated DA release, which may reflect D2/D3 receptor selectivity.

This is the first report that we are aware of that has compared the response of DA agonist in sub-anatomical striatal brain regions to distinguish their selectivity for D2- or D3-autoreceptors. Agonists for the DA D2 and D3 receptors, when perfused across a slice, can bind and activate their respective receptors located on both pre- and post-synaptic surfaces. In this study, voltammetry was used to characterize DA release

during agonist perfusion, however only presynaptic autoreceptors that regulate DA release were evaluated. Shifts in voltammetric dose response curves are most often associated with receptor functionality, but changes in receptor sensitivity and density cannot be ruled out (*160*). Using slice FSCV, DA D2 and D3 agonists give distinct dose response curves and EC_{50} values that are dependent on the brain region examined. The dose response curves and EC_{50} of DA D2 agonists exhibit less variation across the CPu, NAc core, and shell as compared to the more D3 selective agonists, which demonstrated a significant shift to lower EC_{50}s in their dose response curves and a reduction in EC_{50} values from the CPu to the NAc shell. Additionally, the EC_{50} values obtained from these voltammetry studies (for D2 and D3 agonists) directly correlate with D2 and D3 receptor density, as measured by autoradiography (*20, 119-122, 154, 155, 158*). This correlation suggests that voltammetry can be used to determine receptor density in different regions of the brain. Taken together, these results indicate that DA D2 agonists are relatively more potent in the CPu than DA D3 agonists. These results suggest that combining slice voltammetry and receptor localization may be a novel method to characterize agonists as more D2- or D3-preferring.

3.3.3 The efficacy of dopamine D2 and D3 agonists

The relative maximum response of DA D2 and D3 agonists in the dorsal and ventral striatum were used to determine if there was a difference in efficacy between these agonists across these regions. In order to directly compare the maximum inhibition of each of the agonists for decreasing DA release, the efficacy of each agonist at a concentration of 1 µM was compared. This concentration was chosen to evaluate drug efficacy because all drugs respond to this agonist concentration. This comparison

was used to determine the relative activity of each agonist to decrease DA release in each of these brain regions, which we believe reflects the preference of these drugs to activate D2 or D3 receptors. This comparison was conducted for each brain region and the efficacies are expressed as percent of the drug effect relative to the pre-drug value (Table 3.1). Thus, a low percentage reflects high efficacy for the given agonist.

The DA D3 agonists exhibited the highest efficacy (greatest inhibition of electrically stimulated DA release) at 1 µM in the NAc shell, with 19 ± 2% and 29 ± 3% maximal stimulated DA release as a percent of pre-drug values (defined as a 100%) for 7-OH-DPAT and (+)-PD 128907, respectively. The DA D3 agonists in the CPu showed an efficacy of 48 ± 9% for 7-OH-DPAT and 43 ± 5% for (+)-PD 128907, which suggests that the D3 agonists have the ability to decrease DA release, but when compared to the ability of D2 agonists, do not produce a maximum effect at this concentration. In contrast, but consistent with the homogenous distribution of the D2 receptor, the efficacy of D2 agonist quinpirole was approximately the same across the different brain regions, 28 ± 6% for CPu, 34 ± 6% for NAc core, and 33 ± 4% for NAc shell. As for quinpirole, B-HT 920 exhibited a similar effect with values of 18 ± 3%, 28 ± 6%, and 30 ± 2% for the CPu, NAc core, and shell, respectively.

3.3.4 Effect of dopamine D2 and D3 agonists on dopamine uptake in the striatum

The main mechanism by which D2 and D3 agonists regulate extracellular DA levels is by inhibiting DA release, although D2 receptors are also known to influence DA synthesis as well. However, there is considerable evidence indicating that both DA D2 and D3 receptors regulate DA transporter function (*108, 152, 161-166*). If DA D2 or D3 agonists modulate the activity of the DA transporter, then this would suggest another

mechanism for these agonists to regulate extracellular DA levels. Many of the initial findings that linked the ability of DA D2 and D3 agonists to modulate V_{max} of the DA transporter used rotating disk voltammetry or chronoamperometry (*108, 163, 166*). An advantage of using electrochemical techniques is their rapid data collection rate, which is on the order of seconds and therefore provides the temporal resolution to discriminate differences in uptake rates. The objective of the following experiments was to evaluate DA uptake rates in the presence of increasing concentrations of DA D2 and D3 agonists.

As described in Section 2.2.5, the Michaelis-Menten based kinetic model was used to evaluate release ($[DA]_p$) and uptake kinetics (V_{max} and K_m). When analyzing DA current versus time plots, K_m values were fixed at 0.16 µM, allowing for manipulation of DA peak amplitude (release) and DA uptake (V_{max}) in the presence or absence of a DA D2 or D3 agonist in striatal regions (*139, 140*). The effect of 0.001, 0.01, 0.03, 0.1, 0.3, 1, 3, and 10 µM of quinpirole, B-HT 920, 7-OH-DPAT, or (+)-PD 128907 on DA uptake was evaluated. The results show a significant decrease in V_{max} in the presence of D2 or D3 receptor agonist only in the CPu and at very high concentrations of the agonist (quinpirole: $F_{7,90} = 13$; $P < 0.0001$; B-HT 920: $F_{8,71} = 8.9$; $P < 0.0001$; 7-OH DPAT: $F_{8,117} = 4.8$; $P < 0.0001$; (+)-PD 128907: $F_{7,66} = 16$; $P < 0.0001$; Figure 3.5).

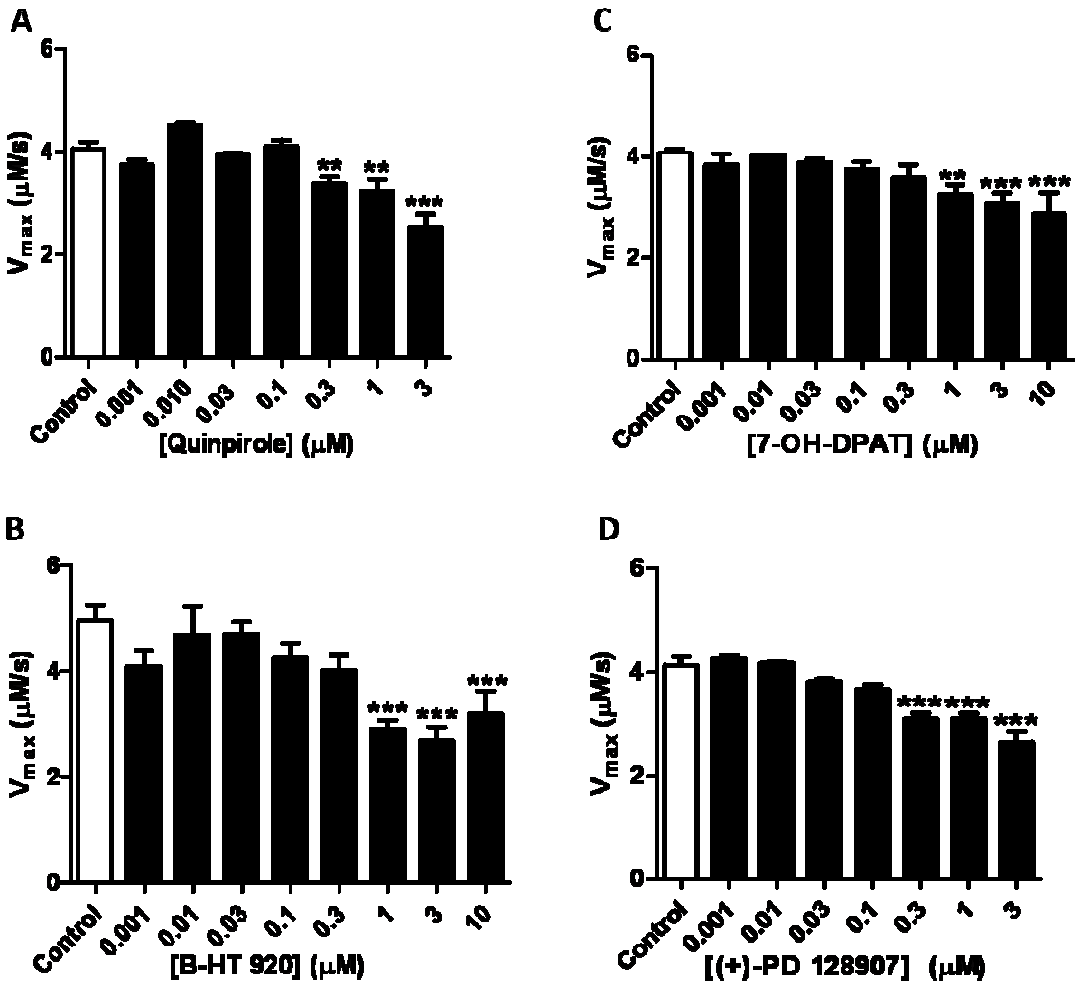

Figure 3.5 Effect of dopamine (DA) D2 and D3 agonist concentrations on electrically evoked DA uptake rates in the caudate putamen (CPu). (A) quinpirole, (B) B-HT 920, (C) 7-OH-DPAT, (D) (+)-PD 128907. Each concentration-uptake rate curve was analyzed with one-way ANOVA (** $P < 0.01$; *** $P < 0.001$).

No difference (one-way ANOVA (Dunnett's test)) in DA uptake rates was observed in the NAc core ($F_{6,38}$ = 0.67; *P* = 0.67) or shell ($F_{7,79}$ = 1.9; *P* = 0.085) (Figure 3.6 parts A and B) with increasing concentration of quinpirole. Similarly, increasing concentrations of the D2 agonist B-HT 920 did not affect DA uptake rates in the NAc core ($F_{7,50}$ = 2.2; *P* = 0.057), and shell ($F_{7,50}$ = 2.1; *P* = 0.062), as shown in Figure 3.6 parts C and D, respectively. DA uptake rates were also evaluated in the absence and presence of the D3 agonist, 7-OH-DPAT or (+)-PD 128907. Similar to the DA D2 agonists quinpirole and B-HT 920, DA uptake rates were not significantly different in the NAc when increasing concentrations of 7-OH-DPAT or (+)-PD 128907 were added to the slices, NAc core [7-OH-DPAT: ($F_{7,72}$ = 0.67; *P* = 0.69); (+)-PD 128907: ($F_{7,46}$ = 1.7; *P* = 0.15)] shown in Figure 3.7 parts A and C, respectively or NAc shell [7-OH-DPAT: ($F_{6,105}$ = 1.4; *P* = 0.23); (+)-PD 128907: ($F_{7,110}$ = 1.6; *P* = 0.14)] shown in Figure 3.7 parts B and D, respectively.

Our results from mouse brain slices show only a decrease in V_{max} at the highest concentrations of agonists applied in the CPu. However, previous electrochemical studies reported an increase in DA clearance in the presence of a D2 agonist, and a decrease in DA clearance by D2-like receptor antagonist (*163, 166, 170*). However, these data are not conclusive because Dickinson *et al.* reported no difference in DA clearance in the presence of raclopride, a known D2 antagonist (*80*). These previous studies, which evaluated the effect of DA agonists or antagonists on DA clearance, did not use FSCV, but other electrochemical methods.

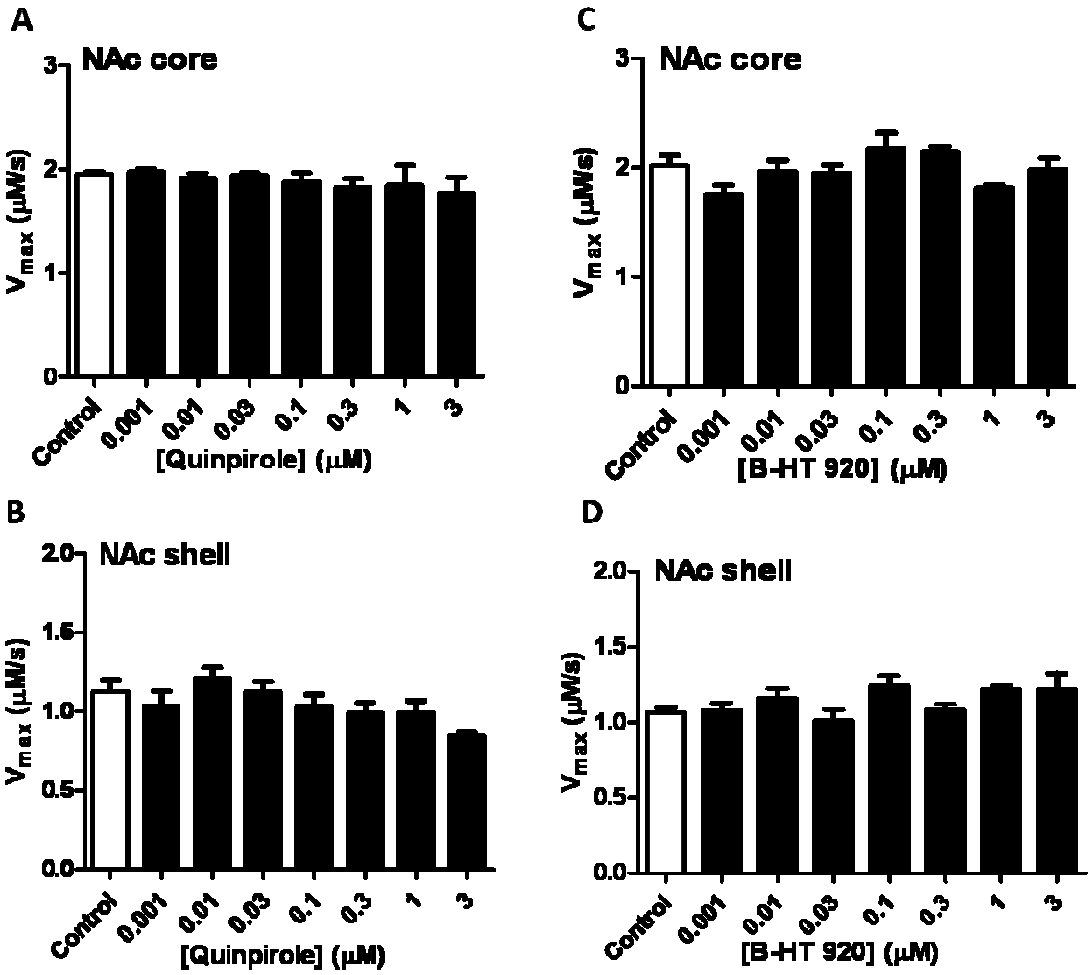

Figure 3.6 Effect of the dopamine (DA) D2 agonist concentration on DA uptake in nucleus accumbens (NAc). Specifically, the effects of quinpirole on the NAc core (A) and NAc shell (B), and B-HT 920 on the NAc core (C) and NAc shell (D).

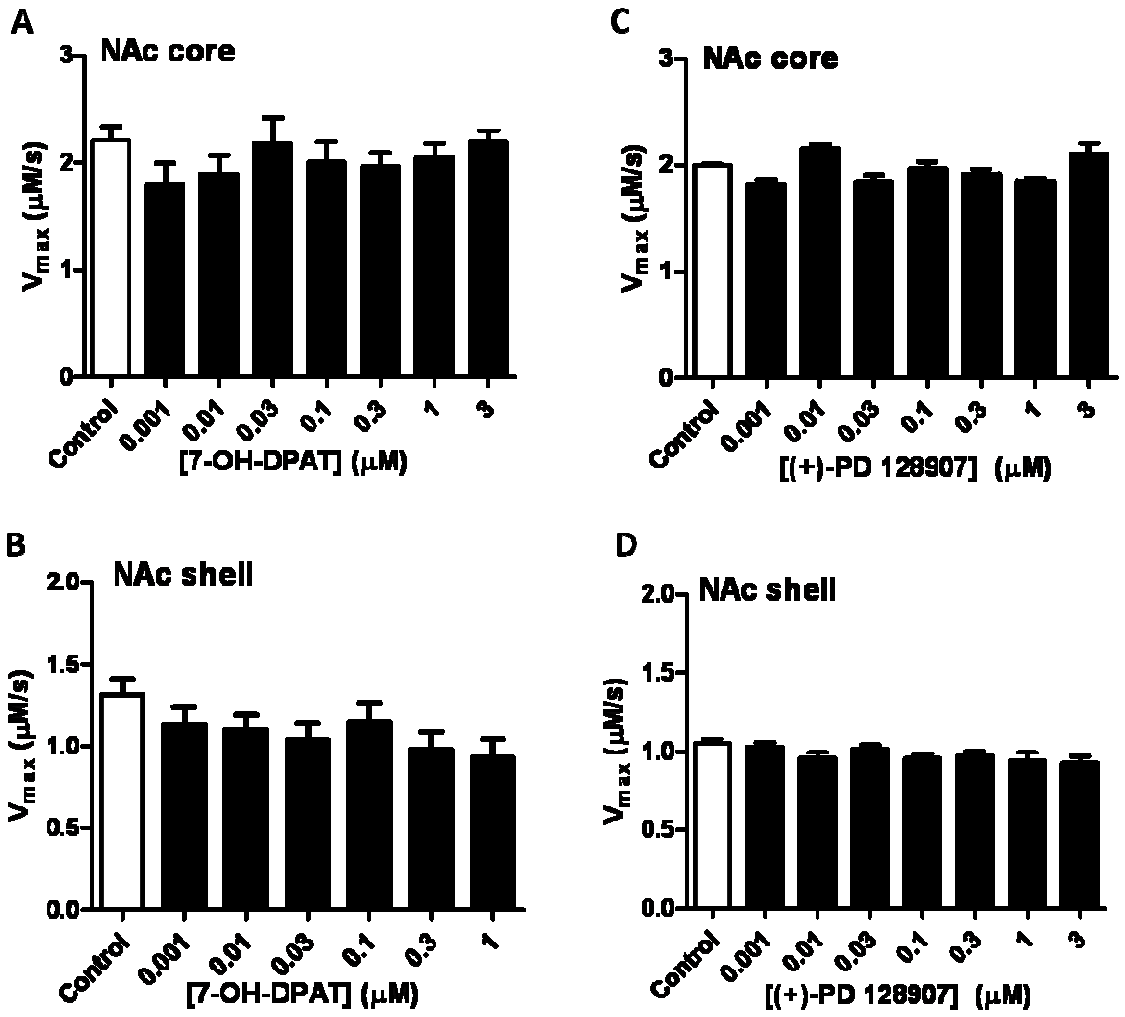

Figure 3.7 Effect of the dopamine (DA) D3 agonist concentration on DA uptake in nucleus accumbens (NAc). Specifically, the effects of 7-OH-DPAT on the NAc core (A) and NAc shell (B), and (+)-PD 128907 on the NAc core (C) and NAc shell (D).

The discrepancy in uptake rates between our results and these previous studies could be a result of different experimental parameters used in FSCV as compared to chronoamperometry or rotating disk voltammetry, such as brain slices versus an intact system (*in vivo*), or inducing DA depolarization by employing one pulse stimulation (endogenous DA release) versus applying exogenous DA. Interestingly, most FSCV experiments that measure the effect of D2-agonists on DA peak amplitude do not report uptake rates (*67, 69-71, 73, 76, 82, 102*). This approach is most likely due to an *a priori* assumption that only electrically stimulated DA release (or DA amplitude) has been altered in the presence of agonists (*126*). A study by Joseph *et al.* measured the DA uptake rate using FSCV, and in the presence of quinpirole noted that the uptake rate in CPu was not different (*70*). Joseph *et al.* suggested that alterations in DA uptake kinetics are not observed because (1) DA uptake rates are maximally accelerated or (2) temporal resolution of FSCV is not adequate to resolve these elevated DA uptake rates (*70*).

DA transporter activity is regulated by either receptors or second-messenger linked signal transduction pathways. Briefly, activation of protein kinase C (PKC), extracellular signal-regulated kinases 1 and 2 (ERK1/2) and phosphatidylinositol-3-kinase (PI3K) have all been shown to influence DA transporter activity (*171-173*). Although voltammetric studies suggest modulation of DA transport via DA receptors, only recently have the second-messenger pathways between DA receptors and transporters been examined (*152, 162, 165*). Specifically, Bolan *et al.* demonstrated that D2 receptor activation enhanced cell surface expression of the DA transporter by ERK1/2 (*162*). Additionally, Lee *et al*. demonstrated a direct protein-protein interaction

between the D2 receptor and the DA transporter, and this direct physical coupling promoted DA transporter expression to the cell surface (*165*). For example, an increase in V_{max} was observed with no difference in K_m (*165*). In a subsequent study, acute D3 receptor activation was shown to modulate DA transporter activity by both ERK1/2 and PI3K, but prolonged D3 receptor activation induced a reduction in the cell surface DA transporter expression (*152*). In our study, cumulative dose response curves were used to evaluate the DA uptake rate and as a result, the slice was bathed with an agonist for at least 2 hours before concentrations greater than 0.3 µM are applied. Our agonist results suggest low concentrations do not influence DA uptake rate, which may represent acute activation. However, a combination of prolonged exposure and agonist concentrations greater than 0.3 µM do demonstrate a significant decrease in DA uptake rate in the CPu, in agreement with previous findings (*152*). Because this decrease in DA uptake rate was observed with both D2 and D3 agonists, we speculate that a possible mechanism for receptors regulating transporter expression and/or function may be through the ERK1/2 pathway. However, future studies would have to assess this proposed mechanism.

The fact that DA uptake rate is influenced only by high concentrations of agonist in the CPu, while no difference in uptake is observed in the NAc core and shell suggests that this may be a brain region specific phenomenon. The DA transporter density within the striatum is known to vary depending on the sub-anatomical location, with the CPu having the greatest density of DA transporters, while the NAc core and shell have considerably less (*90, 96, 148, 149*). We hypothesize this lack of agonist effect on DA uptake rate in the NAc may be a result of fewer DA transporters as compared to the

CPu. The density of DA transporters is reduced in the NAc as compared to the CPu, while D2-like receptor density remains the same or is increased in the NAc. Taken together, these data suggest fewer DA transporters are coupled and/or are not responsive to D2-like receptor agonists in the accumbens. Hence, no effect of these agonists in the NAc core or shell is observed versus the CPu.

3.3.5 Effect of dopamine antagonists in the CPu

DA D2 and D3 receptor antagonists block their respective receptors and activate DA synthesis and release in presynaptic terminals (*174-176*). To demonstrate reversibility of the electrically evoked DA signal, an antagonist was applied to brain slices immediately after agonist application. The objective was to determine if DA D2-like and D3 antagonists can selectively reverse their respective agonist response. The CPu was chosen as the brain region to characterize these antagonist effects, because it is known to exhibit the greatest discrepancy between DA D2 and D3 receptor levels. In these studies only one concentration of the DA D2 or D3 receptor agonist (300 nM) was applied to the slice. This agonist concentration was chosen based on the dose response curves that we generated demonstrating approximately 40 – 60% decrease in the DA release. Immediately after agonist application, a non-selective DA D2 or selective D3 antagonist (10 µM) was applied to the slice. As shown by Schmitz *et al.,* even after a ten minute perfusion with 500 nM of quinpirole the DA peak amplitude as recorded by FSCV was attenuated for at least an additional 22 minutes after the removal of quinpirole, demonstrating the response of the agonist was not washed out when the buffer was changed to aCSF (*125*). Immediately after quinpirole either sulpiride (a non-selective DA antagonist) or nafadotride (a selective DA D3 antagonist) was perfused

over the slice. The D2 agonist effect in the CPu was reversed fully only by the sulpiride (Figure 3.8A), while nafadotride increased electrically stimulated DA levels to approximately 70% of the pre-drug value (Figure 3.7B). Hence, the D3 antagonist had the ability to increase maximal stimulated DA release by only 10% in the CPu. Similarly, after 7-OH-DPAT perfusion in the CPu, an approximately 40% decrease in the electrically stimulated DA response was observed. However, upon perfusion of sulpiride or nafadotride the electrically stimulated DA response returned to pre-drug levels (100%; Figure 3.8 parts C and D). Thus, it appears that the effect of a DA D2 agonist is only reversible after infusion of a non-selective D2 antagonist, suggesting that nafadotride is acting primarily at either available DA D3 receptors within the CPu, where there is low density of these receptors present, or alternatively, nafadotride is elevating DA levels by interacting at available DA D2 receptors (*20, 154, 155*).

However, we believe that nafadotride is not acting at the D2 receptors because with the application of such a high concentration (10 µM), we would expect to observe a greater response due to the higher D2 receptor functionality and/or density present within the CPu. Nafadotride is unable to fully reverse the effect of quinpirole because of the lower abundance of D3 receptors available within this brain region, and the levoisomer of nafadotride is known to have a greater affinity to the DA D3 receptors than to the D2 receptors (*177*). Within the CPu, we have demonstrated that sulpiride can fully reverse the effects of quinpirole, while nafadotride is unable to reverse these effects. Because only the non-selective DA antagonist reversed the agonist response, this further supports the hypothesis that the DA D2 receptors are more functional in the CPu than the D3 receptors.

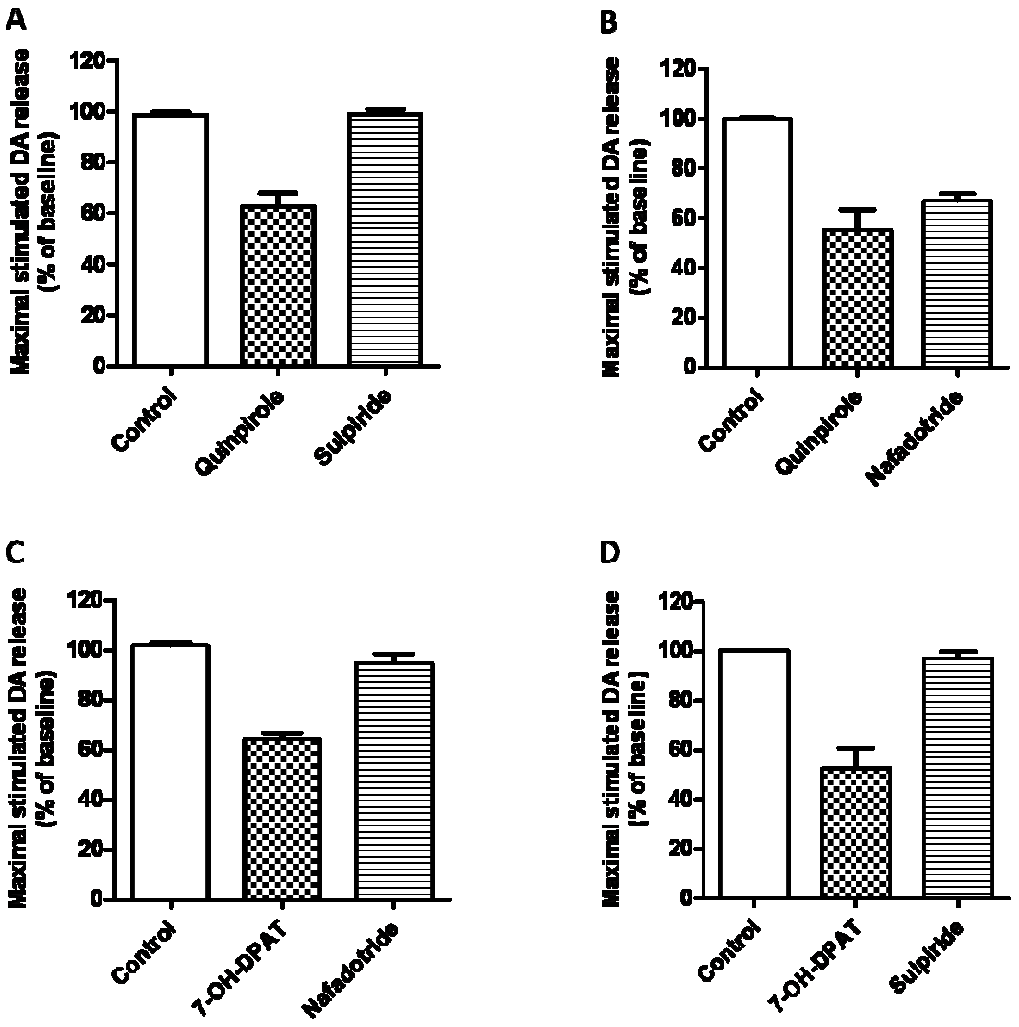

Figure 3.8 Effect of 300 nM quinpirole reversed with 10 µM sulpiride or partially reversed by nafadotride (A and B, respectively) or 7-OH-DPAT reversed with 10 µM nafadotride or sulpiride (C and D, respectively) on electrically evoked dopamine in dorsal CPu (n = 3 for each trial).

However, when the DA D3 agonist 7-OH-DPAT is applied to the CPu, both antagonists, sulpiride and nafadotride, reverse the DA response. The ability for both antagonists to reverse the DA D3 agonist is a result of sulpiride being a non-selective DA antagonist, with a high affinity for D2 and D3 receptors. As a result of sulpiride's promiscuity, it is able to reverse the effect of the D3 agonist in the CPu. Previous work using slice FSCV showed that higher concentrations of sulpiride and similar non-selective DA antagonists like clozapine and haloperidol had the ability to attenuate the 7-OH-DPAT-induced inhibition of electrically stimulated DA release in the NAc core (*76*). Our results with quinpirole-sulpiride and 7-OH-DPAT-sulpiride demonstrate that sulpiride is indeed a non-selective DA antagonist with high affinity for both the D2 and D3 receptors. In order to demonstrate exclusive receptor reversibility of the D3 receptor in the CPu, a very selective D2 antagonist would need to be applied. Unfortunately, many of the classic antipsychotic DA antagonists are not very selective.

The D3 antagonist nafadotride is described as a highly potent, preferential D3 antagonist. When an excess of nafadotride is applied to the CPu, it easily reverses the agonist effects. This reversal is most likely a result of its ability to compete with 7-OH-DPAT for available DA D3 receptors. Additionally, based on the results with quinpirole-nafadotride in the CPu (Figure 3.7B), it appears that nafadotride is not very effective at activating the DA D2 receptor, suggesting that nafadotride is a more selective D3 receptor antagonist. Taken together, these agonist-antagonist treatments suggest that within the CPu a non-selective DA antagonist in excess concentration can easily reverse the inhibition of D2- and D3-receptor agonists, but a selective D3 antagonist can reverse only the effects of a D3 agonist.

3.4 Conclusions

The results presented here demonstrate that the striatal region of the brain can be used as a tool to determine whether or not agonists are selective for D2- or D3-autoreceptors. The advantage of studying these effects in the striatum is the distinct localization of D2 and D3 receptors. Using slice FSCV we demonstrated that the D2 receptor functionality is uniform in the striatum. Specifically, commercially available D2 agonists (quinpirole and B-HT 920) showed similar EC_{50} values throughout the striatum. However, the D3 receptor functionality is localized in the NAc shell. More specifically, DA agonists with more D3-like properties (7-OH-DPAT and (+)-PD 128907 demonstrated a significant leftward shift in their dose response curves, which correspond with a reduction in EC_{50} values from the dorsal CPu to the NAc shell. Our results, which examine autoreceptor function, complement the autoradiography work that has mapped the distribution of DA D2 and D3 receptors. Although FSCV cannot distinguish receptor density from sensitivity, these results demonstrate a simple and fast method for determining DA functionality with D2 and D3 receptors. We believe that by exploiting the unique receptor density within the striatum, voltammetry may be used as a tool to characterize D2-like agonists as either D2- or D3-preferring. Mapping these receptors can offer powerful insight into the neuropathology of disorders involving these receptors, as well the mode of action of pharmacological agents.

CHAPTER 4

Aberrant Striatal Dopamine Dynamics in Brain-Derived Neurotrophic Factor-Deficient Mice

(Portions from Bosse, Maina, *et al., Accepted in Journal of Neurochemistry*)

4.1 Introduction

As a trophic factor, brain-derived neurotrophic factor (BDNF) plays an important role in neurogenesis, survival, growth, and synaptic plasticity of neurons to ensure normal development and maintenance of the adult mammalian brain (*21, 22, 178, 179*). BDNF is one of the most abundant neurotrophic factors in the mammalian brain with the highest levels of mRNA and protein occurring in the hippocampus, substantia nigra (SN), ventral tegmental area (VTA), and frontal cortex (*24, 180*). For example, within the VTA approximately 90% of the dopaminergic neurons contain BDNF mRNA (*181*). Both anterograde and retrograde transport of BDNF is known to occur in the midbrain dopamine (DA) neurons. Anterograde transport involves axonal movement of BDNF from cell bodies in the midbrain to nerve terminals in the striatum (*24, 180*). Besides anterograde transport, corticostriatal glutamate afferents are known to supply BDNF to the DA rich striatum (*24, 180*). Released BDNF interacts with its receptor tyrosine kinase B (TrkB) locally causing rapid physiological effects on neuronal transmission by activating downstream signaling pathways (see Section 1.2.3).

In cultured cells, BDNF increases the density of tyrosine hydroxylase (TH)-positive fibers (a marker of DA neurons), DA release, and uptake rates (*182-184*). In brain slices, exogenous BDNF is known to increase the turnover ratio between DA and its catabolite 3,4-dihydroxyphenylacetic acid (DOPAC) as well as potentiating the

activity-dependent release of DA (*29-31*). In organotypic brain slice cultures of rat hippocampus, BDNF enhances quantal neurotransmitter release by increasing the number of docked synaptic vesicles within presynaptic terminals (*185*).

The role of BDNF is critical for an organism's survival because mice lacking BDNF (null mutants; $BDNF^{-/-}$) exhibit impaired motor function/coordination and do not survive beyond three weeks of age (*34, 186*). The $BDNF^{-/-}$ mice have a reduced number of vesicles docked at presynaptic active zones, as well as reduced long-term potentiation (LTP) in the hippocampus as compared to wildtype mice (*187*). Mice that have been engineered to have reduced endogenous BDNF levels appear to be hyperactive, a phenotype that is often associated with a dysregulation of the nigrostriatal DA system (*34, 188*). Accordingly, numerous studies have highlighted that BDNF heterozygous ($BDNF^{+/-}$) mice exhibit increased tissue DA concentrations (reflective of intracellular levels) in the striatum, as well as decreased DA release in superfused striatal tissue fragments (*35, 189*). Furthermore, BDNF conditional knockout mice show reduced electrically evoked DA release in the caudate putamen (CPu) and nucleus accumbens (NAc) shell, but not in the core as measured by amperometry (*39*). Taken together, these studies suggest that BDNF can augment striatal DA function in a region-specific manner, but the mechanism of how BDNF modulates DA function remains elusive.

BDNF appears to modulate DA release-regulating receptors. $BDNF^{-/-}$ and $BDNF^{+/-}$ mice have reduced DA D3 receptor levels in the CPu, NAc core and shell, and the Islands of Calleja (*36-38*). A recent study in BDNF conditional knockout mice also shows altered DA D2 receptor expression in the CPu (*39*). However, others have

reported that BDNF deficiency in mice does not alter the expression of DA D2 receptors, TH, or the DA transporter (*37, 133*). Furthermore, it has been hypothesized that, in the NAc, BDNF regulates expression of DA D3 receptors and not extracellular DA levels (*188*). Taken together, these results suggest that reduced BDNF levels can regulate the DA system. Our general hypothesis is that BDNF strongly regulates many facets of DA transmission in the striatal complex.

BDNF hypofunction has been linked to numerous DA related neurological diseases, such as Parkinson's disease, Alzheimer's disease, Huntington's disease, schizophrenia, attention deficit hyperactivity disorder (ADHD), addiction, and depression (*42, 46, 53, 54, 112, 113, 115-117, 190*). Understanding the role of low, endogenous BDNF levels in modulating presynaptic DA dynamics will provide critical information that may lead to better treatment options for these neurological diseases. The main objective of this study was to understand how BDNF modulates the DA system in the striatal complex that can be divided into three discrete brain regions that include the CPu, NAc core and shell (*10*). Complementary neurochemical methods such as slice fast scan cyclic voltammetry (FSCV) and *in vivo* microdialysis (performed by *Kelly Bosse, Ph.D*.) were used. Slice FSCV provides real-time (every 100 ms) measurement of presynaptic dynamics such as DA release and uptake in brain slices. Inherent advantage of FSCV is that it employs microelectrodes (diameter ~ 7 microns) that provide good spatial resolution to probe the DA system in sub-anatomical regions of the striatum (NAc core and shell). The use of FSCV to evaluate the dopaminergic system provides an opportunity to probe DA autoreceptor functionality and the ability of exogenous BDNF to influence presynaptic DA dynamics in wildtype and $BDNF^{+/-}$ mice.

In vivo microdialysis in freely moving mice was used to measure extracellular basal levels of DA by use of the zero net flux method, as well as extracellular levels of DA catabolites DOPAC and homovanillic acid (HVA). Coupling microdialysis to HPLC-electrochemical detection provides the sensitivity to measure the low levels of extracellular DA in the brain. Finally, brain tissue analysis was performed to evaluate the effect of low BDNF levels on DA synthesis by measuring the accumulation of L-DOPA, the DA synthesis precursor.

4.2 Materials and methods

Wildtype and $BDNF^{+/-}$ mice offspring were raised as a colony in house and genotyped as described in Section 2.2. BDNF protein levels in $BDNF^{+/-}$ mice are ~ 50% less compared to those in wildtype mice, as quantified using enzyme-linked immunosorbent assay (ELISA) in our laboratory (*142*). Male $BDNF^{+/-}$ and wildtype mice aged 8 – 16 weeks were used for *in vivo* microdialysis, slice FSCV, and L-DOPA tissue content experiments.

4.2.1 *In vivo* microdialysis

Kelly Bosse, Ph.D. performed all the microdialysis experiments on adult mice with the assistance from Marion France. The microdialysis experiments conducted by Dr. Bosse involved stereotaxic surgery, probe implantation, sample collection, HPLC separation with electrochemical detection, chromatographic analysis, statistical data analysis, and graphing. Analyses of L-DOPA content in the tissue was performed by Kelly E. Bosse, Ph.D. with assistance from Joseph Roberts.

In vivo microdialysis experiments were performed as described in Section 2.5. Briefly, a microdialysis probe was inserted through a guide cannula implanted in the

CPu of mice during stereotaxic surgery. Following overnight perfusion of the probe with artificial cerebrospinal fluid (aCSF) at a flow rate of 0.4 µL/min, dialysate samples were collected every 20 minutes at a flow rate of 1.1 µL/min from freely moving mice. The dialysate was analyzed for DA, DOPAC, and HVA using HPLC separation and electrochemical quantification (Section 2.6). The zero net flux technique (Section 2.5) was utilized to estimate basal extracellular levels of DA in the CPu (*103, 143*). A second set of experiments, examined extracellular DA levels after a local perfusion with a high K^+ aCSF that induces neuronal depolarization and vesicular-mediated release (Section 2.5). L-DOPA accumulation was measured by tissue content analysis in both genotypes as described in Section 2.7.

4.2.2 Slice FSCV

Slice FSCV experiments were performed as previously described in Section 2.4 with minor modifications. Electrically stimulated (350 µA, 60 Hz, 4 ms wide) DA release and uptake rates following single or multiple (5) pulse stimulation were evaluated in the CPu, NAc core, and NAc shell. Additionally, the effect of exogenous BDNF perfusion on DA release and uptake rates in the CPu was evaluated. BDNF was dissolved in oxygenated aCSF to a final concentration of 100 ng/mL. Upon obtaining stable baseline recordings, BDNF (PeproTech inc., Rocky Hill, NJ) was perfused (1 mL/min flow rate) over a slice from $BDNF^{+/-}$ or wildtype mice for 30 minutes and DA recordings were made every 5 minutes. BDNF activity was inhibited by perfusing the slice with 1 µM K252a (Figure 4.1), a TrkB receptor antagonist (Tocris Bioscience, Ellisville, MO). Following the 30 minute perfusion with K252a, the same slice was perfused with 100 ng/mL BDNF for another 30 minutes with DA recordings every 5 minutes. Dose-response plots for DA

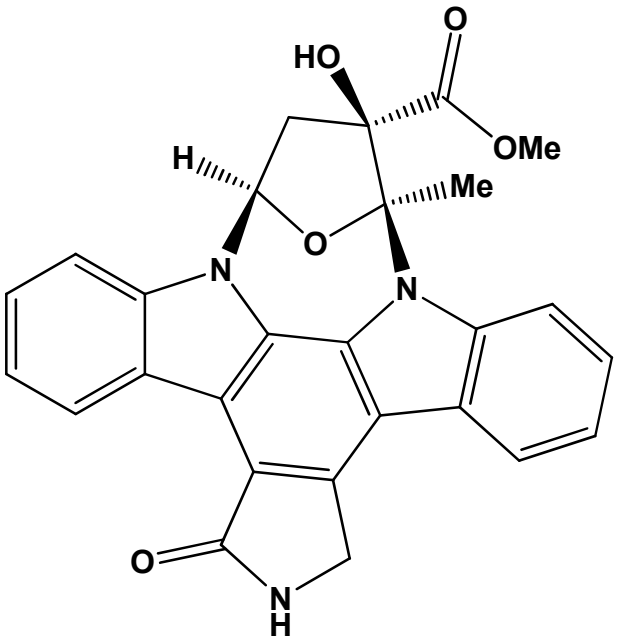

Figure 4.1 Chemical structure of K252a, tyrosine kinase B inhibitor.

release and uptake rates were also generated with both BDNF (50, 100, and 200 ng/mL) and K252a (0.1 0.3, 1 and 3 µM). Each concentration was perfused over a slice for 30 minutes.

To assess DA D2 and D3 autoreceptor functionality, the DA D3 receptor agonist 7-OH-DPAT or DA D2 receptor agonist quinpirole was perfused with cumulative concentrations (0.001 – 10 µM) at a flow rate of 1 mL/min following stable baseline recordings. The log of the concentration of the agonists plotted against normalized concentration of DA to obtain a dose-response curve for each genotype, from which the corresponding EC_{50} values were obtained. Previous findings from Sections 3.3.1 and 3.3.2 suggest that D2 autoreceptor functionality is homogenous across the striatal regions whereas D3 autoreceptor functionality is greatest in the NAc shell (*94*). Therefore, D2 autoreceptor functionality was evaluated only in the CPu, whereas D3 receptor was evaluated in the NAc shell.

4.2.3 Data analysis

Kelly Bosse, Ph.D. performed all the data and statistical analyses of the microdialysis results.

All values are reported as means ± standard errors of the means (SEMs) of at least four different animals, with and the statistical significance defined as $P < 0.05$. Zero net flux data were analyzed by linear regression to determine the x-intercept (DA_{ext}) and slope (E_d) for individual wildtype and $BDNF^{+/-}$ mice. Differences in DA_{ext} between genotypes were determined by a two-tailed Student's t-test. Differences in high K^+-stimulated extracellular DA levels were assessed using a two-way ANOVA with genotype as the independent variable and time as the repeated measure. Bonferroni

multiple comparison analysis was used for post-test. Area under the DA concentration curve was calculated from the four 20-minutes samples following high-K^+ perfusion (from 80 to 140 minutes) using the trapezoidal method (GraphPad Prism software). Data are reported as area under curve (AUC) in arbitrary units ± SEMs, and statistical significance was determined by Student's t-test. Levels of L-DOPA were expressed in ng and normalized to mg wet weight of brain tissue. Pair-wise comparisons using Student's t-test (two-tailed) were made to evaluate genotypic differences on DA release per pulse ($[DA]_p$) and uptake rate (V_{max}) evaluated with FSCV, L-DOPA tissue accumulation, and extracellular catabolite levels (DOPAC and HVA). When five-pulse stimulation was used in FSCV, the AUC of the current versus time plots was used to determine DA release by normalizing the data obtained from one electrode placement as a ratio of AUC (5p)/ AUC (1p). Two-way ANOVA with Bonferroni post-test was used to test the interaction between genotype and treatment (BDNF perfusion) or region (multiple pulse effect) on DA release with FSCV. One-way ANOVA (Dunnett's post-test) was used to determine the dose dependent effect of BDNF or K252a on DA release and uptake rates. Additionally, Student's-t test (two-tailed) was used to evaluate the genotype difference in autoreceptor functionality when quinpirole or 7-OH-DPAT was perfused on brain slices. Effect of quinpirole or 7-OH-DPAT treatments on DA uptake rate was evaluated using a one-way ANOVA with Tukey post-test, where means were compared to the pre-drug values.

4.3 Results

4.3.1 Basal and stimulated extracellular concentrations of dopamine in the CPu

Microdialysis results were obtained by Kelly E. Bosse, Ph.D.

To determine the impact of low endogenous levels of BDNF on DA dynamics, basal and K^+-stimulated extracellular DA concentrations were evaluated using *in vivo* microdialysis in the CPu of $BDNF^{+/-}$ mice. The basal concentrations of extracellular DA were estimated with the zero net flux method (Figure 4.2). This quantitative microdialysis technique approximates relative *"in vivo"* probe recovery using extraction fraction (E_d) values determined from the slopes of the zero net flux regression lines (*143*). The extraction fraction is considered to be a measurement of transporter-mediated uptake and often changes in E_d values are thought to be reflective of alterations in neurotransmitter uptake (*86*). Apparent extracellular DA levels, corrected for recovery, were significantly higher in $BDNF^{+/-}$ mice (12 ± 0.4 nM, n = 6) as compared to wildtype (5 ± 0.2 nM, n = 6, $P < 0.001$; Figure 4.2, inset). However, average E_d values were not different between the wildtype (0.21 ± 0.04) and $BDNF^{+/-}$ (0.23 ± 0.02) mice.

Genotypic differences in non-specific, depolarization-mediated DA transmission were also assessed using microdialysis. In line with the zero net flux data, $BDNF^{+/-}$ mice exhibited elevated mean baseline concentrations of extracellular DA (2.3 ± 0.2 nM, n = 12, averaged from three samples) compared to wildtype mice (1.2 ± 0.2 nM, n = 12, $P < 0.001$) as measured by conventional microdialysis. A 20 minute perfusion of high-K^+ (120 mM) aCSF through the microdialysis probe resulted in elevated extracellular concentrations of DA (Figure 4.3). Two-way ANOVA analysis revealed a significant main effect of time ($F_{6,66} = 24.29$), genotype ($F_{1,66} = 11.83$), and genotype x time

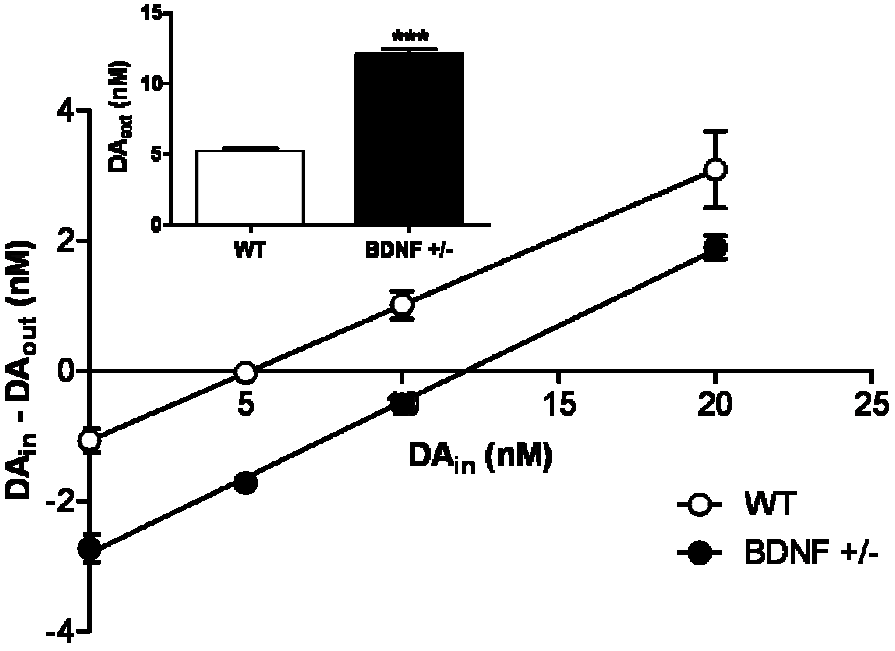

Figure 4.2 Linear regression analysis of dopamine (DA) levels in the CPu of wildtype (WT) and BDNF$^{+/-}$ mice determined by zero net flux. The x-intercept (point of zero net flux) represents an estimate of basal extracellular DA levels (DA_{ext}). Inset shows the mean ± SEM apparent DA_{ext} values (n = 6 mice per group). ****P* < 0.001 compared to WT mice (Student's t-test). *Figure courtesy of Kelly E. Bosse, Ph.D. and Tiffany A. Mathews, Ph.D.*

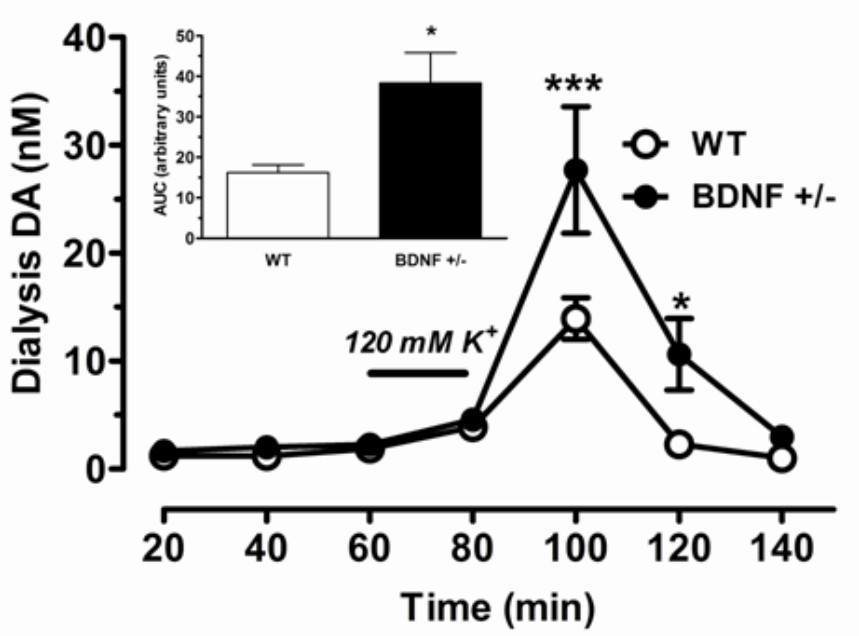

Figure 4.3 Extracellular dopamine (DA) concentrations in the CPu of wildtype (WT) and $BDNF^{+/-}$ mice following 20 minute perfusion of high-potassium (120 mM K^+) aCSF. Data are means ± SEM (n = 6 mice per group). **P* < 0.05; ****P* < 0.001, compared to WT mice (two-way ANOVA). Inset shows the area under the curve (AUC) for the cumulative increase in extracellular DA over four 20 min samples (80 – 140 min) following high-K^+ perfusion. Data are mean AUC ± SEM. **P* < 0.05 compared to WT mice (Student's t-test). *Figure courtesy of Kelly E. Bosse, Ph.D. and Tiffany A. Mathews, Ph.D.*

interaction ($F_{6,66}$ = 3.44). These findings indicate that while high-K^+ administration increased dialysate DA levels in both wildtype and $BDNF^{+/-}$ mice, the extent of increase was different with respect to genotype. Subsequent Bonferroni post-test results show that the peak increase in DA following high-K^+ stimulation in $BDNF^{+/-}$ mice (10-fold; 28 ± 6 nM) was potentiated relative to the increase observed in wildtype mice (6-fold; 14 ± 2 nM, $P < 0.001$). AUC analysis verified that $BDNF^{+/-}$ mice have a significantly greater cumulative increase in dialysate DA following high-K^+ perfusion as compared to wildtype mice ($P < 0.05$; Figure 4.3, inset).

4.3.2 L-DOPA and catabolite concentrations in the CPu

Tissue content studies to determine L-DOPA levels were performed by Kelly E. Bosse, Ph.D. with assistance from Joseph Roberts.

DA synthesis was determined by measuring the tissue accumulation of L-DOPA in the CPu following inhibition of L-aromatic acid decarboxylase with NSD-1015. No statistical difference was detected between the average striatal tissue levels of L-DOPA in wildtype mice (380 ± 25 ng/mg wet weight (ww), n = 13) and $BDNF^{+/-}$ mice (430 ± 40 ng/mg ww, n = 11, $P = 0.28$; Figure 4.4A). DA catabolism was evaluated by measuring the extraneuronal concentration of the DA catabolites, DOPAC and HVA, from baseline dialysis samples.

The mean extracellular concentrations, determined from triplicate analysis, for both DOPAC (wildtype: 410 ± 70 nM, n = 16; $BDNF^{+/-}$: 330 ± 90 nM, n = 10, $P = 0.66$) and HVA (wildtype: 465 ± 65 nM, n = 16; $BDNF^{+/-}$: 560 ± 120 nM, n = 10, $P = 0.47$) were also comparable across the two genotypes (Figure 4.4B). Together, these data indicate

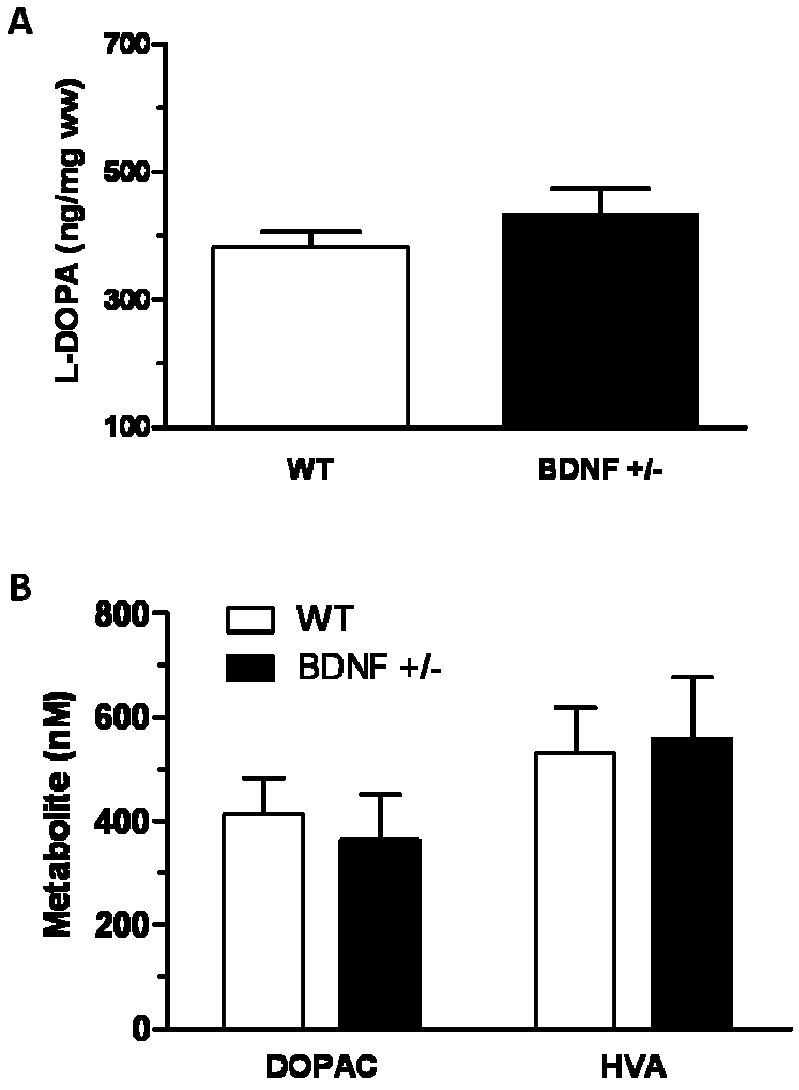

Figure 4.4 Dopamine (DA) synthesis and catabolism in the caudate putamen (CPu) of wildtype (WT) and BDNF$^{+/-}$ mice. (A) L-DOPA tissue accumulation following treatment with NSD-1015 and GBL. Data are means ± SEMs and expressed as L-DOPA ng/mg wet weight (ww) of tissue (n = 11 – 13 mice per group). (B) Extracellular concentration of the DA catabolites DOPAC and HVA, as measured by microdialysis. Data are means ± SEMs of uncorrected baseline values (n = 10 – 16 mice per group). *Figure courtesy of Kelly E. Bosse, Ph.D. and Tiffany A. Mathews, Ph.D.*

that constitutive depletion of BDNF does not result in altered rates of DA synthesis or catabolism.

4.3.3 Electrically evoked dopamine release and uptake rates in the striatum

FSCV was used to examine single pulse, electrically stimulated DA release and uptake rates in the CPu and NAc. As described previously (Section 2.2.5), the Michaelis-Menten based kinetic model was used to evaluate DA release ($[DA]_p$), uptake rate (maximum velocity; V_{max}), and affinity of DA for the DA transporter (apparent K_m) by fitting DA current versus time traces. For analysis, K_m values were fixed to 0.16 µM, allowing for non-linear fitting of DA peak amplitude (release) and DA uptake (V_{max}). Representative false color plots (Figure 4.5 parts A and B), and their corresponding DA concentration versus time plots (Figure 4.5 parts C and D) are shown for wildtype and $BDNF^{+/-}$ mice brain slices in the CPu. Electrically stimulated DA release was reduced by ~ 37% in $BDNF^{+/-}$ mice (1.2 ± 0.1 µM, n = 26) as compared to wildtype mice (1.9 ± 0.1 µM, n = 23; Figure 4.5E). The rate at which DA was cleared from the extracellular space by the DA transporter (uptake rate) was also attenuated by ~ 36% in $BDNF^{+/-}$ mice (2.7 ± 0.1 µM/s, n = 26) relative to the rates obtained in wildtype mice (4.2 ± 0.1 µM/s, n = 23; Figure 4.5F). A two-tailed t-test revealed that the decreases in both parameters, DA release and uptake rate, were significant in $BDNF^{+/-}$ mice as compared to wildtype mice ($P < 0.0001$).

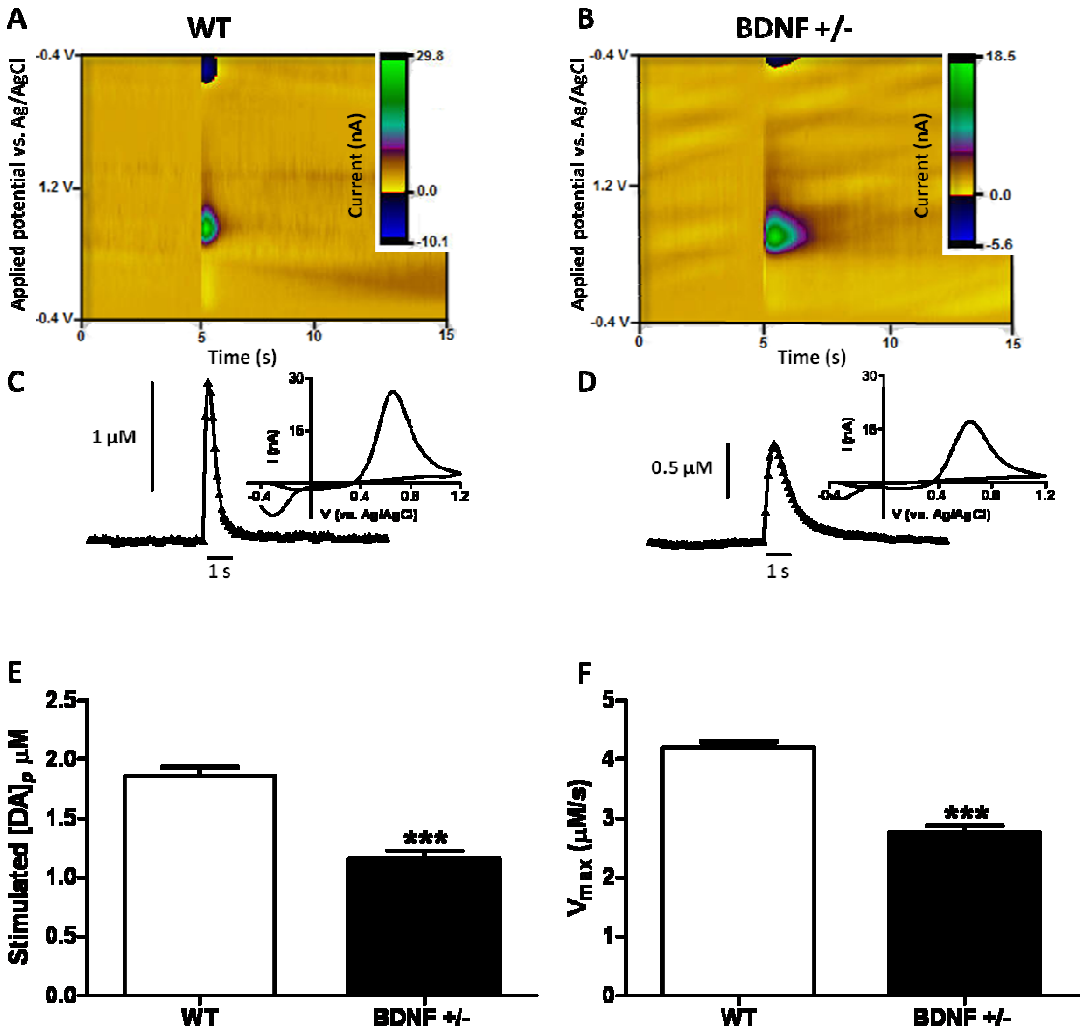

Figure 4.5 Electrically evoked dopamine (DA) release measured using slice FSCV following single-pulse stimulation in dorsal caudate putamen (CPu) of wildtype (WT) and BDNF$^{+/-}$ mice. Representative color plots from (A) WT and (B) BDNF$^{+/-}$ mice display time (x-axis), applied potential versus Ag/AgCl reference electrode (y-axis), and current in pseudo-color. The concentration versus time traces from (C) WT and (D) BDNF$^{+/-}$ mice are shown below their corresponding color plots, and the insets display the corresponding cyclic voltammograms. (E) Maximum electrically evoked DA release and (F) DA uptake rates measured from several locations within the CPu. Data are means ± SEMs (n = 23 – 26 mice per group). ***P < 0.0001 as compared to WT mice (Student's t-test).

To determine if presynaptic DA dynamics are similar or different across the discrete sub-regions of the striatum, recordings were made from the NAc core and shell. Similarly, electrically evoked DA release was significantly lower in the NAc of $BDNF^{+/-}$ mice as compared to wildtype mice. In the NAc core, an ~ 36% reduction in DA release was observed (wildtype: 1.1 ± 0.2 µM, n = 8 and $BDNF^{+/-}$: 0.7 ± 0.08 µM, n = 9; Figure 4.6A). An ~ 33% reduction in evoked DA release was observed in the NAc shell (wildtype: 0.6 ± 0.05 µM, n = 12 and $BDNF^{+/-}$: 0.4 ± 0.04 µM, n = 12; Figure 4.6A). A two-tailed t-test revealed a significant decrease in DA release between the two genotypes (NAc core: P = 0.024 and NAc shell: P = 0.034). However, no significant genotype difference in uptake rates was observed in the NAc core (wildtype: 2.3 ± 0.2 µM/s, n = 8 and $BDNF^{+/-}$: 2.0 ± 0.2 µM/s, n = 9) and NAc shell (wildtype: 1.2 ± 0.08 µM/s, n = 12 and $BDNF^{+/-}$: 1.1 ± 0.08 µM/s, n = 12; Figure 4.6B). A two-tailed t-test revealed no genotype difference in the uptake rates (NAc core: P = 0.22 and NAc shell: P = 0.22).

To better understand how low, endogenous BDNF levels influence electrically evoked DA release, the number of stimulation pulses (p) was varied from 1 to 5. Upon electrode placement and obtaining a stable baseline, both 1 pulse and 5 pulse FSCV measurements were made in the same location, to reduce the impact of regional variation. Area under curve (AUC) in arbitrary units was used to analyze the maximal evoked DA release levels.

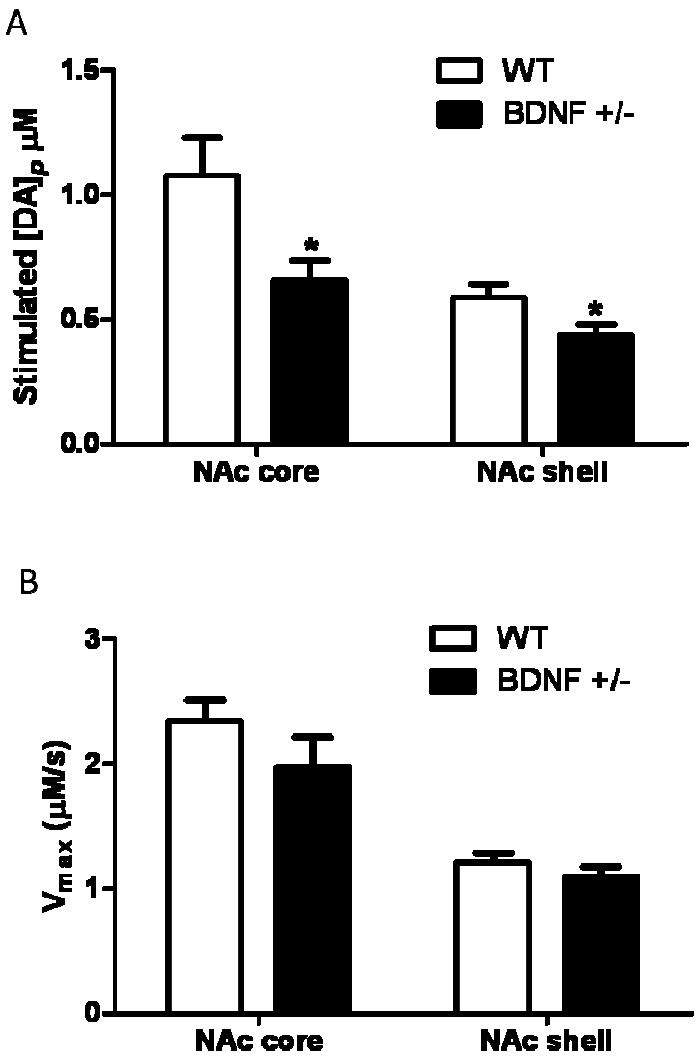

Figure 4.6 Single pulse electrically evoked dopamine (DA) release (A) and maximum velocity (V_{max}, uptake rate) (B) measured using slice FSCV in nucleus accumbens (NAc) of wildtype (WT) and $BDNF^{+/-}$ mice. Data are means ± SEMs (n = 8 – 12 mice per group). *$P < 0.05$ as compared to WT mice (Student's t-test).

Increasing the number of pulses led to an increase in stimulated DA release in both wildtype and $BDNF^{+/-}$ mice (Figure 4.7 parts A and B, respectively). The data was then normalized to a ratio (DA_{5p}/DA_{1p}, AUC; Figure 4.7C). The ratios for wildtype mice were: CPu, 1.5 ± 0.1, n = 12; NAc core, 2.1 ± 0.3, n = 8; and NAc shell, 3.0 ± 0.4, n = 9. Additionally, the ratios for $BDNF^{+/-}$ mice were: CPu, 1.7 ± 0.1, n = 13; NAc core, 2.2 ± 0.3, n = 6; and NAc shell, 2.2 ± 0.3, n = 9. Two-way ANOVA analysis revealed a significant main effect of striatal region ($F_{1,40}$ = 20.25, P < 0.0001) and genotype x striatal region interaction ($F_{1,40}$ = 4.60, P = 0.038). However, no significance genotype effect was observed ($F_{1,40}$ = 2.26, P = 0.14). Bonferroni post-test revealed only a significant difference (P < 0.001) between NAc shell and CPu of wildtype mice, but not $BDNF^{+/-}$ mice. Taken together, these results indicate a reduction in stimulated DA_{5p} release in the NAc shell of BDNF-deficient mice.

4.3.4 Effect of exogenous BDNF on electrically evoked dopamine release

Numerous reports suggest that exogenously applied BDNF is able to enhance DA release (*29-31*). To understand how exogenous of BDNF influences presynaptic DA dynamics, electrically evoked DA release (Figure 4.8A), and uptake rates (Figure 4.8B) were monitored every 5 minutes following direct application of BDNF (100 ng/mL) to a slice for 30 minutes. Two-way ANOVA of electrically stimulated DA release showed a significant main effect of treatment ($F_{1,36}$ = 33.01, P < 0.0001), genotype ($F_{1,36}$ = 218.5, P < 0.0001), and a genotype x treatment interaction ($F_{1,36}$ = 15.56, P < 0.001). Bonferroni post-test revealed that exogenous application of BDNF significantly increases DA release by ~ 17% in $BDNF^{+/-}$ mice (P < 0.001, n = 5), with no effect in wildtype mice (n = 5). BDNF-mediated increase in electrically evoked DA release was

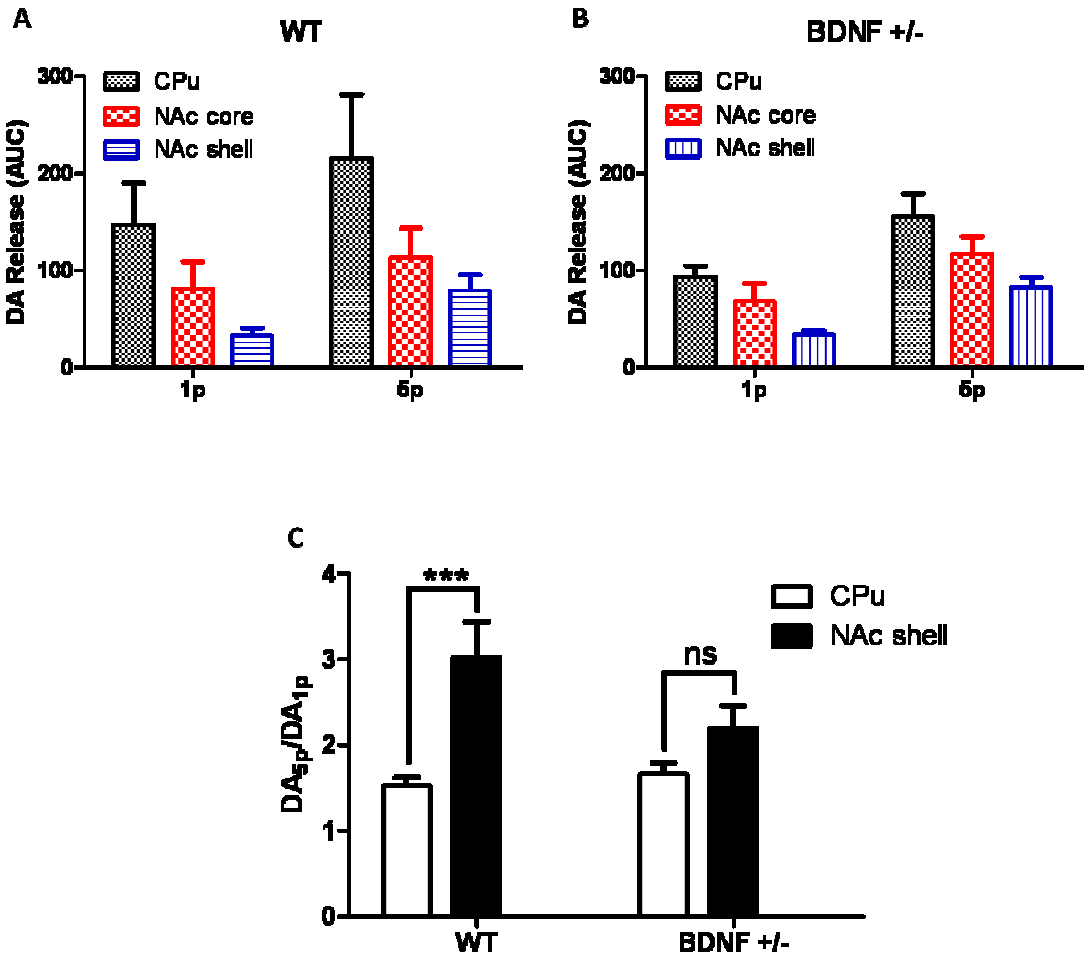

Figure 4.7 Effect of single and multiple pulse (1p and 5p) stimulation on dopamine (DA) release on brain slices, measured as area under curve (AUC) using FSCV. AUC obtained in caudate putamen (CPu) and nucleus accumbens (NAc core and NAc shell) of wildtype (WT) (A) and $BDNF^{+/-}$ (B) mice. (C) Ratio of DA release (DA_{5p}/DA_{1p}) in WT and $BDNF^{+/-}$ mice. Data are means ± SEMs (n = 6 – 13 mice per group), two-way ANOVA (Bonferroni post-test), ***P < 0.001, no significance (ns, P > 0.05). NAc core AUC ratio exempted for clarity.

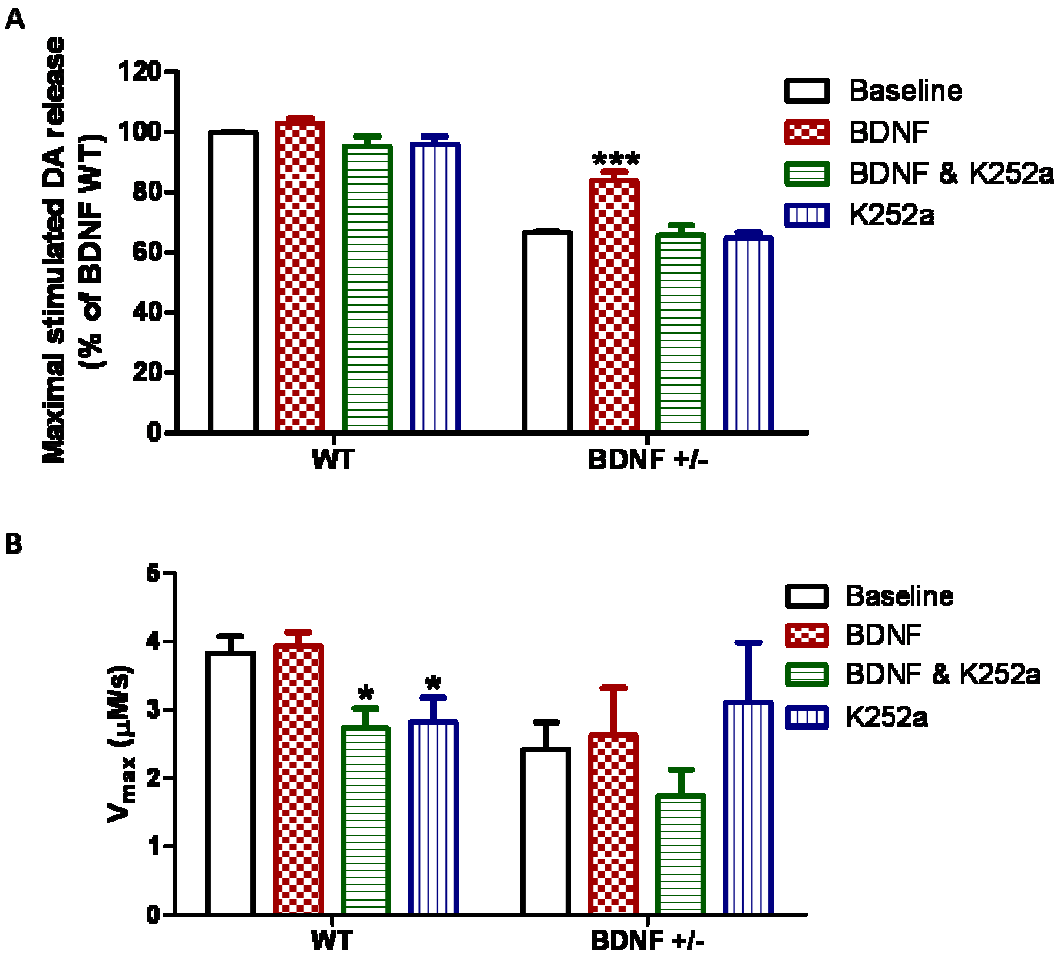

Figure 4.8 Effect of exogenous application of BDNF (100 ng/mL) on dopamine (DA) release and uptake rates in the caudate putamen (CPu) of wildtype (WT) and $BDNF^{+/-}$ mice. (A) Normalized single pulse, electrically evoked DA release (represented as % of WT baseline) and (B) DA uptake rates in WT and $BDNF^{+/-}$ mice before and after 30 minute perfusion of either 100 ng/mL BDNF, 1 µM K252a, or both in the CPu. Data are means ± SEM (n = 4 – 5 mice per treatment group). ****P* < 0.001 compared to untreated $BDNF^{+/-}$ mice (two-way ANOVA). **P* < 0.05 as compared to WT mice baseline (one-way ANOVA).

blocked by perfusion of TrkB inhibitor K252a in $BDNF^{+/-}$ mice. No change in DA uptake rate was observed after BDNF perfusion in either wildtype or $BDNF^{+/-}$ mice. However, perfusion of K252a on slices from wildtype mice lowered the uptake rate significantly as analyzed using one-way ANOVA (Dunnett's post-test, $P < 0.05$, n = 5 mice per group).

Increasing concentrations of exogenous BDNF (50, 100, and 200 ng/mL) led to a dose-dependent increase in electrically stimulated DA release in $BDNF^{+/-}$ mice brain slices (Figure 4.9A). One-way ANOVA ($F_{3,36} = 9.42$; $P < 0.0001$, n = 5) followed by Dunnett's post-test revealed that each concentration of BDNF increased DA release significantly. However, no difference in V_{max} (DA uptake rates) was observed upon increasing BDNF concentration in $BDNF^{+/-}$ mice ($F_{3,36} = 0.013$; $P = 1.00$; n = 5; Figure 4.9B).

Our results from a single 30-minute treatment with 1 µM K252a showed a significant reduction in DA uptake rates in wildtype mice but not $BDNF^{+/-}$ mice (Figure 4.8). To determine whether inhibition of the TrkB receptor is able to modulate DA dynamics in a dose-dependent manner, increasing concentrations of K252a (0.1, 0.3, 1 and 3 µM) were perfused on brain slices of wildtype mice and single pulse electrically evoked DA release and uptake rates were monitored. Perfusion of increasing concentrations of K252a reduced the stimulated DA release significantly (relative to baseline; Figure 4.10A) as analyzed using one-way ANOVA ($F_{4,25} = 4.06$; $P = 0.011$, n = 3). Interestingly, Dunnett's post-test revealed a significant ($P < 0.05$) reduction in stimulated DA release only at the highest concentration (3 µM), but not the other concentrations of K252a applied. Increasing the concentration of K252a led to a reduction in V_{max} in a dose-dependent manner (Figure 4.10B). One-way ANOVA

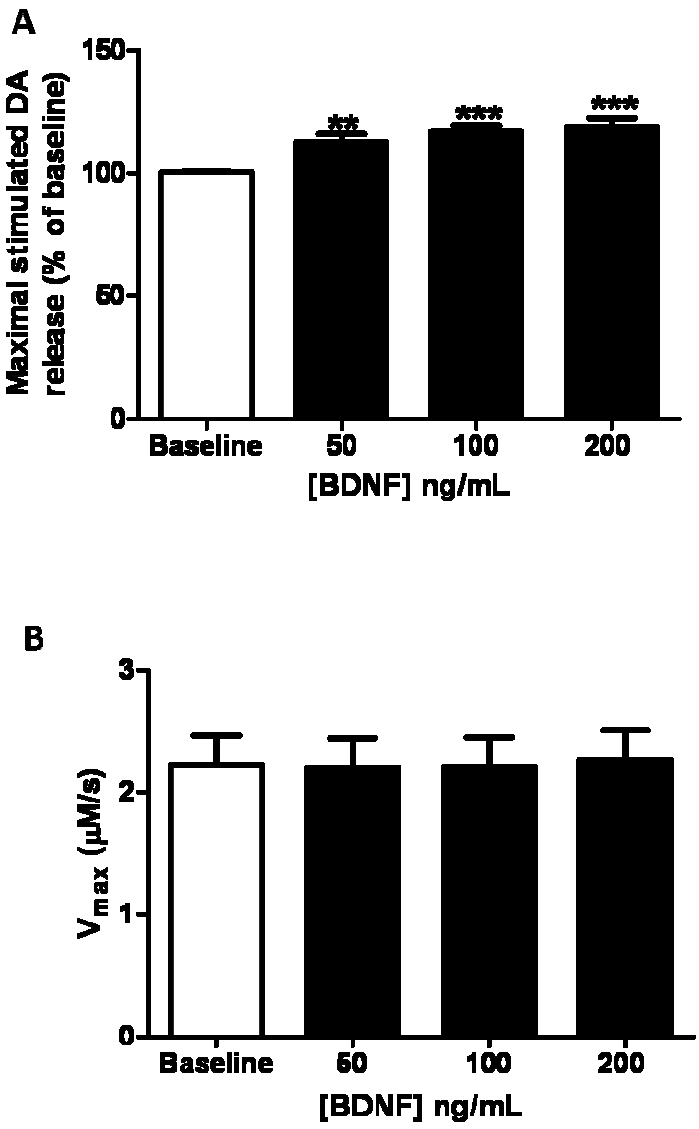

Figure 4.9 Effect of increasing concentrations of BDNF (50, 100, and 200 ng/mL) on dopamine (DA) release and uptake rates in the caudate putamen (CPu) of $BDNF^{+/-}$ mice. (A) Normalized single pulse electrically evoked DA release (represented as % of baseline) and (B) Corresponding maximum velocity (V_{max}) after perfusion of increasing concentrations of BDNF. Data are means ± SEM (n = 5 mice). ***P* < 0.01, ****P* < 0.001 for baseline compared to BDNF treatments (one-way ANOVA, Dunnett's post-test).

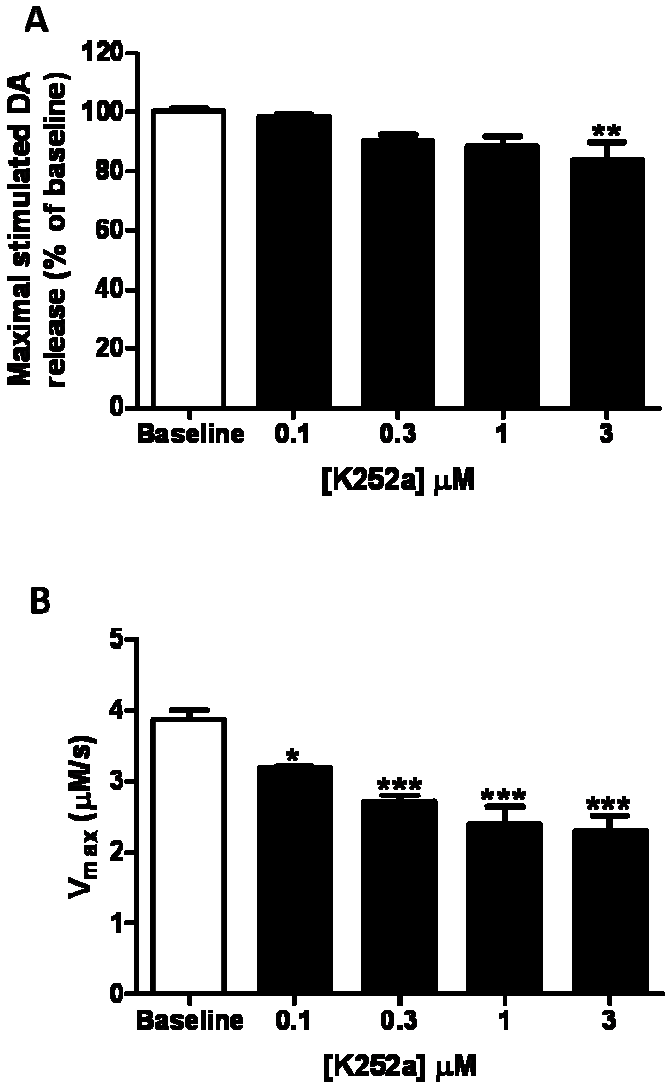

Figure 4.10 Effect of increasing concentrations of K252a (0.1 – 3 μM) on dopamine (DA) release and uptake rates in the caudate putamen (CPu) of wildtype mice. (A) Normalized single pulse electrically evoked DA release (represented as % of baseline) and (B) corresponding maximum velocity (V_{max}) after perfusion of increasing concentrations of K252a. Data are means ± SEMs (n = 3 mice). *P < 0.05, **P < 0.01, ***P < 0.001 for baseline as compared to K252a treatments (one-way ANOVA, Dunnett's post-test).

analysis ($F_{4,25}$ = 14.93; P < 0.0001, n = 3) followed by Dunnett's post-test revealed that each concentration of K252a significantly decreased V_{max}.

4.3.5 Dopamine D3 and D2 autoreceptor functionality in BDNF$^{+/-}$ mice

Increasing concentrations of the DA D3 agonist 7-OH-DPAT were perfused over a mouse brain slice to evoke D3 autoreceptor-mediated inhibition of DA release. Single pulse electrically stimulated DA release was monitored in BDNF$^{+/-}$ and wildtype mice in the NAc shell due to its high D3 receptor expression and sensitivity to D3 activation (Section 3.3.2) (*36*). The log concentration of the D3 agonist was plotted against the normalized concentration of DA to obtain dose response curves for each genotype and corresponding EC_{50} values.

The EC_{50} value for wildtype mice was 39 ± 6 nM (n = 9) and 118 ± 16 nM (n = 5) for the BDNF$^{+/-}$ mice. Analysis of the EC_{50} values using Student's t-test revealed a significant difference (P < 0.0001; Figure 4.11A). This suggests a reduction in DA D3 presynaptic receptor function in the NAc shell of BDNF$^{+/-}$ as compared to wildtype mice. Additionally, we evaluated the effect of increasing 7-OH-DPAT concentration on DA uptake rates. In the NAc shell, 7-OH-DPAT did not alter the uptake rates in either wildtype (Figure 4.11B) or BDNF$^{+/-}$ mice (Figure 4.11C) as analyzed using one-way ANOVA with Dunnett's post-test (wildtype: $F_{6,48}$ = 0.93, P = 0.48, n = 9 and BDNF$^{+/-}$: $F_{6,33}$ = 1.26, P = 0.30, n = 5).

Similarly, the DA D2 receptor agonist quinpirole was used to probe the effect of low levels of BDNF on the functionality of D2 autoreceptor in the CPu. Increasing concentrations of quinpirole were perfused over a slice and FSCV was used to monitor electrically stimulated DA release and uptake rates. The log concentration of quinpirole

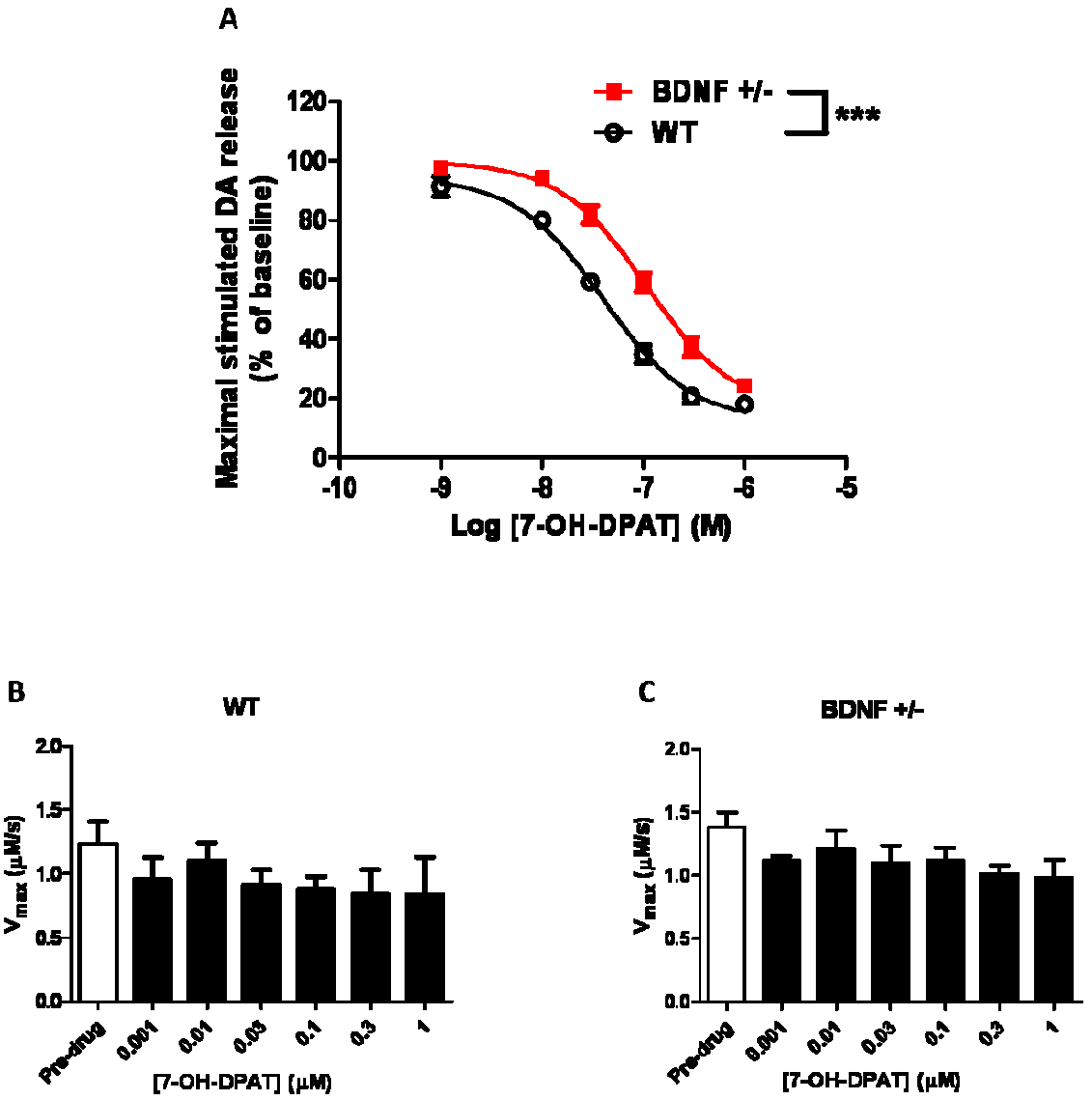

Figure 4.11 Effect of the dopamine (DA) D3 agonist 7-OH-DPAT on DA release and uptake rates as measured using FSCV in the nucleus accumbens (NAc) shell. (A) Dose response curves for inhibition of electrically stimulated DA efflux in the wildtype (WT) and $BDNF^{+/-}$ mice. Effect of 7-OH-DPAT concentrations on maximum velocity (V_{max}) in the NAc shell of WT mice (B) and $BDNF^{+/-}$ mice (C). Analysis of the EC_{50} values using Student's-t test revealed significant reduction in DA D3 receptor functionality (****P* < 0.0001). No change in uptake rates was observed for either genotype (one-way ANOVA, Dunnett's post-test, n = 5 for $BDNF^{+/-}$ mice and n = 9 for WT mice).

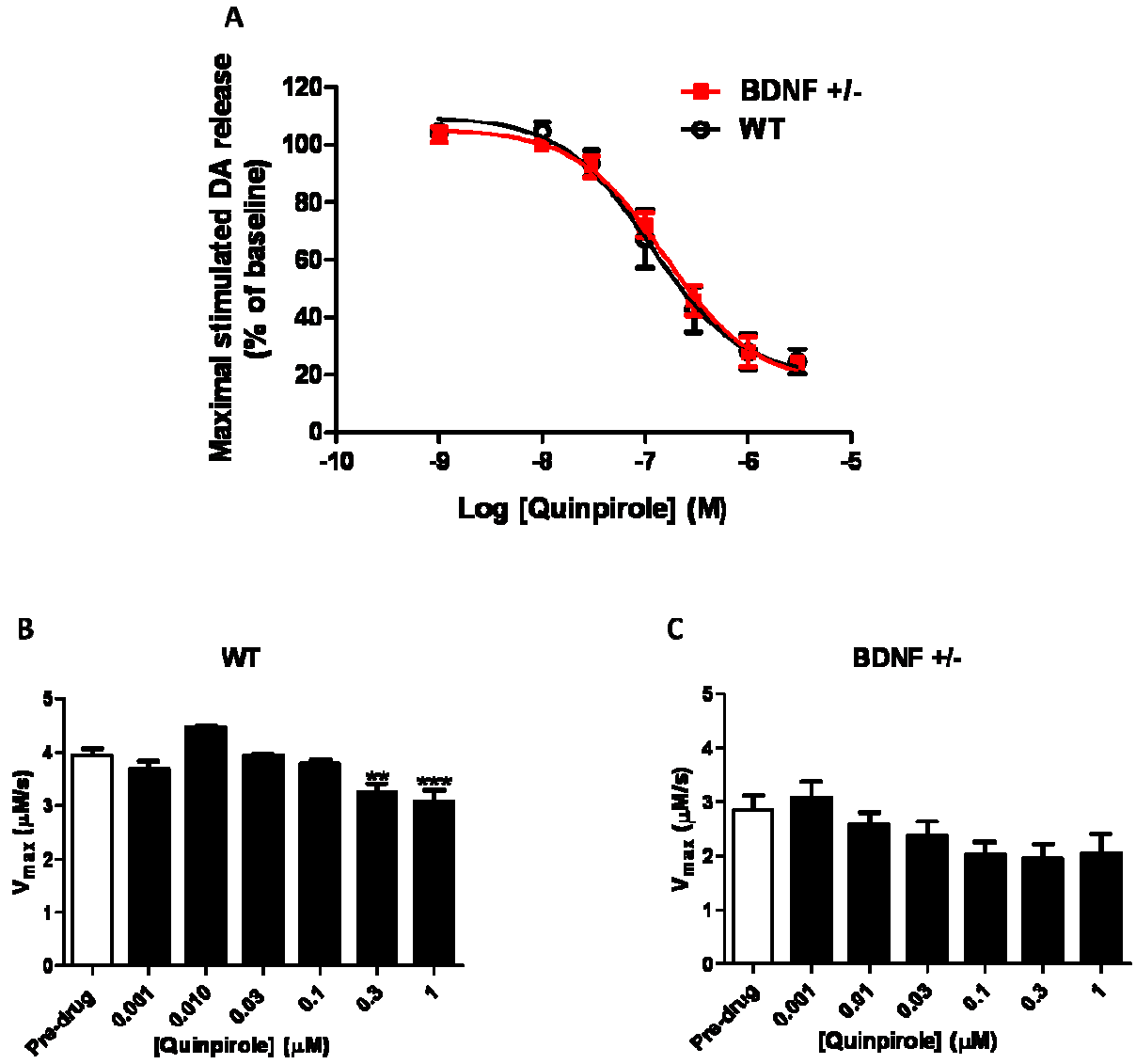

Figure 4.12 Effect of dopamine (DA) D2 agonist quinpirole on DA release and uptake rates measured using FSCV in the caudate putamen (CPu). (A) Dose response curves for inhibition of electrically stimulated DA efflux in wildtype (WT) and BDNF$^{+/-}$ mice. The effect of quinpirole on maximum velocity (V_{max}) in WT mice (B) and BDNF$^{+/-}$ mice (C). Analysis of the EC_{50} values using Student's-t test revealed no significant change in DA D2 receptor functionality. Concentrations greater than 0.1 μM reduced the uptake rate in WT mice with no change in uptake rate observed in BDNF$^{+/-}$ mice (one-way ANOVA, Dunnett's post-test), $^{**}P < 0.01$, $^{***}P < 0.001$ (n = 5 for BDNF$^{+/-}$ mice and n = 7 for wildtype mice).

was plotted against the normalized concentration of DA to obtain dose response curves for each genotype (Figure 4.12A) and the corresponding EC_{50} values. The EC_{50} value for wildtype and $BDNF^{+/-}$ mice were 114 ± 35 nM (n = 7) and 156 ± 32 nM (n = 5), respectively. The EC_{50} values were not different as analyzed using Student's-t test. The results show a significant decrease in V_{max} (uptake rate) in the presence of high concentrations of quinpirole in the CPu of wildtype mice ($F_{6,52} = 6.67$, $P < 0.0001$, n = 7; Figure 4.12B), but not in $BDNF^{+/-}$ mice ($F_{6,65} = 2.05$, $P = 0.074$, n = 5; Figure 4.12C).

4.4 Discussion

4.4.1 Hyperdopaminergic state due to reduced dopamine release and clearance

There is considerable evidence suggesting the neurotrophic factor, BDNF modulates the striatal DA system (*35, 37, 133, 182, 191, 192*). In the present study, two complementary techniques, *in vivo* microdialysis and slice voltammetry were employed to probe the role of low endogenous BDNF levels on striatal DA dynamics. Electrically evoked DA release and uptake rates in the CPu were attenuated in $BDNF^{+/-}$ mice as compared to their wildtype littermates. Exogenous BDNF perfusion partially restored the reduced DA release observed in $BDNF^{+/-}$ mice. On the other hand, BDNF-deficient mice exhibited no differences in DA synthesis or catabolism in the CPu. Interestingly, in the NAc core and shell only electrically stimulated DA release was attenuated in $BDNF^{+/-}$ mice, while no difference was observed in DA uptake rates. Together, these findings suggest that BDNF regulates presynaptic DA homeostasis by altering DA release, which appear to influence extracellular DA levels leading to a compensatory response by DA transporter.

This is the first study to use the microdialysis technique of zero net flux to estimate "true" basal extracellular levels of DA in BDNF-deficient mice. Extraneuronal DA levels in BDNF-deficient mice were elevated (~ 12 nM) in the CPu compared to basal DA levels from wildtype mice (~ 5 nM). The slice FSCV results indicate reduced uptake rates likely account for the increased basal levels of DA in $BDNF^{+/-}$ mice. Furthermore, previous studies in the $BDNF^{+/-}$ mice have shown that DA transporter expression is not altered, suggesting that low endogenous BDNF levels may alter the function of the DA transporter (*37, 133*). One possible mechanism as to how BDNF may mediate DA transporter activity is through the second-messengers linked to BDNF-TrkB signal transduction pathways. Specifically, activation of protein kinase C (PKC), extracellular signal-regulated kinases 1 and 2 (ERK1/2), and phosphatidylinositol-3-kinase (PI3K) pathways have been linked to regulation of DA transporter activity (*171-173*).

Extracellular levels of neurotransmitters measured by microdialysis represent a balance between release and uptake processes, the effect of BDNF-deficiency on DA exocytotic release and DA transporter-mediated uptake was differentiated with slice FSCV. Both stimulated release and the velocity of DA uptake was reduced in $BBDNF^{+/-}$ mice. Interestingly, this decrease in stimulated DA release and DA uptake rates in $BDNF^{+/-}$ mice was similar to presynaptic DA dynamics observed in DA transporter heterozygous mice ($DAT^{+/-}$ mice; with a 50% reduction in DA transporter expression) (*193*). In $DAT^{+/-}$ mice, the decrease in stimulated DA release was hypothesized to be a compensatory response to the excess extracellular DA levels due to the reduced uptake. To determine if the low endogenous BDNF levels can directly contribute to the

blunted DA release or uptake observed, exogenous BDNF was applied to the slice for 30 minutes. DA release upon stimulation was elevated by ~ 17% in the $BDNF^{+/-}$ mice, while exogenous BDNF application lead to no alteration in DA uptake rates. Slice FSCV measures DA release mainly from the readily releasable pool of vesicles (*63, 194*). Since BDNF is thought to enhance quantal neurotransmitter release by increasing the number of docked synaptic vesicles as well as increasing DA firing frequency within presynaptic terminals, further experiments are necessary to determine if the decrease in electrically stimulated DA release in BDNF-deficient mice is due to a decrease in one or both of these parameters (*185*). Indeed, $BDNF^{+/-}$ mice have impaired hippocampal presynaptic transmitter release that is associated with fewer docked vesicles in the active zone and lower synaptosomal levels of synaptobrevin and synaptophysin, which assist in vesicle docking and fusion (*185, 187, 195*). These effects are reversed with addition of exogenous BDNF (*187*).

4.4.2 Reduced multiple-pulse electrically stimulated dopamine release in nucleus accumbens

Neuronal DA transmission is dynamic, resulting from a combination of tonic DA release (~ 4 Hz; ‘rhythmic firing’) and short, but intense burst firing of DA neurons (phasic firing) (*196*). Extracellular DA levels measured over a period of 10 – 20 minutes by *in vivo* microdialysis are thought to primarily reflect tonic DA release, where burst firing is averaged over this period (*103*). DA transients resulting from bursts of DA cell firing in the VTA are detected in the NAc using *in vivo* FSCV (*56, 65, 91, 101, 197-199*). FSCV is ideal for measuring DA transients due to its fast temporal resolution (~ 100 ms), since DA transients are typically a few milliseconds in duration, FSCV allows for

discrete detection of multiple bursts (*89, 197*). Results demonstrate that BDNF$^{+/-}$ mice have reduced singe-pulse electrically stimulated DA release in the striatum (CPu and NAc) as compared to their wildtype controls.

To better understand the role of low BDNF levels on DA release, the number of stimulation pulses for DA release was varied (1p versus 5p) in the striatal complex (CPu, NAc core and shell) in both wildtype and BDNF$^{+/-}$ mice. When examining pulse trains, the AUC of the current versus time plot was examined and not the discrete parameters of DA release and uptake. In both genotypes, the CPu showed the greatest amount of electrically stimulated DA release, while the NAc shell had the least, which is consistent with previous reports (*101*). When the AUC ratio (DA_{5p}/DA_{1p}) was evaluated, wildtype mice had the lowest DA ratio in the CPu, while the shell had a significantly greater ratio. Interestingly, the DA_{5p}/DA_{1p} ratio in the BDNF$^{+/-}$ mice was not different between the CPu and NAc. Taken together, these results suggest that mice with low endogenous BDNF levels may have impaired DA burst firing in the NAc shell. However, to truly understand if burst firing is compromised in these mice future studies will need to use *in vivo* FSCV to probe DA burst firing.

4.4.3 Reduced dopamine D3 autoreceptor function

Stimulation of DA D2-like receptors on presynaptic nerve terminals results in feedback inhibition, which homeostatically regulates extracellular levels of DA via inhibition of DA synthesis and release (*19, 20*). Our microdialysis data show that basal extracellular DA levels are elevated in BDNF$^{+/-}$ mice as compared to wildtype mice, hypothesized to result from the reduced DA uptake rates. However, the long-term consequences of elevated extracellular DA levels may lead to either a change in

autoreceptor expression or function in the CPu (*14*). Furthermore, numerous studies in BDNF-deficient mice have demonstrated that BDNF modulates release-regulating DA D3 receptor expression (*36, 37, 200*). For example, both mice lacking BDNF (BDNF knockout) and $BDNF^{+/-}$ mice have reduced DA D3 levels in the CPu and NAc (*36, 37*).

Since our dialysis results indicate increased extracellular DA levels in the CPu, our first step was to determine if these elevated extracellular levels lead to alterations in presynaptic DA D2 receptor function. Interestingly, DA D2 autoreceptor function was not altered by the increase in extracellular DA levels in the CPu, which has a high density of D2 receptors (Section 3.3.1) (*17, 158*). This finding suggests release- and synthesis-regulating DA D2 autoreceptors are not affected by the hyperdopaminergic state observed in the CPu. Furthermore, our results are consistent with a previous study that reported DA D2 receptor expression is not affected by BDNF deficiency in the NAc shell (*36*). However, future work needs to evaluate the functionality of DA D2 autoreceptor in other regions such NAc shell to determine whether modulation of DA D2 receptors is region-specific in $BDNF^{+/-}$ mice.

Although no changes were seen in DA D2 receptors in the CPu, the next step was to determine if $BDNF^{+/-}$ mice showed a decrease in DA D3 autoreceptor functionality in the NAc, as has been previously documented (*36, 37*). Slice FSCV results in the NAc shell indicated that $BDNF^{+/-}$ mice had diminished DA D3 autoreceptor function compared to their wildtype littermates. This finding further highlights that low BDNF levels directly regulate DA D3 receptor function. Although we have not evaluated extracellular DA levels in the NAc using *in vivo* microdialysis, based on our slice voltammetry release and uptake results we would expect to see no difference in

extracellular DA levels. If this hypothesis does turn out to be valid it would further support the hypothesis that BDNF expression directly regulates presynaptic D3 autoreceptors with no influence from extracellular DA levels. To our knowledge, this is the first time that presynaptic DA D3 autoreceptor function has been shown to be reduced, since previous studies utilized radioligands, which map both pre- and post-synaptic DA D3 receptor density. Overall, a more careful evaluation of D2-like autoreceptors must be made in the striatum by examining not only extracellular DA levels but also proteins such as BDNF to better understand how it controls the functionality and/or expression of these receptors.

4.4.4 Exogenous BDNF increases electrically stimulated dopamine release

Interestingly, both *in vivo* microdialysis and slice voltammetry show opposite differences in stimulated DA release in BDNF-deficient mice. To better under if BDNF regulates DA release exogenous application of BDNF was applied to brain slices. When a 100 ng/mL of BDNF was exogenously applied to a brain slice, only $BDNF^{+/-}$ mice showed a ~ 17% increase in electrically stimulated DA release, while no difference in DA uptake. However, exogenous BDNF did not affect electrically-stimulated DA release in wildtype mice. These findings suggests that the BDNF receptor; TrkB, in BDNF-deficient mice is either (1) supersensitive and/or (2) exogenous application of BDNF enhances DA release. This is not the first evidence suggesting that TrkB activation via BDNF leads to an increase in synaptic transmission. For example, Lohof *et al.* were the first to show that BDNF can acutely potentiate both stimulated synaptic responses and the frequency of miniature synaptic events (*201*). Several subsequent reports have shown that exogenously applied BDNF is indeed capable of enhancing synaptic events

such as DA release both *in vivo* and *in vitro* (*29-31*). BDNF signaling is mediated by the TrkB receptor (*10, 22*). To examine whether the TrkB receptor can mediate DA dynamics of release and uptake, a potent non-selective Trk receptor antagonist, K252a, was perfused over the slice for 30 minutes and DA dynamics were monitored every 5 minutes (*202*). Perfusion of K252a alone had no effect on electrically stimulated DA release in either genotype. When the slices were treated with both BDNF and the TrkB receptor antagonist, the BDNF-mediated increase in electrically evoked DA was blocked in the $BDNF^{+/-}$ mice suggesting that the TrkB receptor mediates DA release.

However, K252a rapidly reduced the rate of DA uptake in the wildtype mice, but not in the $BDNF^{+/-}$ mice. Considering no alterations were observed in DA transport when exogenous BDNF was applied to the slices, these differences in DA uptake were surprising in the presence of K252a. Upon increasing the concentration of K252a from 0.1 to 3 µM exhibited that K252a reduces the V_{max} in a dose-dependent manner with no effect on electrically stimulated DA release at lower concentrations. This is in agreement with previous work where inhibition of tyrosine kinases by genistein or tyrphostin 23 resulted in a rapid (5 – 15 minute), dose-dependent decrease in [^{3}H]DA uptake rate in synaptosomal preparation (*203*).

The mechanisms underlying the ability of 1) exogenous BDNF to potentiate DA release and 2) TrkB receptor inhibition with K252a to modulate DA uptake rate are not known. However, previous studies have shown that BDNF perfusion to hippocampal cells and nerve-muscle cultures rapidly increases cytoplasmic Ca^{2+} (*204, 205*). Additionally, extracellular Ca^{2+} influx through voltage-gated Ca^{2+} ion channels and *N*-methyl-D-aspartate receptors is required for BDNF-induced synaptic potentiation (*204-*

208). BDNF signaling through TrkB receptor increases intracellular Ca^{2+} concentration, suggesting that TrkB activation may result in modulating downstream signaling events, and consequently increasing DA available for release (*209*).

TrkB receptors undergo rapid BDNF-induced internalization and K252a prevents TrkB internalization induced by BDNF (*207, 208, 210*). Current evidence suggests that inhibition of tyrosine kinases, PI3K, MAPK, and ERK1/2 decreases DA transporter activity by decreasing V_{max} (*152, 172, 173, 203, 211, 212*). Therefore, inhibition of the TrkB receptor using K252a appears to inhibit the BDNF-signaling events and ultimately reducing DA transporter function. More studies are required to determine the specific BDNF-signaling pathways that may be involved. Noteworthy, high concentrations of K252a may have non-specific binding to other kinases including those that modulate DA transporter activity directly such as Ca^{2+}/calmodulin-dependent protein kinases II (CaMKII) (*213*).

4.4 Conclusions

The main goal of this work was to understand how low, endogenous BDNF levels regulate presynaptic DA dynamics in the striatal complex. The present results show that electrically stimulated DA release and DA uptake rates are attenuated in the CPu of mice expressing low BDNF levels compared to their wildtype littermates. Conversely, DA release but not DA uptake was decreased in the NAc of $BDNF^{+/-}$ mice. DA synthesis and metabolism were not altered, indicating that the increased basal extracellular DA levels observed in the CPu of $BDNF^{+/-}$ mice using microdialysis is likely related to a decrease in DA uptake function. Although our results highlight a change in DA transporter function, we hypothesize that the alterations in DA release detected in $BDNF^{+/-}$ mice is the primary mechanism by which endogenous BDNF regulates

presynaptic DA dynamics. Thus, the alterations observed in the DA transporter function are a compensatory response to reduced stimulated release. Exogenous BDNF rescues DA release in a dose-dependent manner. Exact mechanism of how BDNF increases the amount of DA released is unknown but our results combined with those obtained by Pozzo-Miller *et al.* would suggest alterations in either the number of vesicles in the readily releasable pool or alterations in the proteins required for the docking of the vesicles in BDNF-deficient mice. Furthermore, the results not only indicate alterations in DA release and uptake, but that low BDNF levels reduce DA D3 autoreceptor function.

Overall the results obtained reveal significant impairment in DA functions in mice with reduced endogenous levels of BDNF. We hypothesize that the combination of low endogenous BDNF levels with the observed hyperdopaminergic system may have detrimental consequences for addiction liability and neurological disorders. Specifically, the hyperdopaminergic state due to low BDNF levels suggests that BDNF hypofunction may play crucial role in disorders related to enhanced dopaminergic transmission, such as ADHD. Finally, this work has implications for the development of therapeutic agents that will target BDNF signaling and possibly expression may lead to significant alterations in the DA system.

CHAPTER 5

The Impact of Low Endogenous BDNF Levels and Aging on Striatal Dopamine Dynamics

5.1 Introduction

The age-related decline in structure and function of neuronal systems affects both motor and memory functions (*102, 133, 214, 215*). These age-related neuronal adaptations parallel human aging as well (*216, 217*). Dopamine (DA) neuron dysregulation has been found to play a major role in motor and cognitive impairment in rodents, non-human primates, and humans (*218-222*). Studies in humans have shown that a decline in the number of dopaminergic neurons in the substantia nigra (SN) occurs during the normal process of aging, and is accelerated in Parkinson's disease patients (*222-225*). Parkinson's disease is a neurological disorder that is associated with greater than 80% loss of DA neurons in the striatum. The most severe symptoms associated with Parkinson's disease involve dysregulation in the control of motor function, such as bradykinesia, resting tremor, and rigidity (*10, 40, 226, 227*).

The cause of normal age-related motor deficits is hypothesized to involve alterations in the function of DA neurons, not neuronal loss, as demonstrated in animal models of aging (*214, 221, 228*). There is considerable evidence that the reductions of DA function are related to a decrease in DA release, DA uptake rate, and vesicular monoamine transporter 2 (VMAT2) activity (*214, 221, 229*). However, others have reported that age-related DA dysfunction involves neuronal changes, such as reductions in both tyrosine hydroxylase (TH) and DA transporter densities in the SN of aged rodents (*230*). Moreover, the reduction in DA neuron function and/or structure is

associated with a decrease in locomotor activity in both aged rodents and humans (*214, 221, 224, 225*). However, the exact cause of the normal aging process on the DA system remains unknown.

Survival of neurons depends on continuous support from neurotrophic factors such as brain derived-neurotrophic factor (BDNF) and glial cell line-derived neurotrophic factor (GDNF). Specifically, it has been reported that dopaminergic neuron degeneration and/or dysfunction may be linked to age-related decreases in the levels of GDNF, BDNF, and neurotrophin 3 (NT-3) (*231-233*). Neurotrophins such as BDNF, GDNF, and NT-3 are involved in the regulation of growth, differentiation, survival, and maintenance of nigrostriatal DA neurons that control motor coordination (*21, 234*). Reduced expression of these trophic factors is proposed to enhance the vulnerability of DA neurons to degeneration and/or dysfunction from external stressors and neurotoxins with age (*231, 233*). In the normal process of aging, BDNF levels are known to decline by 14 – 52% in the nigrostriatal system of 24 – 26 month old rats (*179, 235*). Additionally, there is considerable evidence indicating that low levels of BDNF and aging are linked to neurodegenerative disorders such as Huntington’s disease, Parkinson’s disease, and Alzheimer’s disease (*41, 42, 46, 115-117, 236, 237*). Specifically, BDNF deficiency may be a critical mediator in Parkinson's disease, as surviving nigrostriatal DA neurons have reduced levels of BDNF. Additionally, there is a considerable sub-population of Parkinson’s disease patients that have the val66met single nucleotide BDNF gene polymorphism (*41, 42, 116, 238, 239*). These results suggest a link between BDNF levels and age-related degeneration and/or dysfunction of DA neurons.

With respect to animal models, BDNF$^{+/-}$ mice aged 11 to 21 months have reduced locomotor activity in beam walking, which is an assessment of fine motor coordination, as compared to their wildtype littermates (*34, 132*). BDNF$^{+/-}$ mice also exhibit enhanced age-related decline in accelerated rotarod performance (*133*). These reductions in motor coordination in BDNF-deficient mice are hypothesized to be associated with attenuation in nigrostriatal DA system function, because dopaminergic axonal innervations in the dorsal striatum, SN, VTA, and NAc (core and shell) do not differ between wildtype and BDNF$^{+/-}$ mice at 26 months of age (*240*). With respect to key modulators of the striatal dopaminergic system, such as TH, DA transporter, and VMAT2 expression, BDNF-deficient mice at 21 months of age are not different from wildtype mice (*133*). Although DA transporter and VMAT2 expression are not different between the two genotypes at 21 months of age, the function of the DA transporter (from 12 months) and VMAT2 (from 3 months) is attenuated with age in the BDNF$^{+/-}$ mice as compared to wildtype mice (*133*). With respect to stimulated DA release, high K^+- artificial cerebrospinal fluid (aCSF) in aged BDNF$^{+/-}$ mice exhibited a reduced DA response compared to wildtype mice (*133*). Taken together, these findings emphasize the crucial role of BDNF in augmenting DA dynamics during the aging process.

To better understand if lifelong decrements in BDNF levels and the aging process influence the dopaminergic system, BDNF$^{+/-}$ mice were evaluated at ~ 18 months of age and compared to their wildtype littermate controls. To understand how striatal DA dynamics adapt with respect to time, the results from ~ 18 month old mice were compared with the younger (~ 3 month old) mice (CHAPTER 4). Characterization of the ~ 3 month old BDNF$^{+/-}$ mice showed a hyperdopaminergic phenotype,

characterized by both reduced DA uptake rates and elevated basal DA levels that are believed to be attributed to the DA system compensating for reduced DA release (CHAPTER 4). Therefore, we hypothesized that a lifetime with ~ 50% reduction in BDNF protein levels would cause significant impairments on the DA system in $BDNF^{+/-}$ mice compared to the wildtype mice. DA dynamics at ~ 18 months of age were evaluated using slice FSCV to measure electrically stimulated DA release and DA uptake rates. Additionally, *in vivo* microdialysis in freely moving mice was used to measure extracellular basal levels of DA by use of the zero net flux method, as well as extracellular levels of DA catabolites, 3,4-dihydroxyphenylacetic acid (DOPAC) and homovanillic acid (HVA).

5.2 Materials and methods

Johnna A. Birbeck performed all the microdialysis experiments on aged mice (~ 18 months of age), which involved stereotaxic surgery, probe implantation, and sample collection. Sample analysis included HPLC separation with electrochemical detection and chromatographic data analysis.

Wildtype and $BDNF^{+/-}$ mice offspring were raised as a colony in house and genotyped as described in Section 2.2. Male and female ($BDNF^{+/-}$ and wildtype) mice aged to at least 18 months were used for all neurochemical measurements. *In vivo* microdialysis experiments were performed as described in Section 2.5. Upon stereotaxic surgery, a microdialysis probe was implanted for neurotransmitter sampling. The dialysate from the CPu containing the analytes of interest (DA, DOPAC, and HVA) was analyzed by HPLC coupled to an electrochemical detector. Zero net flux technique was used to estimate basal extracellular levels of DA in the CPu of a freely behaving

mouse as described in Section 2.5. Slice FSCV experiments were performed as previously described in Section 2.4 with minor modifications.

5.2.1 Data analysis

Johnna A. Birbeck performed all the microdialysis samples analysis that included chromatographic analysis, statistical data analysis and graphing. Microdialysis results from the aged mice were directly compared to those of young adult mice, the results were obtained by Kelly E. Bosse, Ph.D., and the details of her contributions can be found in CHAPTER 4.

All values are reported as means ± standard errors of the means (SEMs). Zero net flux data were analyzed by linear regression to determine the x-intercept (DA_{ext}) and slope (E_d) for individual wildtype and $BDNF^{+/-}$ mice. Differences in DA_{ext} between genotypes were determined by a two-tailed Student's t-test. To evaluate the impact of aging on DA dynamics, data for young adult mice (~ 3 months, CHAPTER 4) and the aged mice (~ 18 months) were compared. Two-way ANOVA with a Bonferroni post-test was used to determine the impact of the independent variables of genotype and aging on stimulated DA release ($[DA]_p$) and uptake rates (V_{max}) evaluated with FSCV and extracellular catabolite levels (DOPAC and HVA) as measured by *in vivo* microdialysis. Results from one and five pulse stimulation were analyzed by determining the area under the curve (AUC) from the resulting current versus time plots to determine DA release (DA_{1p} and DA_{5p}, respectively). Data obtained from the one and five pulse stimulations were normalized as a ratio (DA_{5p}/DA_{1p}), because the electrode placement in the slice was not changed during the one and five pulse measurements. With respect to the one and five pulse stimulation parameters, a two-way ANOVA with a Bonferroni

post-test was used to determine the impact of the independent variables of genotype and brain region of interest. In all cases, statistical significance was defined as $P < 0.05$.

5.3 Results

5.3.1 DOPAC levels in aged BDNF-deficient mice

Johnna Birbeck performed all the microdialysis samples analyses that included chromatographic analysis, statistical data analysis and graphing. Microdialysis results from the aged mice were directly compared to those of young adult mice, the results were obtained by Kelly E. Bosse, Ph.D., and the details of her contributions can be found in CHAPTER 4.

To determine the long-term effect of low endogenous levels of BDNF on DA dynamics, *in vivo* microdialysis was used to determine striatal basal DA levels and extracellular concentrations of DA catabolites (DOPAC and HVA) in the CPu of aged $BDNF^{+/-}$ and wildtype mice. The basal concentrations of extracellular DA were determined using the zero net flux method (Figure 5.1). Apparent extracellular DA levels (DA_{ext}), corrected for recovery, did not differ ($P = 0.34$; two-tailed t-test) in aged $BDNF^{+/-}$ mice (7 ± 1 nM; n = 14) as compared to wildtype mice (6 ± 0.8 nM; n = 9). An advantage of the zero net flux method is that it approximates relative "*in vivo"* probe recovery from the slopes of the linear regression analyses, which is more commonly referred to as extraction fraction (E_d). Previous studies have suggested that changes in the slope relate to alterations in transporter. The average extraction fraction did not differ between aged wildtype (0.48 ± 0.06) and $BDNF^{+/-}$ mice (0.35 ± 0.06). To better understand the long-term consequences of low, endogenous BDNF levels on basal DA levels, a second

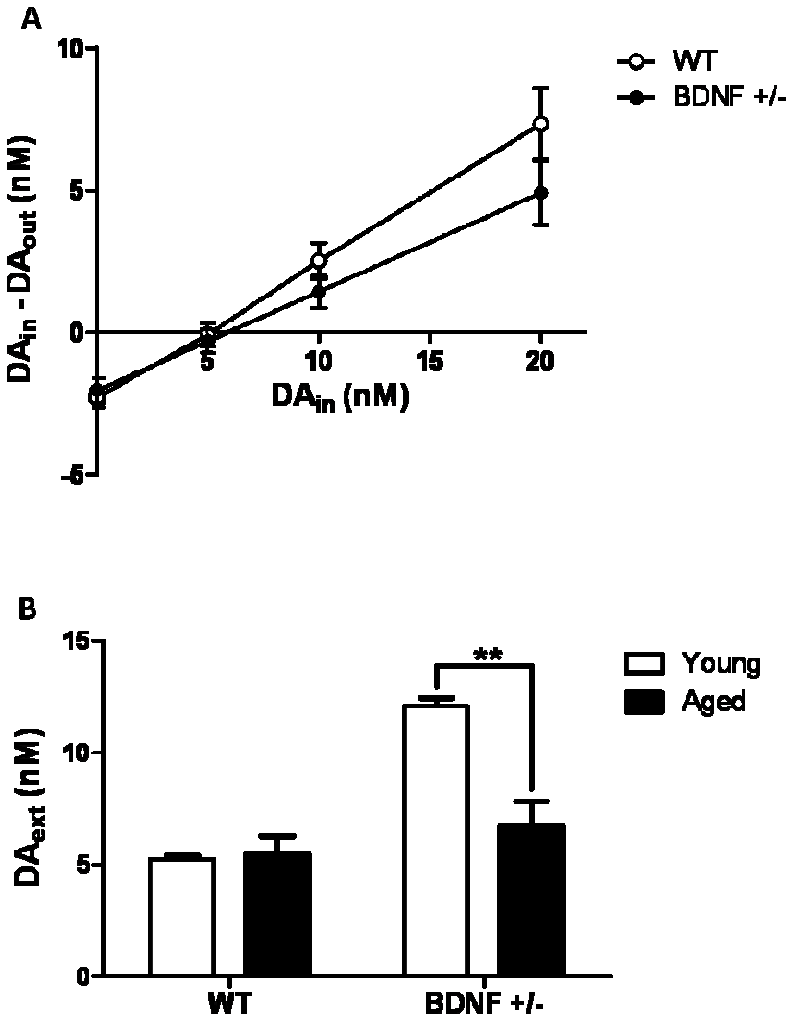

Figure 5.1 Basal extracellular levels of dopamine (DA) in the caudate putamen (CPu) of wildtype (WT) and BDNF$^{+/-}$ mice as measured using zero net flux. (A) Linear regression analysis of basal DA levels in aged mice (~ 18 months old), determined by zero net flux. The x-intercept represents an estimate of basal DA levels (DA_{ext}) and the slope of the line corresponds to the extraction fraction (E_d). (B) Summary of basal DA levels (DA_{ext}) from the CPu of young (~ 3 months old) mice and aged mice. Data are means ± SEMs of the apparent DA_{ext} (n = 6 – 14 mice). ***P* = 0.01, comparison of DA_{ext} levels between young and aged BDNF$^{+/-}$ mice using Student's t-test. *Figure courtesy of Johnna A. Birbeck, Kelly E. Bosse, Ph.D., and Tiffany A. Mathews, Ph.D.*

comparison was made between young (~ 3 months old, Figure 5.1B) and aged (~ 18 months old) mice. The basal DA levels in young adult (~ 5 nM) and aged (~ 6 nM) wildtype mice were not different (P = 0.86) as determined by zero net flux. In contrast, $BDNF^{+/-}$ mice showed a significant decrease in basal DA levels (young mice ~ 12 nM vs aged mice ~ 6 nM; $P < 0.01$).

DA catabolism was evaluated by measuring extracellular levels of DA catabolites, DOPAC and HVA, from baseline dialysis samples (average of three samples). Elevated extracellular DOPAC concentrations were observed in the CPu of $BDNF^{+/-}$ versus wildtype controls, where DOPAC levels for aged $BDNF^{+/-}$ mice were 910 ± 160 nM (n = 7), as compared to 460 ± 80 nM in aged wildtype mice (n = 14, Figure 5.2A). DOPAC concentrations in the young adult mice (Section 4.3.2) were ~ 410 nM (wildtype) and ~ 330 nM ($BDNF^{+/-}$). Two-way ANOVA revealed a significant main effect of aging ($F_{1,43}$ = 10.77, P = 0.002), genotype ($F_{1,43}$ = 5.10, P = 0.03), and genotype x aging interaction ($F_{1,43}$ = 6.38 P = 0.02). A Bonferroni post-test revealed that aging has a significant effect on extracellular DOPAC levels in $BDNF^{+/-}$ mice ($P < 0.01$), but not in wildtype mice ($P > 0.05$). Extracellular HVA concentrations were not different between aged wildtype and $BDNF^{+/-}$ mice (wildtype: 490 ± 70 nM, n = 14; $BDNF^{+/-}$: 690 ± 100 nM, n = 7; Figure 5.2B). Two-way ANOVA (Bonferroni post-test) analysis comparing the HVA levels in the young adult mice (wildtype: ~ 465 nM; $BDNF^{+/-}$: ~ 560 nM) and the aged mice was carried out. There was no age-related or genotype difference in HVA levels (Figure 5.2B). These data indicate that aging in BDNF-deficient mice results in an elevation of DA catabolism process.

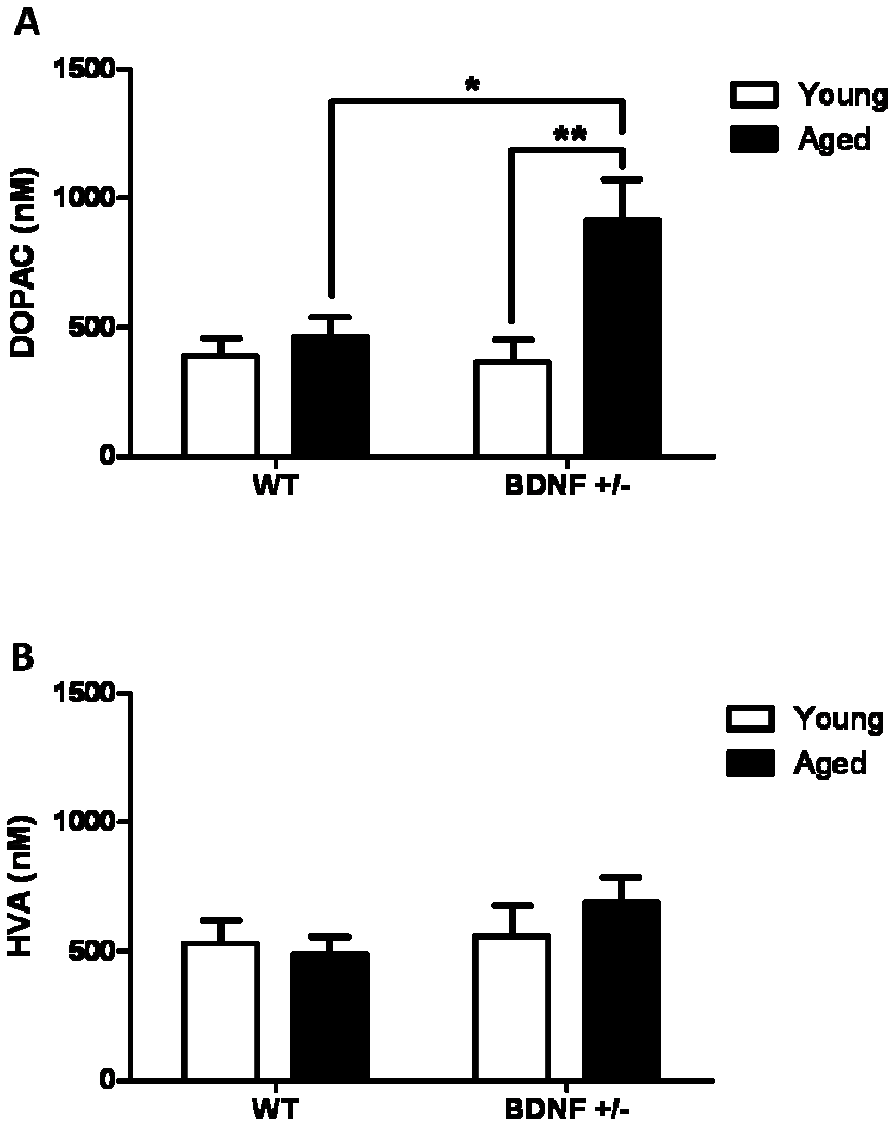

Figure 5.2 Dopamine catabolism in the caudate-putamen (CPu) of young and aged wildtype (WT) and BDNF$^{+/-}$ mice. (A) Extracellular DOPAC levels, as measured by microdialysis. (B) Extracellular HVA levels, determined by microdialysis. Data are reported as the mean ± SEM of uncorrected baseline values for young (~ 3 months) and aged (~ 18 months) mice (n = 7 – 16 mice). Two-way ANOVA (Bonferroni post-test) comparisons in DOPAC levels (*P < 0.05, **P < 0.01). *Figure courtesy of Johnna A. Birbeck, Kelly E. Bosse, Ph.D., and Tiffany A. Mathews, Ph.D.*

5.3.2 Aging differences in electrically stimulated dopamine release and uptake rates

FSCV was used to examine single pulse, electrically stimulated DA release and uptake rates in the CPu and NAc of aged mice (~ 18 months). As described previously (Section 2.2.5), the Michaelis-Menten based kinetic model was used to evaluate single pulse stimulated DA release concentration ($[DA]_p$) and uptake rate (maximum velocity, V_{max}) by fitting DA concentration versus time FSCV traces. No difference was observed in electrically stimulated DA release in the CPu between aged $BDNF^{+/-}$ (2.0 ± 0.2 µM, n = 14) and wildtype (1.7 ± 0.1 µM, n = 15) mice (Figure 5.3A). However, a comparison between stimulated DA release concentrations in the young adult (Section 4.3.3) and aged mice using two-way ANOVA revealed significant main effects of aging ($F_{1,101}$ = 12.54, P = 0.0006), genotype ($F_{1,101}$ = 4.19, P = 0.04), and genotype x aging interaction ($F_{1,101}$ = 21.22, P < 0.0001). Aging led to an increase in stimulated DA release in the CPu of $BDNF^{+/-}$ mice (young: 1.2 µM; aged: 2.0 µM; P < 0.001)), but no effect of aging was observed in the wildtype mice (P > 0.05; Bonferroni post-test; Figure 5.3A). DA uptake rates were not different in the CPu of aged $BDNF^{+/-}$ mice (3.9 ± 0.2 µM/s, n = 14) relative to the rates obtained from aged wildtype mice (3.9 ± 0.1 µM/s, n = 15; Figure 5.3B). A comparison between DA uptake rates in the young adult (Section 4.3.3) and aged mice using two-way ANOVA revealed significant main effects of aging ($F_{1,121}$ = 4.78, P = 0.03), genotype ($F_{1,121}$ = 17.23, P < 0.0001), and genotype x aging interaction ($F_{1,121}$ = 14.93, P = 0.0002). Bonferroni post-test revealed only a significant increase (P < 0.001) in V_{max} of $BDNF^{+/-}$ mice (young: 2.7 µM/s; aged: 3.9 µM/s; P = 0.0005; Figure 5.3B).

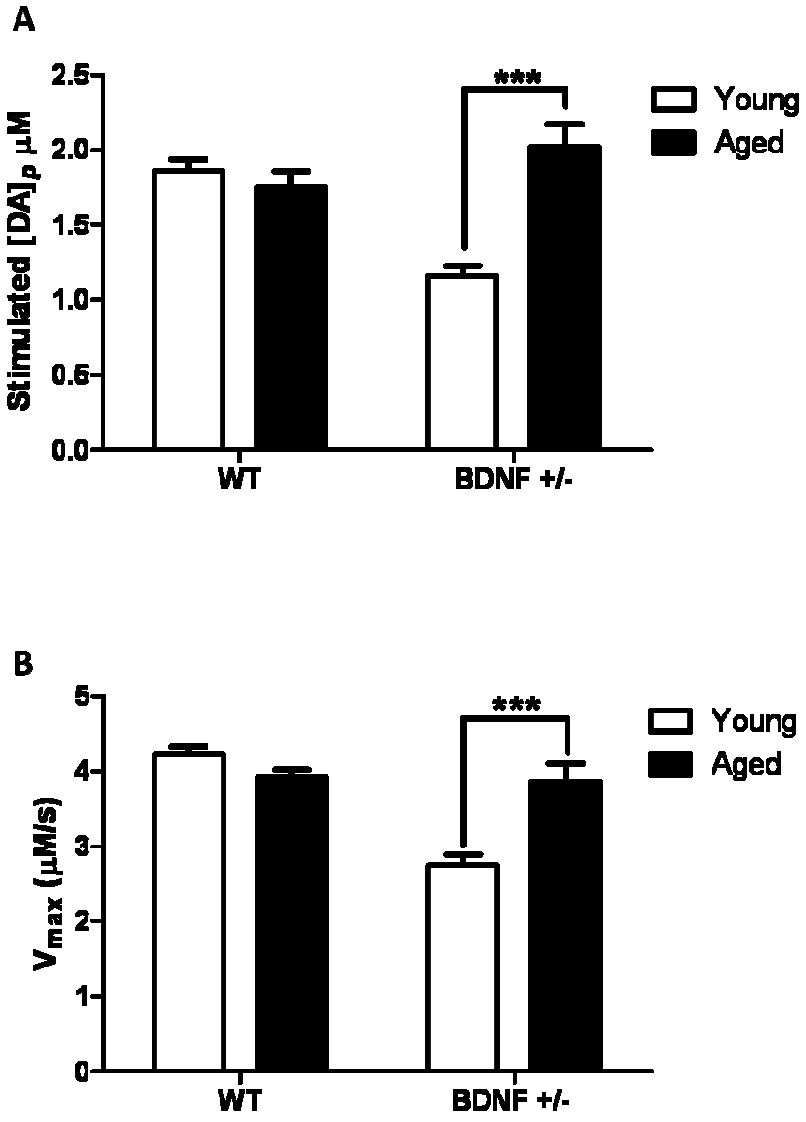

Figure 5.3 Presynaptic dopamine (DA) dynamics in young and aged mice in the caudate putamen (CPu). Single pulse electrically evoked DA release (A) and maximum velocity (V_{max}, uptake rate) (B) measured using FSCV in the caudate putamen (CPu) of wildtype (WT) and $BDNF^{+/-}$ mice. Data are reported as means ± SEMs for young (~ 3 months) and aged (~ 18 months) mice (n = 14 – 26 mice per group). ****P* < 0.001 for aging effect in $BDNF^{+/-}$ mice (two-way ANOVA, Bonferroni post-test).

In the NAc core, electrically evoked DA release did not differ between aged wildtype (0.7 ± 0.2 µM, n = 12) and BDNF$^{+/-}$ (1.0 ± 0.1 µM, n = 8) mice (Figure 5.4A). A comparison between stimulated DA concentrations in the young adult (Section 4.3.3) and aged mice using two-way ANOVA did not reveal significant effects of aging and genotype, but a significant genotype x aging interaction ($F_{1,33}$ = 14.47, *P* = 0.0006) was observed. Interestingly, wildtype mice showed a significant decrease (Bonferroni post-test, *P* < 0.05) in stimulated DA release as a result of aging (young: 1.1 µM; aged: 0.7 µM; *P* < 0.05; Figure 5.4A). In contrast, BDNF$^{+/-}$ mice showed a significant increase (Bonferroni post-test, *P* < 0.05) in stimulated DA release in the NAc core as a result of aging (young: 0.7 µM; aged: 1.0 µM; *P* = 0.03, Figure 5.4A). DA uptake rates did not differ in the NAc core of aged wildtype mice (2.0 ± 0.2 µM/s, n = 12) compared to aged BDNF$^{+/-}$ mice (2.6 ± 0.2 µM/s, n = 8; Figure 5.4B). Two-way ANOVA (Bonferroni post-test) comparisons between DA uptake rates in the NAc core of young adult (wildtype: 2.3 µM/s and BDNF$^{+/-}$: 2.0 µM/s) and aged mice did not indicate any genotype difference or aging effect (Figure 5.4B).

Similar to the CPu and NAc core, no difference in evoked DA release was observed between aged wildtype (0.3 ± 0.04 µM, n = 11) and BDNF$^{+/-}$ (0.4 ± 0.03 µM, n = 12) mice in the NAc shell (Figure 5.5A). However, a significant decrease (two-way ANOVA: Bonferroni post-test, *P* < 0.01) in stimulated DA release was observed in NAc shell of wildtype mice (young: 0.6 µM; aged: 0.3 µM; Figure 5.5A). In contrast to the other striatal regions, BDNF$^{+/-}$ mice showed no aging effect (Bonferroni post-test, *P* > 0.05) in stimulated DA release in the NAc shell (Figure 5.4A).

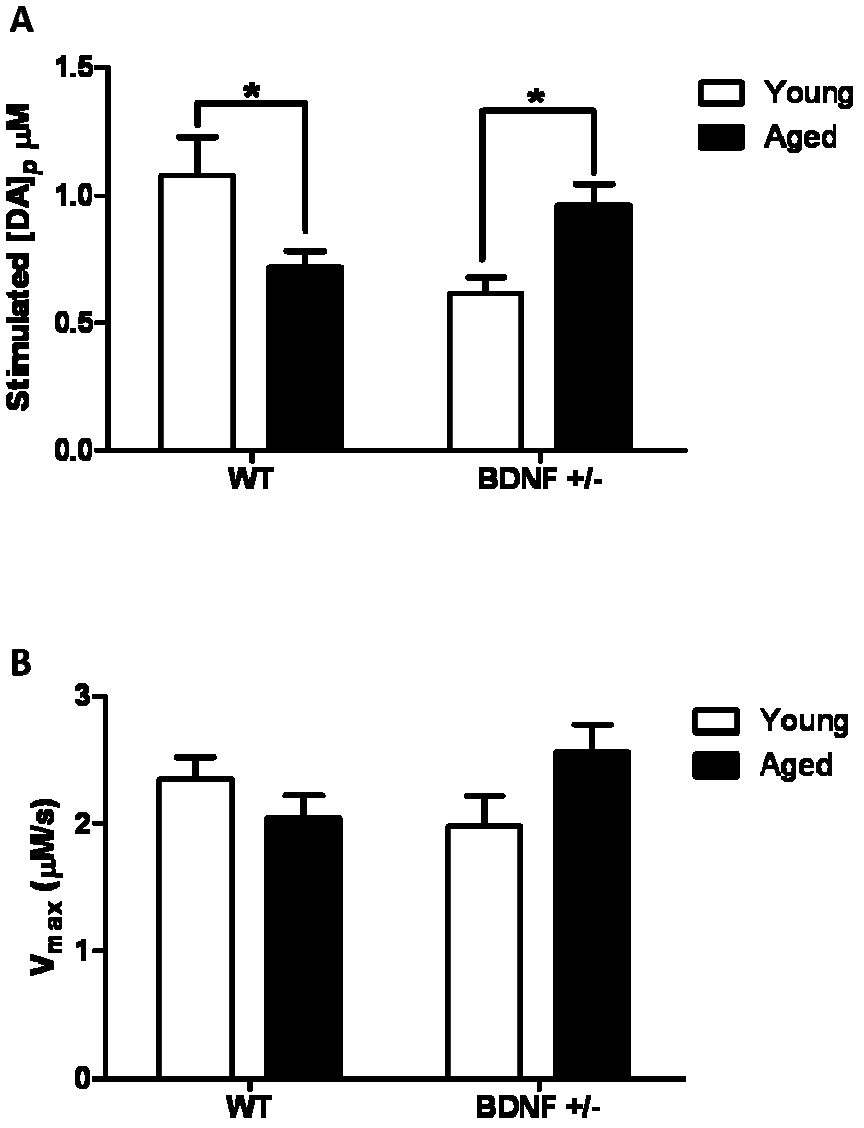

Figure 5.4 Presynaptic dopamine (DA) dynamics from the nucleus accumbens (NAc) core measured using FSCV. (A) Single pulse electrically evoked DA release and (B) maximum velocity (V_{max}, DA uptake rate) between young and aged wildtype (WT) and $BDNF^{+/-}$ mice. Data are reported as means ± SEMs for young (~ 3 months) and old (~ 18 months) mice (n = 8 – 12 mice per group). *P < 0.05 for aging effect comparisons in stimulated DA release (two-way ANOVA, Bonferroni post-test).

Additionally, no genotype difference (two-way ANOVA) in DA uptake rates were observed in the NAc shell of aged mice (wildtype: 0.8 ± 0.1 µM/s, n = 11; $BDNF^{+/-}$: 1.0 ± 0.1 µM/s, n = 12; Figure 5.5B). A significant decrease (Bonferroni post-test, $P < 0.01$) in DA uptake rates was observed in the NAc shell of aged wildtype mice (young: 1.2 µM/s; vs. aged: 0.8 µM/s; $P = 0.005$, Figure 5.5B). No aging effect was observed in DA uptake rates of $BDNF^{+/-}$ mice (Figure 5.5B).

To better understand the combined effects of low BDNF levels and aging on electrically evoked DA release, the numbers of stimulation pulses (p) were varied from 1 to 5. Once a stable electrically evoked DA release was obtained in a given location, stimulation parameters were varied from 1p to 5p. Area under the curve (AUC) was used to monitor the maximal evoked DA release. Increasing the number of pulses led to an increase in the stimulated DA release in both wildtype and $BDNF^{+/-}$ mice (Figure 5.6A and 5.6B, respectively). To reduce the variation from one placement to the other, AUC data was normalized a ration (DA_{5p}/DA_{1p}; Figure 5.6C). Striatal ratios for aged wildtype mice were CPu: 1.2 ± 0.1, n = 15, NAc core: 1.8 ± 0.2, n = 14, and NAc shell: 2.1 ± 0.1, n = 12. Striatal ratios for aged $BDNF^{+/-}$ mice were CPu: 1.2 ± 0.04, n = 11, NAc core: 1.5 ± 0.07, n = 6, and NAc shell: 2.5 ± 0.1, n = 7. Two-way ANOVA analysis revealed a significant effect of the striatal region of interest ($F_{2,59} = 44.04$, $P < 0.0001$). However, no difference was observed between the aged genotypes ($F_{1,59} = 0.2072$, $P = 0.65$). Also there was no genotype x striatal region interaction ($F_{2,59} = 4.129$, $P = 0.021$).

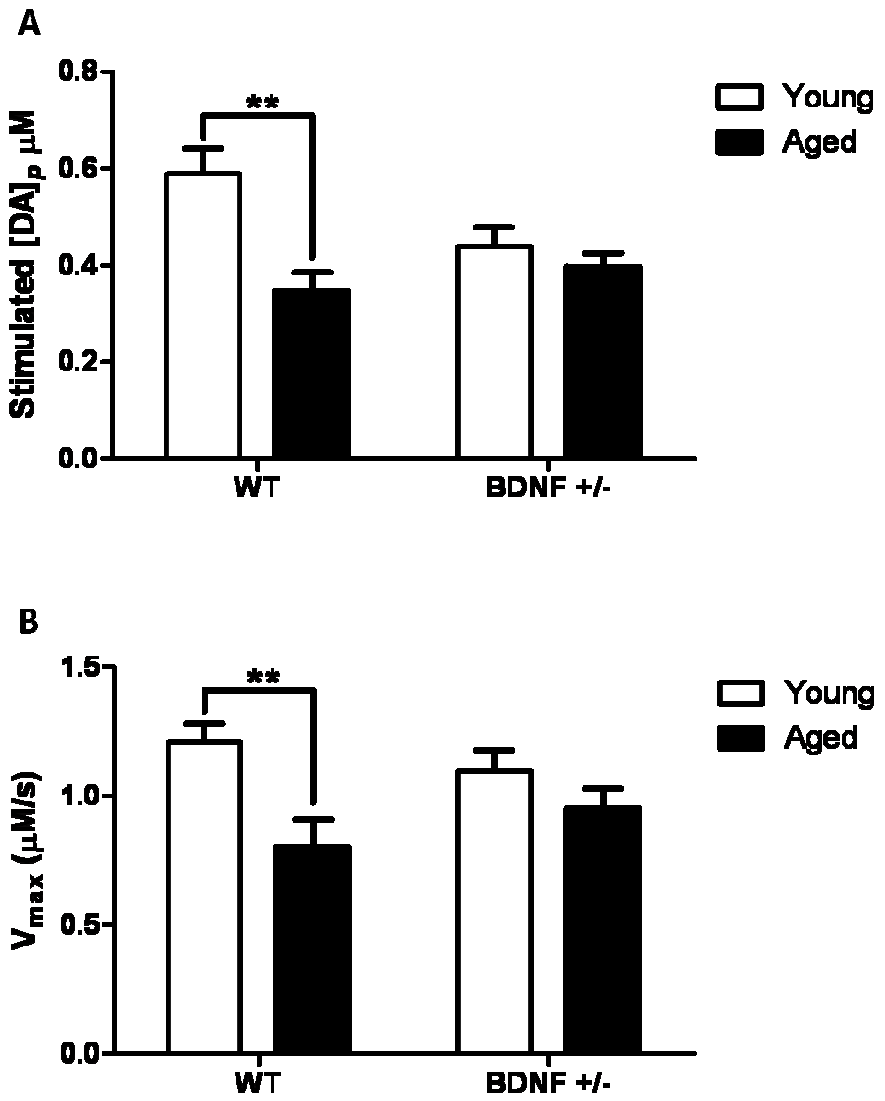

Figure 5.5 Presynaptic dopamine (DA) dynamics from the nucleus accumbens (NAc) shell measured using FSCV. (A) Single pulse electrically evoked DA release and (B) maximum velocity (V_{max}, uptake rate) in the NAc shell of young and aged wildtype (WT) and $BDNF^{+/-}$ mice. Data are reported as means ± SEMs for young (~ 3 months) and old (~ 18 months) mice (n = 11 – 12 mice per group). ***P* < 0.01 for aging effect comparison (two-way ANOVA, Bonferroni post-test).

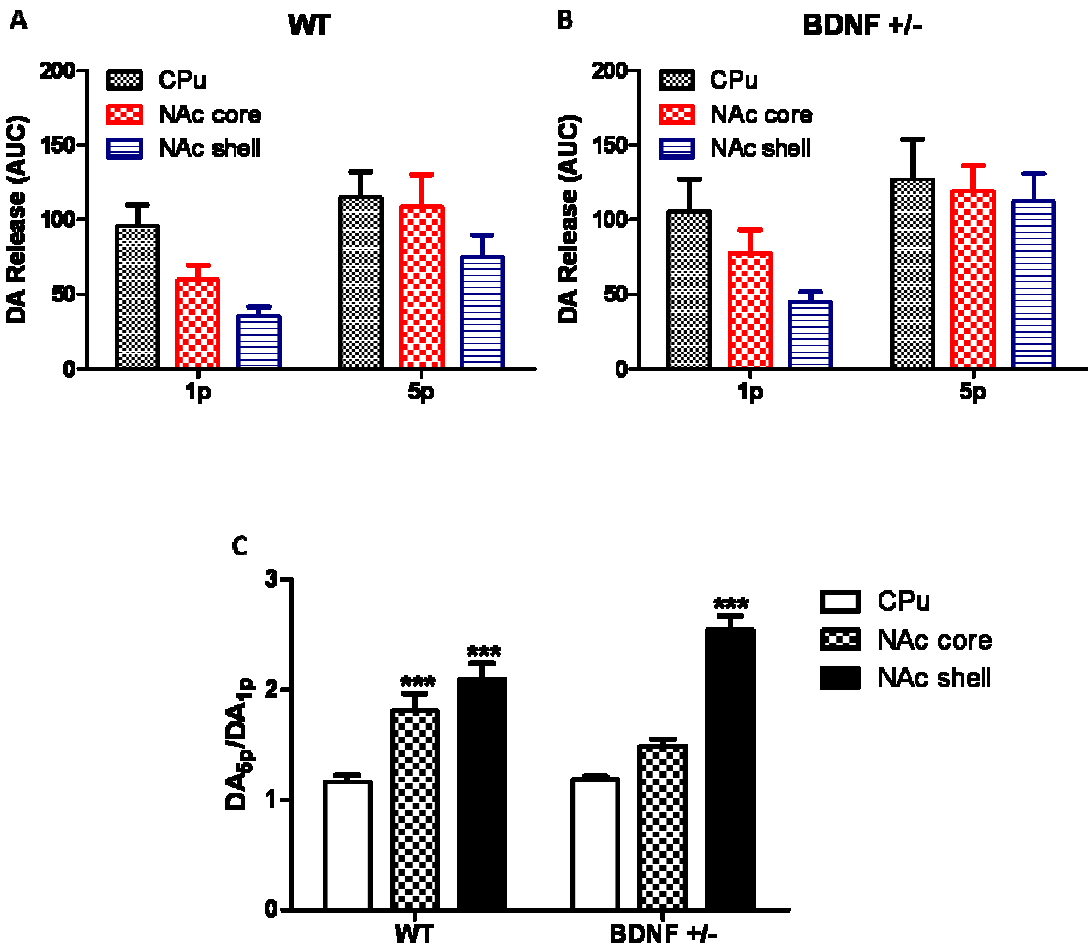

Figure 5.6 Effect of single (1p) or multiple pulse (5p) stimulation on electrically evoked dopamine (DA) across the striatum in aged wildtype (WT) and BDNF$^{+/-}$ mice, measured using FSCV. (A) Release in the caudate putamen (CPu) and nucleus accumbens (NAc) core and shell in aged wildtype mice are reported as area under the curve (AUC). (B) Release in the CPu, and NAc core and shell in aged BDNF$^{+/-}$ mice. (C) Ratio of DA release (DA_{5p}/DA_{1p}) in aged WT and BDNF$^{+/-}$ mice. Data are reported as means ± SEMs (n = 6 – 15 mice per group), analyzed using two-way ANOVA (Bonferroni post-test), ***P < 0.001 (differences within groups).

Bonferroni post-test revealed a significant difference ($P < 0.001$) between NAc shell and CPu in both aged wildtype and aged $BDNF^{+/-}$ mice (Figure 5.6C). A significant difference was observed between the CPu and NAc core of the aged wildtype mice ($P < 0.001$), whereas no difference was observed in the aged $BDNF^{+/-}$ mice (Figure 5.6C).

To further understand the impact of aging on DA release upon multiple pulse stimulations, the DA release ratios (DA_{5p}/DA_{1p}) of young adult (~ 3 months) and aged (~ 18 months) mice were compared using a two-tailed t-test (Figure 5.7). Aging significantly decreased electrically evoked DA release in the CPu ($P < 0.001$; Figure 5.7A) and NAc shell ($P < 0.05$) of wildtype mice, but no difference was observed in NAc core ($P > 0.05$). In the $BDNF^{+/-}$ mice, aging led to a signficant decrease in DA release in CPu ($P = 0.03$) and NAc core ($P = 0.04$; Figure 5.7B). Interestingly, in the NAc shell of aged $BDNF^{+/-}$ mice, DA_{5p} was significantly increased ($P = 0.02$) as a result of aging, in line with aging-related increase in single pulse DA release observed in the CPu and NAc core. These results indicate that in the absence or presence of BDNF, aging reduces DA release (DA_{5p}) in both genotypes, except in the NAc core of wildtype mice where no change was observed.

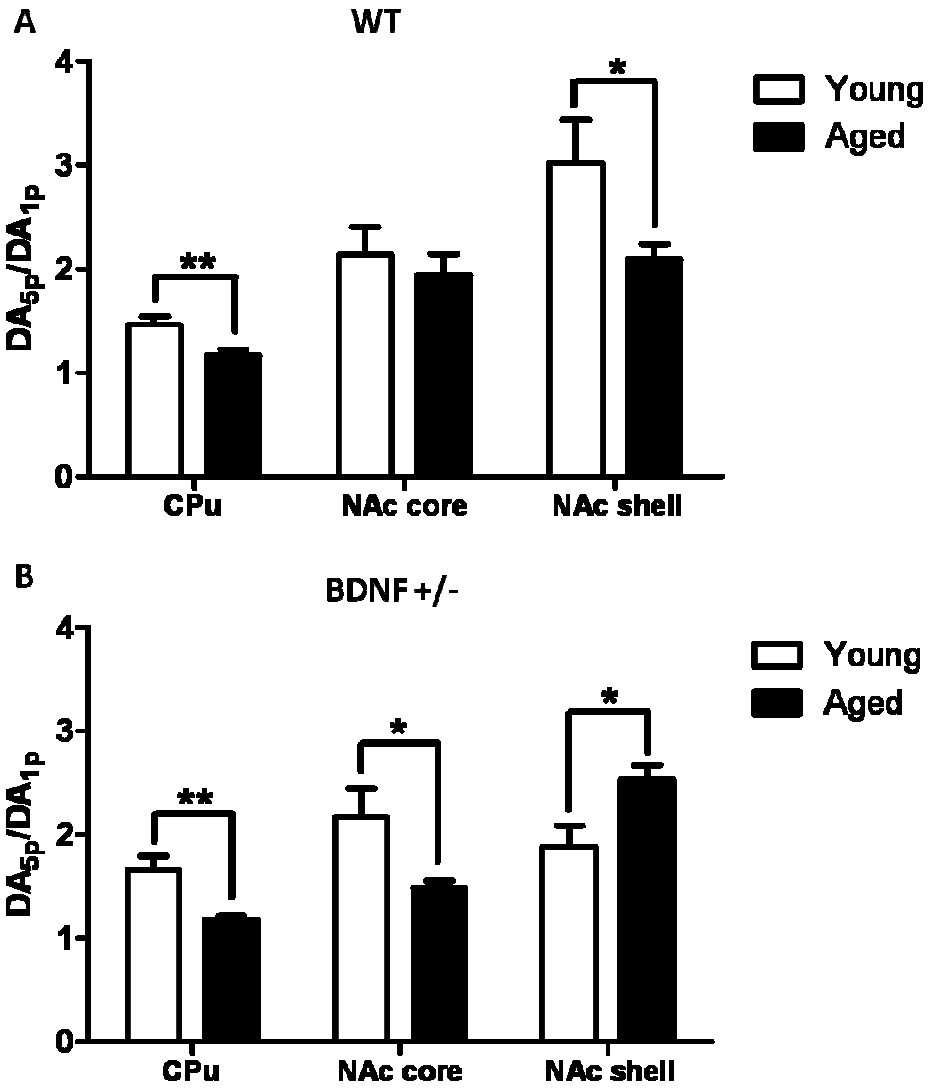

Figure 5.7 Effect of aging on 1 and 5 pulse stimulations of dopamine (DA) release measured by FSCV. (A) The effect of age on stimulated DA release in young and aged wildtype (WT) mice across the striatum. (B) The effect of age and reduced BDNF expression on stimulated DA release in young and aged $BDNF^{+/-}$ mice in the CPu, NAc core, and shell. Data are shown as means ± SEMs of DA release (DA_{5p}/DA_{1p}) in WT and $BDNF^{+/-}$ mice (n = 6 – 13 mice per group). $^{**}P < 0.05$, $^{**}P < 0.01$ for the effect of age on the brain region of interest (Student's t-test).

5.4 Discussion

The main objective of the present study was to determine the long-term effect of low endogenous BDNF levels on DA dynamics. This was accomplished by using slice FSCV and *in vivo* microdialysis to probe DA dynamics in aged $BDNF^{+/-}$ and wildtype mice. Contrary to our hypothesis that low BDNF levels would greatly attenuate DA dynamics in aged mice, no genotypic differences in stimulated DA release, DA uptake, or basal extracellular DA levels were observed. Interestingly, extracellular levels of DOPAC were elevated in aged $BDNF^{+/-}$ mice as compared to aged wildtype mice, while no genotypic difference was observed in HVA levels. Overall, aged $BDNF^{+/-}$ mice appear to have an elevated catabolism process as compared to the wildtype mice.

To further understand the impact of aging and low endogenous BDNF levels on DA dynamics, the results from the aged mice (~ 18 months) were compared to those obtained from young adult mice (~ 3 months). Three-month-old $BDNF^{+/-}$ mice have a hyperdopaminergic phenotype that is attributed to both reduced electrically evoked DA release and reduced function of the DA transporter (CHAPTER 4). These DA alterations, as measured by FSCV, were not observed in aged $BDNF^{+/-}$ mice. A significant decrease in basal extracellular DA levels, as measured by the zero net flux method, was observed in aged $BDNF^{+/-}$ mice as compared to their younger counterparts, but no difference in basal extracellular DA levels between young and aged wildtype mice was observed. The basal levels of DA determined from aged and young wildtype, as well as aged $BDNF^{+/-}$ mice were all similar (~ 6 nM) and are consistent with striatal DA_{ext} values previously reported for adult C57BL/6 mice (*241*). However, aged mice with reduced BDNF expression exhibited a significant increase in DOPAC levels

as compared to aged wildtype mice. However, no age-related difference in HVA levels were observed between young and old mice.

BDNF$^{+/-}$ mice have a hyperdopaminergic phenotype at the age of ~ 3 – 4 months due to reduced DA transport (CHAPTER 4). Surprisingly, at this age, levels of DOPAC are not altered as expected due to the elevated basal extracellular DA levels in these mice. Aged (11 – 24 months) wildtype (C57Bl/6) and DAT$^{+/-}$ mice have an elevated DOPAC/DA ratio, although at a greater magnitude in the DAT$^{+/-}$ mice (*242*). Similarly, we observed elevated DOPAC levels in the aged BDNF$^{+/-}$ mice. Increased DOPAC levels are mainly attributed to an elevated catabolism rate (*242-244*). However, we did not observe significant change in HVA levels with age in either BDNF$^{+/-}$ or wildtype mice. Tissue content DA levels were not altered in the aged DAT$^{+/-}$ mice but decreased DA levels were observed from the age of 11 months in wildtype mice (*242*). In our study, extraneuronal DA levels were attenuated in the old BDNF$^{+/-}$ mice as compared to the young mice, but no change was observed with age in wildtype mice. Taken together, the age-related high rate of catabolism appears to reduce the elevated extracellular DA levels in the BDNF-deficient mice, similar to levels for wildtype mice.

Dysregulation of motor function in Parkinson's disease patients is attributed to loss of more than 80% of DA neurons in the striatum (*10, 40, 226, 245*). However, age-related motor deficits are thought to mainly involve alterations in functional parameters of the DA system, not neuronal loss, as demonstrated in animal models of aging (*214, 221, 228*). Specifically, it is believed that changes, such as decreased DA uptake by the DA transporter, reduced DA release, and decreased VMAT2 activity, may lead to the age-related motor deficits (*214, 221, 229*). In wildtype mice, aging decreased electrically

evoked DA release (1p stimulation) in the NAc (core and shell), but no difference in stimulated DA release in the CPu was observed. Interestingly, DA uptake rates were significantly decreased only in the NAc shell, but not in the NAc core or CPu of aged wildtype mice as compared to the young adult mice. Overall, wildtype mice show an age-related decrease in presynaptic DA release and uptake functions that is region-specific. Currently, it is not known which parameter within the DA system is the primary effect of aging. The FSCV data suggests that both DA release and DA uptake are reduced with age. However, this decrease in both parameters is not parallel across all brain regions, as the CPu appears resistant to changes in DA release and uptake, while the NAc core shows no difference in DA uptake between young and aged wildtype mice. These results suggest that the NAc shell is most susceptible to age-related alterations in wildtype mice, which is interesting because aging research has generally not been focused on the NAc. Most aging research has focused on the CPu, due to its role in regulating movement, as seen in the neurodegenerative disease of Parkinson's. The primary functions associated with the NAc are natural or biological rewards, like eating, drinking, procreation, and investigation (*246*). Additionally, it is interesting that the anatomically distinct region of the NAc shell is more susceptible to presynaptic DA changes as compared to the core. Although these voltammetry results are unable to pinpoint an exact mechanism, they do suggest a need for further evaluation of DA parameters within the VTA-NAc region during the normal aging process.

In contrast to wildtype mice, aged $BDNF^{+/-}$ mice exhibit a potentiation in electrically stimulated DA release (1p stimulation) in the CPu and NAc core, but no difference in DA release was seen in the NAc shell. DA uptake rates were significantly

elevated only in the CPu, while no difference in DA uptake was seen in the NAc core or shell of aged BDNF$^{+/-}$ mice. These results are very surprising, because our initial hypothesis was that the DA dynamics of aged BDNF$^{+/-}$ mice would be more susceptible to the combined effects of age and low BDNF levels as compared to wildtype mice. Overall, a lifetime of low endogenous BDNF levels in mice appear to lead to enhancement in electrically stimulated DA release and DA uptake rates in the CPu. The presynaptic DA dynamics in aged BDNF$^{+/-}$ mice appear to 'normalize', as measured by voltammetry and dialysis, such that they appear neurochemically similar to the wildtype mice. Others who have examined the effect of aging in BDNF$^{+/-}$ mice have shown that they have reduced locomotor activity in beam walking and accelerated rotarod performance as compared to the aged wildtype (11 – 21 months old) mice (*34, 133, 134*).

Exactly how BDNF mediates DA dynamics remains unknown, although it has been hypothesized that intracellular BDNF prevents synaptic fatigue (*185, 187, 247*). This suggests that BDNF may enhance long-term potentiation (LTP) induction at high-frequency stimuli. Our previous findings demonstrated that three-month-old adult mice with low BDNF levels have reduced DA available for release in the NAc shell when the number of stimulation pulses is increased as compared to three-month-old wildtype mice (Section 4.4.2). To understand how aging and BDNF deficiency affect DA release, we evaluated electrically stimulated DA release in the striatal complex using 1 and 5 pulse stimulation parameters (*101*). No genotype difference was observed in DA release as the number of stimulation pulses increased in aged wildtype and BDNF$^{+/-}$ mice. To understand the impact of the presence or reduction of BDNF and aging on DA

release, three-month-old adult and aged (~ 18 months) mice were compared. Aged wildtype mice exhibited a significant decrease in DA_{5p} release in the CPu and NAc shell, with no difference in NAc core as compared to their younger counterparts. Aged $BDNF^{+/-}$ mice showed a signficant decrease in DA_{5p} release in the CPu and NAc core compared to the younger $BDNF^{+/-}$ mice. Taken together, these multiple pulse stimulation results indicate a reduction in DA release upon aging in both genotypes. In contrast, an increase in DA_{5p} release was observed in the NAc shell of $BDNF^{+/-}$ mice. This difference highlights an enhanced DA release in the NAc shell of aged $BDNF^{+/-}$ mice that was not observed upon single pulse stimulation. The NAc shell is known to be more responsive to multiple pulse stimulation, which is in line with burst firing during rewarding events (*56, 101, 197*).

These findings demonstrate that low BDNF levels in early life may have detrimental consequences on DA system functions in the striatum, such as reduced DA release, DA uptake, and elevated basal DA levels. However, the DA system appears to adapt with age. In mice deficient in BDNF, the presynaptic DA dynamics appear to neurochemically adapt such that they appear more like wildtype mice. However, the contribution of age and BDNF levels to this phenomenon is unknown and future studies must be performed to better understand if this is a gradual shift or a sudden change. In either case, it will be very interesting to understand what molecular targets may contribute to this shift in the aging $BDNF^{+/-}$ mice. A simplistic hypothesis is that an enhanced catabolism process in the CPu is able to significantly decrease the elevated basal extracellular DA levels in young adult mice. If these changes, either in monoamine oxidase (MAO) expression or function, are indeed enough to regulate extracellular DA

levels, then the system could try compensating by enhancing DA release and DA uptake rates during the aging process. To confirm this hypothesis, studies evaluating MAO must be conducted to better detail its role.

5.5 Conclusions

In wildtype mice, age-related reductions in DA release were observed in the striatal complex, with the NAc shell being more susceptible to reduction in DA clearance as well. No significant alterations were observed in basal DA concentrations or catabolism processes due to aging. Overall, only a decline in presynaptic DA function was observed in the aged wildtype mice.

Despite the fact that reduced BDNF levels are linked to a dysfunctional DA system in human and animal models, our current study failed to find BDNF-related reduction in presynaptic DA dynamics in aged BDNF-deficient mice (*41, 133, 190, 231, 233, 236*). In fact, stimulated DA release, DA uptake rates, and catabolism by MAO appear enhanced. The hyperdopaminergic phenotype observed in three-month-old BDNF-deficient mice was reversed with age, leading to normal levels of basal DA levels. Increase in DA release in BDNF-deficient mice highlights enhancement in dopaminergic neuron presynaptic function with age. These findings from aged mice highlight adaptations in the dopaminergic system as a result of the normal aging process in mice with reduced BDNF levels. Future studies are required to examine different discrete time points to determine at what age the neurochemical adaptations ‘switch’ to make the BDNF-deficient mice appear more like aged wildtype mice. The role of BDNF appears to be more important in the development of the DA system, but not for the maintenance of the neurons (*248*). During neuronal development, low BDNF levels

may alter DA transmission. However, at old age, low endogenous BDNF levels alone do not appear to be critical in DA dysregulation.

CHAPTER 6

Effect of Low Endogenous BDNF levels on Dopamine Transporter Function

6.1 Introduction

Extracellular dopamine (DA) signaling is terminated primarily through rapid reuptake by the DA transporter, regulating the lifetime of extraneuronal DA following its release. The Na^+ and Cl^- dependent DA transporter consists of 12 transmembrane regions, each with functional roles (*10, 249*). The first five regions from the N-terminal of the DA transporter are thought to be involved in ion-dependent substrate transport (*250*). Methamphetamine and other DA transporter inhibitors target the transmembrane regions six through eight, while the remaining regions through the C-terminus are involved in substrate affinity and stereoselectivity (*249-252*).

Drugs of abuse such as methamphetamine and cocaine are known to increase extracellular DA by interacting with the DA transporter, albeit different mechanisms (*10, 253*). Methamphetamine competitively inhibits DA reuptake at the DA transporter, as well as reversing DA transport, these effects combined lead to increased extraneuronal DA levels (*5-7, 253*). Once inside the neuron, methamphetamine modulates vesicular monoamine transporter (VMAT) activity (*6, 254-257*). As a potent competitive DA antagonist at the VMAT, methamphetamine limits sequestration of cytoplasmic DA into vesicles (*255*). This results in DA efflux that is independent of the presynaptic neuron firing activity.

Besides being a highly addictive substance, prolonged high doses of methamphetamine are known to be neurotoxic (*258-261*). Specifically, animal models

indicate numerous neurochemical impairments within the striatal DA system, such as long-lasting intracellular depletions of DA, its catabolites 3,4-dihydroxyphenylacetic acid (DOPAC) and homovanillic acid (HVA), as well as tyrosine hydroxylase (TH) activity (*259-261*). The ability of methamphetamine to induce dopaminergic deficits appears to be region specific, with the caudate putamen (CPu) being more susceptible and the nucleus accumbens (NAc) being relatively resistant to the long-term DA system dysregulation (*262, 263*). Moreover, neurotoxicity of methamphetamine appears to be dependent on age, brain-derived neurotrophic factor (BDNF) levels, gender, stress, and temperature (*35, 258-260, 264*).

With respect to methamphetamine neurotoxicity, Dluzen and co-workers showed that there is less severe damage to the nigrostriatal dopaminergic system in BDNF heterozygous mutant ($BDNF^{+/-}$) mice as compared to their wildtype littermates (*35, 134*). However, the role of low BDNF levels on the reduced neurotoxicity is still a subject of considerable debate. Our findings from CHAPTER 4 show that $BDNF^{+/-}$ mice have attenuated DA uptake rates as compared to their wildtype littermates (Figure 4.4), suggesting that expression or function of the DA transporter is reduced. Interestingly, autoradiographic methods show no difference in DA transporter expression between wildtype and $BDNF^{+/-}$ mice (*37, 133*).

The main objective of this study was to evaluate DA transporter function in a mouse model with low endogenous BDNF levels. Slice FSCV was used to probe the effects of methamphetamine by monitoring inhibition of DA uptake, as previously reported (*14, 62, 68, 90, 265, 266*). Methamphetamine induces rapid and reversible competitive inhibition of DA uptake through the DA transporter (*6, 14, 62*). Therefore,

methamphetamine was used as tool to probe DA transporter kinetic parameters such as maximum velocity (V_{max}), apparent Michaelis-Menten constant (apparent K_m), and stimulated DA concentration per pulse $[DA]_p$ using slice FSCV from wildtype and $BDNF^{+/-}$ mice. We hypothesized that decreased DA transporter function in the $BDNF^{+/-}$ mice will manifest as a decrease in methamphetamine's affinity towards the DA transporter. Additionally, *in vivo* microdialysis was used to evaluate the role of BDNF levels on methamphetamine-induced DA release in freely moving mice.

6.2 Materials and methods

Kelly Bosse, Ph.D. performed all the microdialysis experiments on young mice (3 – 4 months of age). Johnna A. Birbeck performed all the microdialysis experiments on aged mice (~ 18 months of age). In all cases, microdialysis experiments conducted by either Dr. Bosse or Johnna Birbeck involved stereotaxic surgery, probe implantation, sample collection, methamphetamine injection, HPLC separation with electrochemical detection, and chromatographic data analysis.

BDNF wildtype and $BDNF^{+/-}$ mice were raised as a colony in house and genotyped as described in Section 2.2. Male ($BDNF^{+/-}$ and wildtype) mice aged ~ 3 – 4 months (young) or both male and female mice aged ~ 18 months were used for slice FSCV experiments and *in vivo* microdialysis. Slice FSCV experiments were performed as previously described in Section 2.4 with minor modifications. Single pulse stimulation was used to electrically evoke DA release in the caudate putamen (CPu) every five minutes. Upon obtaining a stable baseline, increasing concentrations (0.01 – 10 µM) of methamphetamine (Sigma-Aldrich, St. Louis, MO) were perfused over brain slices from either young or aged (wildtype or $BDNF^{+/-}$) mice. Each concentration of

methamphetamine was perfused for 30 minutes, with DA being electrically evoked every five minutes.

In vivo microdialysis experiments in young adult and aged mice were performed by *Kelly E. Bosse, Ph.D.* and *Johnna A. Birbeck*, respectively, as described in Section 2.5. Briefly, upon stereotaxic surgery, a microdialysis probe was implanted in the CPu for sampling. After recovery and equilibration, at least three dialysate baseline samples were collected for 20 minutes. An intraperitoneal (i.p.) injection of methamphetamine (1.0 mg/kg) was administered immediately after collection of the third baseline sample. At least six dialysate samples containing methamphetamine-induced DA release were collected every 20 minutes. The extraneuronal DA concentration from each dialysate sample was determined through separation and quantification using HPLC coupled to an electrochemical detector as described in Section 2.6.

6.2.1 Data analysis

Kelly E. Bosse, Ph.D. and Johnna A. Birbeck performed statistical analysis and graphing of the microdialysis data.

All values are reported as means ± standard errors of the means (SEMs) of at least five animals. Slice FSCV data were analyzed by fitting the current versus time traces to a Michaelis-Menten kinetic based model to determine changes in $[DA]_p$, V_{max}, and apparent K_m (“apparent” affinity of DA for its transporter) (*62, 68, 90, 138*). Competitive inhibition of DA uptake is reflected as an increase in apparent K_m (*62, 68*). The relationship between inhibition constant (K_i) and apparent K_m is described by Equation 4, where [i] is the concentration of inhibitor (e.g. methamphetamine) and K_m is the Michaelis-Menten constant. As previously reported, K_i values were calculated from

the slope of a linear regression plot of methamphetamine concentration versus the apparent K_m values (Equation 5), where the K_m was 0.16 µM, as previously reported (*62, 68, 139, 140*). Apparent K_m values resulting from effect of higher concentrations of methamphetamine (> 0.3 µM) were excluded to properly fit the linear regression. At these high concentrations, methamphetamine reduced stimulated DA release besides inhibiting DA uptake. The DA uptake process obeys the Michaelis-Menten kinetics with the assumption that each stimulation pulse releases a constant amount of DA (*14, 62*).

$$\text{Apparent } K_m = K_m \times (1 + [i]/K_i) \quad \textbf{(4)}$$

$$\text{Slope} = \Delta y/\Delta x = K_m/K_i \quad \textbf{(5)}$$

Dose response curves were plotted as log concentration (M) of methamphetamine versus percent of baseline (maximal stimulated DA release) and the data were fitted using a non-linear regression curve to determine the half maximal effective concentration (IC_{50}; concentration of inhibitor at which DA release is half the maximum). Differences in methamphetamine's effect on DA apparent K_m values and stimulated DA release were assessed using a two-way ANOVA with genotype as the independent variable and concentration of methamphetamine as the repeated measure. The effect of methamphetamine on V_{max} was analyzed using a one-way ANOVA with a Dunnett's post-test to compare pre-drug V_{max} values to treatments. Finally, the effect of BDNF levels on methamphetamine-induced extracellular DA levels as measured by microdialysis was assessed using a two-way ANOVA, with genotype as the independent variable and time as the repeated measure. In all cases, statistical significance is defined as $P < 0.05$.

6.3 Results

Methamphetamine dose-dependently inhibited DA uptake in both genotypes ($P < 0.0001$). Representative pre-drug and 0.3 µM methamphetamine induced concentration versus time traces and their corresponding cyclic voltammograms from wildtype mice are shown in Figure 6.1A. In the presence of methamphetamine, the "apparent" affinity of DA for its transporter is decreased, as evaluated by linear and non-linear fitting (Figure 6.1B – E). Dose dependent decrease in affinity of DA for its transporter is represented as an increase in apparent K_m values. Young (~ 3 months) and aged (~ 18 months) mice show dose dependent increase in the apparent K_m values in both wildtype and BDNF$^{+/-}$ mice (Figures 6.1B & C). Analysis of the non-linear dose response curves for the young BDNF$^{+/-}$ and wildtype mice using two-way ANOVA revealed significant effects of methamphetamine treatment ($F_{7,142} = 65.77$, $P < 0.0001$), genotype ($F_{1,142} = 12.93$, $P = 0.0004$), and genotype x treatment interaction ($F_{7,142} = 3.15$, $P = 0.0040$). The apparent K_m values were attenuated in the young BDNF$^{+/-}$ mice as compared to their wildtype littermates (Figure 6.1B). Higher apparent K_m values indicate greater uptake inhibition in the young wildtype than in the BDNF$^{+/-}$ mice. Data analysis for the aged mice using two-way ANOVA revealed a significant main effect of methamphetamine treatment ($F_{6,317} = 96.50$, $P < 0.0001$), but with no genotype difference ($F_{1,317} = 0.018$, $P = 0.89$) or genotype x treatment interaction ($F_{1,317} = 0.14$, $P = 0.99$). Overall, the effect of BDNF levels on methamphetamine treatment was only observed in the young mice.

To quantitatively characterize DA uptake inhibition, K_i values were calculated from the linear regression of apparent K_m values using Equation 5 (Figure 6.1D). A low K_i value represents high drug potency while a high K_i value represents low drug potency

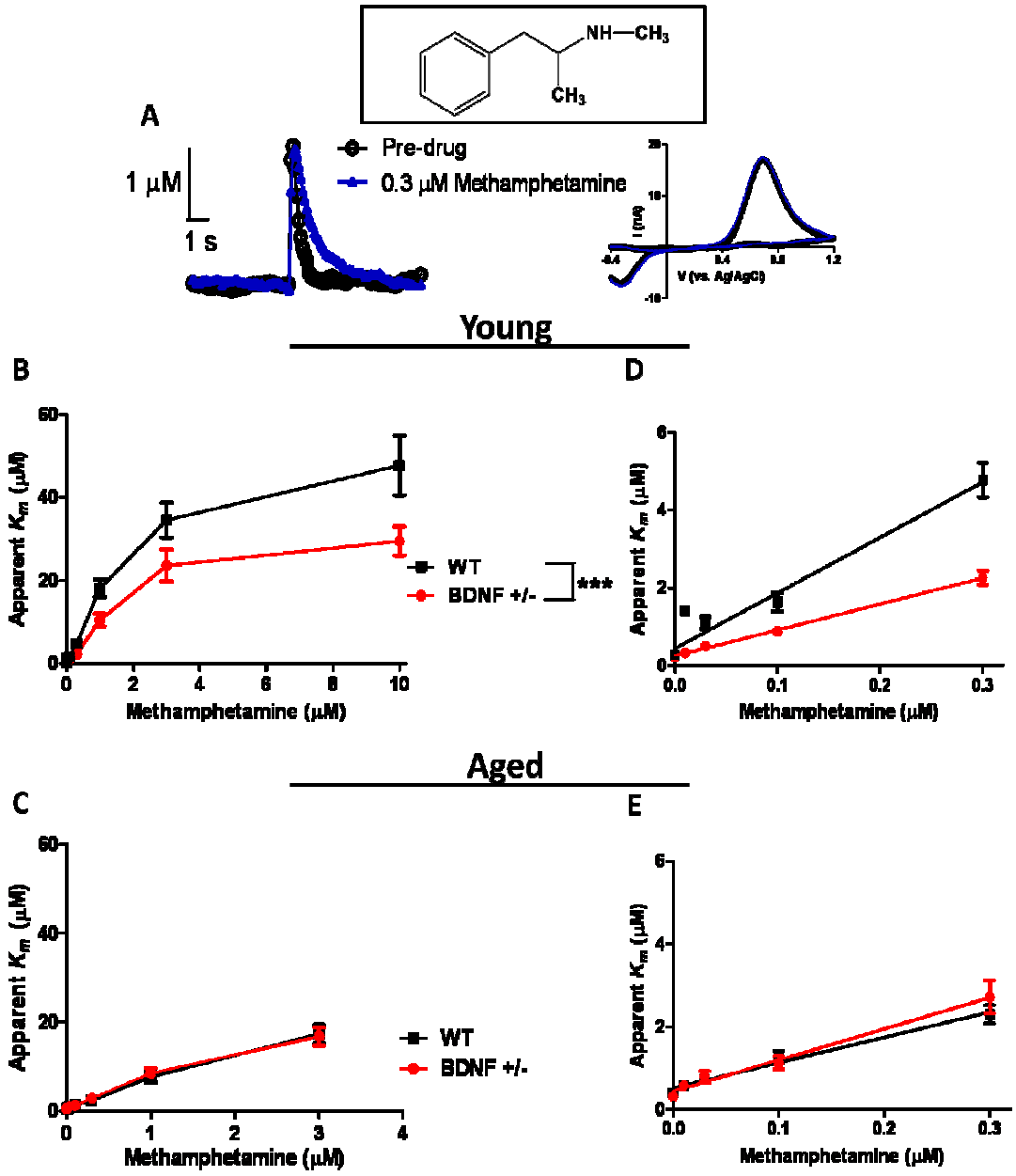

Figure 6.1 Effect of methamphetamine (inset, chemical structure) on apparent K_m values obtained using slice FSCV in young (~ 3 months) and aged (~ 18 months) mice of wildtype (WT) and BDNF$^{+/-}$ mice. (A) Representative concentration versus time plots (left) and cyclic voltammograms (right), before (pre-drug) and after perfusion of 0.3 µM methamphetamine in WT mice. (B & C) Non-linear fitting of dose-dependent increase in apparent K_m values with increasing methamphetamine concentrations in young and aged mice, respectively. (D & E) Linear regression plots of the apparent K_m values in young and aged mice, respectively, with omission of methamphetamine concentrations greater than 0.3 µM, because they significantly reduce DA release upon electrical stimulation. Data are reported means ± SEMs (n = 6 – 14 mice per group), analyzed using two-way ANOVA, ***$P < 0.0001$.

(*62*). The K_i for methamphetamine was lower in young wildtype (0.011 ± 0.001 µM, n = 7) as compared to the $BDNF^{+/-}$ (0.024 ± 0.001 µM, n = 6) mice, suggesting that methamphetamine is more potent in the wildtype mice than the $BDNF^{+/-}$ mice. In contrast, the calculated K_i values for methamphetamine from the aged mice (Figure 6.1E) were similar for both genotypes (wildtype; 0.026 ± 0.002 µM, n = 14 and $BDNF^{+/-}$ mice; 0.021 ± 0.002 µM, n = 12). Overall these results suggest that methamphetamine potency is decreased in young mice with low endogenous BDNF levels as compared to wildtype littermates, with no potency difference in the aged mice.

To determine the role of low endogenous BDNF levels on DA release, electrically evoked DA release was evaluated with increasing methamphetamine concentrations. Methamphetamine limits the presynaptic neuron's ability to use VMAT by disrupting the proton gradient required for sequestration of cytoplasmic DA into vesicles (*255*) Methamphetamine causes DA efflux that is independent of electrical stimulation or neuron firing activity (*255*). The maximal electrically stimulated DA release, normalized as percent of baseline, significantly decreased in a dose-dependent manner with increasing concentrations of methamphetamine in both genotypes (Figure 6.2). In this study, IC_{50} values obtained from the dose-response curves are defined as the concentration of methamphetamine required to attenuate electrically stimulated DA release by 50%, relative to the pre-drug baseline. The IC_{50} values from young mice were 0.055 ± 0.003 µM (wildtype, n = 7) and 0.060 ± 0.003 µM ($BDNF^{+/-}$, n = 6). The IC_{50} values from aged mice were 0.066 ± 0.002 µM (wildtype, n = 14) and 0.066 ± 0.002 µM ($BDNF^{+/-}$, n = 12), which were similar to the IC_{50} values of the young mice. Two-way ANOVA revealed that methamphetamine treatment significantly reduced stimulated DA

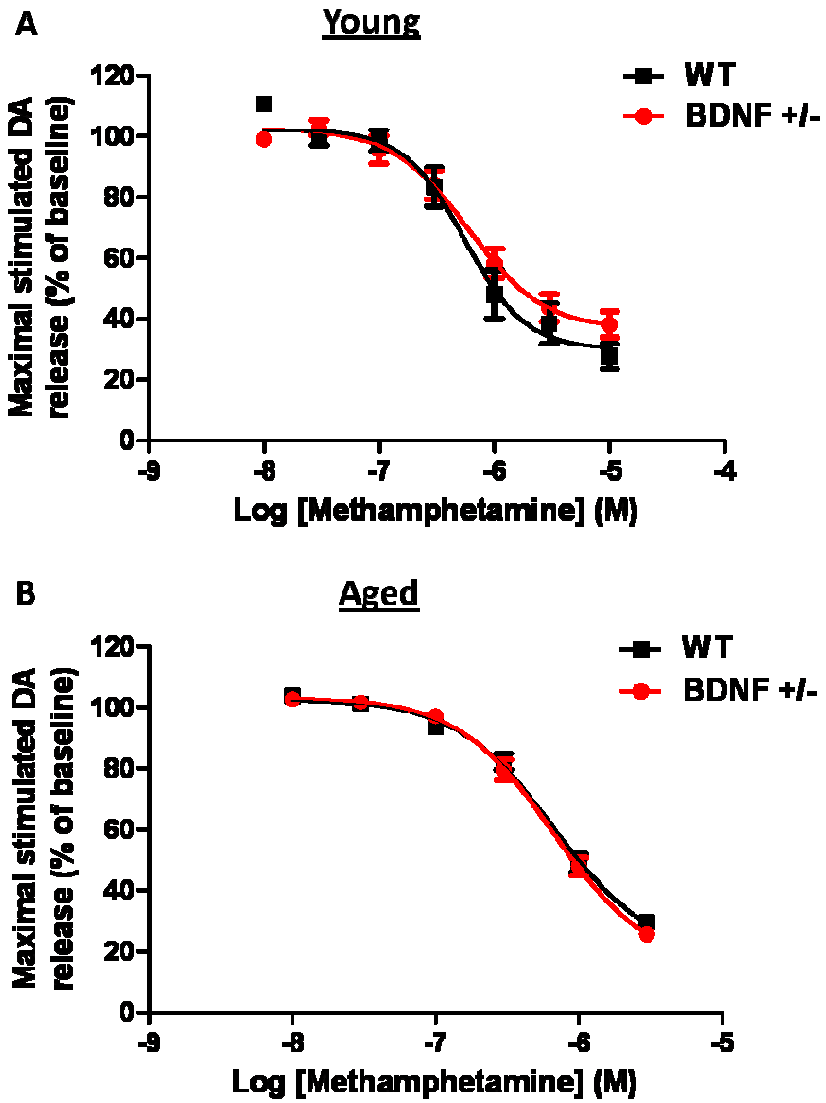

Figure 6.2 Effect of methamphetamine on electrically stimulated dopamine (DA) release as measured using slice FSCV. Dose-dependent decrease in maximal stimulated DA release relative to percentage of baseline in: (A) young adult mice (~ 3 months) and (B) aged (~ 18 months) mice in both wildtype (WT) and BDNF$^{+/-}$ mice. Data are means ± SEMs (n = 6 – 14 mice per group), analyzed using two-way ANOVA.

release in both young ($F_{7,143} = 66.74$, $P < 0.0001$, Figure 6.2A) and aged ($F_{6,326} = 346.8$, $P < 0.0001$; Figure 6.2B) mice. However, no main effect of genotype was observed in young ($F_{1,143} = 0.35$, $P = 0.56$) or aged ($F_{1,326} = 0.52$, $P = 0.47$) mice. Overall, the results suggest that BDNF expression does not play a role in the methamphetamine-induced vesicular depletion of DA.

Perfusion of methamphetamine did not alter the maximum velocity (V_{max}) in either genotype (Figure 6.3), as analyzed by one-way ANOVA (Dunnett's post-test). No difference was observed between the pre-drug V_{max} and V_{max} after methamphetamine treatments in ~ 3 month old wildtype ($F_{7,98} = 1.37$, $P = 0.23$) or $BDNF^{+/-}$ mice ($F_{8.73} = 0.90$, $P = 0.52$), Figures 6.3A and 6.3C, respectively. Similarly, increasing concentration of methamphetamine did not affect the V_{max} in the ~ 18 month old wildtype ($F_{6,179} = 0.44$, $P = 0.85$; Figure 6.3B) or $BDNF^{+/-}$ ($F_{6,143} = 0.89$, $P = 0.51$; Figure 6.3D) mice.

Genotypic differences in methamphetamine-induced DA release were assessed using *in vivo* microdialysis. *Microdialysis results were obtained by Johnna A. Birbeck and Kelly E. Bosse, Ph.D.* Methamphetamine i.p. injection (1.0 mg/kg) resulted in a 300 – 500% increase in extracellular concentrations of DA, relative to percent baseline, in both young and aged wildtype and $BDNF^{+/-}$ mice (Figure 6.4). Two-way ANOVA analysis revealed a significant main effect of methamphetamine treatment ($F_{8,115} = 14.87$, $P < 0.0001$), but no genotype effect ($F_{1,115} = 0.12$, $P = 0.73$), or treatment x genotype interaction ($F_{8,115} = 0.53$, $P = 0.83$) in young mice. Similarly, aged mice revealed a significant main effect of methamphetamine treatment ($F_{8,231} = 9.36$, $P < 0.0001$), but no

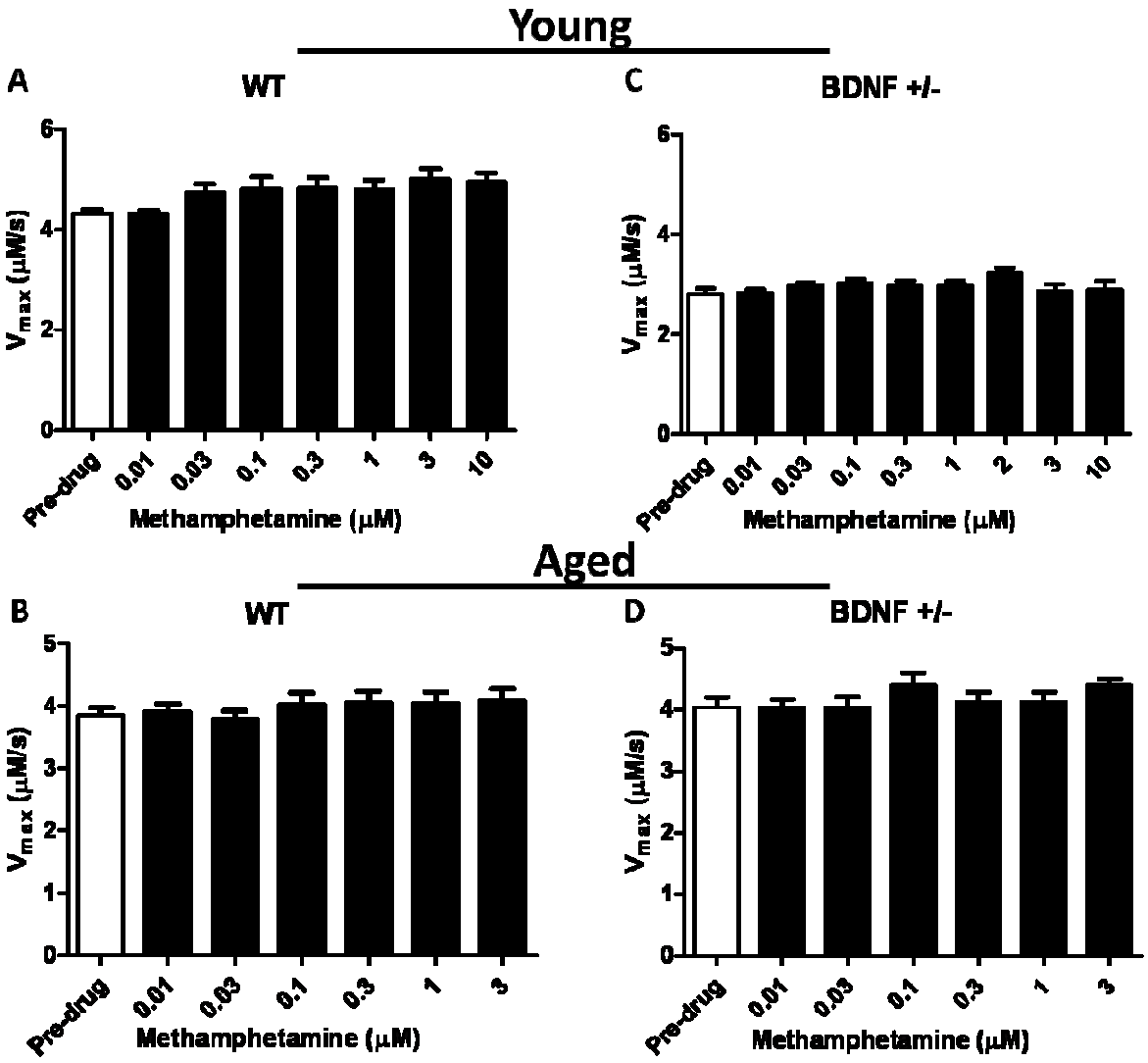

Figure 6.3 Effect of methamphetamine concentration on dopamine uptake, quantified by maximum velocity (V_{max}), as measured using slice FSCV in the caudate putamen (CPu). V_{max} values were not different after perfusion of methamphetamine in young adult (~ 3 months) wildtype and $BDNF^{+/-}$ mice (A & C, respectively), and aged (~ 18 months) wildtype and $BDNF^{+/-}$ mice (B & D, respectively). Data are reported as means ± SEMs (n = 6 – 14 mice per group).

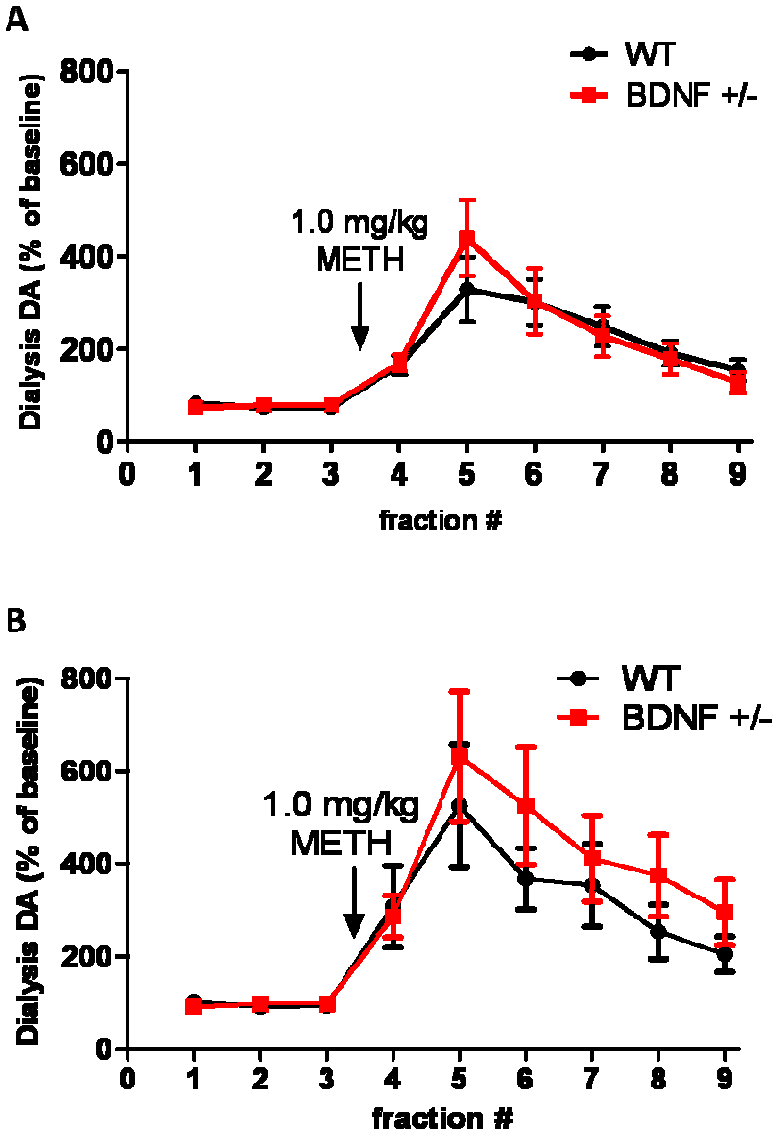

Figure 6.4 The acute effect intraperitoneal injection of methamphetamine (METH; 1.0 mg/kg) on extracellular dopamine (DA) concentrations in the caudate putamen (CPu) of young and aged (wildtype (WT) and BDNF$^{+/-}$) mice. Extracellular DA levels are expressed as a percentage relative to baseline in (A) young (~ 3 months) and (B) aged (~ 18 months) mice. METH-induced extracellular DA levels are not different between the genotypes in young and aged mice. Each fraction number (#) was collected for a period of 20 minutes. Data are reported as means ± SEMs (n = 7 - 20 mice per group). *Figure courtesy of Johnna A. Birbeck, Kelly E. Bosse, Ph.D., and Tiffany A. Mathews, Ph.D.*

genotype effect ($F_{1,231}$ = 2.44, P = 0.11), or treatment x genotype interaction ($F_{8,231}$ = 0.35, P = 0.94). Overall, these findings indicate that low BDNF levels did not alter methamphetamine-induced DA release *in vivo*.

6.4 Discussion

The primary objective of the present study was to determine the effect of low endogenous BDNF levels on DA transporter function throughout the animal's lifetime. This study was prompted by our previous findings that showed reduced DA uptake rates in young adult $BDNF^{+/-}$ mice as compared to their wildtype littermates (CHAPTER 4). To determine the extent of how low endogenous BDNF levels may alter or disrupt DA transport function, a competitive inhibitor of DA transporter methamphetamine was used. Slice FSCV was used to probe DA transporter function due to its fast temporal resolution (milliseconds) providing a relative comparison of DA uptake kinetic parameters. It has been previously reported that BDNF deficiency does not alter the expression of DA transporter; therefore, we predicted that $BDNF^{+/-}$ mice have altered DA uptake function leading to the observed decrease in uptake rates (*37, 133*). A dose-dependent increase in apparent K_m values with increasing methamphetamine concentration was observed in both genotypes and age groups. Interestingly, young BDNF-deficient mice appear to have a lower apparent K_m as compared to their wildtype littermates, suggesting a reduction in DA transport function. However, such BDNF-dependent reduction in DA transport function was not observed in the aged $BDNF^{+/-}$ mice suggesting the mice adapt with time.

DA uptake rates through the DA transporter are described by Michaelis-Menten kinetics with the following assumptions: (1) each electrical stimulation releases a

constant amount of DA, (2) the primary mechanism from clearing DA from the synapse is by the DA transporter, and (3) the uptake process is saturable (*14, 267, 268*). In slice FSCV, the K_m value is inversely related to DA's affinity for its transporter. In the presence of a competitive inhibitor like methamphetamine, the apparent K_m increases linearly indicating a low affinity of DA for its transporter (*14, 62*). Overall, the concentration of DA needed to reach V_{max} in the presence of methamphetamine is greater than the concentration of DA needed in its absence.

An inverse relationship exists between K_i and potency of an uptake inhibitor; with a high K_i value representing lower inhibitor potency while a low K_i value represents higher potency of the inhibitor. In this study, K_i values were calculated from the apparent K_m values (see Equation 5). Young wildtype mice had a lower K_i value as compared to young $BDNF^{+/-}$ or the aged mice. Overall, the K_i values obtained for methamphetamine (0.011 – 0.026 µM) from both genotypes were lower than previously reported K_i from C57Bl/6J mice (0.47 µM) using FSCV (*62*). Our K_i values were lower than previously reported because concentrations of methamphetamine greater than 0.3 µM reduce the electrically-stimulated DA release, in agreement with John and Jones observations with high concentrations of DA releasers (*62*). A net decrease in the amount of DA available for release alters the uptake process, an effect observed with amphetamines and not other uptake inhibitors such as cocaine (*68, 193*). However, this effect on stimulated DA release in the presence of methamphetamine does not appear to be dependent on BDNF levels.

Maximum velocity (V_{max}), which is proposed to be proportional to the number of DA transporters, was not altered by methamphetamine perfusion. This observation is in

agreement with other studies that have shown that both amphetamine and methamphetamine do not alter the V_{max} during DA inhibition (*62, 269*). Acute treatment of brain slices using methamphetamine is unlikely to cause degeneration of DA neurons or alter DA transporter density. With respect to age, there is evidence that aged BDNF-deficient mice, greater than 18 months old show no difference in DA transporter expression (*133*). Taken together, these findings further imply that low BDNF levels play a major role in altering DA transport function at a young age (~ 3 months of age) but low endogenous BDNF levels appear to have no overt effect on DA transporter expression.

Normally, transport of extracellular DA into the neuron is unidirectional, with the inward transport rate being greater than the rate of outward transport (*14, 270*). The presence of high extracellular concentrations DA for prolonged periods of time is thought to lower the rate of inward DA transport (reuptake) by the DA transporter (*14*). In addition, methamphetamine is hypothesized to favor the DA transporter to face inward most of the time, promoting DA efflux (*267*). If one of the functional consequence of the observed decreased V_{max} in the young $BDNF^{+/-}$ mice is the presence of more inward facing DA transporters, then this would suggests that the effect of inhibition of DA transport by methamphetamine is reduced. Indeed, our results show reduced DA inhibition (higher K_i value) in young $BDNF^{+/-}$ mice as compared to wildtype mice.

There is considerable evidence showing that protein kinases, such as protein kinase C (PKC) and Ca^{2+}/calmodulin-dependent protein kinase II (CaMKII) regulate DA transporter functions, including its orientation through phosphorylation (*213, 271-274*). Specifically, PKC activation causes phosphorylation of DA transporter at the N-terminus, an event required for amphetamine-mediated DA efflux (*272, 274*).

Interestingly, BDNF signaling through TrkB receptor activation is known to regulate numerous intracellular signaling pathways like PKC (*10, 22*). However, our current findings are unable to determine the exact role of reduced BDNF levels on protein kinases in the modulation of DA transporter.

It has been hypothesized that neurotoxic regiments of amphetamine molecules release sequestered DA from vesicles into the more oxidizing intracellular environment, facilitating the formation of reactive oxygen species such as superoxide radicals, hydroxyl radicals, and quinines (*131, 275*). Furthermore, it is hypothesized that DA neurons are more susceptible to degeneration due to the increased formation of reactive oxygen species that can destroy numerous biological functions within DA neurons. Intraneuronal sequestration of DA is important in preventing formation of reactive oxygen species because VMAT2 knock-out mice have increased methamphetamine-induced neurotoxicity (*276*). However, DA transporter knock-out mice are protected against methamphetamine-induced DA depletion and reactive oxygen species production in the striatum (*277*). This is attributed to reduced access of methamphetamine into the neuron (*277*). Interestingly, previous work has shown that a neurotoxic dose of methamphetamine causes more damage to the nigrostriatal dopaminergic system of wildtype mice as compared to $BDNF^{+/-}$ mice (*35, 134*). Others have shown that pre-treatment with BDNF protects neurons (*29, 278, 279*). Our findings suggest that young $BDNF^{+/-}$ mice would appear to be more resistant to a neurotoxic regiment of methamphetamine because they have decreased DA transporter function as compared to wildtype mice. Finally, our initial characterization and these methamphetamine results suggest that, due to the reduced DA transporter function in

the young BDNF$^{+/-}$ mice, methamphetamine access into the neuron is decreased. Thus, young BDNF$^{+/-}$ mice would be more resistant to methamphetamine neurotoxicity as compared to the young wildtype or aged mice.

6.5 Conclusions

The results herein suggest that low endogenous BDNF levels may modulate DA transporter function as evaluated using methamphetamine. Young BDNF$^{+/-}$ mice have reduced effectiveness of methamphetamine in competitively inhibiting DA uptake as compared to wildtype mice. The reduced apparent K_m values in young BDNF$^{+/-}$ mice as compared to wildtype littermates, further suggests that the observed functional decrease in DA uptake may be a result of the reduced affinity of DA for its transporter. Overall, the methamphetamine results confirm our hypothesis that, only young BDNF$^{+/-}$ mice have reduced DA uptake function, with no change in DA transporter density because the V_{max} was not altered. DA transport function in the aged mice was not different, as hypothesized because DA uptake rates in wildtype and BDNF$^{+/-}$ mice were similar.

Most often the addictive properties of drugs of abuse such as methamphetamine involve the mesolimbic dopaminergic system (*10*). However, the actions of abused drugs are not limited to only one system or brain region, but involve the interaction of numerous neurotransmitters, small molecules, and proteins. More specifically, recent studies have suggested that BDNF may play a pivotal role in addiction (*53, 54, 112, 113, 280*). Our finding highlights that; BDNF may modulate the DA transporter, a common target for drugs of abuse such as cocaine and methamphetamine.

CHAPTER 7

Conclusions and Future Directions

Brain-derived neurotrophic factor (BDNF) hypofunction is implicated in several neurological disorders and diseases that affect the dopamine (DA) system, such as Parkinson's disease, Alzheimer's disease, Huntington's disease, schizophrenia, attention deficit hyperactivity disorder (ADHD), addiction, and depression (*42, 46, 53, 54, 112, 113, 115-117, 190*). However, it is not known whether the BDNF hypofunction is the cause of these diseases/disorders or a result. Overall, our findings indicate that BDNF hypofunction can modulate presynaptic DA dynamics in the striatum, suggesting that low levels BDNF may play a role in the susceptibility to DA-related neurological diseases and disorders. The specific conclusions from the work undertaken here, as well as the studies needed to better understand the role of the BDNF on DA system are summarized in this chapter.

7.1 Characterization of dopamine D2 and D3 autoreceptors

Slice fast scan cyclic voltammetry (FSCV) and DA agonists were used to characterize the functionality of the DA D2 and D3 autoreceptors in the mouse striatum. The DA D2 agonists studied demonstrated that the DA D2 autoreceptors have a similar functionality in the caudate putamen (CPu), nucleus accumbens (NAc) core and NAc shell. However, the DA D3 autoreceptors functionality is localized in discrete regions, with the largest response to DA D3 agonists being in the NAc shell, followed by NAc core, and then the CPu. The analytical method developed provides a unique way of probing presynaptic DA D2 and D3 receptors. The findings complement autoradiography studies, which are unable to differentiate expression of presynaptic and

post-synaptic DA D2 and D3 receptors (*20, 119-122, 154, 155, 158*). Taken together these findings suggest that presynaptic DA D2 receptors are homogenously distributed in the striatum, while DA D3 autoreceptors are localized in the NAc shell. Furthermore, the Mathews' laboratory developed this slice FSCV assay to determine how low levels of endogenous BDNF influence presynaptic DA D2 and D3 autoreceptor functionality within the striatum (CHAPTER 4).

Taking advantage of the expression of each of the DA D2-like autoreceptors within the discrete striatal regions will be useful to differentiate the specificity of D2-like drug candidates, by determining DA D2 or D3 drug preference. Using slice voltammetry to characterize DA agonists and antagonists as either more D2- or D3-preferring will provide critical information regarding potential therapeutic selectivity, potency, efficacy, and dose dependency. Using slice FSCV assay to map presynaptic DA D2 and D3 autoreceptor functionality will also offer insight into the neurological diseases when used in genetically modified animal models.

7.2 Effect of low BDNF levels on dopamine dynamics

The overarching objectives of the "BDNF project" were to understand if and how low endogenous BDNF levels alter presynaptic DA dynamics using the complementary neurochemical techniques of *in vivo* microdialysis and slice FSCV. Our findings suggest that BDNF is indeed a powerful modulator of presynaptic DA dynamics. Low levels of BDNF appear to cause hyperdopaminergia in the CPu, characterized by elevated extracellular basal DA concentration and decreased DA uptake rates (Figure 7.1).

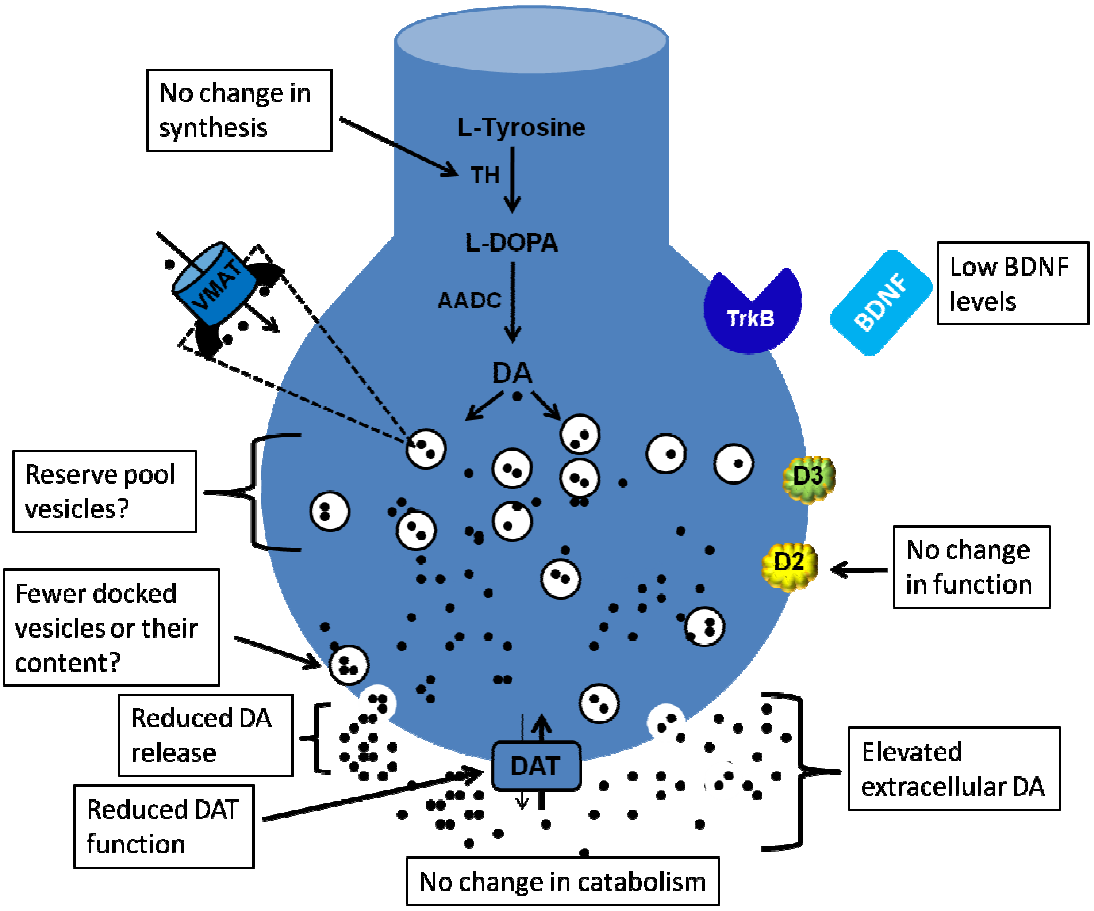

Figure 7.1 Schematic diagram showing the impact of low endogenous brain-derived neurotrophic factor (BDNF) levels on dopamine (DA) dynamics as measured using *in vivo* microdialysis and slice FSCV in the caudate putamen (CPu). $BDNF^{+/-}$ mice have reduced BDNF levels, elevated extracellular DA levels (hyperdopaminergia), reduced DA uptake function, and reduced DA release as compared to wildtype mice. Abbreviations: TH, tyrosine hydroxylase; L-DOPA, L-3,4-dihydroxyphenylalanine; AADC, L-aromatic amino acid decarboxylase; VMAT, vesicular monoamine transporter; DAT, DA transporter; TrkB, tyrosine kinase B.

To further probe the observed decrease in DA transporter uptake rates in $BDNF^{+/-}$ mice, the DA transporter substrate methamphetamine was used as a tool to evaluate the DA transporter kinetics. Low, endogenous BDNF levels in young mice lead to reduction in the affinity of DA for its transporter (CHAPTER 6). Therefore, the observed reduction in striatal DA uptake rate is primarily due to reduction in DA transport function. We hypothesize that the observed decrease in DA uptake in $BDNF^{+/-}$ mice could be a result of the DA system trying to overcompensate for the increase in basal extracellular DA levels. Future studies are warranted to determine if this combination of low BDNF levels and a hyperdopaminergic system increase the susceptibility to neurological disorders.

Slice voltammetry revealed that young $BDNF^{+/-}$ mice have decreased stimulated DA release in the CPu. This finding was surprising because *in vivo* microdialysis showed an increase in extracellular basal DA levels with no difference in DA synthesis rates. Furthermore, evidence from the Pozzo-Miller laboratory suggests that in the hippocampus, BDNF enhances quantal neurotransmitter release by increasing the number of docked synaptic vesicles within presynaptic terminals (*185*). Taken together, these findings suggest that similar to the hippocampus, the CPu may have fewer docked vesicles, which may lead to the observed decrease in stimulated DA release. Furthermore, this decrease in DA release can be quickly reversed with an acute perfusion of 100 ng/mL of BDNF over the slice (see Figure 4.7A), suggesting that a primary role of BDNF is to regulate DA release. Taken together, our overarching hypothesis is that at a very young age, extracellular DA levels are low due to the decrease in docked vesicles and/or their content. As a result of these low extracellular

DA levels, the DA system tries to compensate by decreasing the function of the DA transporter. However, due to the increase in extracellular DA levels observed in mice aged ~ 3 months, it appears that the system overcompensates. Therefore to better understand these paradoxical findings, future experiments should focus on determining whether and how BDNF signaling modulates DA vesicular recruitment and/or mobilization of the vesicle pools.

Although the findings obtained using slice FSCV provide an important foundation toward understanding how low BDNF levels modulate presynaptic DA dynamics, *in vivo* FSCV will deliver important details regarding burst-firing patterns in the BDNF-deficient mice. Unlike *in vivo* microdialysis, which predominantly measures tonic extracellular DA levels (‘baseline’) and averages phasic (or burst) firing over a period of 20 minutes, *in vivo* FSCV measures DA every 100 ms allowing for a unique insight into naturally occurring DA transients (phasic firing) (*56, 75, 89, 196*). Furthermore, *in vivo* voltammetry is not limited to measuring naturally occurring DA, but can measure electrically stimulated DA release, which provides a sufficient amount of DA, permitting evaluation of DA uptake parameters *in vivo* (*64, 65, 281, 282*).

Our results and other studies indicate that exogenous BDNF can acutely potentiate DA release in the CPu (CHAPTER 4) (*29-31, 201*). Exactly how BDNF mediates presynaptic DA mechanisms however, remains elusive. Extracellular BDNF binds to the tyrosine kinase (TrkB) receptor, and upon activation, numerous downstream intracellular signaling cascades are initiated including phospholipase C, γ (PLCγ), phosphotidylinositol-3 kinase (PI3K), and mitogen-activated protein kinase (MAPK) pathways (CHAPTER 1) (*10, 283*). However, in order for exogenous BDNF to

acutely modulate DA release, a rapid signaling event may be required. Signaling via the PLCγ pathway appears to be the most likely intracellular pathway which BDNF could rapidly increase DA release in the CPu. Activation of the PLCγ leads to synthesis of inositol 1,4,5 triphosphate (IP3), through its receptor, IP3 then stimulates sarcoplasmic reticulum to release Ca^{2+} (Figure 7.2) (*23, 209, 284*).

Several studies have linked cytoplasmic Ca^{2+} concentration in modulation of neurotransmitter trafficking and docking of vesicles (*209, 285, 286*). For example, Neal *et al.* demonstrated that increased intracellular Ca^{2+} and influx of extracellular Ca^{2+} are important in enhancing BDNF-mediated DA release from amacrine cells of rabbit eye retina (*209*). However, no studies have evaluated the role of BDNF-signaling mediated Ca^{2+} release and regulation of presynaptic DA release in the striatum. To determine the mechanism through which BDNF mediates DA release, future experiments are required to determine if and how PLCγ pathway activation is involved in striatal DA release.

There are a few limitations of using BDNF to probe DA dynamics. First, purchasing BDNF is expensive, making most researchers to use very low concentrations to better understand its therapeutic benefits. Secondly, as a large protein (27 kDa), BDNF cannot easily pass through the blood-brain barrier, and the only effective delivery method is direct infusions into the brain. For example, phase I/II clinical trials using recombinant human BDNF have been unsuccessful in amyotrophic lateral sclerosis patients mainly due to poor delivery method and a short half-life (*287*). However, recent studies have identified 7,8-dihydroxyflavone, a selective high-affinity TrkB agonist that initiates TrkB dimerization, autophosphorylation, and activation of downstream signaling cascades (*288-291*).

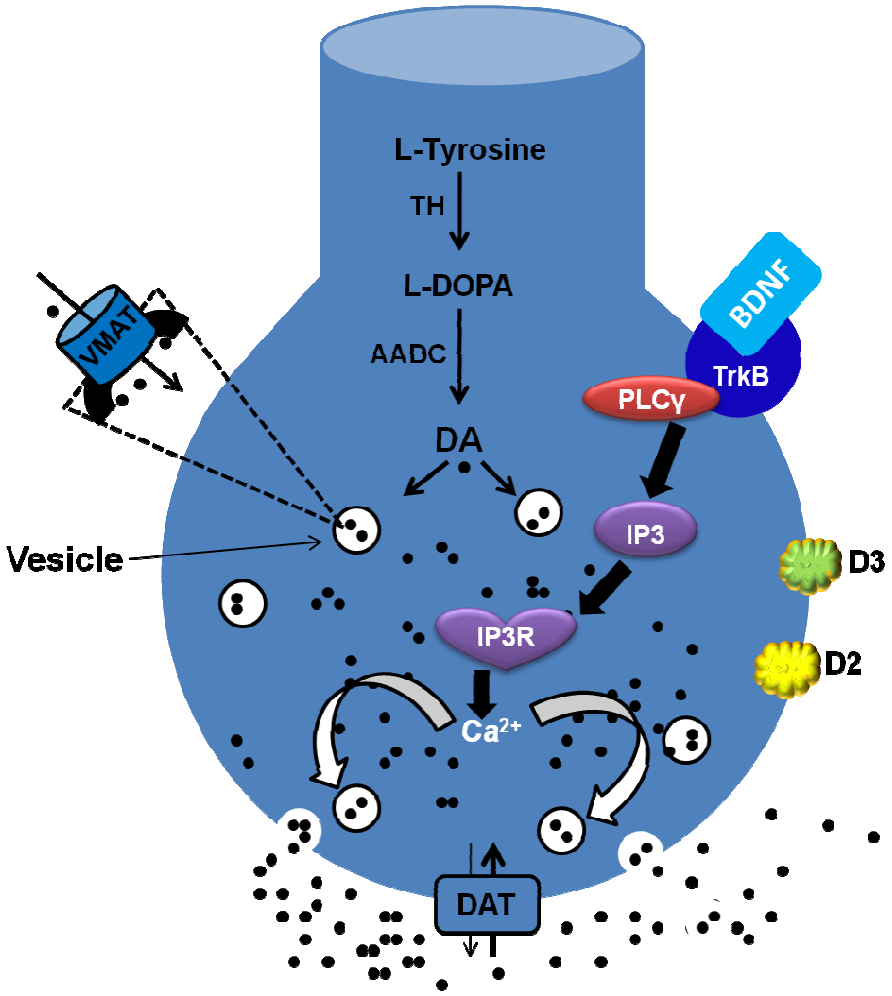

Figure 7.2 Schematic representation of the possible mechanism through which exogenous brain-derived neurotrophic factor (BDNF) signaling through tyrosine kinase B (TrkB) receptor acutely increases dopamine (DA) release in the presynaptic terminal. Abbreviations used: TH, tyrosine hydroxylase; L-DOPA, 3,4-dihydroxyphenylalanine; AADC, L-aromatic amino acid decarboxylase; VMAT, vesicular monoamine transporter; DAT, DA transporter; PLCγ, phospholipase Cγ; PI3K, phosphatidylinositol-3-kinase; IP3, inositol-1,4,5-triphosphate; IP3R, IP3 receptor.

Now that there an opportunity to use 7,8-dihydroxyflavone, one of the most critical questions regarding this small molecule is whether it can modulate neurotransmitter dynamics, or simply put, how does it influence the DA system? Future studies will use 7,8-dihydroxyflavone to probe DA dynamics with neurochemical techniques including FSCV and microdialysis to provide a better understanding of TrkB-signaling role in neurotransmission and therapeutic relevance of the TrkB receptor agonist.

Although the majority of this dissertation research has focused on the dorsal striatum (caudate-putamen; CPu), another brain region of interest is the nucleus accumbens (NAc). This region is involved in addiction and there is considerable evidence that low BDNF levels may predispose individuals to addiction (*53, 54, 112, 113, 280*). Thus, the primary question is whether low endogenous BDNF levels in the NAc have the same effect as they do in the CPu. In the NAc, electrically stimulated DA release is reduced, with no difference in DA uptake rates, further suggesting that BDNF is a key mediator of DA release. Additionally, low, endogenous BDNF levels appear to lead to reduction in the release-regulating DA D3 autoreceptor function in the NAc shell. Taken together, these alterations in the NAc suggest the impact of low endogenous BDNF levels throughout the striatum. Although initial characterization has focused on using only slice voltammetry to examine DA alterations in the NAc, future studies will determine basal extracellular DA levels in NAc using microdialysis. By examining both dorsal and ventral striatum, we hope to have a better understanding of how low BDNF levels influence DA dynamics in a brain region dependent manner.

7.3 Low BDNF levels, aging and dopamine dynamics

Finally, our last study was to evaluate age-related impact of the low endogenous BDNF levels on presynaptic striatal DA dynamics. For example, there is a natural age-related decline in striatal presynaptic dopaminergic functions of stimulated DA release and clearance observed in NAc of wildtype mice. In contrast, DA release, uptake, and catabolism appear to be enhanced in aged BDNF-deficient mice. These results suggest that aging plays a significant role in 'normalizing' the hyperdopaminergic phenotype observed in ~ 3 month old $BDNF^{+/-}$ mice, highlighting possible neuronal DA adaptations during the aging process. Taken together, the role of endogenous BDNF levels appear to be more critical during the development of DA system and not for long term maintenance of presynaptic DA function. Future studies will examine discrete time points to determine at what age the neurochemical adaptations 'switch' to make the BDNF-deficient mice appear more like wildtype mice. Once the approximate time point is known, future studies will then focus on the neurobiology or neurochemistry to understand what is leading to this 'normalization' in the BDNF-deficient mice.

Overall, the intrinsic function of reduced BDNF levels appears to be concomitant reduction of DA release in young BDNF-deficient mice. However, in the aged BDNF-deficient mice, DA is release is similar to wildtype mice. These results suggest that, excess extracellular basal DA are reduced through increased DA uptake and DA catabolism over the animal's lifetime. Future experiments will focus on determining whether the increase in catabolism is due to increased expression of the DA transporter and/or monoamine oxidase (MAO) or its function.

The overarching goals of this these studies are to better understand how low endogenous BDNF levels modulate DA neuronal transmission within the striatum. Our findings suggest that, in young animals that there are significant alterations in numerous presynaptic functions within the striatum, which may ultimately lead to increase susceptibility to neurological diseases. Although these findings provide the necessary foundation in understanding this complex relationship between BDNF and DA, obviously future studies will examine how BDNF signaling mediates dopaminergic system with age or in the presence of either an illicit drug or therapeutic drug to better understand the complex relationship between BDNF signaling and DA system.

REFERENCES

1. Cooper, J. R., Bloom, F. E., and Roth, R. H. (1996) *The biochemical basis of neuropharmacology*, 7 ed., Oxford University Press, New York.
2. Siegel, G. J., Agranoff, B. W., and Albers, R. W. (1999) *Basic Neurochemistry: Molecular, Cellular & Medical Aspects* 6ed., Lippincott-Raven, Philadephia.
3. Wise, R. A., and Rompre, P. P. (1989) Brain dopamine and reward, *Annu Rev Psychol 40*, 191-225.
4. Missale, C., Nash, S. R., Robinson, S. W., Jaber, M., and Caron, M. G. (1998) Dopamine receptors: from structure to function, *Physiol Rev 78*, 189-225.
5. Kuczenski, R., Segal, D., and Aizenstein, M. (1991) Amphetamine, cocaine, and fencamfamine: relationship between locomotor and stereotypy response profiles and caudate and accumbens dopamine dynamics, *J. Neurosci. 11*, 2703-2712.
6. Fleckenstein, A. E., Volz, T. J., Riddle, E. L., Gibb, J. W., and Hanson, G. R. (2007) New Insights into the Mechanism of Action of Amphetamines, *Annual Review of Pharmacology and Toxicology 47*, 681-698.
7. Di Chiara, G., and Imperato, A. (1985) Ethanol preferentially stimulates dopamine release in the nucleus accumbens of freely moving rats, *Eur J Pharmacol 115*, 131-132.
8. Mathews, T. A., John, C. E., Lapa, G. B., Budygin, E. A., and Jones, S. R. (2006) No role of the dopamine transporter in acute ethanol effects on striatal dopamine dynamics, *Synapse 60*, 288-294.
9. Paxinos, G., and Franklin, K. B. J. (2001) *The Mouse Brain in Stereotaxic Coordinates*, Second ed., Academic Press, San Diego.

10. Nestler, E. J., Hyman, S. E., and Malenka, R. C. (2009) *Molecular Basis of Neuropharmacology: A Foundation for Clinical Neuroscience* Second ed., McGraw-Hill, New York.

11. von Bohlen und Halbach, O., and Dermietzel, R. (2002) *Neurotransmitters and Neuromodulators, Handbook of Receptors and Biological Effects*, Wiley-VCH Verlag GmbH & Co. KGaA, Weinheim.

12. Pierce, R. C., and Kumaresan, V. (2006) The mesolimbic dopamine system: the final common pathway for the reinforcing effect of drugs of abuse?, *Neurosci Biobehav Rev 30*, 215-238.

13. Carter, A. R., Chen, C., Schwartz, P. M., and Segal, R. A. (2002) Brain-Derived Neurotrophic Factor Modulates Cerebellar Plasticity and Synaptic Ultrastructure, *J. Neurosci. 22*, 1316-1327.

14. Jones, S. R., Joseph, J. D., Barak, L. S., Caron, M. G., and Wightman, R. M. (1999) Dopamine neuronal transport kinetics and effects of amphetamine, *J Neurochem 73*, 2406-2414.

15. Mortensen, O. V., and Amara, S. G. (2003) Dynamic regulation of the dopamine transporter, *Eur J Pharmacol 479*, 159-170.

16. Amara, S. G., and Kuhar, M. J. (1993) Neurotransmitter transporters: recent progress, *Annu Rev Neurosci 16*, 73-93.

17. Jackson, D. M., and Westlind-Danielsson, A. (1994) Dopamine receptors: molecular biology, biochemistry and behavioural aspects, *Pharmacol Ther 64*, 291-370.

18. Kebabian, J. W., and Calne, D. B. (1979) Multiple receptors for dopamine, *Nature 277*, 93-96.

19. Benkert, O., Grunder, G., and Wetzel, H. (1992) Dopamine autoreceptor agonists in the treatment of schizophrenia and major depression, *Pharmacopsychiatry 25*, 254-260.

20. Sokoloff, P., Giros, B., Martres, M. P., Bouthenet, M. L., and Schwartz, J. C. (1990) Molecular cloning and characterization of a novel dopamine receptor (D3) as a target for neuroleptics, *Nature 347*, 146-151.

21. McAllister, A. K., Katz, L. C., and Lo, D. C. (1999) Neurotrophins and synaptic plasticity, *Annu Rev Neurosci 22*, 295-318.

22. Lu, B. (2003) BDNF and activity-dependent synaptic modulation, *Learn Mem 10*, 86-98.

23. Kaplan, D. R., and Miller, F. D. (2000) Neurotrophin signal transduction in the nervous system, *Current Opinion in Neurobiology 10*, 381-391.

24. Altar, C. A., Cai, N., Bliven, T., Juhasz, M., Conner, J. M., Acheson, A. L., Lindsay, R. M., and Wiegand, S. J. (1997) Anterograde transport of brain-derived neurotrophic factor and its role in the brain, *Nature 389*, 856-860.

25. Altar, C. A., Siuciak, J. A., Wright, P., Ip, N. Y., Lindsay, R. M., and Wiegand, S. J. (1994) In situ hybridization of trkB and trkC receptor mRNA in rat forebrain and association with high-affinity binding of [125I]BDNF, [125I]NT-4/5 and [125I]NT-3, *Eur J Neurosci 6*, 1389-1405.

26. Poo, M. M. (2001) Neurotrophins as synaptic modulators, *Nat Rev Neurosci 2*, 24-32.

27. Nestler, E. J. (2001) Molecular basis of long-term plasticity underlying addiction, *Nat Rev Neurosci 2*, 119-128.

28. Altar, C. A., Boylan, C. B., Fritsche, M., Jackson, C., Hyman, C., and Lindsay, R. M. (1994) The Neurotrophins NT-4/5 and BDNF Augment Serotonin, Dopamine, and GABAergic Systems during Behaviorally Effective Infusions to the Substantia Nigra, *Experimental Neurology 130*, 31-40.

29. Siuciak, J. A., Boylan, C., Fritsche, M., Altar, C. A., and Lindsay, R. M. (1996) BDNF increases monoaminergic activity in rat brain following intracerebroventricular or intraparenchymal administration, *Brain Res 710*, 11-20.

30. Altar, C. A., Fritsche, M., and Lindsay, R. M. (1998) Cell body infusions of brain-derived neurotrophic factor increase forebrain dopamine release and serotonin metabolism determined with in vivo microdialysis, *Adv Pharmacol 42*, 915-921.

31. Goggi, J., Pullar, I. A., Carney, S. L., and Bradford, H. F. (2002) Modulation of neurotransmitter release induced by brain-derived neurotrophic factor in rat brain striatal slices in vitro, *Brain Res 941*, 34-42.

32. Goggi, J., Pullar, I. A., Carney, S. L., and Bradford, H. F. (2003) Signalling pathways involved in the short-term potentiation of dopamine release by BDNF, *Brain Research 968*, 156-161.

33. Nestler, E. J., and Carlezon, W. A. (2006) The Mesolimbic Dopamine Reward Circuit in Depression, *Biological psychiatry 59*, 1151-1159.

34. Dluzen, D. E., Gao, X., Story, G. M., Anderson, L. I., Kucera, J., and Walro, J. M. (2001) Evaluation of nigrostriatal dopaminergic function in adult +/+ and +/- BDNF mutant mice, *Exp Neurol 170*, 121-128.

35. Dluzen, D. E., Anderson, L. I., McDermott, J. L., Kucera, J., and Walro, J. M. (2002) Striatal dopamine output is compromised within +/- BDNF mice, *Synapse 43*, 112-117.

36. Guillin, O., Diaz, J., Carroll, P., Griffon, N., Schwartz, J. C., and Sokoloff, P. (2001) BDNF controls dopamine D3 receptor expression and triggers behavioural sensitization, *Nature 411*, 86-89.

37. Joyce, J. N., Renish, L., Osredkar, T., Walro, J. M., Kucera, J., and Dluzen, D. E. (2004) Methamphetamine-induced loss of striatal dopamine innervation in BDNF heterozygote mice does not further reduce D3 receptor concentrations, *Synapse 52*, 11-19.

38. Saylor, A. J., Meredith, G. E., Vercillo, M. S., Zahm, D. S., and McGinty, J. F. (2006) BDNF heterozygous mice demonstrate age-related changes in striatal and nigral gene expression, *Exp Neurol 199*, 362-372.

39. Cordeira, J. W., Frank, L., Sena-Esteves, M., Pothos, E. N., and Rios, M. (2010) Brain-Derived Neurotrophic Factor Regulates Hedonic Feeding by Acting on the Mesolimbic Dopamine System, *J. Neurosci. 30*, 2533-2541.

40. Marsden, C. D. (1990) Parkinson's disease, *Lancet 335*, 948-952.

41. Howells, D. W., Porritt, M. J., Wong, J. Y. F., Batchelor, P. E., Kalnins, R., Hughes, A. J., and Donnan, G. A. (2000) Reduced BDNF mRNA Expression in the Parkinson's Disease Substantia Nigra, *Experimental Neurology 166*, 127-135.

42. Mogi, M., Togari, A., Kondo, T., Mizuno, Y., Komure, O., Kuno, S., Ichinose, H., and Nagatsu, T. (1999) Brain-derived growth factor and nerve growth factor

concentrations are decreased in the substantia nigra in Parkinson's disease, *Neuroscience Letters 270*, 45-48.

43. Parain, K., Murer, M. G., Yan, Q., Faucheux, B., Agid, Y., Hirsch, E., and Raisman-Vozari, R. (1999) Reduced expression of brain-derived neurotrophic factor protein in Parkinson's disease substantia nigra, *Neuroreport 10*, 557-561.

44. Warby, S. C., Graham, R. K., and Hayden, M. R. (1993) Huntington Disease.

45. MacDonald, M. E., Ambrose, C. M., Duyao, M. P., Myers, R. H., Lin, C., Srinidhi, L., Barnes, G., Taylor, S. A., James, M., Groot, N., MacFarlane, H., Jenkins, B., Anderson, M. A., Wexler, N. S., Gusella, J. F., Bates, G. P., Baxendale, S., Hummerich, H., Kirby, S., North, M., Youngman, S., Mott, R., Zehetner, G., Sedlacek, Z., Poustka, A., Frischauf, A.-M., Lehrach, H., Buckler, A. J., Church, D., Doucette-Stamm, L., O'Donovan, M. C., Riba-Ramirez, L., Shah, M., Stanton, V. P., Strobel, S. A., Draths, K. M., Wales, J. L., Dervan, P., Housman, D. E., Altherr, M., Shiang, R., Thompson, L., Fielder, T., Wasmuth, J. J., Tagle, D., Valdes, J., Elmer, L., Allard, M., Castilla, L., Swaroop, M., Blanchard, K., Collins, F. S., Snell, R., Holloway, T., Gillespie, K., Datson, N., Shaw, D., and Harper, P. S. (1993) A novel gene containing a trinucleotide repeat that is expanded and unstable on Huntington's disease chromosomes, *Cell 72*, 971-983.

46. Zuccato, C., and Cattaneo, E. (2009) Brain-derived neurotrophic factor in neurodegenerative diseases, *Nat Rev Neurol 5*, 311-322.

47. Gauthier, L. R., Charrin, B. C., Borrell-Pages, M., Dompierre, J. P., Rangone, H., Cordelieres, F. P., De Mey, J., MacDonald, M. E., Lessmann, V., Humbert, S., and Saudou, F. (2004) Huntingtin controls neurotrophic support and survival of

neurons by enhancing BDNF vesicular transport along microtubules, *Cell 118*, 127-138.

48. Kuntsi, J., McLoughlin, G., and Asherson, P. (2006) Attention deficit hyperactivity disorder, *Neuromolecular Med 8*, 461-484.

49. Solanto, M. V. (2002) Dopamine dysfunction in AD/HD: integrating clinical and basic neuroscience research, *Behav Brain Res 130*, 65-71.

50. Kim, B.-N., Cummins, T. D. R., Kim, J.-W., Bellgrove, M. A., Hong, S.-B., Song, S.-H., Shin, M.-S., Cho, S.-C., Kim, J.-H., Son, J.-W., Shin, Y.-M., Chung, U.-S., and Han, D.-H. (2011) Val/Val genotype of brain-derived neurotrophic factor (BDNF) Val66Met polymorphism is associated with a better response to OROS-MPH in Korean ADHD children, *The International Journal of Neuropsychopharmacology FirstView*, 1-12.

51. Kent, L., Green, E., Hawi, Z., Kirley, A., Dudbridge, F., Lowe, N., Raybould, R., Langley, K., Bray, N., Fitzgerald, M., Owen, M. J., O'Donovan, M. C., Gill, M., Thapar, A., and Craddock, N. (2005) Association of the paternally transmitted copy of common Valine allele of the Val66Met polymorphism of the brain-derived neurotrophic factor (BDNF) gene with susceptibility to ADHD, *Mol Psychiatry 10*, 939-943.

52. Aureli, A., Del Beato, T., Sebastiani, P., Marimpietri, A., Melillo, C. V., Sechi, E., and Di Loreto, S. (2010) Attention-deficit hyperactivity disorder and intellectual disability: a study of association with brain-derived neurotrophic factor gene polymorphisms, *Int J Immunopathol Pharmacol 23*, 873-880.

53. Bolanos, C. A., and Nestler, E. J. (2004) Neurotrophic mechanisms in drug addiction, *Neuromolecular Med 5*, 69-83.

54. McGinty, J. F., Whitfield Jr, T. W., and Berglind, W. J. (2010) Brain-derived neurotrophic factor and cocaine addiction, *Brain Research 1314*, 183-193.

55. Schultz, K. N., and Kennedy, R. T. (2008) Time-resolved microdialysis for in vivo neurochemical measurements and other applications, *Annu Rev Anal Chem (Palo Alto Calif) 1*, 627-661.

56. Wightman, R. M., and Robinson, D. L. (2002) Transient changes in mesolimbic dopamine and their association with 'reward', *Journal of Neurochemistry 82*, 721-735.

57. Michael, D. J., and Wightman, R. M. (1999) Electrochemical monitoring of biogenic amine neurotransmission in real time, *Journal of Pharmaceutical and Biomedical Analysis 19*, 33-46.

58. Hochstetler, S. E., Puopolo, M., Gustincich, S., Raviola, E., and Wightman, R. M. (2000) Real-time amperometric measurements of zeptomole quantities of dopamine released from neurons, *Anal Chem 72*, 489-496.

59. Shippenberg, T. S., He, M., and Chefer, V. (1999) The use of microdialysis in the mouse: conventional versus quantitative techniques, *Psychopharmacology (Berl) 147*, 33-34.

60. Mas, M., Gonzalez-Mora, J. L., Louilot, A., Sole, C., and Guadalupe, T. (1990) Increased dopamine release in the nucleus accumbens of copulating male rats as evidenced by in vivo voltammetry, *Neurosci Lett 110*, 303-308.

61. Sabeti, J., Adams, C. E., Burmeister, J., Gerhardt, G. A., and Zahniser, N. R. (2002) Kinetic analysis of striatal clearance of exogenous dopamine recorded by chronoamperometry in freely-moving rats, *J Neurosci Methods 121*, 41-52.

62. John, C. E., and Jones, S. R. (2007) Voltammetric characterization of the effect of monoamine uptake inhibitors and releasers on dopamine and serotonin uptake in mouse caudate-putamen and substantia nigra slices, *Neuropharmacology 52*, 1596-1605.

63. Ortiz, A. N., Kurth, B. J., Osterhaus, G. L., and Johnson, M. A. (2010) Dysregulation of intracellular dopamine stores revealed in the R6/2 mouse striatum, *Journal of Neurochemistry 112*, 755-761.

64. Kraft, J. C., Osterhaus, G. L., Ortiz, A. N., Garris, P. A., and Johnson, M. A. (2009) In vivo dopamine release and uptake impairments in rats treated with 3-nitropropionic acid, *Neuroscience 161*, 940-949.

65. Park, J., Aragona, B. J., Kile, B. M., Carelli, R. M., and Wightman, R. M. (2010) In vivo voltammetric monitoring of catecholamine release in subterritories of the nucleus accumbens shell, *Neuroscience 169*, 132-142.

66. Aragona, B. J., Cleaveland, N. A., Stuber, G. D., Day, J. J., Carelli, R. M., and Wightman, R. M. (2008) Preferential Enhancement of Dopamine Transmission within the Nucleus Accumbens Shell by Cocaine Is Attributable to a Direct Increase in Phasic Dopamine Release Events, *J. Neurosci. 28*, 8821-8831.

67. Fawaz, C. S., Martel, P., Leo, D., and Trudeau, L. E. (2009) Presynaptic action of neurotensin on dopamine release through inhibition of D(2) receptor function, *BMC Neurosci 10*, 96.

68. Jones, S. R., Garris, P. A., and Wightman, R. M. (1995) Different effects of cocaine and nomifensine on dopamine uptake in the caudate-putamen and nucleus accumbens, *J Pharmacol Exp Ther 274*, 396-403.

69. Jones, S. R., Lee, T. H., Wightman, R. M., and Ellinwood, E. H. (1996) Effects of intermittent and continuous cocaine administration on dopamine release and uptake regulation in the striatum: in vitro voltammetric assessment, *Psychopharmacology (Berl) 126*, 331-338.

70. Joseph, J. D., Wang, Y. M., Miles, P. R., Budygin, E. A., Picetti, R., Gainetdinov, R. R., Caron, M. G., and Wightman, R. M. (2002) Dopamine autoreceptor regulation of release and uptake in mouse brain slices in the absence of D(3) receptors, *Neuroscience 112*, 39-49.

71. Kennedy, R. T., Jones, S. R., and Wightman, R. M. (1992) Dynamic observation of dopamine autoreceptor effects in rat striatal slices, *J Neurochem 59*, 449-455.

72. Khalid, M., Aoun, R. A., and Mathews, T. A. (2011) Altered striatal dopamine release following a sub-acute exposure to manganese, *Journal of Neuroscience Methods In Press, Uncorrected Proof*.

73. Mateo, Y., Lack, C. M., Morgan, D., Roberts, D. C., and Jones, S. R. (2005) Reduced dopamine terminal function and insensitivity to cocaine following cocaine binge self-administration and deprivation, *Neuropsychopharmacology 30*, 1455-1463.

74. Phillips, P. E., Johns, J. M., Lubin, D. A., Budygin, E. A., Gainetdinov, R. R., Lieberman, J. A., and Wightman, R. M. (2003) Presynaptic dopaminergic function

is largely unaltered in mesolimbic and mesostriatal terminals of adult rats that were prenatally exposed to cocaine, *Brain Res 961*, 63-72.

75. Phillips, P. E., Robinson, D. L., Stuber, G. D., Carelli, R. M., and Wightman, R. M. (2003) Real-time measurements of phasic changes in extracellular dopamine concentration in freely moving rats by fast-scan cyclic voltammetry, *Methods Mol Med 79*, 443-464.

76. Roberts, C., Cummins, R., Gnoffo, Z., and Kew, J. N. (2006) Dopamine D3 receptor modulation of dopamine efflux in the rat nucleus accumbens, *Eur J Pharmacol 534*, 108-114.

77. Wightman, R. M., Amatore, C., Engstrom, R. C., Hale, P. D., Kristensen, E. W., Kuhr, W. G., and May, L. J. (1988) Real-time characterization of dopamine overflow and uptake in the rat striatum, *Neuroscience 25*, 513-523.

78. Cadoni, C., and Di Chiara, G. (2000) Differential changes in accumbens shell and core dopamine in behavioral sensitization to nicotine, *Eur J Pharmacol 387*, R23-25.

79. Chefer, V. I., Zapata, A., Shippenberg, T. S., and Bungay, P. M. (2006) Quantitative no-net-flux microdialysis permits detection of increases and decreases in dopamine uptake in mouse nucleus accumbens, *Journal of Neuroscience Methods 155*, 187-193.

80. Dickinson, S. D., Sabeti, J., Larson, G. A., Giardina, K., Rubinstein, M., Kelly, M. A., Grandy, D. K., Low, M. J., Gerhardt, G. A., and Zahniser, N. R. (1999) Dopamine D2 receptor-deficient mice exhibit decreased dopamine transporter

function but no changes in dopamine release in dorsal striatum, *J Neurochem 72*, 148-156.

81. Humpel, C., Ebendal, T., and Olson, L. (1996) Microdialysis: a way to study in vivo release of neurotrophic bioactivity: a critical summary, *J Mol Med 74*, 523-526.

82. Mathews, T. A., Brookshire, B. R., Budygin, E. A., Hamre, K., Goldowitz, D., and Jones, S. R. (2009) Ethanol-induced hyperactivity is associated with hypodopaminergia in the 22-TNJ ENU-mutated mouse, *Alcohol 43*, 421-431.

83. Mathews, T. A., Fedele, D. E., Coppelli, F. M., Avila, A. M., Murphy, D. L., and Andrews, A. M. (2004) Gene dose-dependent alterations in extraneuronal serotonin but not dopamine in mice with reduced serotonin transporter expression, *J Neurosci Methods 140*, 169-181.

84. Parsons, L. H., and Justice, J. B., Jr. (1994) Quantitative approaches to in vivo brain microdialysis, *Crit Rev Neurobiol 8*, 189-220.

85. Robertson, G. S., Tham, C. S., Wilson, C., Jakubovic, A., and Fibiger, H. C. (1993) In vivo comparisons of the effects of quinpirole and the putative presynaptic dopaminergic agonists B-HT 920 and SND 919 on striatal dopamine and acetylcholine release, *J Pharmacol Exp Ther 264*, 1344-1351.

86. Smith, A. D., and Justice, J. B. (1994) The effect of inhibition of synthesis, release, metabolism and uptake on the microdialysis extraction fraction of dopamine, *J Neurosci Methods 54*, 75-82.

87. Kissinger, P. T., and Heineman, W. R. (1983) Cyclic voltammetry, *Journal of Chemical Education 60*, 702.

88. Van Benschoten, J. J., Lewis, J. Y., Heineman, W. R., Roston, D. A., and Kissinger, P. T. (1983) Cyclic voltammetry experiment, *Journal of Chemical Education 60*, 772-null.

89. Robinson, D. L., Venton, B. J., Heien, M. L., and Wightman, R. M. (2003) Detecting subsecond dopamine release with fast-scan cyclic voltammetry in vivo, *Clin Chem 49*, 1763-1773.

90. Jones, S. R., Garris, P. A., Kilts, C. D., and Wightman, R. M. (1995) Comparison of dopamine uptake in the basolateral amygdaloid nucleus, caudate-putamen, and nucleus accumbens of the rat, *J Neurochem 64*, 2581-2589.

91. Addy, N. A., Daberkow, D. P., Ford, J. N., Garris, P. A., and Wightman, R. M. (2010) Sensitization of rapid dopamine signaling in the nucleus accumbens core and shell after repeated cocaine in rats, *J Neurophysiol 104*, 922-931.

92. Budygin, E. A., John, C. E., Mateo, Y., and Jones, S. R. (2002) Lack of cocaine effect on dopamine clearance in the core and shell of the nucleus accumbens of dopamine transporter knock-out mice, *J Neurosci 22*, RC222.

93. Marcus, M. M., Nomikos, G. G., and Svensson, T. H. (1996) Differential actions of typical and atypical antipsychotic drugs on dopamine release in the core and shell of the nucleus accumbens, *Eur Neuropsychopharmacol 6*, 29-38.

94. Maina, F. K., and Mathews, T. A. (2010) Functional Fast Scan Cyclic Voltammetry Assay to Characterize Dopamine D2 and D3 Autoreceptors in the Mouse Striatum, *ACS Chemical Neuroscience 1*, 450-462.

95. Kreiss, D. S., Bergstrom, D. A., Gonzalez, A. M., Huang, K. X., Sibley, D. R., and Walters, J. R. (1995) Dopamine receptor agonist potencies for inhibition of cell

firing correlate with dopamine D3 receptor binding affinities, *Eur J Pharmacol 277*, 209-214.

96. Cragg, S. J., Hille, C. J., and Greenfield, S. A. (2000) Dopamine release and uptake dynamics within nonhuman primate striatum in vitro, *J Neurosci 20*, 8209-8217.

97. Rice, M. E., Richards, C. D., Nedergaard, S., Hounsgaard, J., Nicholson, C., and Greenfield, S. A. (1994) Direct monitoring of dopamine and 5-HT release in substantia nigra and ventral tegmental area in vitro, *Exp Brain Res 100*, 395-406.

98. Giros, B., Jaber, M., Jones, S. R., Wightman, R. M., and Caron, M. G. (1996) Hyperlocomotion and indifference to cocaine and amphetamine in mice lacking the dopamine transporter, *Nature 379*, 606-612.

99. Perez, X. A., Parameswaran, N., Huang, L. Z., O'Leary, K. T., and Quik, M. (2008) Pre-synaptic dopaminergic compensation after moderate nigrostriatal damage in non-human primates, *J Neurochem 105*, 1861-1872.

100. Johnson, M. A., Rajan, V., Miller, C. E., and Wightman, R. M. (2006) Dopamine release is severely compromised in the R6/2 mouse model of Huntington's disease, *J Neurochem 97*, 737-746.

101. Zhang, L., Doyon, W. M., Clark, J. J., Phillips, P. E., and Dani, J. A. (2009) Controls of tonic and phasic dopamine transmission in the dorsal and ventral striatum, *Mol Pharmacol 76*, 396-404.

102. Zhang, T., Zhang, L., Liang, Y., Siapas, A. G., Zhou, F. M., and Dani, J. A. (2009) Dopamine signaling differences in the nucleus accumbens and dorsal striatum exploited by nicotine, *J Neurosci 29*, 4035-4043.

103. Justice, J. B., Jr. (1993) Quantitative microdialysis of neurotransmitters, *J Neurosci Methods 48*, 263-276.

104. Torto, N., Laurell, T., Gorton, L., and Marko-Varga, G. (1999) Recent trends in the application of microdialysis in bioprocesses, *Analytica Chimica Acta 379*, 281-305.

105. Davies, M. I., Cooper, J. D., Desmond, S. S., Lunte, C. E., and Lunte, S. M. (2000) Analytical considerations for microdialysis sampling, *Adv Drug Deliv Rev 45*, 169-188.

106. Weiss, D. J., Lunte, C. E., and Lunte, S. M. (2000) In vivo microdialysis as a tool for monitoring pharmacokinetics, *TrAC Trends in Analytical Chemistry 19*, 606-616.

107. Pugsley, T. A., Davis, M. D., Akunne, H. C., MacKenzie, R. G., Shih, Y. H., Damsma, G., Wikstrom, H., Whetzel, S. Z., Georgic, L. M., Cooke, L. W., and et al. (1995) Neurochemical and functional characterization of the preferentially selective dopamine D3 agonist PD 128907, *J Pharmacol Exp Ther 275*, 1355-1366.

108. Zapata, A., and Shippenberg, T. S. (2002) D(3) receptor ligands modulate extracellular dopamine clearance in the nucleus accumbens, *J Neurochem 81*, 1035-1042.

109. Kennedy, R. T., Thompson, J. E., and Vickroy, T. W. (2002) In vivo monitoring of amino acids by direct sampling of brain extracellular fluid at ultralow flow rates and capillary electrophoresis, *J Neurosci Methods 114*, 39-49.

110. Chefer, V. I., Zakharova, I., and Shippenberg, T. S. (2003) Enhanced responsiveness to novelty and cocaine is associated with decreased basal dopamine uptake and release in the nucleus accumbens: quantitative microdialysis in rats under transient conditions, *J Neurosci 23*, 3076-3084.

111. Erickson, B. E. (2000) Product Review: Electrochemical detectors for liquid chromatography, *Analytical Chemistry 72*, 353 A-357 A.

112. Ghitza, U. E., Zhai, H., Wu, P., Airavaara, M., Shaham, Y., and Lu, L. (2010) Role of BDNF and GDNF in drug reward and relapse: A review, *Neuroscience & Biobehavioral Reviews 35*, 157-171.

113. Pierce, R. C., and Bari, A. A. (2001) The role of neurotrophic factors in psychostimulant-induced behavioral and neuronal plasticity, *Rev Neurosci 12*, 95-110.

114. Mogi, M., Togari, A., Kondo, T., Mizuno, Y., Komure, O., Kuno, S., Ichinose, H., and Nagatsu, T. (1999) Brain-derived growth factor and nerve growth factor concentrations are decreased in the substantia nigra in Parkinson's disease, *Neurosci Lett 270*, 45-48.

115. Ferrer, I., Goutan, E., Marin, C., Rey, M. J., and Ribalta, T. (2000) Brain-derived neurotrophic factor in Huntington disease, *Brain Res 866*, 257-261.

116. Murer, M. G., Yan, Q., and Raisman-Vozari, R. (2001) Brain-derived neurotrophic factor in the control human brain, and in Alzheimer's disease and Parkinson's disease, *Progress in Neurobiology 63*, 71-124.

117. Zajac, M., Pang, T., Wong, N., Weinrich, B., Leang, L., Craig, J., Saffery, R., and Hannan, A. (2010) Wheel running and environmental enrichment differentially

modify exon-specific BDNF expression in the hippocampus of wild-type and pre-motor symptomatic male and female Huntington's disease mice, *Hippocampus 20*, 621-636.

118. Chen, Y. C., Choi, J. K., Andersen, S. L., Rosen, B. R., and Jenkins, B. G. (2005) Mapping dopamine D2/D3 receptor function using pharmacological magnetic resonance imaging, *Psychopharmacology (Berl) 180*, 705-715.

119. Stanwood, G. D., McElligot, S., Lu, L., and McGonigle, P. (1997) Ontogeny of dopamine D3 receptors in the nucleus accumbens of the rat, *Neurosci Lett 223*, 13-16.

120. Tarazi, F. I., Moran-Gates, T., Wong, E. H., Henry, B., and Shahid, M. (2008) Differential regional and dose-related effects of asenapine on dopamine receptor subtypes, *Psychopharmacology (Berl) 198*, 103-111.

121. Tupala, E., Hall, H., Bergstrom, K., Sarkioja, T., Rasanen, P., Mantere, T., Callaway, J., Hiltunen, J., and Tiihonen, J. (2001) Dopamine D(2)/D(3)-receptor and transporter densities in nucleus accumbens and amygdala of type 1 and 2 alcoholics, *Mol Psychiatry 6*, 261-267.

122. Tupala, E., and Tiihonen, J. (2008) Cortical dopamine D(1) receptors in type 1 and type 2 alcoholics measured with human whole hemisphere autoradiography, *Psychiatry Res 162*, 1-9.

123. Zapata, A., and Shippenberg, T. S. (2005) Lack of functional D2 receptors prevents the effects of the D3-preferring agonist (+)-PD 128907 on dialysate dopamine levels, *Neuropharmacology 48*, 43-50.

124. Patel, J., Trout, S. J., Palij, P., Whelpton, R., and Kruk, Z. L. (1995) Biphasic inhibition of stimulated endogenous dopamine release by 7-OH-DPAT in slices of rat nucleus accumbens, *Br J Pharmacol 115*, 421-426.

125. Schmitz, Y., Schmauss, C., and Sulzer, D. (2002) Altered dopamine release and uptake kinetics in mice lacking D2 receptors, *J Neurosci 22*, 8002-8009.

126. Wu, Q., Reith, M. E., Walker, Q. D., Kuhn, C. M., Carroll, F. I., and Garris, P. A. (2002) Concurrent autoreceptor-mediated control of dopamine release and uptake during neurotransmission: an in vivo voltammetric study, *J Neurosci 22*, 6272-6281.

127. Guiard, B. P., David, D. J., Deltheil, T., Chenu, F., Le Maitre, E., Renoir, T., Leroux-Nicollet, I., Sokoloff, P., Lanfumey, L., Hamon, M., Andrews, A. M., Hen, R., and Gardier, A. M. (2008) Brain-derived neurotrophic factor-deficient mice exhibit a hippocampal hyperserotonergic phenotype, *Int J Neuropsychopharmacol 11*, 79-92.

128. Nibuya, M., Nestler, E., and Duman, R. (1996) Chronic antidepressant administration increases the expression of cAMP response element binding protein (CREB) in rat hippocampus, *J. Neurosci. 16*, 2365-2372.

129. Miyazaki, I., and Asanuma, M. (2008) Dopaminergic neuron-specific oxidative stress caused by dopamine itself, *Acta Med Okayama 62*, 141-150.

130. Asanuma, M., Miyazaki, I., Diaz-Corrales, F. J., Miyoshi, K., Ogawa, N., and Murata, M. (2008) Preventing effects of a novel anti-parkinsonian agent zonisamide on dopamine quinone formation, *Neuroscience Research 60*, 106-113.

131. Stokes, A. H., Hastings, T. G., and Vrana, K. E. (1999) Cytotoxic and genotoxic potential of dopamine, *Journal of Neuroscience Research 55*, 659-665.

132. Dluzen, D. E., McDermott, J. L., Anderson, L. I., Kucera, J., Joyce, J. N., Osredkar, T., and Walro, J. M. (2004) Age-related changes in nigrostriatal dopaminergic function are accentuated in +/- brain-derived neurotrophic factor mice, *Neuroscience 128*, 201-208.

133. Boger, H. A., Mannangatti, P., Samuvel, D. J., Saylor, A. J., Bender, T. S., McGinty, J. F., Fortress, A. M., Zaman, V., Huang, P., Middaugh, L. D., Randall, P. K., Jayanthi, L. D., Rohrer, B., Helke, K. L., Granholm, A. C., and Ramamoorthy, S. (2011) Effects of brain-derived neurotrophic factor on dopaminergic function and motor behavior during aging, *Genes Brain Behav 10*, 186-198.

134. Dluzen, D. E., and McDermott, J. L. (2004) Developmental and genetic influences upon gender differences in methamphetamine-induced nigrostriatal dopaminergic neurotoxicity, *Ann N Y Acad Sci 1025*, 205-220.

135. Lack, A. K., Diaz, M.R., Chappell, A., DuBois, D.W. & McCool, B.A. . (2007) Chronic ethanol and withdrawal differentially modulate pre- and postsynaptic function at glutamatergic synapses in rat basolateral amygdala, *J Neurophysiol 98*, 3185-3196.

136. John, C. E., and Jones, S. R. (2006) Exocytotic release of dopamine in ventral tegmental area slices from C57BL/6 and dopamine transporter knockout mice, *Neurochem Int 49*, 737-745.

137. Budygin, E. A., Phillips, P. E., Wightman, R. M., and Jones, S. R. (2001) Terminal effects of ethanol on dopamine dynamics in rat nucleus accumbens: an in vitro voltammetric study, *Synapse 42*, 77-79.

138. Heien, M. L., Phillips, P. E., Stuber, G. D., Seipel, A. T., and Wightman, R. M. (2003) Overoxidation of carbon-fiber microelectrodes enhances dopamine adsorption and increases sensitivity, *Analyst 128*, 1413-1419.

139. Near, J. A., Bigelow, J. C., and Wightman, R. M. (1988) Comparison of uptake of dopamine in rat striatal chopped tissue and synaptosomes, *J Pharmacol Exp Ther 245*, 921-927.

140. Wu, Q., Reith, M. E., Wightman, R. M., Kawagoe, K. T., and Garris, P. A. (2001) Determination of release and uptake parameters from electrically evoked dopamine dynamics measured by real-time voltammetry, *J Neurosci Methods 112*, 119-133.

141. Wightman, R. M., and Zimmerman, J. B. (1990) Control of dopamine extracellular concentration in rat striatum by impulse flow and uptake, *Brain Res Brain Res Rev 15*, 135-144.

142. Bosse, K. E., and Mathews, T. A. (2011) Ethanol-induced increases in extracellular dopamine are blunted in brain-derived neurotrophic factor heterozygous mice, *Neuroscience Letters 489*, 172-176.

143. Lonnroth, P., Jansson, P. A., and Smith, U. (1987) A microdialysis method allowing characterization of intercellular water space in humans, *Am J Physiol 253*, E228-231.

144. Cosford, R. J., Vinson, A. P., Kukoyi, S., and Justice, J. B., Jr. (1996) Quantitative microdialysis of serotonin and norepinephrine: pharmacological influences on in vivo extraction fraction, *J Neurosci Methods 68*, 39-47.

145. Budygin, E. A., Mathews, T. A., Lapa, G. B., and Jones, S. R. (2005) Local effects of acute ethanol on dopamine neurotransmission in the ventral striatum in C57BL/6 mice, *Eur J Pharmacol 523*, 40-45.

146. Zaborszky, L., Alheid, G. F., Beinfeld, M. C., Eiden, L. E., Heimer, L., and Palkovits, M. (1985) Cholecystokinin innervation of the ventral striatum: a morphological and radioimmunological study, *Neuroscience 14*, 427-453.

147. Yamada, S., Takaki, T., Yokoo, H., and Tanaka, M. (1995) Differential effects of dopamine antagonists on evoked dopamine release from slices of striatum and nucleus accumbens in rats, *J Pharm Pharmacol 47*, 259-262.

148. Cragg, S. J., Hille, C. J., and Greenfield, S. A. (2002) Functional domains in dorsal striatum of the nonhuman primate are defined by the dynamic behavior of dopamine, *J Neurosci 22*, 5705-5712.

149. Cragg, S. J. (2003) Variable dopamine release probability and short-term plasticity between functional domains of the primate striatum, *J Neurosci 23*, 4378-4385.

150. Jones, S. R., O'Dell, S. J., Marshall, J. F., and Wightman, R. M. (1996) Functional and anatomical evidence for different dopamine dynamics in the core and shell of the nucleus accumbens in slices of rat brain, *Synapse 23*, 224-231.

151. Zocchi, A., Girlanda, E., Varnier, G., Sartori, I., Zanetti, L., Wildish, G. A., Lennon, M., Mugnaini, M., and Heidbreder, C. A. (2003) Dopamine

responsiveness to drugs of abuse: A shell-core investigation in the nucleus accumbens of the mouse, *Synapse 50*, 293-302.

152. Zapata, A., Kivell, B., Han, Y., Javitch, J. A., Bolan, E. A., Kuraguntla, D., Jaligam, V., Oz, M., Jayanthi, L. D., Samuvel, D. J., Ramamoorthy, S., and Shippenberg, T. S. (2007) Regulation of dopamine transporter function and cell surface expression by D3 dopamine receptors, *J Biol Chem 282*, 35842-35854.

153. Gainetdinov, R. R., Sotnikova, T. D., Grekhova, T. V., and Rayevsky, K. S. (1996) In vivo evidence for preferential role of dopamine D3 receptor in the presynaptic regulation of dopamine release but not synthesis, *Eur J Pharmacol 308*, 261-269.

154. Levesque, D., Diaz, J., Pilon, C., Martres, M. P., Giros, B., Souil, E., Schott, D., Morgat, J. L., Schwartz, J. C., and Sokoloff, P. (1992) Identification, characterization, and localization of the dopamine D3 receptor in rat brain using 7-[3H]hydroxy-N,N-di-n-propyl-2-aminotetralin, *Proc Natl Acad Sci U S A 89*, 8155-8159.

155. Diaz, J., Pilon, C., Le Foll, B., Gros, C., Triller, A., Schwartz, J. C., and Sokoloff, P. (2000) Dopamine D3 receptors expressed by all mesencephalic dopamine neurons, *J Neurosci 20*, 8677-8684.

156. Sokoloff, P., Guillin, O., Diaz, J., Carroll, P., and Griffon, N. (2002) Brain-derived neurotrophic factor controls dopamine D3 receptor expression: implications for neurodevelopmental psychiatric disorders, *Neurotox Res 4*, 671-678.

157. Sokoloff, P., Diaz, J., Le Foll, B., Guillin, O., Leriche, L., Bezard, E., and Gross, C. (2006) The dopamine D3 receptor: a therapeutic target for the treatment of neuropsychiatric disorders, *CNS Neurol Disord Drug Targets 5*, 25-43.

158. Bouthenet, M. L., Souil, E., Martres, M. P., Sokoloff, P., Giros, B., and Schwartz, J. C. (1991) Localization of dopamine D3 receptor mRNA in the rat brain using in situ hybridization histochemistry: comparison with dopamine D2 receptor mRNA, *Brain Res 564*, 203-219.

159. Zapata, A., Witkin, J. M., and Shippenberg, T. S. (2001) Selective D3 receptor agonist effects of (+)-PD 128907 on dialysate dopamine at low doses, *Neuropharmacology 41*, 351-359.

160. Jones, S. R., Gainetdinov, R. R., Hu, X. T., Cooper, D. C., Wightman, R. M., White, F. J., and Caron, M. G. (1999) Loss of autoreceptor functions in mice lacking the dopamine transporter, *Nat Neurosci 2*, 649-655.

161. Batchelor, M., and Schenk, J. O. (1998) Protein kinase A activity may kinetically upregulate the striatal transporter for dopamine, *J Neurosci 18*, 10304-10309.

162. Bolan, E. A., Kivell, B., Jaligam, V., Oz, M., Jayanthi, L. D., Han, Y., Sen, N., Urizar, E., Gomes, I., Devi, L. A., Ramamoorthy, S., Javitch, J. A., Zapata, A., and Shippenberg, T. S. (2007) D2 receptors regulate dopamine transporter function via an extracellular signal-regulated kinases 1 and 2-dependent and phosphoinositide 3 kinase-independent mechanism, *Mol Pharmacol 71*, 1222-1232.

163. Cass, W. A., and Gerhardt, G. A. (1994) Direct in vivo evidence that D2 dopamine receptors can modulate dopamine uptake, *Neurosci Lett 176*, 259-263.

164. De Mei, C., Ramos, M., Iitaka, C., and Borrelli, E. (2009) Getting specialized: presynaptic and postsynaptic dopamine D2 receptors, *Curr Opin Pharmacol 9*, 53-58.

165. Lee, F. J., Pei, L., Moszczynska, A., Vukusic, B., Fletcher, P. J., and Liu, F. (2007) Dopamine transporter cell surface localization facilitated by a direct interaction with the dopamine D2 receptor, *Embo J 26*, 2127-2136.

166. Meiergerd, S. M., Patterson, T. A., and Schenk, J. O. (1993) D2 receptors may modulate the function of the striatal transporter for dopamine: kinetic evidence from studies in vitro and in vivo, *J Neurochem 61*, 764-767.

167. O'Neill, C., Evers-Donnelly, A., Nicholson, D., O'Boyle, K. M., and O'Connor, J. J. (2009) D2 receptor-mediated inhibition of dopamine release in the rat striatum in vitro is modulated by CB1 receptors: studies using fast cyclic voltammetry, *J Neurochem 108*, 545-551.

168. Levant, B. (1998) Differential distribution of D3 dopamine receptors in the brains of several mammalian species, *Brain Res 800*, 269-274.

169. Le Foll, B., Gallo, A., Le Strat, Y., Lu, L., and Gorwood, P. (2009) Genetics of dopamine receptors and drug addiction: a comprehensive review, *Behav Pharmacol 20*, 1-17.

170. Rothblat, D. S., and Schneider, J. S. (1997) Regionally specific effects of haloperidol and clozapine on dopamine reuptake in the striatum, *Neurosci Lett 228*, 119-122.

171. Loder, M. K., and Melikian, H. E. (2003) The dopamine transporter constitutively internalizes and recycles in a protein kinase C-regulated manner in stably transfected PC12 cell lines, *J Biol Chem 278*, 22168-22174.

172. Carvelli, L., Moron, J. A., Kahlig, K. M., Ferrer, J. V., Sen, N., Lechleiter, J. D., Leeb-Lundberg, L. M., Merrill, G., Lafer, E. M., Ballou, L. M., Shippenberg, T. S., Javitch, J. A., Lin, R. Z., and Galli, A. (2002) PI 3-kinase regulation of dopamine uptake, *J Neurochem 81*, 859-869.

173. Moron, J. A., Zakharova, I., Ferrer, J. V., Merrill, G. A., Hope, B., Lafer, E. M., Lin, Z. C., Wang, J. B., Javitch, J. A., Galli, A., and Shippenberg, T. S. (2003) Mitogen-activated protein kinase regulates dopamine transporter surface expression and dopamine transport capacity, *J Neurosci 23*, 8480-8488.

174. Kapur, S., and Seeman, P. (2001) Does fast dissociation from the dopamine d(2) receptor explain the action of atypical antipsychotics?: A new hypothesis, *Am J Psychiatry 158*, 360-369.

175. Deutch, A. Y., Moghaddam, B., Innis, R. B., Krystal, J. H., Aghajanian, G. K., Bunney, B. S., and Charney, D. S. (1991) Mechanisms of action of atypical antipsychotic drugs. Implications for novel therapeutic strategies for schizophrenia, *Schizophr Res 4*, 121-156.

176. Carlsson, A., and Lindqvist, M. (1963) Effect of Chlorpromazine or Haloperidol on Formation of 3methoxytyramine and Normetanephrine in Mouse Brain, *Acta Pharmacol Toxicol (Copenh) 20*, 140-144.

177. Sautel, F., Griffon, N., Sokoloff, P., Schwartz, J. C., Launay, C., Simon, P., Costentin, J., Schoenfelder, A., Garrido, F., Mann, A., and et al. (1995)

Nafadotride, a potent preferential dopamine D3 receptor antagonist, activates locomotion in rodents, *J Pharmacol Exp Ther 275*, 1239-1246.

178. Thoenen, H. (1995) Neurotrophins and neuronal plasticity, *Science 270*, 593-598.

179. Croll, S. D., Ip, N. Y., Lindsay, R. M., and Wiegand, S. J. (1998) Expression of BDNF and trkB as a function of age and cognitive performance, *Brain Res 812*, 200-208.

180. Conner, J. M., Lauterborn, J. C., Yan, Q., Gall, C. M., and Varon, S. (1997) Distribution of brain-derived neurotrophic factor (BDNF) protein and mRNA in the normal adult rat CNS: evidence for anterograde axonal transport, *J Neurosci 17*, 2295-2313.

181. Seroogy, K. B., and Gall, C. M. (1993) Expression of neurotrophins by midbrain dopaminergic neurons, *Exp Neurol 124*, 119-128.

182. Hyman, C., Hofer, M., Barde, Y. A., Juhasz, M., Yancopoulos, G. D., Squinto, S. P., and Lindsay, R. M. (1991) BDNF is a neurotrophic factor for dopaminergic neurons of the substantia nigra, *Nature 350*, 230-232.

183. Hyman, C., Juhasz, M., Jackson, C., Wright, P., Ip, N. Y., and Lindsay, R. M. (1994) Overlapping and distinct actions of the neurotrophins BDNF, NT-3, and NT-4/5 on cultured dopaminergic and GABAergic neurons of the ventral mesencephalon, *J Neurosci 14*, 335-347.

184. Hoglinger, G. U., Sautter, J., Meyer, M., Spenger, C., Seiler, R. W., Oertel, W. H., and Widmer, H. R. (1998) Rat fetal ventral mesencephalon grown as solid tissue

cultures: influence of culture time and BDNF treatment on dopamine neuron survival and function, *Brain Res 813*, 313-322.

185. Tyler, W. J., and Pozzo-Miller, L. D. (2001) BDNF enhances quantal neurotransmitter release and increases the number of docked vesicles at the active zones of hippocampal excitatory synapses, *J Neurosci 21*, 4249-4258.

186. Conover, J. C., and Yancopoulos, G. D. (1997) Neurotrophin regulation of the developing nervous system: analyses of knockout mice, *Rev Neurosci 8*, 13-27.

187. Pozzo-Miller, L. D., Gottschalk, W., Zhang, L., McDermott, K., Du, J., Gopalakrishnan, R., Oho, C., Sheng, Z.-H., and Lu, B. (1999) Impairments in High-Frequency Transmission, Synaptic Vesicle Docking, and Synaptic Protein Distribution in the Hippocampus of BDNF Knockout Mice, *J. Neurosci. 19*, 4972-4983.

188. Saylor, A. J., and McGinty, J. F. (2008) Amphetamine-induced locomotion and gene expression are altered in BDNF heterozygous mice, *Genes, Brain and Behavior 7*, 906-914.

189. Dluzen, D. E., Story, G. M., Xu, K., Kucera, J., and Walro, J. M. (1999) Alterations in Nigrostriatal Dopaminergic Function within BDNF Mutant Mice, *Experimental Neurology 160*, 500-507.

190. Angelucci, F., Brene, S., and Mathe, A. A. (2005) BDNF in schizophrenia, depression and corresponding animal models, *Mol Psychiatry 10*, 345-352.

191. Lapchak, P. A., Beck, K. D., Araujo, D. M., Irwin, I., Langston, J. W., and Hefti, F. (1993) Chronic intranigral administration of brain-derived neurotrophic factor produces striatal dopaminergic hypofunction in unlesioned adult rats and fails to

attenuate the decline of striatal dopaminergic function following medial forebrain bundle transection, *Neuroscience 53*, 639-650.

192. Spina, M. B., Squinto, S. P., Miller, J., Lindsay, R. M., and Hyman, C. (1992) Brain-derived neurotrophic factor protects dopamine neurons against 6-hydroxydopamine and N-methyl-4-phenylpyridinium ion toxicity: involvement of the glutathione system, *J Neurochem 59*, 99-106.

193. Jones, S. R., Gainetdinov, R. R., Wightman, R. M., and Caron, M. G. (1998) Mechanisms of amphetamine action revealed in mice lacking the dopamine transporter, *J Neurosci 18*, 1979-1986.

194. Yavich, L., and MacDonald, E. (2000) Dopamine release from pharmacologically distinct storage pools in rat striatum following stimulation at frequency of neuronal bursting, *Brain Research 870*, 73-79.

195. Calhoun, M., Jucker, M., Martin, L., Thinakaran, G., Price, D., and Mouton, P. (1996) Comparative evaluation of synaptophysin-based methods for quantification of synapses, *Journal of Neurocytology 25*, 821-828.

196. Grace, A. A., and Bunney, B. S. (1984) The control of firing pattern in nigral dopamine neurons: burst firing, *J Neurosci 4*, 2877-2890.

197. Sombers, L. A., Beyene, M., Carelli, R. M., and Wightman, R. M. (2009) Synaptic overflow of dopamine in the nucleus accumbens arises from neuronal activity in the ventral tegmental area, *J Neurosci 29*, 1735-1742.

198. Rebec, G. V., Christensen, J. R., Guerra, C., and Bardo, M. T. (1997) Regional and temporal differences in real-time dopamine efflux in the nucleus accumbens during free-choice novelty, *Brain Res 776*, 61-67.

199. Rebec, G. V., Grabner, C. P., Johnson, M., Pierce, R. C., and Bardo, M. T. (1997) Transient increases in catecholaminergic activity in medial prefrontal cortex and nucleus accumbens shell during novelty, *Neuroscience 76*, 707-714.

200. Saylor, A., and McGinty, J. (2010) An intrastriatal brain-derived neurotrophic factor infusion restores striatal gene expression in Bdnf heterozygous mice, *Brain Structure and Function*, 1-8.

201. Lohof, A. M., Ip, N. Y., and Poo, M. M. (1993) Potentiation of developing neuromuscular synapses by the neurotrophins NT-3 and BDNF, *Nature 363*, 350-353.

202. Knusel, B., and Hefti, F. (1992) K-252 compounds: modulators of neurotrophin signal transduction, *J Neurochem 59*, 1987-1996.

203. Hoover, B. R., Everett, C. V., Sorkin, A., and Zahniser, N. R. (2007) Rapid regulation of dopamine transporters by tyrosine kinases in rat neuronal preparations, *J Neurochem 101*, 1258-1271.

204. Berninger, B., Garcia, D. E., Inagaki, N., Hahnel, C., and Lindholm, D. (1993) BDNF and NT-3 induce intracellular Ca2+ elevation in hippocampal neurones, *Neuroreport 4*, 1303-1306.

205. Stoop, R., and Poo, M. M. (1996) Synaptic modulation by neurotrophic factors, *Prog Brain Res 109*, 359-364.

206. Kang, H., and Schuman, E. M. (1995) Long-lasting neurotrophin-induced enhancement of synaptic transmission in the adult hippocampus, *Science 267*, 1658-1662.

207. Du, J., Feng, L., Yang, F., and Lu, B. (2000) Activity- and Ca(2+)-dependent modulation of surface expression of brain-derived neurotrophic factor receptors in hippocampal neurons, *J Cell Biol 150*, 1423-1434.

208. Du, J., Feng, L., Zaitsev, E., Je, H. S., Liu, X. W., and Lu, B. (2003) Regulation of TrkB receptor tyrosine kinase and its internalization by neuronal activity and Ca2+ influx, *J Cell Biol 163*, 385-395.

209. Neal, M., Cunningham, J., Lever, I., Pezet, S., and Malcangio, M. (2003) Mechanism by which brain-derived neurotrophic factor increases dopamine release from the rabbit retina, *Invest Ophthalmol Vis Sci 44*, 791-798.

210. Hendry, I. A., Stockel, K., Thoenen, H., and Iversen, L. L. (1974) The retrograde axonal transport of nerve growth factor, *Brain Res 68*, 103-121.

211. Ramamoorthy, S., Shippenberg, T. S., and Jayanthi, L. D. (2011) Regulation of monoamine transporters: Role of transporter phosphorylation, *Pharmacology & Therapeutics 129*, 220-238.

212. Doolen, S., and Zahniser, N. R. (2001) Protein tyrosine kinase inhibitors alter human dopamine transporter activity in Xenopus oocytes, *J Pharmacol Exp Ther 296*, 931-938.

213. Fog, J. U., Khoshbouei, H., Holy, M., Owens, W. A., Vaegter, C. B., Sen, N., Nikandrova, Y., Bowton, E., McMahon, D. G., Colbran, R. J., Daws, L. C., Sitte, H. H., Javitch, J. A., Galli, A., and Gether, U. (2006) Calmodulin kinase II interacts with the dopamine transporter C terminus to regulate amphetamine-induced reverse transport, *Neuron 51*, 417-429.

214. Yurek, D. M., Hipkens, S. B., Hebert, M. A., Gash, D. M., and Gerhardt, G. A. (1998) Age-related decline in striatal dopamine release and motoric function in brown Norway/Fischer 344 hybrid rats, *Brain Res 791*, 246-256.

215. Willig, F., Palacios, A., Monmaur, P., M'Harzi, M., Laurent, J., and Delacour, J. (1987) Short-term memory, exploration and locomotor activity in aged rats, *Neurobiol Aging 8*, 393-402.

216. Bennett, D. A., Beckett, L. A., Murray, A. M., Shannon, K. M., Goetz, C. G., Pilgrim, D. M., and Evans, D. A. (1996) Prevalence of Parkinsonian Signs and Associated Mortality in a Community Population of Older People, *New England Journal of Medicine 334*, 71-76.

217. Kluger, A., Gianutsos, J. G., Golomb, J., Ferris, S. H., George, A. E., Franssen, E., and Reisberg, B. (1997) Patterns of motor impairement in normal aging, mild cognitive decline, and early Alzheimer's disease, *J Gerontol B Psychol Sci Soc Sci 52*, P28-39.

218. Volkow, N. D., Wang, G. J., Fowler, J. S., Ding, Y. S., Gur, R. C., Gatley, J., Logan, J., Moberg, P. J., Hitzemann, R., Smith, G., and Pappas, N. (1998) Parallel loss of presynaptic and postsynaptic dopamine markers in normal aging, *Ann Neurol 44*, 143-147.

219. Volkow, N. D., Gur, R. C., Wang, G. J., Fowler, J. S., Moberg, P. J., Ding, Y. S., Hitzemann, R., Smith, G., and Logan, J. (1998) Association between decline in brain dopamine activity with age and cognitive and motor impairment in healthy individuals, *Am J Psychiatry 155*, 344-349.

220. Gerhardt, G. A., Cass, W. A., Yi, A., Zhang, Z., and Gash, D. M. (2002) Changes in somatodendritic but not terminal dopamine regulation in aged rhesus monkeys, *J Neurochem 80*, 168-177.

221. Hebert, M. A., and Gerhardt, G. A. (1998) Normal and drug-induced locomotor behavior in aging: comparison to evoked DA release and tissue content in fischer 344 rats, *Brain Res 797*, 42-54.

222. Ingram, S. L., and Amara, S. G. (2000) Arachidonic acid stimulates a novel cocaine-sensitive cation conductance associated with the human dopamine transporter, *J Neurosci 20*, 550-557.

223. Long, J. M., Mouton, P. R., Jucker, M., and Ingram, D. K. (1999) What counts in brain aging? Design-based stereological analysis of cell number, *J Gerontol A Biol Sci Med Sci 54*, B407-417.

224. Cabello, C. R., Thune, J. J., Pakkenberg, H., and Pakkenberg, B. (2002) Ageing of substantia nigra in humans: cell loss may be compensated by hypertrophy, *Neuropathol Appl Neurobiol 28*, 283-291.

225. Ma, S. Y., Ciliax, B. J., Stebbins, G., Jaffar, S., Joyce, J. N., Cochran, E. J., Kordower, J. H., Mash, D. C., Levey, A. I., and Mufson, E. J. (1999) Dopamine transporter-immunoreactive neurons decrease with age in the human substantia nigra, *J Comp Neurol 409*, 25-37.

226. Hornykiewicz, O., and Kish, S. J. (1987) Biochemical pathophysiology of Parkinson's disease, *Adv Neurol 45*, 19-34.

227. Leenders, K. L., Salmon, E. P., Tyrrell, P., Perani, D., Brooks, D. J., Sager, H., Jones, T., Marsden, C. D., and Frackowiak, R. S. (1990) The nigrostriatal

dopaminergic system assessed in vivo by positron emission tomography in healthy volunteer subjects and patients with Parkinson's disease, *Arch Neurol 47*, 1290-1298.

228. Grondin, R., Cass, W. A., Zhang, Z., Stanford, J. A., Gash, D. M., and Gerhardt, G. A. (2003) Glial cell line-derived neurotrophic factor increases stimulus-evoked dopamine release and motor speed in aged rhesus monkeys, *J Neurosci 23*, 1974-1980.

229. Cruz-Muros, I., Afonso-Oramas, D., Abreu, P., Rodriguez, M., Gonzalez, M. C., and Gonzalez-Hernandez, T. (2008) Deglycosylation and subcellular redistribution of VMAT2 in the mesostriatal system during normal aging, *Neurobiol Aging 29*, 1702-1711.

230. Himi, T., Cao, M., and Mori, N. (1995) Reduced expression of the molecular markers of dopaminergic neuronal atrophy in the aging rat brain, *J Gerontol A Biol Sci Med Sci 50*, B193-200.

231. Yurek, D. M., and Fletcher-Turner, A. (2001) Differential expression of GDNF, BDNF, and NT-3 in the aging nigrostriatal system following a neurotoxic lesion, *Brain Res 891*, 228-235.

232. Yurek, D. M., and Seroogy, K. B. (2000) Differential expression of neurotrophin and neurotrophin receptor mRNAs in and adjacent to fetal midbrain grafts implanted into the dopamine-denervated striatum, *J Comp Neurol 423*, 462-473.

233. Yurek, D. M., and Fletcher-Turner, A. (2000) Lesion-induced increase of BDNF is greater in the striatum of young versus old rat brain, *Exp Neurol 161*, 392-396.

234. Strand, A. D., Baquet, Z. C., Aragaki, A. K., Holmans, P., Yang, L., Cleren, C., Beal, M. F., Jones, L., Kooperberg, C., Olson, J. M., and Jones, K. R. (2007) Expression profiling of Huntington's disease models suggests that brain-derived neurotrophic factor depletion plays a major role in striatal degeneration, *J Neurosci 27*, 11758-11768.

235. Katoh-Semba, R., Semba, R., Takeuchi, I. K., and Kato, K. (1998) Age-related changes in levels of brain-derived neurotrophic factor in selected brain regions of rats, normal mice and senescence-accelerated mice: a comparison to those of nerve growth factor and neurotrophin-3, *Neurosci Res 31*, 227-234.

236. Nagatsu, T., and Sawada, M. (2007) Biochemistry of postmortem brains in Parkinson's disease: historical overview and future prospects, *J Neural Transm Suppl*, 113-120.

237. Silhol, M., Bonnichon, V., Rage, F., and Tapia-Arancibia, L. (2005) Age-related changes in brain-derived neurotrophic factor and tyrosine kinase receptor isoforms in the hippocampus and hypothalamus in male rats, *Neuroscience 132*, 613-624.

238. Guerini, F. R., Beghi, E., Riboldazzi, G., Zangaglia, R., Pianezzola, C., Bono, G., Casali, C., Di Lorenzo, C., Agliardi, C., Nappi, G., Clerici, M., and Martignoni, E. (2009) BDNF Val66Met polymorphism is associated with cognitive impairment in Italian patients with Parkinson’s disease, *European Journal of Neurology 16*, 1240-1245.

239. Masaki, T., Matsushita, S., Arai, H., Takeda, A., Itoyama, Y., Mochizuki, H., Kamakura, K., Ohara, S., and Higuchi, S. (2003) Association between a

polymorphism of brain-derived neurotrophic factor gene and sporadic Parkinson's disease, *Ann Neurol 54*, 276-277.

240. Luellen, B. A., Bianco, L. E., Schneider, L. M., and Andrews, A. M. (2007) Reduced brain-derived neurotrophic factor is associated with a loss of serotonergic innervation in the hippocampus of aging mice, *Genes Brain Behav 6*, 482-490.

241. He, M., and Shippenberg, T. S. (2000) Strain differences in basal and cocaine-evoked dopamine dynamics in mouse striatum, *J Pharmacol Exp Ther 293*, 121-127.

242. Dluzen, D. E., Ji, J., and McDermott, J. L. (2010) Age-related changes in nigrostriatal dopaminergic function in heterozygous mutant dopamine transporter knock-out mice, *Neurosci Lett 476*, 66-69.

243. Jones, S. R., Gainetdinov, R. R., Jaber, M., Giros, B., Wightman, R. M., and Caron, M. G. (1998) Profound neuronal plasticity in response to inactivation of the dopamine transporter, *Proceedings of the National Academy of Sciences 95*, 4029-4034.

244. Gainetdinov, R. R., Jones, S. R., and Caron, M. G. (1999) Functional hyperdopaminergia in dopamine transporter knock-out mice, *Biol Psychiatry 46*, 303-311.

245. Jankovic, J., and Aguilar, L. G. (2008) Current approaches to the treatment of Parkinson's disease, *Neuropsychiatr Dis Treat 4*, 743-757.

246. Kelley, A. E. (1999) Functional specificity of ventral striatal compartments in appetitive behaviors, *Ann N Y Acad Sci 877*, 71-90.

247. Gottschalk, W., Pozzo-Miller, L. D., Figurov, A., and Lu, B. (1998) Presynaptic modulation of synaptic transmission and plasticity by brain-derived neurotrophic factor in the developing hippocampus, *J Neurosci 18*, 6830-6839.

248. Baker, S. A., Stanford, L. E., Brown, R. E., and Hagg, T. (2005) Maturation but not survival of dopaminergic nigrostriatal neurons is affected in developing and aging BDNF-deficient mice, *Brain Res 1039*, 177-188.

249. Giros, B., and Caron, M. G. (1993) Molecular characterization of the dopamine transporter, *Trends Pharmacol Sci 14*, 43-49.

250. Torres, G. E., Carneiro, A., Seamans, K., Fiorentini, C., Sweeney, A., Yao, W. D., and Caron, M. G. (2003) Oligomerization and trafficking of the human dopamine transporter. Mutational analysis identifies critical domains important for the functional expression of the transporter, *J Biol Chem 278*, 2731-2739.

251. Buck, K. J., and Amara, S. G. (1994) Chimeric dopamine-norepinephrine transporters delineate structural domains influencing selectivity for catecholamines and 1-methyl-4-phenylpyridinium, *Proc Natl Acad Sci U S A 91*, 12584-12588.

252. Kitayama, S., Shimada, S., Xu, H., Markham, L., Donovan, D. M., and Uhl, G. R. (1992) Dopamine transporter site-directed mutations differentially alter substrate transport and cocaine binding, *Proc Natl Acad Sci U S A 89*, 7782-7785.

253. Fleckenstein, A. E., Haughey, H. M., Metzger, R. R., Kokoshka, J. M., Riddle, E. L., Hanson, J. E., Gibb, J. W., and Hanson, G. R. (1999) Differential effects of psychostimulants and related agents on dopaminergic and serotonergic transporter function, *Eur J Pharmacol 382*, 45-49.

254. Chu, P.-W., Hadlock, G. C., Vieira-Brock, P., Stout, K., Hanson, G. R., and Fleckenstein, A. E. (2010) Methamphetamine alters vesicular monoamine transporter-2 function and potassium-stimulated dopamine release, *Journal of Neurochemistry 115*, 325-332.

255. Fleckenstein, A. E., Volz, T. J., and Hanson, G. R. (2009) Psychostimulant-induced alterations in vesicular monoamine transporter-2 function: Neurotoxic and therapeutic implications, *Neuropharmacology 56*, 133-138.

256. Nickell, J. R., Krishnamurthy, S., Norrholm, S., Deaciuc, G., Siripurapu, K. B., Zheng, G., Crooks, P. A., and Dwoskin, L. P. (2010) Lobelane Inhibits Methamphetamine-Evoked Dopamine Release via Inhibition of the Vesicular Monoamine Transporter-2, *Journal of Pharmacology and Experimental Therapeutics 332*, 612-621.

257. Ugarte, Y. V., Rau, K. S., Riddle, E. L., Hanson, G. R., and Fleckenstein, A. E. (2003) Methamphetamine rapidly decreases mouse vesicular dopamine uptake: role of hyperthermia and dopamine D2 receptors, *European Journal of Pharmacology 472*, 165-171.

258. Dluzen, D. E., McDermott, J. L., and Darvesh, A. S. (2010) Relationships among gender, age, time, and temperature in methamphetamine-induced striatal dopaminergic neurotoxicity, *Neuroscience 167*, 985-993.

259. Miller, D. B., O'Callaghan, J. P., and Ali, S. F. (2000) Age as a Susceptibility Factor in the Striatal Dopaminergic Neurotoxicity Observed in the Mouse following Substituted Amphetamine Exposure, *Annals of the New York Academy of Sciences 914*, 194-207.

260. O'Callaghan, J. P., and Miller, D. B. (1994) Neurotoxicity profiles of substituted amphetamines in the C57BL/6J mouse, *Journal of Pharmacology and Experimental Therapeutics 270*, 741-751.

261. Kogan, F. J., Nichols, W. K., and Gibb, J. W. (1976) Influence of methamphetamine on nigral and striatal tyrosine hydroxylase activity and on striatal dopamine levels, *Eur J Pharmacol 36*, 363-371.

262. Cass, W. A. (1997) Decreases in evoked overflow of dopamine in rat striatum after neurotoxic doses of methamphetamine, *J Pharmacol Exp Ther 280*, 105-113.

263. Chu, P.-W., Seferian, K. S., Birdsall, E., Truong, J. G., Riordan, J. A., Metcalf, C. S., Hanson, G. R., and Fleckenstein, A. E. (2008) Differential regional effects of methamphetamine on dopamine transport, *European Journal of Pharmacology 590*, 105-110.

264. Dluzen, D. E. (2004) The effect of gender and the neurotrophin, BDNF, upon methamphetamine-induced neurotoxicity of the nigrostriatal dopaminergic system in mice, *Neurosci Lett 359*, 135-138.

265. Budygin, E. A., Oleson, E. B., Mathews, T. A., Lack, A. K., Diaz, M. R., McCool, B. A., and Jones, S. R. (2007) Effects of chronic alcohol exposure on dopamine uptake in rat nucleus accumbens and caudate putamen, *Psychopharmacology (Berl) 193*, 495-501.

266. Mateo, Y., Budygin, E. A., John, C. E., Banks, M. L., and Jones, S. R. (2004) Voltammetric assessment of dopamine clearance in the absence of the

dopamine transporter: no contribution of other transporters in core or shell of nucleus accumbens, *J Neurosci Methods 140*, 183-187.

267. Horn, A. S. (1990) Dopamine uptake: A review of progress in the last decade, *Progress in Neurobiology 34*, 387-400.

268. Nicholson, C. (1995) Interaction between diffusion and Michaelis-Menten uptake of dopamine after iontophoresis in striatum, *Biophysical journal 68*, 1699-1715.

269. Bennett, B. A., Hollingsworth, C. K., Martin, R. S., and Harp, J. J. (1998) Methamphetamine-induced alterations in dopamine transporter function, *Brain Research 782*, 219-227.

270. Schenk, J. O., Wright, C., and Bjorklund, N. (2005) Unraveling neuronal dopamine transporter mechanisms with rotating disk electrode voltammetry, *Journal of Neuroscience Methods 143*, 41-47.

271. Goodwin, J. S., Larson, G. A., Swant, J., Sen, N., Javitch, J. A., Zahniser, N. R., De Felice, L. J., and Khoshbouei, H. (2009) Amphetamine and methamphetamine differentially affect dopamine transporters in vitro and in vivo, *J Biol Chem 284*, 2978-2989.

272. Kantor, L., Hewlett, G. H., Park, Y. H., Richardson-Burns, S. M., Mellon, M. J., and Gnegy, M. E. (2001) Protein kinase C and intracellular calcium are required for amphetamine-mediated dopamine release via the norepinephrine transporter in undifferentiated PC12 cells, *J Pharmacol Exp Ther 297*, 1016-1024.

273. Giambalvo, C. T. (1988) Protein kinase C and dopamine release--II. Effect of dopamine acting drugs in vivo, *Biochem Pharmacol 37*, 4009-4017.

274. Khoshbouei, H., Sen, N., Guptaroy, B., Johnson, L., Lund, D., Gnegy, M. E., Galli, A., and Javitch, J. A. (2004) N-terminal phosphorylation of the dopamine transporter is required for amphetamine-induced efflux, *PLoS Biol 2*, E78.

275. Cubells, J. F., Rayport, S., Rajendran, G., and Sulzer, D. (1994) Methamphetamine neurotoxicity involves vacuolation of endocytic organelles and dopamine-dependent intracellular oxidative stress, *J Neurosci 14*, 2260-2271.

276. Fumagalli, F., Gainetdinov, R. R., Wang, Y. M., Valenzano, K. J., Miller, G. W., and Caron, M. G. (1999) Increased methamphetamine neurotoxicity in heterozygous vesicular monoamine transporter 2 knock-out mice, *J Neurosci 19*, 2424-2431.

277. Fumagalli, F., Gainetdinov, R. R., Valenzano, K. J., and Caron, M. G. (1998) Role of dopamine transporter in methamphetamine-induced neurotoxicity: evidence from mice lacking the transporter, *J Neurosci 18*, 4861-4869.

278. Mamounas, L. A., Altar, C. A., Blue, M. E., Kaplan, D. R., Tessarollo, L., and Lyons, W. E. (2000) BDNF promotes the regenerative sprouting, but not survival, of injured serotonergic axons in the adult rat brain, *J Neurosci 20*, 771-782.

279. Siuciak, J. A., Lewis, D. R., Wiegand, S. J., and Lindsay, R. M. (1997) Antidepressant-Like Effect of Brain-derived Neurotrophic Factor (BDNF), *Pharmacology Biochemistry and Behavior 56*, 131-137.

280. McGough, N. N., He, D. Y., Logrip, M. L., Jeanblanc, J., Phamluong, K., Luong, K., Kharazia, V., Janak, P. H., and Ron, D. (2004) RACK1 and brain-derived neurotrophic factor: a homeostatic pathway that regulates alcohol addiction, *J Neurosci 24*, 10542-10552.

281. Garris, P. A., Walker, Q. D., and Wightman, R. M. (1997) Dopamine release and uptake rates both decrease in the partially denervated striatum in proportion to the loss of dopamine terminals, *Brain Res 753*, 225-234.

282. Garris, P. A., and Wightman, R. M. (1995) Distinct pharmacological regulation of evoked dopamine efflux in the amygdala and striatum of the rat in vivo, *Synapse 20*, 269-279.

283. Segal, R. A. (2003) Selectivity in neurotrophin signaling: theme and variations, *Annu Rev Neurosci 26*, 299-330.

284. Toyoshima, C., Nakasako, M., Nomura, H., and Ogawa, H. (2000) Crystal structure of the calcium pump of sarcoplasmic reticulum at 2.6 [angst] resolution, *Nature 405*, 647-655.

285. Reichardt, L. F. (2006) Neurotrophin-regulated signalling pathways, *Philos Trans R Soc Lond B Biol Sci 361*, 1545-1564.

286. Finkbeiner, S., Tavazoie, S. F., Maloratsky, A., Jacobs, K. M., Harris, K. M., and Greenberg, M. E. (1997) CREB: a major mediator of neuronal neurotrophin responses, *Neuron 19*, 1031-1047.

287. Ochs, G., Penn, R. D., York, M., Giess, R., Beck, M., Tonn, J., Haigh, J., Malta, E., Traub, M., Sendtner, M., and Toyka, K. V. (2000) A phase I/II trial of recombinant methionyl human brain derived neurotrophic factor administered by intrathecal infusion to patients with amyotrophic lateral sclerosis, *Amyotrophic Lateral Sclerosis 1*, 201-206.

288. Liu, X., Chan, C.-B., Jang, S.-W., Pradoldej, S., Huang, J., He, K., Phun, L. H., France, S., Xiao, G., Jia, Y., Luo, H. R., and Ye, K. (2010) A Synthetic 7,8-

Dihydroxyflavone Derivative Promotes Neurogenesis and Exhibits Potent Antidepressant Effect, *Journal of Medicinal Chemistry 53*, 8274-8286.

289. Monteggia, L. M. (2011) Toward Neurotrophin-Based Therapeutics, *Am J Psychiatry 168*, 114-116.

290. Jang, S.-W., Liu, X., Yepes, M., Shepherd, K. R., Miller, G. W., Liu, Y., Wilson, W. D., Xiao, G., Blanchi, B., Sun, Y. E., and Ye, K. (2010) A selective TrkB agonist with potent neurotrophic activities by 7,8-dihydroxyflavone, *Proceedings of the National Academy of Sciences 107*, 2687-2692.

291. Andero, R., Heldt, S. A., Ye, K., Liu, X., Armario, A., and Ressler, K. J. (2011) Effect of 7,8-Dihydroxyflavone, a Small-Molecule TrkB Agonist, on Emotional Learning, *Am J Psychiatry 168*, 163-172.

ABSTRACT

EFFECT OF LOW ENDOGENOUS BRAIN-DERIVED NEUROTROPHIC FACTOR LEVELS ON STRIATAL DOPAMINE DYNAMICS

by

FRANCIS KABUI MAINA

December 2011

Advisor: Dr. Tiffany A. Mathews

Major: Chemistry (Analytical)

Degree: Doctor of Philosophy

Many neurological diseases and disorders are a result of alterations with neurotransmitters, neuromodulators, and/or proteins. Specifically, one protein that has been linked to numerous neurological diseases and disorders such as Parkinson's disease, Huntington's disease, addiction, attention deficit hyperactivity disorder (ADHD), and depression is brain-derived neurotrophic factor (BDNF). As a trophic factor, BDNF role is to assist in the growth, survival, and differentiation of neurons. However, there is increasing evidence that BDNF may mediate neurotransmitter dynamics. Our goals were to understand how endogenous BDNF levels and aging modulate the dopamine (DA) dynamics in the mouse striatum. Two complementary neurochemical techniques, slice (*in vitro*) fast scan cyclic voltammetry (FSCV) and *in vivo* microdialysis were used to characterize striatal DA dynamics in wildtype and BDNF heterozygous mutant ($BDNF^{+/-}$) mice.

Overall, our findings highlight that (1) we were able to develop a reliable FSCV assay to characterize DA release-regulating D2 and D3 autoreceptors functionality in the striatum of wildtype (C57BL/6) mice, (2) $BDNF^{+/-}$ mice appear to be

hyperdopaminergic at young age, which may be a consequence of reduced DA release and DA transporter functions, (3) perfusion of exogenous BDNF on brain slices from young $BDNF^{+/-}$ mice increases the electrically evoked DA release in a dose-dependent manner, and (4) neurochemically, aged $BDNF^{+/-}$ mice are more similar to their wildtype littermates. Taken together, these results suggest that, during neuronal development, low BDNF levels can modulate DA dynamics, increasing susceptibility to neurological diseases and disorders. However, a life-time of low BDNF levels alone does not appear to be critical in DA dynamics dysregulation with age.

AUTOBIOGRAPHICAL STATEMENT

Education

2006-2011
Wayne State University (Detroit, Michigan)
Doctor of Philosophy (Ph.D.), Chemistry (Analytical)
Dissertation: Effect of low endogenous brain-derived neurotrophic factor levels on striatal dopamine dynamics (Advisor: Dr. Tiffany A. Mathews)

2000-2004
University of Nairobi (Nairobi, Kenya)
Bachelor of Science (Chemistry)

Employment

August 2006 to August 2011
Wayne State University (Detroit, Michigan)
Research/Teaching Assistant

February 2005 to July 2006
GlaxoSmithKline (Nairobi, Kenya)
In-Process Chemist

Publications

1. Bosse, Kelly E., **Maina, Francis K.,** Birbeck, J., France, M., Roberts, J., and Mathews, Tiffany A. "Aberrant striatal dopamine transmitter dynamics in brain-derived neurotrophic factor-deficient mice reveal a hyperdopaminergic phenotype'' Accepted for Publication in *Journal of Neurochemistry*.

2. **Maina, Francis K.,** Khalid Madiha, Apawu Aaron and Mathews, Tiffany A. "Pre-synaptic dopamine dynamics in striatal brain slices with fast-scan cyclic voltammetry" Accepted for Publication in *Journal of Visualized Experiments*.

3. **Maina, Francis K.** and Mathews, Tiffany A. "A functional fast scan cyclic voltammetry assay to characterize dopamine D2 and D3 autoreceptors in the mouse striatum" *ACS Chemical Neuroscience,* 2010, 1(6): 450-462. (Highlighted in *ACS Chemical Neuroscience, "In This Issue"* by Anirban Mahapatra)

Awards and Membership

- Wayne State University Summer 2011 Dissertation Fellowship Award
- Chemistry Graduate Student Professional Travel Awards (2008-2009 & 2009-2010)
- Member of American Chemical Society